



**UNIVERSIDADE FEDERAL DO PARÁ
INSTITUTO DE GEOCIÊNCIAS
PROGRAMA DE PÓS-GRADUAÇÃO EM GEOLOGIA E GEOQUÍMICA**

TESE DE DOUTORADO

**O SISTEMA FLUVIAL SOLIMÕES-AMAZONAS DURANTE O
QUATERNÁRIO**

Tese apresentada por:

JOSÉ MAX GONZÁLEZ ROZO

Orientador: Prof. Dr. Afonso César Rodrigues Nogueira (UFPA)

**BELÉM
2012**

Dados Internacionais de Catalogação-na-Publicação (CIP)
Biblioteca Geólogo Raimundo Montenegro Garcia de Montalvão

G643s González Rozo, José Max

O Sistema fluvial Solimões-Amazonas durante o Quaternário / José Max Gonzalez Rozo; Orientador: Afonso Cesar Rodrigues Nogueira - 2012.

xxi, 128 fl.: il.

Tese (doutorado em geologia) – Universidade Federal do Pará, Instituto de Geociências, Programa de Pós-Graduação em Geologia e Geoquímica, Belém, 2011.

1. Geologia estratigráfica - Quaternário. 2. Padrão fluvial anastomosado. 3. Padrão fluvial meandrante de múltiplos canais. 4. Barras em crescente. 5. Rio Amazonas. I. Nogueira, Afonso César Rodrigues, *orient.* II. Universidade Federal do Pará III. Título.

CDD 22° ed.: 551.7909811



**Universidade Federal do Pará
Instituto de Geociências**

Programa de Pós-Graduação em Geologia e Geoquímica



O SISTEMA FLUVIAL SOLIMÕES-AMAZONAS DURANTE O QUATERNÁRIO

TESE APRESENTADA POR


JOSÉ MAX GONZÁLEZ ROZO

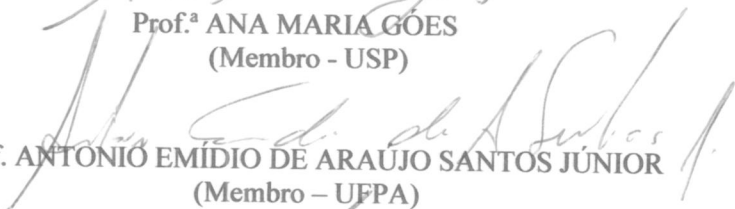
**Como requisito parcial à obtenção do Grau de Doutor em Ciências na Área
de GEOLOGIA**

Data de Aprovação: 03 / 09 / 2012

Banca Examinadora:


Prof. AFONSO CÉSAR RODRIGUES NOGUEIRA
(Orientador – UFPA)


Prof.ª ANA MARIA GOES
(Membro - USP)


Prof. ANTONIO EMÍDIO DE ARAUJO SANTOS JÚNIOR
(Membro – UFPA)


Prof. ARNALDO DE QUEIROZ DA SILVA
(Membro - UFPA)


Prof. JOSÉ CANDIDO STEVAUX
(Membro - UEM)

*A Carmen, mi madre,
cuya mente se perdió en lo mas profundo de um abismo...*

AGRADECIMENTOS

Ao Conselho Nacional de Desenvolvimento Científico e Tecnológico (CNPq) pela bolsa concedida para minha manutenção no Brasil entre 2009-2012.

Ao Programa de Pós-graduação em Geologia e Geoquímica da Universidade Federal do Pará pelo apoio logístico e financeiro.

Ao Afonso César Rodrigues Nogueira, pela orientação e por ter me dado a oportunidade de continuar a pesquisa nos sistemas fluviais Amazônicos.

Ao Werner Truckenbrodt pelas detalhadas revisões dos meus textos e por seus inúmeros questionamentos e sugestões na realização deste trabalho.

Ao Rômulo Simões Angélica pela orientação com a análise dos argilominerais e a sua equipe pela eficiência no processamento das amostras para Difração de Raios X.

Ao Kenneth Campbell do *Natural History Museum of Los Angeles County* pelas discussões sobre a geologia da Amazônia.

Ao André Roy da *Université de Montréal* pelas sugestões no trabalho na área da Amazônia Colombiana, bem como pela ajuda com a análise hidrológica.

Ao Gerald Nanson da *University of Wollongong*, e ao Stephen Tooth da *Aberystwyth University* pelas discussões dos padrões fluviais *anastomosing* and *anabranching*, e também pelas valiosas sugestões na descrição do Rio Amazonas no trecho entre os rios Negro e Madeira.

Ao Bart Makaske da *Wageningen University* pelas discussões e valiosas sugestões na descrição do padrão anastomosado do rio Amazonas no trecho entre os rios Negro e Madeira.

Ao Galen Halverson da *McGill University* pela ajuda na análise dos minerais pesados.

Ao Carlo Soto Castro pela ajuda no sensoriamento remoto, e as inúmeras discussões de como usar melhor esta ferramenta nos sistemas fluviais.

Ao Santiago Duque da Universidad Nacional de Colombia em Leticia, pela disponibilidade de dados hidrológicos da Amazônia Colombiana.

Ao Luiz Saturnino, pela ajuda no trabalho de campo, no processamento das amostras, por estar sempre preste a discutir processos geológicos, e principalmente pela amizade ao longo destes anos.

A Roseane Sarges pela amizade, discussões e por ter acompanhado todo o desenvolvimento desta pesquisa.

Ao Luciano Gandin Machado, pela ajuda no trabalho de campo.

Ao Tasso Guimarães pela amizade, pelas discussões sobre a geologia do Quaternário, e por sua essencial ajuda no desenvolvimento final desta tese.

Ao Lucindo Antunes Filho da Universidade Federal do Amazonas, pela amizade e ajuda.

Ao Artur Gustavo Miranda pela ajuda no processamento das amostras de argilominerais.

Ao Anderson Mendes pela amizade e pela ajuda na análise dos minerais pesados.

Aos colegas da Pós-Graduação Jota Bandeira, Isaac Rudsnitzki, Roberto César e Joelson Soares, por estarem sempre dispostos a discutir processos sedimentares.

A Cleida Freitas pela ajuda nos processos administrativos e sua eficiência na secretaria do PPGG.

A Joelma Lobo pela ajuda na montagem das lâminas de minerais pesados.

Ao sr. Lopes, técnico do Laboratório de Sedimentologia, pela ajuda nas análises granulométricas e no processamento das amostras para argilominerais e minerais pesados.

Ao pessoal do Laboratório de Geocronologia Isotópica (ParaISO), por disponibilizarem a infraestrutura do laboratório para a separação dos minerais pesados.

A Julie Major, pelo seu amor, ajuda, constante incentivo, e pela paciência nas minhas largas ausências. Além da sua valiosa ajuda na revisão dos textos em inglês.

Ao Tiago pela inspiração.

A minha família na Colômbia (Carmen, José, Yojana e Ingrith), e minha família no Canadá (Paul, Carole e Jossé) pela ajuda e constante incentivo.

RESUMO

Um padrão predominantemente anastomosado tem sido descrito para o Rio Amazonas com incremento na estabilidade de montante à jusante. Um padrão meandrante com alguns trechos retilíneos tem sido descrito no alto Rio Amazonas, como também trechos meandantes foram identificados no Rio Solimões no Brasil. Adicionalmente, características meandantes na forma de barras em crescente e meandros abandonados têm sido identificadas em diferentes trechos anastomosados no Rio Amazonas. Estas características meandantes são consideradas raras ou ausentes em sistemas anastomosados. Desta forma, o Rio Amazonas com características meandantes é diferente de muitos outros rios anastomosados que possuem estabilidade lateral e ausência de canais meandantes. A limitada informação do Rio Amazonas principalmente obtida a partir de sensoriamento remoto. A falta do estabelecimento de uma relação clara entre as características meandantes e anastomosadas, bem como da determinação da extensão no tempo e espaço do desenvolvimento do padrão anastomosado, aliada a falta de dados de campo dificulta o entendimento das características deste sistema fluvial. Esta falta de informação ainda é maior quando consideramos características morfológicas e hidrológicas pretéritas do Rio Amazonas. Informações sobre o padrão de canal do Rio Amazonas durante o Pleistoceno são raras, com poucos trabalhos que sugerem um padrão meandrante de um único canal durante esta época. Diferentemente, uma ampla discussão sobre a origem do Rio Amazonas com um sistema transcontinental com fluxo para o leste tem sido desenvolvida nos últimos anos. A falta de consenso do tempo exato que este evento ocorreu e a falta de dados sedimentológicos da Amazônia Central somente aumentam esta discussão. Estudos sistemáticos são necessários para o entendimento: 1) da origem do sistema anastomosado do Rio Amazonas e o desenvolvimento de suas características meandantes; 2) do comportamento do alto Amazonas em comparação com o padrão principalmente anastomosado do Rio Amazonas no Brasil; 3) das características do Rio Amazonas durante o Pleistoceno e as diferenças das condições atuais. Para alcançar este entendimento, o padrão atual do canal do Rio Amazonas foi estudado no trecho entre Manaus e a foz do Rio Madeira. Fácies, morfologia, mudanças no padrão do canal através da análise temporal por sensores remotos, além de datações por luminescência opticamente estimulada (LOE) foram analisadas. Foi determinado um padrão geral anastomosado com canais meandantes secundários e barras em crescente, extensamente distribuídas e relacionadas principalmente à migração sub-recente e atual desses canais. Avulsão, formação de barras transversais e atalhos em corredeira são os mecanismos formadores do atual padrão anastomosado do sistema. Esse padrão principal anastomosado, e os canais meandantes

secundários têm coexistido há pelo menos 7.5 ± 0.85 ka. O trecho do Rio Amazonas na Colômbia foi estudado para definir com maior precisão, as diferenças do padrão de canal com o Rio Amazonas na área de Manaus, e também identificar condições para o desenvolvimento do padrão do canal atual. Morfologia, mudanças do canal através de análise temporal com o uso de sensores remotos e dados de vazão foram analisados. Foi encontrado um padrão meandrante de múltiplos canais neste trecho do rio, que corresponde a um padrão *anabanching* lateralmente ativo. Formação de barras transversais e atalhos em corredeira são os mecanismos formadores do padrão *anabanching* no sistema. Variações em descarga são responsáveis pela dinâmica de deposição e erosão, analisadas através de sensores remotos. A deposição Pleistocena é também estudada para definir desde quando a atual configuração do sistema Solimões-Amazonas tem estado presente, bem como, para entender as condições paleogeográficas anteriores ao Holoceno que levaram ao desenvolvimento do sistema fluvial atual. Afloramentos do Pleistoceno (Formação Içá) são muito restritos no Rio Amazonas entre o trecho colombiano, e a confluência com o Rio Madeira, com a área de Coari tendo as melhores exposições. Na área de Coari, fácies, argilominerais e minerais pesados, além de datações por luminescência opticamente estimulada (LOE) foram analisados. Foi encontrado um padrão meandrante principal estabelecido há pelo menos 133.8 ± 20.9 ka. Este sistema aparentemente foi desenvolvido como um padrão de múltiplos canais meandrantés, similar as condições atuais do Rio Amazonas no trecho colombiano.

Palavras chave: Geologia estratigráfica – Quaternário. Padrão fluvial anastomosado. Padrão fluvial meandrante de múltiplos canais. Barras em crescente. Rio Amazonas.

ABSTRACT

The Amazon River has been considered as having a predominantly anastomosing pattern with increasing stability from upstream to downstream. Meandering and even straight patterns have been recognized in the upper Amazon as well as meandering reaches identified in the Solimões River in Brazil. Additionally, meandering features in the form of scroll bars and oxbow lakes have been also identified in different anastomosing reaches of the Amazon. These meandering features have been considered rare or absent in anastomosing rivers. In this context, it is clear that the Amazon, with its meandering features, is different from many other anastomosing rivers that have laterally stable, non-meandering channels. The limited information on the Amazon River provided mainly by remote sensing data and the lack of field data make difficult to understand the characteristics of this fluvial system, to establish a clear relationship between the meandering and anastomosing features and also to determine to what extent in time and space the anastomosing pattern is developed. The lack of information increases respect to the channel pattern characteristics of the Amazon River prior to present-day conditions. Channel pattern features during Pleistocene have been scarcely described, with a few studies that suggest a main single-channel meandering pattern during that time. In contrast, a broad discussion about the origin of the Amazon River as a transcontinental eastward flow has been developed in recent years with no agreement on the exact time this event took place and very scarce sedimentologic data on the deposits of central Amazonia. To our knowledge, no research has yet been undertaken to understand: 1) the origin of the Amazon's anastomosing pattern and the development of its meandering features; 2) the behavior of the upper reaches of the Amazon, and specifically whether these reaches develop only meandering features, or whether they share the characteristic main anastomosing pattern with meandering secondary channels of the Amazon River in Brazil; 3) the characteristics of the Amazon River during Pleistocene and whether the river was different from the present-day pattern. To reach these goals, the current channel pattern of the Amazon River was studied between Manaus and the mouth of the Madeira River. Sedimentary processes were studied using field data, channel changes were analyzed through a temporal analysis using remote sensing data, morphology was studied and optically stimulated luminescence (OSL) dates were obtained. The river in this area was found to be anastomosing with extensively distributed scroll bars. These scroll bars are mainly formed by sinuous secondary channels and related to subrecent and present-day migration. Avulsion, mid-channel bar formation and chute cut-offs are the formative mechanisms of anastomosis in this system. The main anastomosing pattern and the meandering secondary channels have

coexisted at least since 7.5 ± 0.85 ka. A reach of the Colombian Amazon River (upper Amazon River) was studied to more precisely define differences with the middle Amazon River with respect to channel pattern, and also to identify the triggers for its channel pattern development. Channel changes were analyzed through a temporal analysis using remote sensing data, morphology studied and discharge data was analyzed over three different periods. The river in this area was found to be a multichannel meandering pattern that corresponds to a laterally active anabranching river. Mid-channel bar formation and chute cut-offs are the formative mechanisms of the multichannel pattern in this system. Variations in discharge seem to be responsible for the deposition and erosion dynamics found from remote sensing analysis. To determine for how long the current channel pattern of the Amazon River has existed, and to understand the paleogeographic conditions prior to the Holocene, Pleistocene deposition was studied. Pleistocene deposition (Iça Formation) is very restricted between the upper and the middle reaches of the Amazon River, with the Coari area having the best outcrops. Sedimentary processes were studied using field data, clay and heavy minerals analyzed and optically stimulated luminescence (OSL) dates were obtained. A mainly meandering system was found in this area, developing at least since 133.8 ± 20.9 ka. This system seems to be characterized as a multichannel meandering pattern similar to present-day conditions of the Colombian Amazon River.

Keywords: Stratigraphic geology – Quaternary. Anastomosing pattern. Multichannel meandering pattern. Scroll bars. Amazon River.

LISTA DE ILUSTRAÇÕES

1 CONSIDERAÇÕES INICIAIS

- Figura 1 - Location map of the Amazon River. A) Amazon Basin. B) Regional map of the Amazon River between Iquitos, Peru and Manaus, Brazil. Studied areas are indicated in boxes from upstream to downstream as follow: Colombian Amazon River upstream the Javari River in the Leticia area; The Amazon River in the Coari area and the Amazon River between the confluences of the Negro and Madeira Rivers..... 2

2 THE ANASTOMOSING PATTERN AND THE EXTENSIVELY DISTRIBUTED SCROLL BARS IN THE MIDDLE AMAZON RIVER

- Figura 1 - Location map of the middle Amazon River. A) Amazon Basin. B) Regional map of the Amazon River between Iquitos, Peru and Manaus, Brazil. C) Main localities, rivers, islands and paranás (secondary channels) in the Amazon River between Manaus and the junction with the Madeira River. Topographic profiles in Figure 2A are indicated here..... 11
- Figura 2 - Topographic characteristics of the Amazon River between Manaus and the junction with the Madeira River. A) The island's height roughly corresponds to that of the adjacent floodplain. Note the elevation of the terraces compared with the floodplain. See Figure 1C for the location of the topographic profiles. B) Steep-sided channel margin on Careiro Island, locally characterized by displaced blocks ("terra caída") and great water depth near the bank..... 12
- Figura 3 - Geological setting. A) Geotectonic units of the Amazon region. B) Stratigraphy of Upper Cretaceous to Quaternary sedimentary deposits in the Amazonas Basin, modified from Cunha et al. (2007)..... 12
- Figura 4 - Temporal analysis of the Amazon River between Manaus and the mouth of the Madeira River from 1978 to 2009. A) Detail of the eastern part of the Careiro Paraná, the most active area in the secondary channels. B) Detail of Jacaré and Marati islands. Marati Island is where maximum rates of erosion and deposition are recorded in the studied reach of the Amazon River. Note the northeast migration tendency of the Jacaré Paraná and the erosion of the main channel at location 12. For the specific migration rates see Table 3..... 16
- Figura 5 - Morphologic features of the middle Amazon River. A) Detail of the Eastern Careiro Paraná. Note the scroll bar configuration with the development of oxbow lakes. B) Detail of Jacaré and Marati islands. Note the northeast direction of the migration of the Jacaré Paraná as indicated by the scroll bars. C) Scroll bars showing the migration of the main channel. A), B) and C) also show a Landsat-7 image from August 1, 1997. D) Morphology of ridge and swales characteristic of scroll bars from the main and secondary channels. E) Detail of the swale and ridge

- morphology at Onças Island. Note the development of a lake on the swale. D and E are located southeast of Onças Island as indicated in A. F) Characteristic vegetation developed on scroll bar deposits..... 17
- Figura 6 - Morphostratigraphic units in the study area. Note the asymmetrical distribution of the floodplain deposits, which are mainly on the right margin of the Amazon River. The location of the stratigraphic profiles and samples for grain size analysis are also indicated. Lakes, furos and other rivers are in black. B) Sedimentary deposits described in the area. Radiocarbon dates previously reported (^a and ^b) and the OSL ages obtained in this study indicate local events along the study area. ^a(Latrubesse and Franzinelli, 2002), ^b(Sternberg, 1960). C) Bouguer gravimetric map of the western Amazonas basin, modified from Wanderley Filho (1991); the SW-NE lowest gravimetric trend (bottom right of figure) marks the basin axis.. 18
- Figura 7 - Fluvial deposits. On Careiro Island, floodplain deposition is more common than in the reach downstream where scroll bar deposition is predominant. Location of logs indicated in Figure 6A. The depth at which the samples for OSL dating were collected is indicated in profiles 1, 9, 10, 19 and 20..... 19
- Figura 8 - Scroll bar deposits. A) Scroll bar developed over point bar. Scroll bar morphology is better observed from a satellite image (D3 in Figure 5A). This section corresponds to profile 10, in Figure 7. B) Detail of the point bar deposits: medium to fine sand fining upward with the development of trough cross stratification. C) Backsets structures terminating updip against an upstream-dipping erosion surface, in the sense of Fielding (2006). Flow direction from left to right. B) and C) are located in A). D) Climbing ripples. E) Laminar, flaser and lenticular bedding. D) and E) correspond to profile 19 in Figure 7..... 20
- Figura 9 - Development of irregularly rounded lakes in the floodplain. A) Two migrating secondary channels with the development of oxbow lakes. B) Individual bends in each channel can intersect previously formed oxbow lakes from the same channel or from an adjacent channel. The intersection forms lakes with complex geometry. C) Crevasse splays can develop and partially bury oxbow lakes or intersected oxbow lakes. D) As a result lakes develop with an irregularly rounded geometry. The processes in A), B) and C) developed contemporaneously, but here they are separated to illustrate how these lakes are formed..... 21
- Figura 10 -A) and B) Organic-rich beds in western Careiro Island. Tree trunks embedded in these deposits can be observed. Floodbasin and natural levee deposition overlay the organic-rich beds. C), D) and E) Sand bars in eastern Careiro Island. Note the magnitude of these sand bars in C). Dunes in D) are located above the sand bars, and ripples in E) are located above the dunes. F) Sand bars in the main channel at the confluence of the Negro and Amazon Rivers. Note the scour in the downstream dune flank..... 22

Figura 11 -Depositional model and morphologic characteristics of the studied reach of the Amazon River. Note the migration of secondary channels as well as localized migration in the main channel with the development of scroll bars.....	22
3 RECENT FLUVIAL DYNAMICS OF THE COLOMBIAN AMAZON RIVER	
Figura 1 - Location map of the Colombian Amazon River. A) Amazon Basin. B) Regional map of the Amazon River between Iquitos, Peru and Manaus, Brazil. Here we refer to the Ucayali-Amazonas-Solimões system as the Amazon River. Location of gauging stations considered in the hydrological analysis is indicated here. C) Studied reach of the Amazon River. This map was generated based on the Landsat image June 24 2006. Islands not present at that time were added to the map in order to show the location of all islands studied.	32
Figura 2 - Amazon River margin changes between 1986 and 2006. Sites where maximum migration rates were recorded are indicated here and specific values of migration are shown in Table 4. Areas not considered as channel migration are: (a) Cocha Island, that was accreted to the floodplain by 2001; (b) Caballo Cocha Island, that was isolated from the floodplain by 2001; (c) Yauma Island, that by 2006 was being accreted to the floodplain, with a channel to the south that still remains active during high water stages; (d) Fantasia island, which was accreted to the floodplain by 2006.....	37
Figura 3 - Temporal analysis of the Colombian Amazon River between July 19, 1986 and November 14, 1994. Channels, lakes in islands, islands and recent deposition contours are compared between these two dates.....	39
Figura 4 - Temporal analysis of the Colombian Amazon River between November 14, 1994 and July 20, 2001. Channels, lakes in islands, islands and recent deposition contours are compared between these two dates.....	40
Figura 5 - Temporal analysis of the Colombian Amazon River between July 20, 2001 and June 24, 2006. Channels, lakes in islands, islands and recent deposition contours are compared between these two dates. A, B, C, and D correspond to the location of Figure 6.....	42
Figura 6 - Islands with more significant plan view changes between 1986 and 2006. See Figure 5 for location. (A) Corea Island significantly increased its area in its right margin. Erosion on the right margin of Micos Island since 1994 is also observed. Corea Southeast Island was present in 1994 and 2006, however eroded by 2001, and Piraña Island was formed by 2006. (B) El Tigre Island has been considerably eroded on its upstream side with deposition along the convex side of its secondary channel. (C) Serra Island has been drastically eroded upstream. In contrast Zaragoza Island has been gaining area since 1994. (D) Aramosa Island was increased in area by only	

- 1.3%, however it can be seen how the shape of the island changed by 2006. Note that the right channel of the Amazon River upstream Aramosa Island was completely developed by 2006 in an area occupied by Aramosa Island in 1986..... 45
- Figura 7 - Morphology of the area. Terraces represent higher elevations (100 – 160 m.a.s.l) and the floodplain lower areas (80 – 100 m.a.s.l.). Note the terraces controlling the development of the floodplain and scroll bars on the right margin upstream Apicayu Island and on the left margin downstream Cacao Island. This map was generated based on interpretation of the Landsat images used in the temporal analysis and a SRTM image..... 47
- Figura 8 - Variation of monthly discharge respect to mean monthly discharge (23,817 m³ s⁻¹) for Tamshiyacu gauging station over the period 1986-2006. For each sub period of analysis normal distributions of the Q_{monthly} – Q_{mean} variation are indicated in the upper part. Results of the hydrological and temporal analyses in terms of erosion or deposition periods are indicated in the bottom for comparison. Dash lines indicate the limits of each sub period. Location of Tamshiyacu gauging station is indicated in Figure 1B..... 51
- Figura 9 - Variation of monthly discharge respect to mean monthly discharge (34,908 m³ s⁻¹) for Nazareth gauging station over the period 1986-2006. For each sub period of analysis normal distributions of the Q_{monthly} – Q_{mean} variation are indicated in the upper part. Results of the hydrological and temporal analyses in terms of erosion or deposition periods are indicated in the bottom for comparison. Dash lines indicate the limits of each sub period. Location of Nazareth gauging station is indicated in Figures 1B and 1C..... 52
- Figura 10 -Variation of monthly discharge respect to mean monthly discharge (47,100 m³ s⁻¹) for Olivença gauging station over the period 1986-2006. For each sub period of analysis normal distributions of the Q_{monthly} – Q_{mean} variation are indicated in the upper part. Results of the hydrological and temporal analyses in terms of erosion or deposition periods are indicated in the bottom. Dash lines indicate the limits of each sub period. Location of Olivença gauging station is indicated in Figure 1B 53
- 4 THE MEANDERING PATTERN OF THE AMAZON RIVER DURING THE LATE PLEISTOCENE RECENT FLUVIAL DYNAMICS OF THE COLOMBIAN AMAZON RIVER**
- Figura 1 - Location map of the Coari area A) Lithostratigraphic units in the study area and location of the stratigraphic profiles. Profiles 1 to 11 correspond to Pleistocene deposition and Profiles (a) to (g) correspond to Holocene deposits. B) Geotectonic units of the Amazon region. C) Stratigraphy of Upper Cretaceous to Quaternary sedimentary deposits in the Solimões sedimentary basin, modified from Wanderley Filho et al. (2007)..... 68

- Figura 2 - Regional geologic map. Units present in the Solimões and western Amazonas sedimentary basins, modified from Rossetti et al. (2005). Units individualized and dated by different authors in the reach of the Amazon River between Tabatinga and the mouth of the Madeira River. See Figure 1B for location..... 70
- Figura 3 - Pleistocene fluvial deposits. On the Coari area, channel and point bar deposits are more common than floodplain deposits. Location of logs indicated in Figure 1A. The depth at which the samples for OSL dating were collected is indicated in profiles 1, 3, 4, 8 and 10. Note that ages of the deposits are older in the upper part of the profiles when compared with the ages obtained in the lower parts..... 76
- Figura 4 - Holocene fluvial deposits. On the Coari area, floodplain deposits are more common than deposits associated to the channels. Location of logs indicated in Figure 1A. The depth at which a sample for OSL dating was collected is indicated in profiles (d)..... 78
- Figura 5 - The Iça Formation in the Coari area. A) Typical outcrop of the Solimões and Iça Formations in the area. The Solimões Formation has a characteristic grey colour while the Iça Formation is reddish. B) Detail of the unconformity between the Solimões and Iça Formations, note the ferruginized surface that marks the contact. C) Trough cross stratification in the Iça deposits, note the mudstone clasts in the base of each set. D) Typical mudstone clasts at the base of the point bar and channel deposits in the Iça Formation. E) Overview of the point bar, floodbasin and crevasse splay deposits in profile 3, Figure 3. At the base of these deposits the Solimões Formation outcrops..... 79
- Figura 6 - Holocene deposits in the Coari area. A) Morphology of ridge and swales characteristic of scroll bars from the main and secondary channels. B) Organic-rich beds in floodplain lake deposits. Tree trunks embedded in these deposits can be observed. This picture corresponds to Profile (g), Figure 4. C) Present-day sand bars in the Amazon River. Note the magnitude of these sand bars. At the top of these sediments, dunes are present with wavelengths up to 8.3 m and height up to 30 cm. D) Fining upward cycles from coarse to fine sand with planar cross bedding, which follow the present-day direction of the flow..... 81
- Figura 7 - Relationships of clay minerals (smectite – kaolinite ratio) and heavy minerals (unstable – stable ratio) on the deposits of the Solimões and Iça Formations in the Coari Area. In general smectite – kaolinite ratio varies from 0 to 5 with some values out of this range, see Table 3. In general S/K values are higher for the Solimões Formation than for the Iça Formation. The unstable – stable ratio of heavy minerals varies from 0 to 0.2, see Table 4. In general the u/s ratio for tends to be lower for the Solimões Formation than for the Iça Formation..... 84

- Figura 8 - Relationships of clay minerals (smectite – kaolinite ratio) and heavy minerals (unstable – stable ratio) on the Holocene deposits in the Coari Area. In general smectite – kaolinite ratio varies from 0 to 10 with some values out of this range, see Table 3. The unstable – stable ratio of heavy minerals varies from 0 to 5, see Table 4. S/K and u/s ratios are higher than the values for the Solimões and Iça Formations, see Figure 7 and Tables 3 and 4..... 85
- Figura 9 - Sea level variation in the last 140 ka. Sea level curve by Chappell et al. 1996. D1-D9 ages obtained here related to the deposits described. T1-T3 Fluvial terraces individualized by Soares (2007) in the western Amazonas sedimentary basin. Scroll bar (S) and floodplain (F) deposits in the Manaus area (Rozo et al., 2012). Ages get younger with the general sea level drop from 130 to 18 ka..... 87

LISTA DE TABELAS

2 THE ANASTOMOSING PATTERN AND THE EXTENSIVELY DISTRIBUTED SCROLL BARS IN THE MIDDLE AMAZON RIVER

Table 1 - Percent change in the plan view area of each geoform (channels and islands) in the studied reaches of the Amazon and Madeira Rivers. The values of the plan view area for each date are also indicated. Location of the islands is indicated in Figure 1C.....	14
Table 2 - Percent change in the plan view area of: each category of the pixel class-changes analysis; the river system and the system per year. The period of time over which the change occurred corresponds to 31.1 years. The values of the plan view area of each category of change are also indicated.....	15
Table 3 - Migration rates in the studied reach of the Amazon and the mouth of the Madeira River. The locations are numbered from upstream to downstream and categorized by erosion or deposition. See Figure 4 for the specific location of each site.....	16

3 RECENT FLUVIAL DYNAMICS OF THE COLOMBIAN AMAZON RIVER

Table 1 - Landsat data used in this study. Water level and time variation between image acquisition dates are also indicated. The Landsat images were obtained from: (1) http://glovis.usgs.gov/ ; (2) http://glcf.umiacs.umd.edu/index.shtml ; and (3) http://www.dgi.inpe.br/CDSR/ . Water levels were obtained from Agência Nacional de Águas in Brazil.	34
Table 2 - Percent change in the plan view area of islands, channels and recent deposition in the Colombian Amazon River. The plan view area in each date and for each island is indicated, as well as the total plan view area of islands, channels and recent deposition. Location of the islands is indicated in Figure 1C.	38
Table 3 - Percent change in the plan view area of: each category of the pixel class-changes analysis; the river system and the system per year. The time periods over which the changes occurred correspond to 8.3 years (1986-1994), 6.7 years (1994-2001), 4.9 years (2001-2006) and 19.9 years (1986-2006). The plan view area of each categories of change is also indicated.	43
Table 4 - Migration rates on the margins of the studied reach of the Amazon River. The locations are numbered from upstream to downstream and organized by maximum rates of erosion and deposition over the 1986-2006 period. See Figure 2 for the specific location of each site.	46

4 THE MEANDERING PATTERN OF THE AMAZON RIVER DURING THE LATE PLEISTOCENE RECENT FLUVIAL DYNAMICS OF THE COLOMBIAN AMAZON RIVER

Table 1 - Sedimentary lithofacies.....	77
Table 2 - Sedimentary lithofacies association.....	82
Table 3 - Smectite/kaolinite ratio obtained from X-ray diffractograms of the deposits described in the Coari area. Location of the profiles and samples are indicated in Figures 1A , 7 and 8 respectively. The relationship between the profiles and the S/K ratio is plotted in Figures 7 and 8.....	85
Table 4 - Distribution of heavy mineral assemblages in the deposits described in the Coari area. Location of the profiles and samples are indicated in Figures 1A , 7 and 8 respectively. The relationship between the profiles and the u/s ratio is plotted in Figures 7 and 8. Unstable heavy minerals include hornblende, augite, hyperstene and epidote. Stable heavy minerals include zircon, tourmaline and rutile (ZTR).....	86

SUMÁRIO

	DEDICATÓRIA	Iv
	AGRADECIMENTOS	V
	RESUMO	Vii
	ABSTRACT	Ix
	LISTA DE ILUSTRAÇÕES	Xi
	LISTA DE TABELAS	Xvii
1	CONSIDERAÇÕES INICIAS	1
1.1	INTRODUÇÃO.....	1
1.2	ÁREA DE ESTUDO.....	5
1.3	METODOLOGIA PARA O ESTUDO DOS SISTEMAS FLUVIAIS NO QUATERNÁRIO.....	6
2	THE ANASTOMOSING PATTERN AND THE EXTENSIVELY DISTRIBUTED SCROLL BARS IN THE MIDDLE AMAZON RIVER...	9
	Abstract	10
	Introduction	10
	Study area.....	11
	Geological setting	12
	Methods	13
	Results	14
	Temporal analysis.....	14
	Facies and morphostratigraphic units.....	15
	Terraced deposits.....	15
	Scroll bar deposits.....	15
	Floodplain deposits.....	18
	Channel bar deposits.....	19
	Depositional model	20
	Discussion	21
	Relatively stability of the system.....	21
	Genesis and controls of the system.....	23
	Multichannel development.....	23
	Channel migration and islands stability.....	24

	Development of the Anastomosing pattern.....	24
	Conclusions	25
	Acknowledgements.....	26
	References	26
3	RECENT FLUVIAL DYNAMICS OF THE COLOMBIAN AMAZON RIVER	28
	Abstract	28
	Introduction	29
	Study Area	31
	Materials and methods	33
	Image processing.....	34
	Editing and river dynamics quantification.....	35
	Discharge related to the erosion and deposition patterns.....	36
	Results	36
	Temporal analysis.....	36
	Channel changes between July 19, 1986 and November 14, 1994.....	36
	Channel changes between November 14, 1994 and July 20, 2001.....	40
	Channel changes between July 20, 2001 and June 24. 2006.....	41
	Channel changes between July 19, 1986 and June 24. 2006.....	42
	Migration rates of the margins of the Amazon River.....	45
	Geomorphologic units.. ..	47
	Terraces.....	47
	Scroll bars.....	48
	Floodplain.....	49
	Channel bars.....	49
	Discharge related to erosion and deposition periods.....	49
	Discussion	54
	Fluvial dynamics of the Colombian Amazon River.....	54
	Discharge related to erosion and deposition periods.....	57
	Implication of channel pattern classification.....	59
	Conclusions	60
	Acknowledgements.....	61
	References	62

4	THE MEANDERING PATTERN OF THE AMAZON RIVER DURING THE LATE PLEISTOCENE.....	65
	Abstract.....	65
	Introduction.....	66
	Study area.....	68
	Geological setting.....	69
	Methods.....	71
	Results.....	73
	Lithofacies and depositional processes.....	73
	Pleistocene lithofacies.....	73
	Holocene lithofacies.....	75
	Lithofacies Association.....	77
	Pleistocene lithofacies association.....	77
	Holocene lithofacies association.....	80
	Clay and heavy minerals.....	83
	Discussion.....	87
	The age of the Iça Formation.....	87
	Environmental conditions during the Quaternary.....	89
	Quaternary fluvial characteristics of the Amazon River.....	92
	Conclusions.....	94
	Acknowledgements.....	95
	References.....	95
	REFERÊNCIAS.....	100

1 CONSIDERAÇÕES INICIAIS

1.1 INTRODUÇÃO

Grandes rios são definidos em termos de sua bacia de drenagem, largura, volume de sedimentos transportados e vazão (Potter 1978). Dependendo do critério utilizado existem diferentes classificações destes sistemas fluviais (Inman & Nordstro 1971; Potter 1978; Meade 1996; Gupta 2007). Assim, depender somente de um critério para classificar sistemas fluviais grandes pode ser problemático, uma vez que não existe uma definição exata de quando considerar um sistema fluvial como grande. Apesar da dificuldade na definição de critérios para classificar grandes rios (Inman & Nordstro 1971; Potter 1978; Meade 1996; Gupta 2007), está classicamente estabelecido que estes rios são os maiores transportadores de sedimentos dos continentes para os oceanos. Syvitski *et al.* (2005) tem estimado que aproximadamente 21Gt/ano de sedimentos são transportados por grandes rios para as bacias oceânicas, com maior parte da carga de sedimentos carregada em suspensão. O transporte destas quantidades de sedimentos também está associado com a diversidade de paisagens e fácies fluviais por onde os rios fluem. Grandes rios são caracterizados por amplas planícies de inundação onde sedimentos são temporariamente depositados e remobilizados ao longo do tempo. Estas zonas são caracterizadas pela presença de diferentes padrões de canal, desde meandros de um único canal, até trechos anastomosados.

O Rio Amazonas é o maior sistema fluvial do mundo em termos de descarga média anual ($175.000 \text{ m}^3 \text{ s}^{-1}$) e área de drenagem (691.5000 km^2) (Wohl 2007). Recentemente, a descarga média anual tem sido estimada em $209.000 \text{ m}^3 \text{ s}^{-1}$ (Latrubesse, 2008) e a descarga média anual de sedimentos em 754 Mt/ano (Martinez *et al.*, 2009). O rio tem mais de 6000 km de largura e drenagem transcontinental desde os Andes no Peru até o Oceano Atlântico no Brasil (Figura 1A). No Peru, o rio é conhecido como o Amazonas à jusante da confluência dos rios Marañon e Ucayali (Figura 1B). Na Colômbia, o rio percorre menos de 100 km, e é também conhecido com o Amazonas. No território Brasileiro o rio é denominado Solimões, e o nome Amazonas é somente usado à jusante da confluência com o rio Negro em Manaus (Figura 1B). Neste trabalho, o nome Amazonas é usado em referência a todo o sistema fluvial.

O Rio Amazonas segue um padrão geral de incremento na estabilidade entre os rios Içá e Madeira (Figura 1B) (Mertes *et al.*, 1996). A estabilidade do rio foi avaliada a partir de imagens de satélite, com base na percentagem de mudança da área superficial por ano com valores entre 2%/ano na confluência com o rio Jutai e 0.2 % ao ano na confluência com o Rio Negro (Mertes *et al.*, 1996). Recentemente foram obtidas percentagens de mudança na área superficial no Rio Amazonas de 1.8%/ano na confluência com o Rio Japurá (Peixoto *et al.*,

2009) e 0.7 %/ano entre as confluências dos rios Negro e Madeira (Rozo 2004). Estes valores seguem um padrão geral de incremento na estabilidade obtido por Mertes *et al.* (1996). Entretanto, variações entre estes valores estão relacionadas ao uso de ferramentas de sensoriamento remoto mais acuradas, além de escalas temporais mais amplas (por. exe. Rozo 2004; Peixoto *et al.*, 2009). Estimativas sobre as taxas máximas de migração em diferentes trechos do Rio Amazonas sugerem um padrão similar de incremento na estabilidade de montante à jusante. Taxas de migração de 400 m/ano (Kalliola *et al.*, 1992) e 213 m/ ano (Rozo & Soto 2010) tem sido reportadas no alto Amazonas na área de Iquitos (Peru) e nas proximidades de Leticia (Colômbia) respectivamente (Figura 1B). No Brasil, taxas de 140 m/ano (Mertes *et al.*, 1996) e 42 m/ano (Rozo 2004) tem sido apresentadas para os trechos próximos a Fonte Boa e Manaus, respectivamente (Figura 1B).

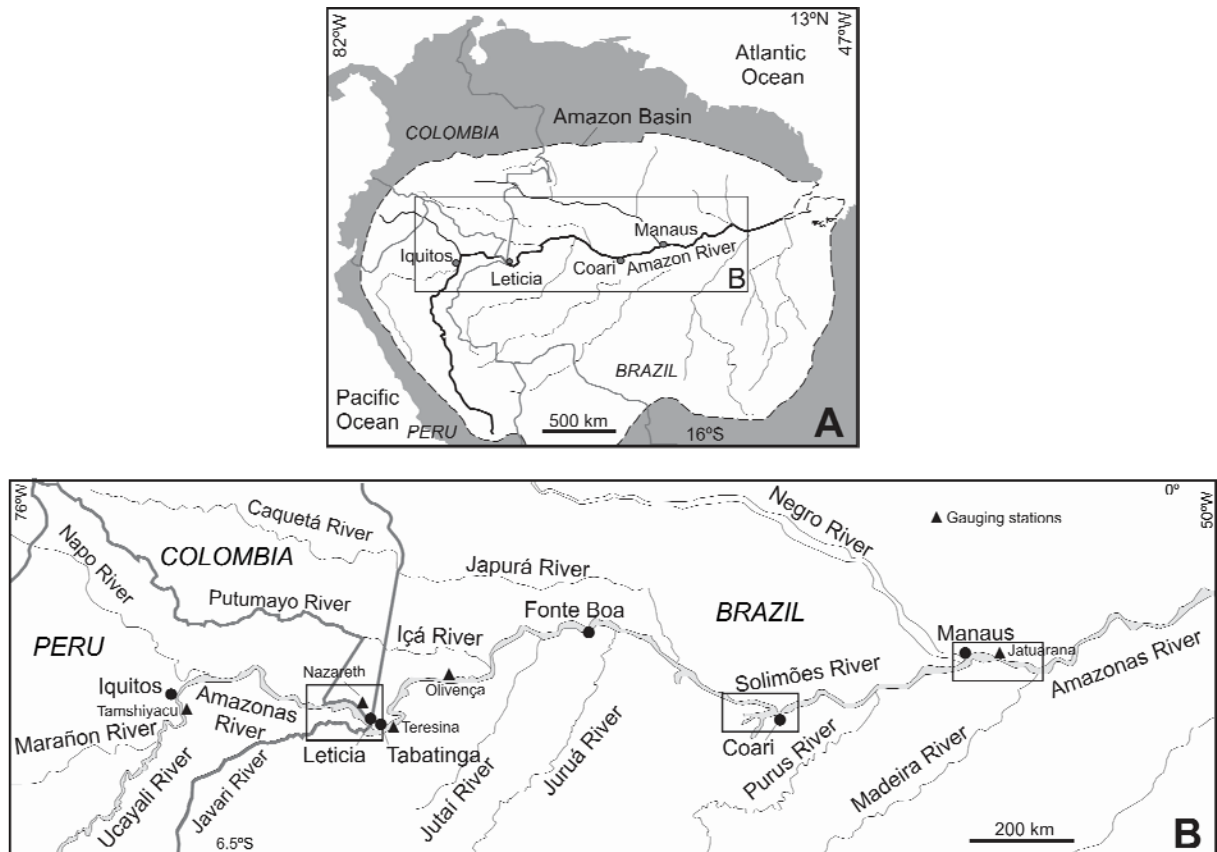


Figura 1. Mapa de localização do Rio Amazonas. A) Bacia Amazônica. B) Rio Amazonas entre Iquitos, Peru e Manaus, Brasil. Áreas estudadas são indicadas nos retângulos de montante a jusante como segue: Rio Amazonas na Colômbia a montante do Rio Javari, na área de Leticia; Rio Amazonas na área de Coari e nas confluências dos rios Negro e Madeira.

As estimativas da percentagem de mudança na área superficial por ano e as taxas de migração são concordantes com as classificações do padrão de canal de diferentes trechos do Rio Amazonas. Kalliola *et al.* (1992) descreve alguns trechos no Peru com um padrão predominantemente meandrante com alguns trechos retilíneos. Baker (1978) demonstrou que o Rio Solimões possui trechos com padrões meandrantés e anastomosados. Um padrão predominantemente anastomosado tem sido descrito para o Rio Amazonas no Brasil (Mertes *et al.*, 1996; Latrubesse & Franzinelli 2002; Rozo 2004). Este padrão fluvial foi identificado com base nos seus múltiplos canais e estabilidade relativa. Ilhas com morfologia tipo *saucer-like*, devido a depósitos de dique marginal que as delimitam, foram primeiramente descritas no Rio Amazonas por Sternberg (1959) e Baker (1978). Mas estes tipos de ilhas não foram discutidos em classificações posteriores do padrão anastomosado no Rio Amazonas. A morfologia tipo *saucer-like* corresponde à descrição de *floodbasins* de Makaske (2001), que representam uma característica fundamental na distinção do padrão anastomosado de outros rios com múltiplos canais.

Latrubesse (2008) descreveu todo o Rio Amazonas como *anabranching*. O termo *anabranching* é aplicado para qualquer tipo de rio com múltiplos canais, enquanto que o anastomosado é um tipo de *anabranching* de baixa energia, com planícies coesivas, ricas em matéria orgânica (Nanson & Knighton 1996). Com base nas informações disponíveis por sensoriamento remoto e descrições de campo ao longo do Rio Amazonas (Sternberg 1959; Baker 1978; Latrubesse & Franzinelli 2002; Rozo 2004; Latrubesse 2008), a porção brasileira deste rio é anastomosado como indicado por Makaske (2001), e também é *anabranching sensu* (Nanson & Knighton 1996).

Características meandrantés na forma de barras em crescente têm sido identificadas em diferentes trechos do Rio Amazonas (Sternberg 1959; Baker 1978; Mertes *et al.*, 1996; Latrubesse & Franzinelli 2002; Rozo 2004; Soares 2007). Estas características meandrantés motivaram Baker (1978) a considerar o rio como anastomosado e meandrante. Rozo (2004) sugeriu que o rio evoluiu de um padrão meandrante de um único canal para um sistema anastomosado com trechos meandrantés durante o Holoceno.

Barras em crescente e lagos de meandro abandonado são consideradas raras ou ausentes em sistemas anastomosados, e sua ausência é sugerida como característica fundamental destes tipos de rios (Smith 1983; Nanson & Croke 1992). No entanto, a presença de canais com migração lateral e desenvolvimento de barras em crescente foi notada em rios anastomosados por vários autores (Bowler *et al.*, 1978; Taylor & Woodyer 1978; Brizga & Finlayson 1990; Nanson & Knighton 1996). Além disso, Makaske (2001) indica que as barras

em crescente não são uma característica dos rios anastomosados, mas elas podem estar presentes. Desta forma, o Rio Amazonas com características meandantes é diferente de muitos outros rios anastomosados (por. ex. Makaske 1998, 2001) que possuem estabilidade lateral e ausência de canais meandantes.

A limitada informação do Rio Amazonas principalmente obtida a partir de sensoriamento remoto (Sternberg 1950, 1959; Baker 1978; Iriondo 1982; Mertes *et al.*, 1996; Latrubesse & Franzinelli 2002; Rozo 2004; Latrubesse 2008) e a falta de dados de campo dificulta o entendimento das características deste sistema fluvial, estabelecimento de uma relação clara entre as características meandantes e anastomosadas, além da determinação da extensão no tempo e espaço do desenvolvimento do padrão anastomosado. Esta falta de informação ainda é maior quando consideramos características morfológicas e hidrológicas pré-terciárias do Rio Amazonas. Informações sobre o padrão de canal do Rio Amazonas durante o Pleistoceno são raras, com poucos trabalhos que sugerem um padrão meandrante de um único canal durante esta época (Soares 2007; Motta 2008). Diferentemente, uma ampla discussão sobre a origem do Rio Amazonas com um sistema transcontinental com fluxo para o leste tem sido desenvolvida nos últimos anos (Hoorn *et al.*, 1995; Rossetti *et al.*, 2005; Campbell *et al.*, 2006; Latrubesse *et al.*, 2007; Figueiredo *et al.*, 2009; Hoorn *et al.*, 2010; Latrubesse *et al.*, 2010; Wilkinson *et al.*, 2010). A falta de consenso do tempo exato que este evento ocorreu e a falta de dados sedimentológicos da Amazonia central somente aumentam esta discussão. Assim, o desenvolvimento do Rio Amazonas como é atualmente conhecido pode ter ocorrido em algum momento entre o final do Mioceno e o final do Pleistoceno.

Estudos sistemáticos são necessários para o entendimento: 1) da origem do sistema anastomosado do Rio Amazonas e o desenvolvimento de suas características meandantes; 2) do compartimento do alto Amazonas em comparação com o padrão principalmente anastomosado do Rio Amazonas no Brasil; 3) das características do Rio Amazonas durante o Pleistoceno e as diferenças das condições atuais.

Com estes propósitos, três áreas foram selecionadas ao longo do Rio Amazonas, com uma distância geográfica considerável entre elas e um intervalo em tempo desde o Pleistoceno ao recente. A primeira área corresponde ao Rio Amazonas entre as confluências dos rios Negro e Madeira (Figura 1B). A segunda área corresponde ao Rio Amazonas na Colômbia. (Figura 1B). Este trecho é localizado a montante da fronteira Brasileira com a Colômbia. O terceiro trecho corresponde ao Rio Amazonas (rio Solimões no Brasil) na região de Coari (Figura 1B). Esta última área foi selecionada devido aos melhores afloramentos da Formação Iça do Pleistoceno (Caputo, 1984; Rossetti *et al.*, 2005).

1.2 ÁREA DE ESTUDO

A terminologia inclui os termos várzea para se referir a planície de inundação da Amazonia (Moura 1944), paraná e furo (Andrade 1956) para descrever canais secundários. Um paraná é um canal secundário que liga um rio a ele mesmo, dentro da planície de inundação ou com pelo menos uma das margens na planície de inundação. Um furo é um canal secundário que liga um rio a outro, um rio a um lago ou um rio a ele mesmo, neste último caso, fora da planície de inundação. Um pulso de inundação sazonal controla a dinâmica da água no rio Amazonas, com um nível mais alto no mês de junho e um período de águas baixas em dezembro (Junk *et al.*, 1989). A precipitação é responsável pela amplitude meia das flutuações dos níveis do rio, que na Amazônia central podem chegar até 10 m (Irion *et al.*, 1997).

O trecho do médio Amazonas estudado aqui é localizado à jusante de Manaus, entre as confluências dos rios Negro e Madeira (Figura 1B). Neste trecho, o Rio Amazonas é um sistema de múltiplos canais com uma aparência geral anastomosada com canais secundários que exibem um padrão meandrante. Os canais são retos a sinuosos, com sinuosidade entre 1.07 e 1.24 no canal principal e entre 1.03 e 1.52 nos canais secundários. A largura do rio varia de 7.2 a 19.5 km, com variação no canal principal entre 1.6 e 6.5 km. Em Jatuarana (30 km à jusante de Manaus, Figura 1B) a vazão média anual é de $123680 \text{ m}^3 \text{ s}^{-1}$ e o rio tem um gradiente de 2.1 cm km^{-1} (Latrubesse 2008). Ao longo do sistema fluvial, a altura das ilhas corresponde em termos gerais com a altura da planície de inundação. As margens do canal são ingrimes e são localmente caracterizadas por terras caídas e profundidade da lâmina da água de até 9 m.

O trecho do alto Amazonas é localizado a montante da confluência com o Rio Javari, que corresponde ao Rio Amazonas na Colômbia (Figura 1B). Esta área de estudo inclui um trecho do Rio Amazonas no Peru, como também um trecho à jusante no Brasil, onde estão localizadas as cidades de Tabatinga e Benjamin Constant. Neste trecho, o Rio Amazonas é um sistema de múltiplos canais onde o canal principal e os canais secundários apresentam um padrão meandrante. Os canais são estreitos e sinuosos, com sinuosidade entre 1.02 e 1.72 no canal principal e entre 1.03 e 3.08 nos canais secundários. A largura do rio varia entre 1 e 12 km, com variação no canal principal entre 1 e 4.4 km. Em Nazareth (Figura 1B) a vazão média anual é de $34.757 \text{ m}^3 \text{ s}^{-1}$. O gradiente do rio em Teresina (22 km à jusante desta área, Figura 1B) é 3.8 cm km^{-1} diminuindo para 3.4 cm km^{-1} na confluência com o Rio Iça (Rio

Putumayo na Colômbia) e o tamanho de grão da carga de fundo é areia média com $D_{50} = 0.3\text{mm}$ (Latrubesse 2008).

A terceira área de estudo corresponde ao Rio Amazonas na área de Coari (Figura 1B). Neste trecho, o Rio Amazonas (Rio Solimões no Brasil) é um sistema de múltiplos canais com uma aparência geral meandrante. A planície de inundação atual do Rio Amazonas é extensamente distribuída na margem esquerda. Na margem direita do canal, falésias íngremes onde afloram depósitos mais antigos são localmente caracterizadas por terras caídas e uma profundidade da lâmina da água de até 24 m.

1.3 METODOLOGIA PARA O ESTUDO DOS SISTEMAS FLUVIAIS NO QUATERNÁRIO

O enfoque metodológico de cada uma das áreas de estudo foi diferenciado. No trecho do Rio Amazonas entre as confluências dos rios Negro e Madeira e na área de Coari, um trabalho de campo foi desenvolvido, enquanto que o trecho do Rio Amazonas na Colômbia foi estudado através de sensoriamento remoto considerando a distância com as outras duas áreas. O trabalho de campo foi realizado ao longo do Rio Amazonas entre as confluências dos rios Negro e Madeira e na área de Coari durante o período de águas baixas (Outubro-Novembro). Terraços e cortes fluviais recentes foram descritos com base em análises sedimentológicas e fácias. Amostras para análise granulométrica foram coletadas para auxiliar nas descrições sedimentológicas. Amostras para datação por luminescência opticamente estimulada (LOE) também foram coletadas. As datações por LOE foram realizadas segundo os protocolos de regeneração de alíquotas simples (RAS) e múltiplas (RAM). Considerando que a área do Rio Amazonas entre as confluências dos rios Negro e Madeira foi direcionada para a descrição da deposição recente (Holoceno) uma vez que depósitos do Pleistoceno não afloram na área, os depósitos sedimentares foram descritos com o uso da morfoestratigrafia, que permitiu a individualização precisa das unidades.

Diferente da área entre as confluências dos rios Negro e Madeira, a área de Coari que foi selecionada para estudar a deposição no Pleistoceno, a morfoestratigrafia não foi utilizada e a descrição dos depósitos foi feita com base na análise de fácies. A deposição recente em Coari foi descrita da mesma forma que os depósitos do Pleistoceno, no entanto as características morfológicas foram avaliadas com um grau menor de detalhamento. Considerando que na área de Coari os depósitos mais antigos do Quaternário foram descritos em contraste com a área de Manaus, e também devido ao fato de não existir morfologia fluvial atual para relacionar cada um dos depósitos descritos, amostras foram coletadas para

análise de minerais pesados e argilominerais. Os resultados destas análises permitiram a descrição dos depósitos sedimentares e discussões das condições durante a deposição. A fração argila ($< 2 \mu\text{m}$) foi separada por sedimentação e centrifugação e colocada em lâminas de vidro. Dados de difração de raios X (DRX) foram obtidos em três lâminas orientadas (normal, glicolada e aquecida à 550°C). Proporções relativas de argilominerais (esmectita e caulinita) foram estimadas com base nas intensidades relativas dos picos. Minerais pesados na fração 63 a $125 \mu\text{m}$ foram separados de minerais leves por gravidade com o uso de bromofórmio. Lâminas de vidro com os minerais pesados foram preparadas para a identificação no microscópio. Trezentos minerais foram contados em cada lâmina, excluindo os minerais opacos. A somatória do número de minerais de hornblenda, augita, hiperstenio e epidoto dividida pela somatória dos minerais de zircão, turmalina e rútilo (ZTR) determinou a relação instáveis/estáveis.

A análise temporal foi feita nas áreas onde a morfologia fluvial foi estudada, estas áreas incluem os trechos do rio à jusante de Manaus e o Amazonas Colombiano. Nas duas áreas, imagens Landsat foram selecionadas com base nas variações mínimas do nível da água entre as datas em que as imagens foram coletadas. Na área de Manaus duas imagens foram selecionadas cobrindo um período de 31.1 anos, o período máximo coberto entre as imagens Landsat disponíveis, de 16 de Julho de 1978 a 18 de Agosto de 2009. Em contraste, no Rio Amazonas na Colômbia 44 imagens foram inicialmente selecionadas, e depois da análise de variação do nível da água na data em que cada imagem foi coletada quatro imagens foram selecionadas. O máximo período coberto foi de cerca de 20 anos entre a primeira e a última imagem desde 19 Julho de 1986 à 24 de Junho de 2006. As outras duas imagens foram selecionadas serviram para documentar o comportamento do sistema fluvial, estas imagens correspondem à 14 de Novembro de 1994 e 20 de Julho de 2001.

No Rio Amazonas à jusante de Manaus, as imagens Landsat foram georreferenciadas com um erro máximo de dois pixels. Adicionalmente, a imagem mais antiga foi reamostrada para a mesma resolução espacial da imagem mais recente, 30 m. No Amazonas Colombiano as imagens já estavam georreferenciadas com um erro máximo de 1.7 pixels. Segmentação e classificação foram aplicadas durante o processamento das imagens no programa SPRING (versão 5.0.6). Com o processamento digital das imagens, os contornos do sistema fluvial foram obtidos. Correções manuais foram feitas para eliminar áreas de nuvens e sombras no programa *ArcMap*, e também para corrigir erros durante o processo de classificação. Posteriormente, a área superficial do canal, ilhas e outras características fluviais foram calculadas. Além disso, uma análise de classes pixel à pixel foi feita em cada período

analisado. Consequentemente, a área de cada categoria de mudança foi calculada e a porcentagem de mudança na área superficial do sistema fluvial por ano foi obtida. Taxas de migração em metros por ano foram calculadas nos locais onde o rio apresenta tendência maior à erosão ou deposição.

No Rio Amazonas na Colômbia uma análise hidrológica foi desenvolvida. Esta análise foi baseada em dados de descarga disponíveis nas estações hidrológicas de Tamshiyacu (Peru), Nazareth (Colômbia) e Olivença (Brasil) (Figura 1B) para analisar as relações entre os padrões de descarga e o resultado da análise temporal. A geomorfologia nesta área foi avaliada com base em imagens Landsat e SRTM (Shuttle Radar Topographic Mission).

2 THE ANASTOMOSING PATTERN AND THE EXTENSIVELY DISTRIBUTED SCROLL BARS IN THE MIDDLE AMAZON RIVER *

Max G. Rozo¹, Afonso C. R. Nogueira¹, Werner Truckenbrodt¹

¹ *Instituto de Geociências, Universidade Federal do Pará, CP 1611, 66.075-900, Belém/PA, Brasil*

* Accepted for publication in Earth Surface Processes and Landforms

The anastomosing pattern and the extensively distributed scroll bars in the middle Amazon River

Max G. Rozo,* Afonso C. R. Nogueira and Werner Truckenbrodt

Instituto de Geociências, Universidade Federal do Pará, CP 1611, 66.075-900, Belém, PA Brazil

Received 18 January 2011; Revised 20 March 2012; Accepted 22 March 2012

*Correspondence to: M. G. Rozo, Instituto de Geociências, Universidade Federal do Pará, CP 1611, 66.075-900, Belém, PA, Brazil. E-mail: rozo@ufpa.br

ESPL

Earth Surface Processes and Landforms

ABSTRACT: The middle Amazon River, between the confluences of the Negro and Madeira Rivers in Brazil, shows an anastomosing morphology with relatively stable, multiple interconnected channels that locally enclose floodbasins. Additionally, this system is characterized by sinuous secondary channels with meander development, discontinuous natural levees concentrated on the concave banks and extensively distributed scroll bars mainly in the islands, related to subrecent and present-day migration of mainly secondary channels. This distinguishes the Amazon from many other anastomosing rivers that have laterally stable, non-meandering channels. We analyzed sedimentary processes using field data, morphology and channel changes through a temporal analysis using remote sensing data and obtained optically stimulated luminescence (OSL) dating to understand the genesis of this large anastomosing river and the development of its meandering secondary channels. Scroll bars have developed in a multichannel river system at least since 7.5 ± 0.85 ka. Avulsion is inferred to have played a minor role in the formation of this anastomosing system, with only one documented case while mid-channel bar formation and chute cut-offs of the main and secondary channels are the main formative mechanisms of anastomosis in this system. Differences in resistance to erosion control the relatively straight main channel and allow secondary channels to develop a meandering platform. Vegetation contributes to the relative stability of islands and the floodplain. Low gradient and high average aggradation rate (1.1 mm yr^{-1}) are conditions which favor the development of anastomosis. Additionally, stable external conditions, low abandonment rate of older channels and independence from high avulsion frequency suggest a long-lived, semi-static type of anastomosing river in this reach of the Amazon. Copyright © 2012 John Wiley & Sons, Ltd.

KEYWORDS: anastomosing pattern; Amazon River; scroll bars; channel changes

Introduction

The Amazon River is characterized by multiple interconnected channels with relatively stable, vegetated islands. Islands with saucer-like morphology due to bounded natural levees were earlier described in the Amazon by Sternberg (1959) and Baker (1978). The saucer-like morphology corresponds to the description of floodbasins by Makaske (2001), and these represent a key characteristic for distinguishing anastomosing from other multiple channel rivers. Subsequent studies of the different reaches of the Brazilian Amazon, although not discussing saucer-like morphology, have documented it as a predominantly anastomosing river (Mertes *et al.*, 1996; Latrubesse and Franzinelli, 2002; Rozo, 2004). The Amazon River has also been described as predominantly anabranching (Latrubesse, 2008). The term anabranching is applied to any type of multiple channel pattern, whereas anastomosing rivers are a low-energy type with cohesive or organic-rich floodplains (Nanson and Knighton, 1996). From the available remote sensing data and field descriptions of the Amazon (Sternberg, 1959; Baker, 1978; Latrubesse and Franzinelli, 2002; Rozo, 2004; Latrubesse, 2008) it is clear that the Amazon is anastomosing as understood by Makaske (2001) and it is also anabranching *sensu* Nanson and Knighton (1996).

Meandering characteristics, mainly scroll bar patterns and meandering secondary channels, have been recognized in

different reaches of the Amazon River (Sternberg, 1959; Baker, 1978; Kalliola *et al.*, 1992; Mertes *et al.*, 1996; Latrubesse and Franzinelli, 2002; Rozo, 2004; Soares *et al.*, 2010). These meandering features led Baker (1978) to consider the river as having both anastomosing and meandering patterns. Rozo (2004) stated that the river evolved from a single-channel meandering into an anastomosing system with meandering branches. It was also suggested that the river had a mainly meandering pattern during the Late Pleistocene (Soares *et al.*, 2010).

Scroll bar deposits and oxbow lakes have been considered rare or absent in anastomosing rivers, and their absence has also been considered to be a fundamental characteristic of this type of river (Smith, 1983; Nanson and Croke, 1992). However, the presence of laterally migrating channels with the development of scroll morphology has been noted in anastomosing rivers by several authors (Bowler *et al.*, 1978; Taylor and Woodyer, 1978; Brizga and Finlayson, 1990; Nanson and Knighton, 1996). Also, Makaske (2001) indicates that scroll deposits are not a characteristic feature in anastomosing river floodplains, but they may be present. In this context, it is clear that the Amazon, with its meandering secondary channels, is different from many other anastomosing rivers (Makaske, 1998, 2001) that have laterally stable, non-meandering channels.

However, the limited information on the Amazon River provided mainly by remote sensing data (Sternberg, 1950, 1959; Baker, 1978; Iriondo, 1982; Mertes *et al.*, 1996; Latrubesse and

Franzinelli, 2002; Rozo, 2004; Latrubesse, 2008) and the lack of field data make it difficult to understand the characteristics of this fluvial system, to establish a clear relationship between the meandering and anastomosing features and also to compare it with similar rivers that have been studied more extensively. These specifically include anastomosing rivers with depositional models described in temperate humid, montane settings (Smith and Smith, 1980; Smith, 1983; Makaske, 1998) and semi-arid climatic settings (Makaske, 1998).

To our knowledge, no research has yet been undertaken to understand the origin of the Amazon's anastomosing pattern and the development of its meandering secondary channels. Mertes *et al.* (1996) suggested that, at a regional scale, subsidence of the Amazonian sedimentary basins or current uplift of the structural arches that delimit these basins exerts a primary control over the development of the system. The river is confined and stable where it passes through the structural arches and on the downstream side of the arches there is a gradual widening of the river valley and the channels become more active. Abandoned channel belts, which are supposed to be the products of avulsion, were identified in the Upper Amazon River (Dumont and Garcia, 1991; Pärssinen *et al.*, 1996) and in the Solimões River (Mertes *et al.*, 1996; Latrubesse and Franzinelli, 2002). However, avulsions related to the development of the multiple channel pattern in the Amazon River have not been described. Sternberg (1959) discusses the possibility that the Amazon River, downstream of Manaus, will occupy the Careiro Paraná (a secondary channel) over time (Figure 1(C)), leading to a multiple channel pattern. However, the lack of accurate data does not allow conclusions to be drawn about the evolution of this secondary channel.

In this study, the geomorphologic and sedimentologic characteristics of the Amazon River between the confluences of the Negro and Madeira Rivers (Figure 1(C)), are examined to understand the genesis and mechanisms controlling the development of this large anastomosing river, with special attention given to the less common aspect of individual

meandering channels. A temporal analysis between 1978 and 2009 is presented to quantify and monitor fluvial changes and river migration. Also, a preliminary depositional model of the system is presented and compared with models of other anastomosing rivers with laterally stable and non-meandering secondary channels.

Study area

The Amazon River is the largest river in the world in terms of annual discharge ($175\,000\text{ m}^3\text{ s}^{-1}$) and drainage area ($6\,915\,000\text{ km}^2$) (Wohl, 2007). It is more than 6000 km long and runs from the Andes in Peru to the Atlantic Ocean in Brazil (Figure 1(A)). In Peru, the river is known as the Amazonas below the junction of the Marañón and Ucayali Rivers (Figure 1(B)). In Colombia, the river runs for no more than 100 km and it is also known as the Amazonas. After entering Brazil the river is denominated Solimões and the name Amazonas is not used until the junction with the Negro River at Manaus (Figure 1(B)). Here we refer to the Amazon as the entire fluvial system. Local terminology includes the terms 'várzea' to refer to the floodplain (Moura, 1944) and 'paraná' and 'furo' (Andrade, 1956) to describe secondary channels. A paraná is a secondary channel that connects a river to itself, inside the floodplain or with at least one of its margins on the floodplain. A furo is a secondary channel that connects a river to another river or a river to a lake. A furo can also connect a river to itself, but in this case, it has to run outside of the floodplain, on the bedrock. Otherwise it is termed paraná.

The reach of the middle Amazon River studied here is located downstream of Manaus, between the confluences of the Negro and Madeira Rivers (Figure 1(B) and 1(C)). In this reach, the Amazon is a multichannel system with an overall anastomosing appearance and with secondary channels exhibiting a meandering planform (Figure 1(C)). The channels are straight and

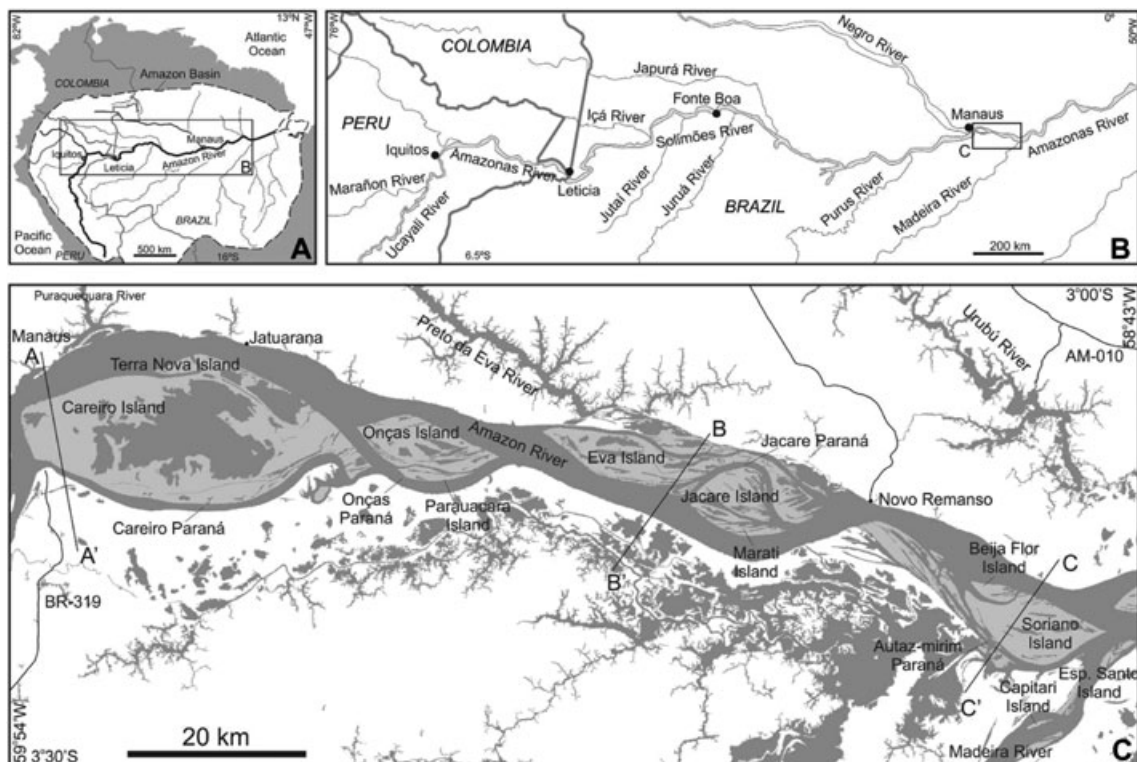


Figure 1. Location map of the middle Amazon River. (A) Amazon Basin. (B) Regional map of the Amazon River between Iquitos, Peru and Manaus, Brazil. (C) Main localities, rivers, islands and paranás (secondary channels) in the Amazon River between Manaus and the junction with the Madeira River. Topographic profiles in Figure 2(A) are indicated here.

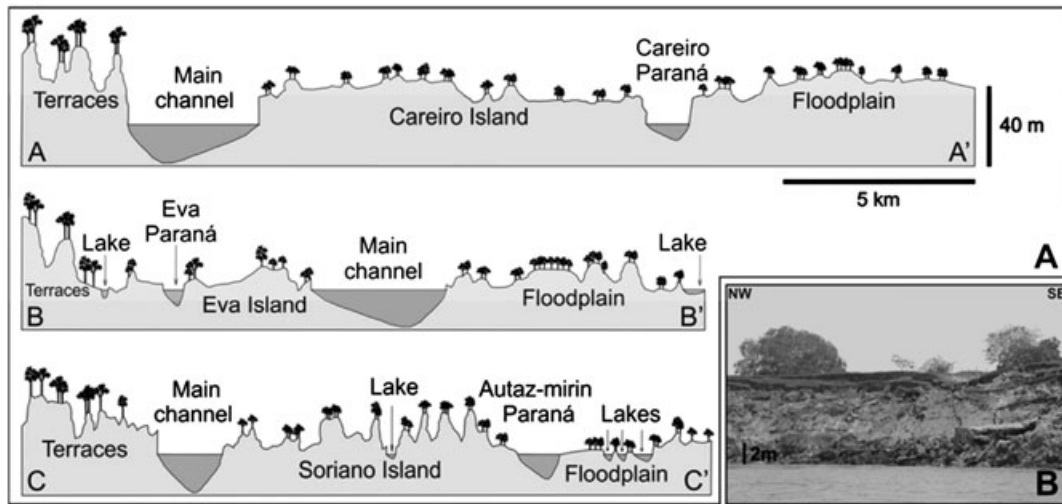


Figure 2. Topographic characteristics of the Amazon River between Manaus and the junction with the Madeira River. (A) The island's height roughly corresponds to that of the adjacent floodplain. Note the elevation of the terraces compared with the floodplain. See Figure 1(C) for the location of the topographic profiles. (B) Steepsided channel margin on Careiro Island, locally characterized by displaced blocks ('terra caída') and great water depth near the bank.

sinuous, with sinuosity varying from 1.07 to 1.24 in the main channel and from 1.03 to 1.52 in secondary channels. The width of the river varies from 7.2 to 19.5 km, with variation in the main channel from 1.6 to 6.5 km. At Jatuarana (30 km downstream of Manaus, see Figure 1(C)) the mean annual discharge is $123\ 680\ \text{m}^3\ \text{s}^{-1}$ and the river has a water surface slope of $2.1\ \text{cm}\ \text{km}^{-1}$ (Latrubesse, 2008). Along this system, the height of islands roughly corresponds to that of the adjacent floodplain (Figure 2(A)). Steep-sided channel margins are locally characterized by slump blocks ('terra caída') and great water-depths, up to 9 m near the bank (Figure 2(B)).

A seasonal flood pulse controls water dynamics of the Amazon, with a high level by June and low water stage around December (Junk *et al.*, 1989). Precipitation is responsible for the mean amplitude of the annual water-level fluctuations which, in the central Amazon region, can reach 10 m (Irion *et al.*, 1997).

Geological setting

The Amazon River system developed on an extensive intracratonic depression located between the Guyana Shield in the north and the Central-Brazilian Shield in the south. This depression is subdivided into the Acre, Solimões, Amazonas and Marajó basins, which are separated from one another by the Iquitos, Purus and Gurupá arcs, respectively (Caputo, 1984) (Figure 3(A)). The terraces of the Amazon River are called 'terras firmes' and in the western part of the Amazonas Basin are formed by fine to coarse-grained siliciclastic deposits of the Upper Cretaceous Alter do Chão Formation (Kristler, 1954; Caputo *et al.*, 1972), the Neogene Novo Remanso Formation (Rozo *et al.*, 2005b) as well as by Pleistocene sediments (Figure 3(B)). Cunha *et al.* (2007) suggested that the Solimões Formation is present in the western Amazonas Basin (Figure 3(B)), however this Neogene unit does not outcrop in the study area. The active Holocene floodplains, or várzeas of the Amazon between the confluences of the Negro and Madeira Rivers are inset into these terraces.

The Quaternary fluvial sediments have been divided by Araujo *et al.* (1974) into ancient and recent deposits, the former constituting terraces unconformably overlying Neogene and Cretaceous formations which outcrop in the area, whereas the recent alluvial sediments flank the present rivers. Mertes *et al.*

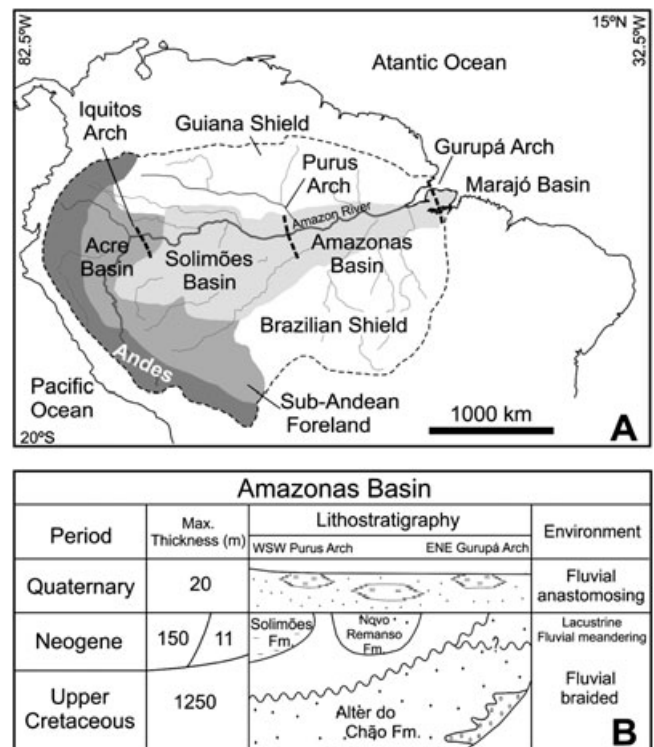


Figure 3. Geological setting. (A) Geotectonic units of the Amazon region. (B) Stratigraphy of Upper Cretaceous to Quaternary sedimentary deposits in the Amazonas Basin, modified from Cunha *et al.* (2007).

(1996) recognized two different geomorphological units flanking the Amazon River, a scroll bar floodplain and a mixed floodplain. The mixed floodplain is equally formed by scroll bars and rounded lakes. Latrubesse and Franzinelli (2002), analyzing the geomorphology of the lower Solimões River, recognized three different Quaternary units: (1) Late Pleistocene scroll bar deposits; (2) a poorly drained 'impeded floodplain' unit characterized by rounded and irregular lakes; and (3) a present-day channel-dominated floodplain where sand bars, levees and scroll bars are being developed. Recently, the Quaternary deposits in the Solimões Basin have been divided based on radiocarbon dates into two Late Pleistocene units: deposits Q1 (43.7–37.4 ka BP) and deposits Q2 (~27.2 ka

BP); and two Holocene units: deposits Q3 (6.73 to 2.48 ka BP) and deposits Q4 (0.24 to 0.13 ka BP) (Rossetti *et al.*, 2005).

Major morphological features and drainage patterns interpreted mainly using remote sensing have demonstrated the influence of intraplate tectonics taking place since the Miocene, the partial link to the Andean Orogeny and reactivation of Precambrian and Phanerozoic structures (Bemerguy *et al.*, 2002). Large strike-slip and extensional movements taking place in the Late Pleistocene to Holocene are suggested to have strongly influenced the current fluvial landscape (Costa *et al.*, 2001; Bemerguy *et al.*, 2002). Proposed evidence for this tectonic influence include: (a) drainage with extensive straight segments, as in the case of the lower courses of the Negro, Preto da Eva and Urubú Rivers, which run parallel to NW-trending normal faults, and alternate grabens and horsts (Sternberg, 1950; Franzinelli and Igreja, 2002; Latrubesse and Franzinelli, 2002); (b) large paleochannel areas and abandoned meanders in the floodplain due to preferential migration related to tilted blocks (Costa *et al.*, 2001; Bemerguy *et al.*, 2002); and (c) damming of lower river courses, which formed lakes associated with tilted blocks and displacement along strike-slip and normal faults (Dumont, 1993).

Methods

Field work was carried out along the Amazon River between Careiro Island and the mouth of the Madeira River in 2003 and 2009 (Figure 1(C)), during the low water season (October – November). Terraces and recent cutbank exposures were described using standard sedimentological and facies analysis that generated stratigraphic profiles for 25 locations (Figures 6(A) and 7). Samples for grain size analysis to support sedimentological descriptions were taken in profiles 12, 18, 23 and 25 as indicated in Figures 6(A) and 7. Samples were also taken in five sand bars (Figure 6(A)).

Five optically stimulated luminescence (OSL) dates were determined at the Laboratory of Glasses and Dating of the Faculty of Technology of São Paulo, Brazil (FATEC–SP). The samples were collected with PVC tubes (60 × 5 cm) in the following profiles and at the following depths: 1 (6.85 m), 9 (9.6 m), 10 (7.9 m), 19 (4.75 m) and 20 (3.70 m) as indicated in Figures 5 and 7. In each case, the sample was taken at the maximum possible depth. Samples were treated with 20% H₂O₂ for 4 h, 20% HF for 45 min, 20% HCl for 2 h, and heavy liquid (SPT) treatments. This was followed by sieving to sort out grain sizes between 100 and 160 µm.

The γ -irradiation was carried out using a Co-60 source. Natural radioactive isotope contents were determined with gamma spectroscopy, using an Inspector portable spectroscopy workstation – Canberra, equipped with an NaI(Tl) detector model 802 and lead shield model 727. The data were calibrated with JG-1(A), JA-3, JB-2, and JB-3 Japanese soil standard samples. Peak energies used were 238, 295, 352, 1120, 1460, 1760, and 2620 keV. The annual dose was calculated using the activity concentration from ²³²Th, ²³⁸U and ⁴⁰K, determined by gamma spectrometry and Bell's equation. OSL measurements were recorded with a Daybreak Nuclear and Medical systems (Model 1100-series automated OSL system). OSL dating of quartz grains was performed using a blue light (470 nm) and detection through ~5 mm Hoya U-340 filters. The OSL ages were obtained by the standardized growth curve (SGC) method, following the single-aliquot regenerative-dose (SAR) protocol (Murray and Wintle, 2000). In this case, samples were preheated to 250 °C for 10 s prior to measurements, and at 200 °C after the test dose.

Remote sensing analysis of fluvial dynamics of the Amazon River between Careiro Island and the mouth of the Madeira River was carried out for a period covering 31.1 years. Most temporal analyses of areas along the Amazon River used Landsat imagery with a spatial resolution of 30 m (Rozo, 2004; Peixoto *et al.*, 2009; Rozo and Soto, 2010), with the exception of radar images with a 16 m spatial resolution used by Mertes *et al.* (1996). Water level fluctuations between the images selected for analysis are more variable among different authors: 82 cm (Rozo, 2004), 1 to 2.9 m (Peixoto *et al.*, 2009) and 52 cm (Rozo and Soto, 2010). Also, images were selected by Mertes *et al.* (1996) from the low water season without considering actual water level fluctuations.

In this study, two Landsat images were selected from Brazil's National Institute for Space Research (INPE) database: a Landsat-3 MSS image acquired on July 16, 1978 with spatial resolution of 80 m and a Landsat-5 TM image from August 18, 2009 with spatial resolution of 30 m. These images were selected based on minimal water level fluctuations (12 cm) and the largest temporal variation (31.1 years) between the acquisition dates available. The Landsat-3 MSS image was resized at a spatial resolution of 30 m. Comparing images adjusted to the same spatial resolution combined with lower water level fluctuations minimized errors in the quantification of changes in the fluvial system. Low cloud coverage was also considered in the selection of images. Daily water level data of the Amazon River, measured at the Careiro gauging station, were obtained from Brazil's National Water Agency (ANA).

The images were processed using ArcGIS and the Brazilian software SPRING. They were georeferenced with a maximum error less than two pixels. The MSS image was resized at the same spatial resolution as the TM image. Segmentation and classification were applied during image processing. The method of segmentation was region growing. Following segmentation, an extraction of the attributes of the regions was carried out, using the classifier Ioseg. The areas classified by the system, following an unsupervised process, were grouped into two predefined classes: water and land. The classified images underwent a process of vector generation from the matrix format of the classified image. Digital processing of the images provided the contours of the fluvial system of the Amazon River.

The classified images were exported as shapefiles into ArcMap. In ArcMap, manual corrections were made to eliminate clouds and shadows and correct any errors during the classification process. Finally, the plan view area of the channel and islands was calculated. These areas were compared, between 1978 and 2009, to determine percentage change in the plan view area of each geomorph. Pixel class-changes for the period were identified. The following categories of change were recognized: (1) no change; (2) deposition: changes from water to islands and water to floodplain; (3) erosion: changes from islands to water and floodplain to water; (4) changes between land categories: from floodplain to islands and vice versa.

The plan view areas of each category (change or no change) were calculated. The percentage of change in each category was estimated with respect to the total plan view area between the banks over which the change occurred (total area of change and no change). The sum of percentage change for the categories of deposition and erosion provided a percentage change in the plan view area of the system. This value was also divided by the number of years over which the change occurred (31.1 years), giving a percentage change in the plan view area of the system per year (Mertes *et al.*, 1996). Land change categories were not added to the percentage change in the plan view area of the system, since islands may be excised parts of the floodplain or vice versa, representing a change in the geomorph classification

but not a real erosional or depositional change. Migration rates in meters per year were calculated at specific locations where there is an evident tendency for the river to erode or deposit.

Results

Temporal analysis

Between July 16, 1978 and August 18, 2009 the plan view area of the Amazon River channel in the study reach was increased while all of the islands suffered size reductions (Table I); these processes represent net erosion in the system. Over the same time period the mouth of the Madeira River registered an increase in size, which also indicates net erosion. In contrast, net deposition in the total plan view area of the islands is indicated by their increase in size (Table I).

The percentage change in the plan view area of the Amazon River system for this period was 17.8% ($0.6\% \text{ yr}^{-1}$), where 82% of the area did not change and 0.2% is the change between land categories (Table II). Islands that were eroded by 2009 represent the largest category of change with 11.3%. Other important changes over this period are areas covered by water in 1978 that by 2009 were occupied by islands with a 3.8% change, and areas of the floodplain that had been eroded by 2009 represent a 2% change. The percentage change in the plan view area of the Madeira River system for this period was 32.4% ($1\% \text{ yr}^{-1}$), 67.4% of the areas did not change and 0.2% was the change between land categories. The change from floodplain to water represents the greatest category of change with 16.3%, followed by water to floodplain with 7.8% and water to islands with 5.1%. In general, in the reaches of the Amazon and Madeira Rivers studied erosion was more prevalent than deposition between 1978 and 2009, with more intense processes acting in the Madeira River (Table II).

Migration rates, in meters per year, of the Amazon River's main channel were estimated at the locations shown in Figure 4 and Table III. The maximum migration rate recorded here is 60 m yr^{-1} for a depositional area located to the east of Marati Island (site 8, Figure 4(B)). Marati Island also shows the maximum rate of erosion with 39 m yr^{-1} (site 7, Figure 4(B)). Erosion is a more common process than deposition, affecting the main islands as well as the right margin of the Amazon River over the study period. Other erosional and depositional areas resulting

from considerable channel migration over the study period are shown in Figure 4 and Table III. The reach of the Madeira River in the study area shows higher migration rates than the reach of the Amazon River (Table III). Erosional rates reached up to 68 m yr^{-1} on the left margin of the Madeira River and depositional rates reached 117 m yr^{-1} at Espiritu Santo Island (sites 14 and 15, respectively, in Figure 4).

The temporal analysis also provides evidence of secondary channel migration, as well as localized migration in the main channel. The Careiro Paraná is very stable in its western part (Figure 4) but toward the east it clearly forms a meander bend where maximum migration rates of 42 m yr^{-1} were found (site 2, Figure 4(A)). South of this bend there is an oxbow lake that is still connected with this secondary channel, and which seems to have originated from a more active meandering stage of this channel (Figures 4(A) and 5(A)). The Onças Paraná is a bend with slow erosion of its right margin. Eva Paraná has a meandering planform with some scroll bar sets following its convex bends. While the channel has been stable during the last 31.1 years, migration is evident at its mouth with more erosion in the concave portion and deposition in the convex margin. Jacaré Paraná exhibits a meandering planform with its first bend clearly migrating northeast. A very large set of scroll bars follow this migration and maximum migration rates in this bend correspond to 18 m yr^{-1} . The bend near the mouth of Jacaré Paraná migrates to the southwest, with a maximum rate of 37 m yr^{-1} and there is also a clear set of scroll bars following this migration. The Autaz-mirim Paraná shows a slight southern migration, and Soriano Island provides further evidence of previous southern migration, since the island consists of a main set of scroll bars migrating in that direction.

In general, no significant changes were observed on the left margin of the Amazon in this reach, thus it has remained unchanged in the last 31.1 years (Figure 4). The stability of this margin is related to the presence of outcrops of the Alter do Chão and Novo Remanso formations that are more resistant to erosion compared with the floodplain deposits on the right margin (Figure 6(A)). The right margin thus exhibits migration related with secondary channels in the case of the Careiro, Onças and Autaz-mirim paranás (Figure 4). Two areas where erosion is due to the main channel are apparent. The first is located downstream of Parauacara Island, with migration rates reaching 20 m yr^{-1} (site 6, Figure 4). The second area is a semi concave bend, directly in front of Marati Island (site 12, Figure 4

Table I. Percentage change in the plan view area of each geoform (channels and islands) in the studied reaches of the Amazon and Madeira Rivers. The values of the plan view area for each date are also indicated. Location of the islands is indicated in Figure 1(C).

Feature	16-Jul-78	18-Aug-09	From 16-Jul-78 to 18-Aug-09	
	Plan view area (km^2)		Change (%)	Process
Channel	685.8	785.6	14.6	
Careiro Island	281.5	219.6	-22.0	
Terra Nova Island	6.2	3.6	-42.7	
Onças Island	50.9	42.9	-15.8	
Parauacara Island	7.4	4.7	-35.7	
Amazon River				Erosion
Eva Island	71.5	65.9	-7.8	
Jacaré Island	26.4	20.8	-21.1	
Marati Island	11.7	5.9	-49.6	
Soriano Island	65.3	61.7	-5.4	
Beija Flor Island	6.7	5.2	-21.9	
Total area of islands	605.1	490.7	-18.9	
Channel	48.6	54.9	12.9	Erosion
Espiritu Santo Island	0.4	3.2	651.5	Deposition
Capitari Island	2.5	0.8	-68.6	Erosion
Total area of Islands	2.9	4.2	44.0	Deposition

Table II. Percentage change in the plan view area of: each category of the pixel class-changes analysis; the river system and the system per year. The period of time over which the change occurred corresponds to 31.1 years. The values of the plan view area of each category of change are also indicated.

Categories	Amazon River				Madeira River							
	16-Jul-78		18-Aug-09		Area of change km ²		Percentage change in the plan view area of the system /year		Area of change km ²		Percentage change in the plan view area of the system /year	
	From	to	each category	the system	each category	the system	each category	the system	each category	the system	each category	the system
Deposition	Water	Islands	3.8	4.6	3.3	5.1	12.9	5.1	7.8	32.4	1.0	
	Water	Floodplain	0.7		5.0							
Erosion	Island	Water	11.3	17.8	2.1	3.3	19.5	3.3	3.3			
	Floodplain	Water	2.0	13.2	10.4	16.3		16.3				
Land change	Island	Floodplain	0.1	0.2	0.0	0.0	0.2	0.0	0.2			
	Floodplain	Islands	0.1		0.1			0.2				
No change			82.0	82.0	43.2	67.4	67.4	43.2	67.4			
Total plan view area between the banks over which the change occurred			1249.0	1523.6	64.1			64.1				

(B)). In this area the rate of erosion increases downstream up to 34 m yr^{-1} . A set of scroll bars in Marati Island follows this migration (Figure 5(B)) and this island is where the maximum depositional rates of migration are found (60 m yr^{-1}) (site 8 Figure 4 (B)). Immediately downstream of Novo Remanso, there is a depositional area directly linked to the main channel (Figure 4). In this area new small bars have been deposited since 1978. A set of scroll bars scaled to the magnitude of the main channel follows this migration towards the northeast (Figure 5(C)). Upstream of Novo Remanso the right margin is a concave erosional bend, and downstream at the same margin, there is a convex depositional bend (Figure 4). This defines a sinuous configuration for this part of the right margin. In contrast, the left margin is mainly linear with an ESE direction. A very slight concave bank exists in the left margin after Novo Remanso, but this bend has remained unchanged at least over the last 31.1 years (Figure 4).

Facies and morphostratigraphic units

The morphostratigraphic analysis of the study area has defined four units which, in order of decreasing age, are: (a) terraced deposits; (b) scroll bar deposits; (c) floodplain deposits; and (d) channel bar deposits (Figure 6(A) and 6(B)).

Terraced deposits

The deposits represent the Alter do Chão (Upper Cretaceous) and Novo Remanso (Neogene) formations (Figure 6(A) and 6 (B)). Three morphologic units can be distinguished: the first unit, with elevations between 20 and 100 m.a.s.l., is characterized by a relief with a medium degree of erosion and trellis drainage pattern. Interfluvies of 1.5 to 2 km in width are supported by ferricrete. The second unit represents flat lower areas, with elevations between 10 and 50 m.a.s.l. A low degree of erosion, sub-trellis drainage and the presence of colluviums with ferricrete fragments characterize this unit. The third unit is restricted to the Novo Remanso area, and is characterized by lower topography with elevations less than 25 m.a.s.l and flatter surfaces than in the previous units.

Elongated-ramified lakes follow the erosive edges of terraced deposits and are more frequent in the southern area where these deposits are in contact with the floodplain (Figure 6(A)). The term elongated-ramified lake is used to describe drainages that have an elongated branch-like form related to the damming of their mouths. These lakes are connected with the main channel through secondary channels. The rivers Puraquequara, Preto da Eva and Urubú follow this configuration (Figure 6(A)). In the case of the Preto da Eva River, the mouth is blocked by scroll bar deposits and it is connected with the Eva Paraná by a small 'furo' channel (Figure 6(A)). The Urubú River is blocked by floodplain sediments (Figure 6(A)) and the channel that connects it with the Amazon runs several kilometers before reaching its mouth.

Restricted floodplains are found in the terraced deposits, in valleys with smooth topography associated with tributaries of the Puraquequara, Preto da Eva and Urubú Rivers. The development of these floodplains results from fluvial captures and dammed mouths of main channels.

Scroll bar deposits

The terms point bar and scroll bar are used here in the sense of Nanson (1980). A point bar is formed in a meandering bend next to the convex bank. It is characterized by a slightly convex-up morphology, coarse sediments and the presence of very scarce vegetation. With fine traction and suspended load deposition, a central ridge is formed extending almost over

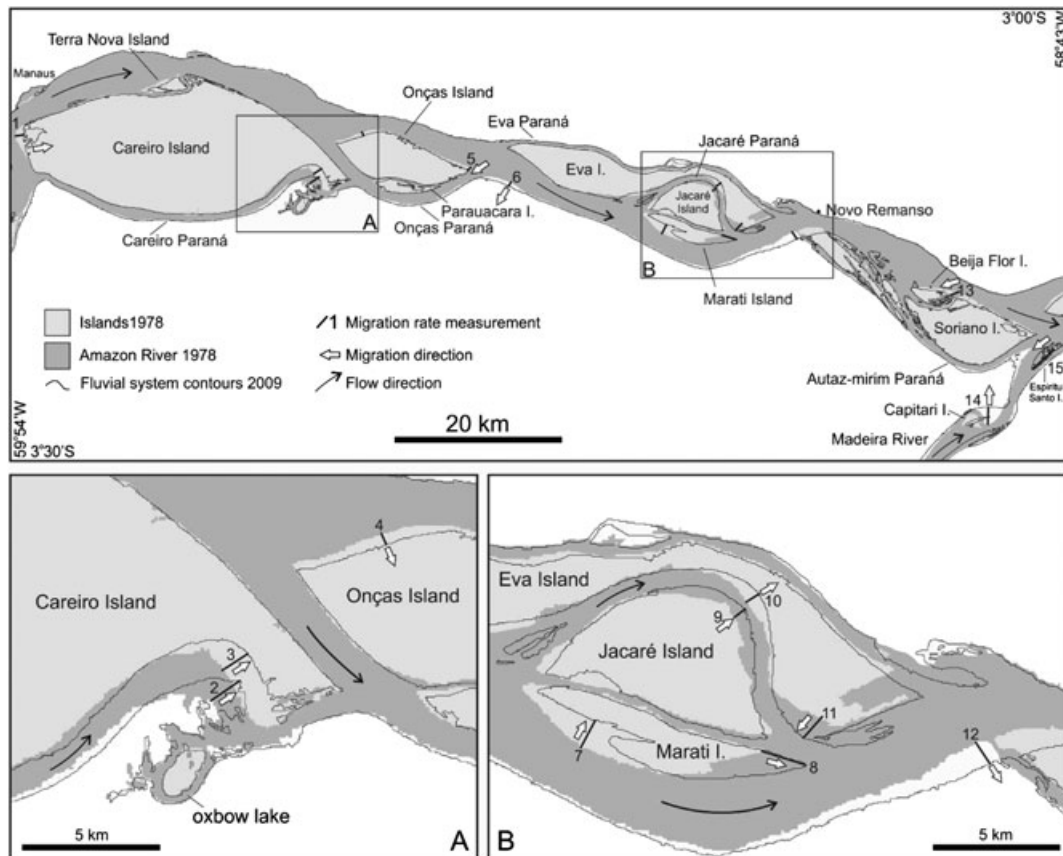


Figure 4. Temporal analysis of the Amazon River between Manaus and the mouth of the Madeira River from 1978 to 2009. (A) Detail of the eastern part of the Careiro Paran , the most active area in the secondary channels. (B) Detail of Jacar  and Marati islands. Marati Island is where maximum rates of erosion and deposition are recorded in the studied reach of the Amazon River. Note the northeast migration tendency of the Jacar  Paran  and the erosion of the main channel at location 12. For the specific migration rates see Table III.

Table III. Migration rates in the studied reach of the Amazon and the mouth of the Madeira River. The locations are numbered from upstream to downstream and categorized by erosion or deposition. See Figure 4 for the specific location of each site.

	Location	Migration (1978 to 2009)			
		meters	meters per year	Process	
Amazon River	1	West of Careiro Island	965	31	Erosion
	3	East of Careiro Island	1142	37	
	4	Northwest of On�as Island	455	15	
	5	East of On�as Island	555	18	
	6	Amazon River right margin	619	20	
	7	Southwest Marati Island	1206	39	
	10	Northeast of Jacar� Paran�	617	20	
	12	Amazon River, South of Novo Remanso	1061	34	
	13	East of Beija Flor Island	1190	38	
	Madeira River	2	East Careiro Paran�	1312	
8		East Marati Island	1869	60	
9		Northeast Jacar� Island	556	18	
11		East of Jacar� Paran�	1159	37	
Madeira River	14	Madeira River	2118	68	Erosion
	15	Espiritu Santo Island	3632	117	Deposition

the entire point bar platform, and this central ridge is denominated a scroll bar. The scroll bar is separated from the convex bank by a swale. It continues to grow mainly by suspended load until it is only flooded near bankfull discharge and colonized by vegetation. With progressive channel migration, a scroll-bar floodplain is developed.

The alluvial islands Careiro, Terra Nova, On as, Paraucara, Eva, Jacar , Marati, Beija Flor, Soriano, Capitari and Espiritu

Santo, together with portions of the right bank of the Amazon River and mainly the left margin of the Madeira River, are composed of scroll bar deposits (Figure 5(A)). The ridge-and-swale morphology is characteristic in these areas (Figure 5(D)) with the development of narrow lakes and minor secondary channels that follow the swales (Figures 5(C) and 5(E)). These scroll bars represent sets of lateral accretion units measuring up to 7.5 km wide at Soriano Island. They follow present-day

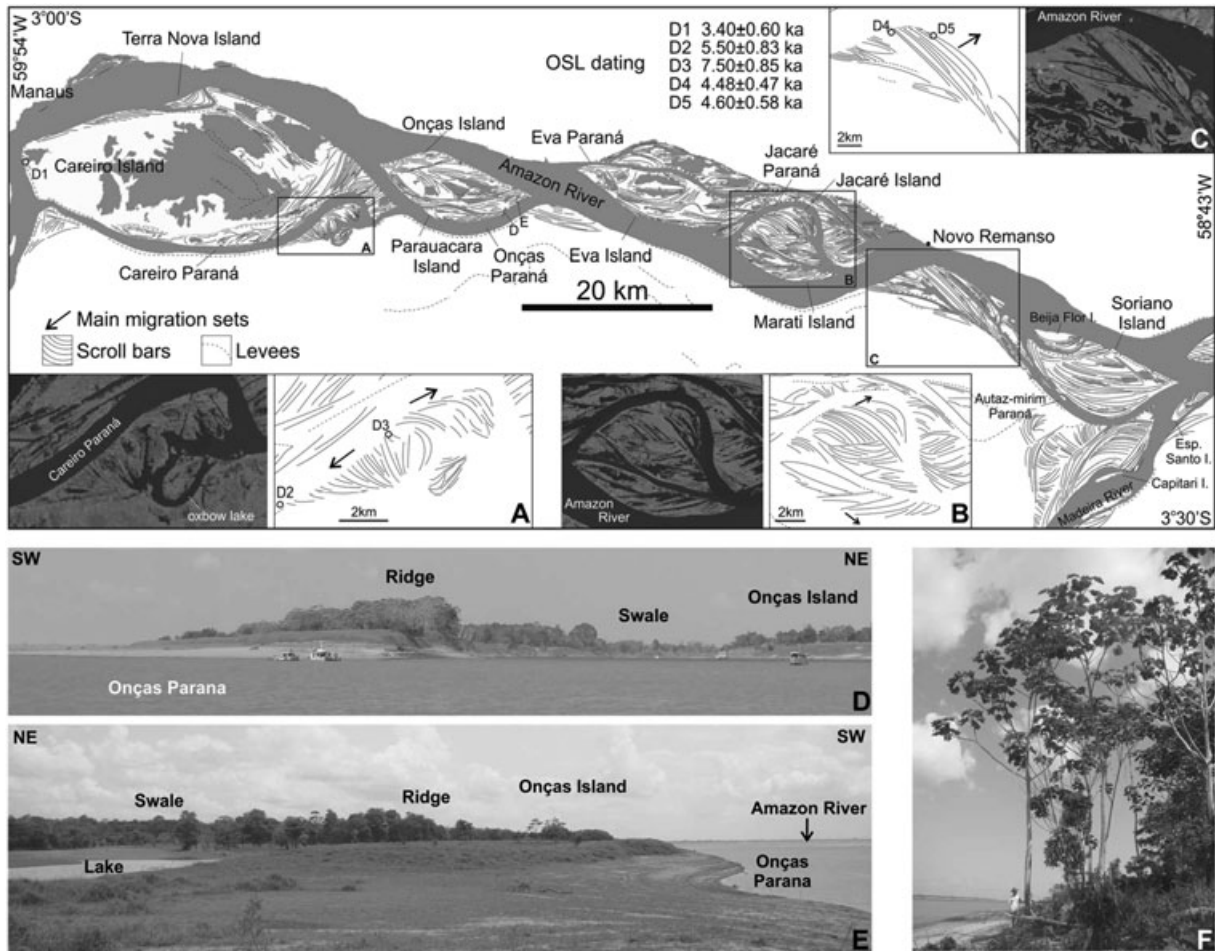


Figure 5. Morphologic features of the middle Amazon River. (A) Detail of the Eastern Careiro Parana. Note the scroll bar configuration with the development of oxbow lakes. (B) Detail of Jacaré and Marati islands. Note the northeast direction of the migration of the Jacaré Parana as indicated by the scroll bars. (C) Scroll bars showing the migration of the main channel. (A), (B) and (C) also show a Landsat-7 image from August 1, 1997. (D) Morphology of ridge and swales characteristic of scroll bars from the main and secondary channels. (E) Detail of the swale and ridge morphology at Onças Island. Note the development of a lake on the swale. D and E are located southeast of Onças Island as indicated in (A). (F) Characteristic vegetation developed on scroll bar deposits.

migration in some parts of the main channel and secondary channels. Some sets are truncated by the main and secondary channels as well. The sets are also separated by successive reactivation surfaces that record changes in migration direction.

The scroll bar deposits consist of silty, fine-grained, moderately to well-sorted sand and greyish clay that form inclined heterolithic stratification according to Thomas *et al.* (1987). The thickness of the inclined heterolithic stratification sets varies from 1.2 to 8.4 m. The strata in each set of scroll bars generally dip up to 10° with the direction of migration being highly variable between individual sets. Subaerial exposure periods are indicated by bioturbation features associated with rather high organic detritus in the form of leaves and trunk fragments (Figure 7).

The individual scroll profiles (Figure 7) are positioned in different parts of the scroll bar deposits, and consequently some show horizontal rather than inclined strata (e.g. Profiles 13 and 20 in Figure 7). This geometry arises from the fact that the profiles were described along-strike. The sedimentary structures found in the scroll bars are also related to the location where the profiles were described, for example trough cross-stratification is common near the channel and in the swale (e.g. Profiles 20 and 21 in Figure 7). Climbing ripples (Figure 8 (D)) are located in the channel limb and swale limb migrating towards the crest of the bar. In the crest of the scroll, ripples and planar lamination is common and ripples migrating in

both directions can also be found. Flaser and lenticular bedding is also present in the scroll bar deposits (Figure 8(E)).

In the study area, evidence for the development of a scroll over a point bar was found only in profile 10 (Figures 7 and 8 (A)), where up to 4 m of medium to fine sand fining upward is found. Trough cross-stratification (Figure 8(B)) is present in this sand set. Backsets structures terminating updip against an upstream-dipping erosion surface, in the sense of Fielding (2006), seem to have developed in this set (Figure 8(C)), indicating upper flow-regime conditions. This sand set with trough cross-stratification is thicker in profile 10 than in any other profile, with the exception of profile 25. Thus, the sand set deposits in profile 10 evidence the top of a point bar over which a scroll bar developed. Over the point bar deposits, an inclined set of medium sand with trough cross-stratification is observed, representing conditions near the channel. Above the previous set, an intercalation of fine sand and clay is found, where the clay is thickening upward, indicating an increase in suspended deposition. In profile 25 (Figure 7), a medium sand set up to 3.4 m thick is found with trough cross-stratification. This sand set overlays the scroll deposits, which can be interpreted as a new point bar developing over older scroll bar deposits.

Vegetation develops once the scroll bar is established and supports soil development. In general, new areas are colonized by fast growing species such as *Cecropia spp.* (Figure 5(F)). This species can grow in height by up to 2.76 m yr^{-1} , according to

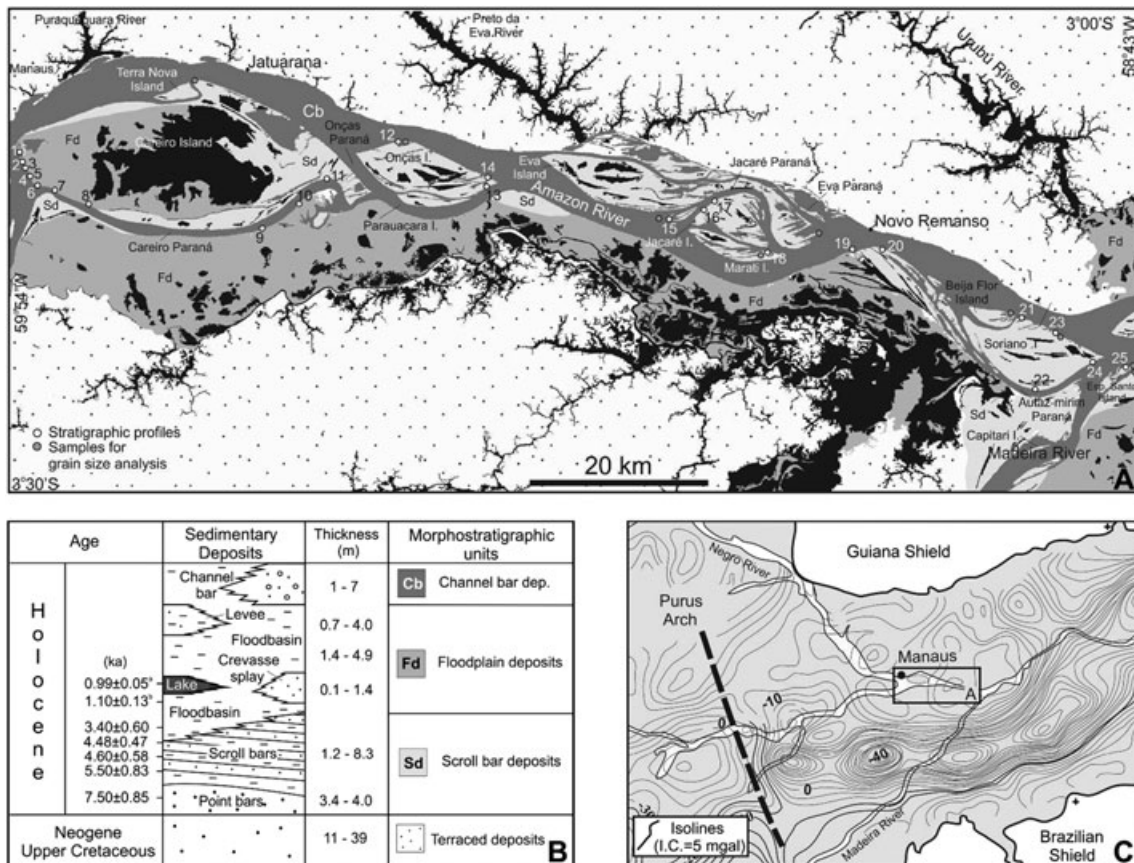


Figure 6. (A) Morphostratigraphic units in the study area. Note the asymmetrical distribution of the floodplain deposits, which are mainly on the right margin of the Amazon River. The location of the stratigraphic profiles and samples for grain size analysis are also indicated. Lakes, furos and other rivers are in black. (B) Sedimentary deposits described in the area. Radiocarbon dates previously reported (a and b) and the OSL ages obtained in this study indicate local events along the study area. ^a (Latrubesse and Franzinelli, 2002), ^b (Sternberg, 1950). (C) Bouguer gravimetric map of the western Amazonas Basin, modified from Wanderley Filho (1991); the SW-NE lowest gravimetric trend (bottom right of figure) marks the basin axis.

measurements in the Atlantic rain forest (southeastern Brazil) (Santos, 2000). Specific growth rates over scroll bars are not yet known. The *Cecropias* in Figure 5(F) are approximately 5 years old based on growth rates for this genus measured by Santos (2000), suggesting that the scroll bars they are growing on are relatively young. In fact, these scroll bars had not yet been deposited in 1978 according to the temporal analysis.

The scroll bars clearly show migration of secondary channels as well as the main channel (Figure 5). The Careiro Paraná at its eastern right margin shows two clear sequences of scroll bar migration (Figure 5(A)). The first is a set migrating northeast with an active depositional area at the right margin of the Careiro Paraná (Site 2 in Figure 4(A)). The second is an ancient set of scroll bars migrating southwest (From D3 to D2 in Figure 5(A)). Rates of migration estimated using OSL dating suggest that the latter set accumulated between 7.5 ± 0.85 ka (D3 in Figures 5(A) and 7) and 5.5 ± 0.83 ka (D2 in Figures 5(A) and 7) with a migration of 5.2 km over 2000 years (2.6 m y^{-1}). Also, in this area an oxbow lake is present which is still connected to the main channel of Careiro Paraná (Figure 5(A)). The scroll bars at Onças Island show the southern migration tendency of the Paraná. The Jacaré Paraná has developed a sinuous channel with northeast migration (Figure 5(B)). Evidence for the migration of the main channel is seen at the southeastern end of Marati Island, where the scroll bars show a migration towards the southeast (Figure 5(B)). Also, the right margin of the Amazon River in front of Novo Remanso indicates migration of the Amazon, with a depositional margin migrating northeast (Figure 5(C)). In this set two OSL ages were obtained: D4 (4.48 ± 0.47 ka) and D5 (4.60 ± 0.58 ka). The age obtained at the eastern extreme of this set (D5) is older than the

age in the western end (D4), when according to the scroll bar migration the opposite should be the case (Figure 5(C)). These two dates are very close to each other, and assuming the error induced by the OSL method of dating, it can only be stated that deposition of this set occurred very rapidly. Soriano Island is the greatest preserved scroll bar set, demonstrating the migration of the Autaz-mirim Paraná to the south (Figure 5).

Floodplain deposits

These deposits, characterized by a mostly flat surface, constitute the western part of Careiro Island, the right side of the main channel of the Amazon, the right side of the confluence of the Madeira River, as well as the area around the mouth of the Urubú River (Figure 6(A)). Irregularly rounded lakes developed from abandoned meanders of secondary channels are common on the floodplain. Individual bends of a secondary channel migrate in the direction of existing oxbow lakes formed from the same channel or from a proximal secondary channel (Figure 9(A)). Meanders can intersect the existing oxbow lakes, preserving part of their original shape (Figure 9(B)). Natural levees formed mainly along concave but also on straight banks of the main and secondary channels are eventually breached by crevasse channels forming crevasse splay deposits. These crevasse splay deposits in the floodplain partially cover the portion of oxbow lakes that were preserved, as well as other oxbow lakes (Figure 9(C)). The above processes preserve part of the original curved outline of the oxbow lakes and forms new lakes with an irregularly rounded geometry (Figure 9(D)). The irregularly rounded as well as oxbow lakes are isolated from secondary channels or connected to the drainage system by small channels

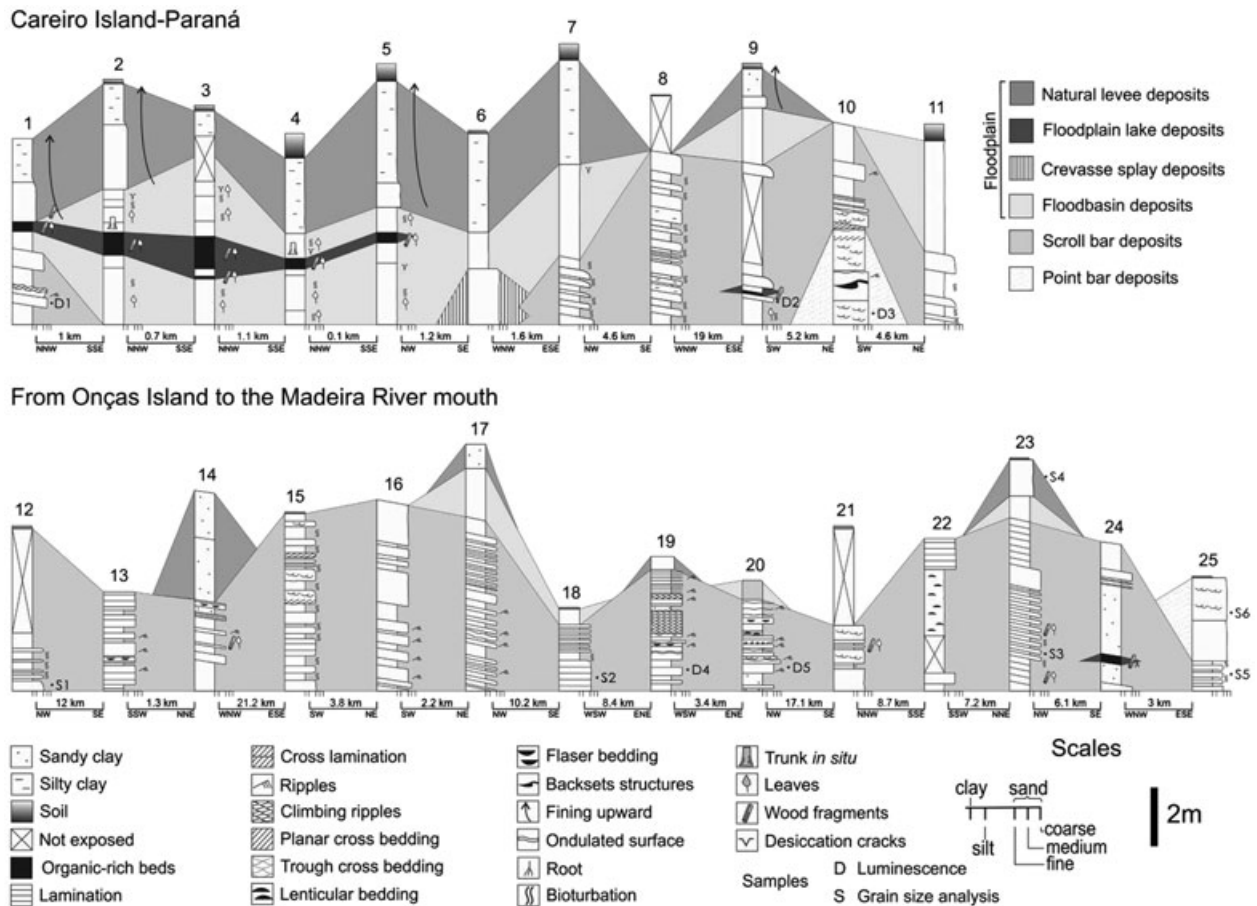


Figure 7. Fluvial deposits. On Careiro Island, floodplain deposition is more common than in the reach downstream where scroll bar deposition is predominant. Location of logs indicated in Figure 6(A). The depth at which the samples for OSL dating were collected is indicated in profiles 1, 9, 10, 19 and 20.

(“furos”), which dry up during the low water season. Some of these lakes are filled with sediments with the preservation of the original contour from which they were formed. Four different types of floodplain deposits were identified in the profiles described along the river banks: floodbasin deposits, floodplain lake deposits, natural levee deposits and crevasse splay deposits.

Floodbasin deposits are characterized by greyish to brown, laminated and massive clays, locally showing distinct bioturbation features and desiccation cracks indicating subaerial exposure. These sediments contain organic detritus and in some locations trunks, the latter reaching up to 30 cm in diameter and oriented in growing position. The thickness of these deposits varies from 0.5 to 4 m. In most of the profiles these deposits overlay scroll bars and are covered by natural levee deposits (Figure 7). Floodplain lake deposits are characterized by dark brown to black clays rich in organic matter (Figure 10(A)). They are more common and thicker (up to 1.4 m) in the western part of Careiro Island compared with other parts of the fluvial system (Figure 7). These deposits are also found on the right margin of the Careiro Paraná near its mouth and near the mouth of the Madeira River (Figure 7). They were observed on the right margin of the Amazon River downstream of Onças Island, but the difficulty in accessing this area impeded their description. These sediments contain leaves and trunks (Figure 10(B)), the latter reaching up to 20 cm in diameter and oriented in horizontal position (Figure 10(A)). Natural levee deposits are massive silt, sandy clay and silty clay. Fining upward cycles, characterized by increasing clay content toward the top of the deposits, were identified in Careiro Island (Figure 7). Their thickness varies from 0.5 to 5 m. They overlay scroll bars, floodbasin and floodplain lake deposits (Figure 7). Crevasse splay deposits

are fine-grained massive sands which were only identified at the base of profile 6 (Figure 7). These deposits occur at a lower topographic elevation than the floodbasin and scroll bar deposits. The location where profile 6 was described corresponds to an active erosional area where previously formed floodplain deposits are being exposed. This suggests that these deposits were accumulated on lower floodplain areas and are interpreted here as crevasse splay. This facies could also be part of point bar deposits, however they are finer than the point bar facies described and do not have any sedimentary structures that would allow further classification. These deposits are also covered by floodbasin and natural levee deposits (Figure 7). Their thickness is up to 2.1 m.

Channel bar deposits

The present-day channel bars of the Amazon River emerge at low water during the dry season and extend up to 3.4 km long, 1 km wide and 7 m high with respect to the river water level at the time of observation (Figure 10(C)). On their surface, there are dunes with wavelengths up to 7.6 m and up to 50 cm high (Figure 10(D)). Over the dunes, ripples are found with heights of 0.5 cm and 8 cm in wavelength (Figure 10(E)). Dunes with wavelengths up to 15 m and heights up to 1 m were observed at the confluence of the Negro and Amazon Rivers. In some troughs between the dunes clay deposition during falling stages is observed (Figure 10(F)). The bars are composed of fine-grained, moderately to well sorted sand. At the base of the deposits, planar cross-bedding is present while at the top several sets of cross-lamination are found. Orientation of these structures corresponds to the present-day direction of the flow.

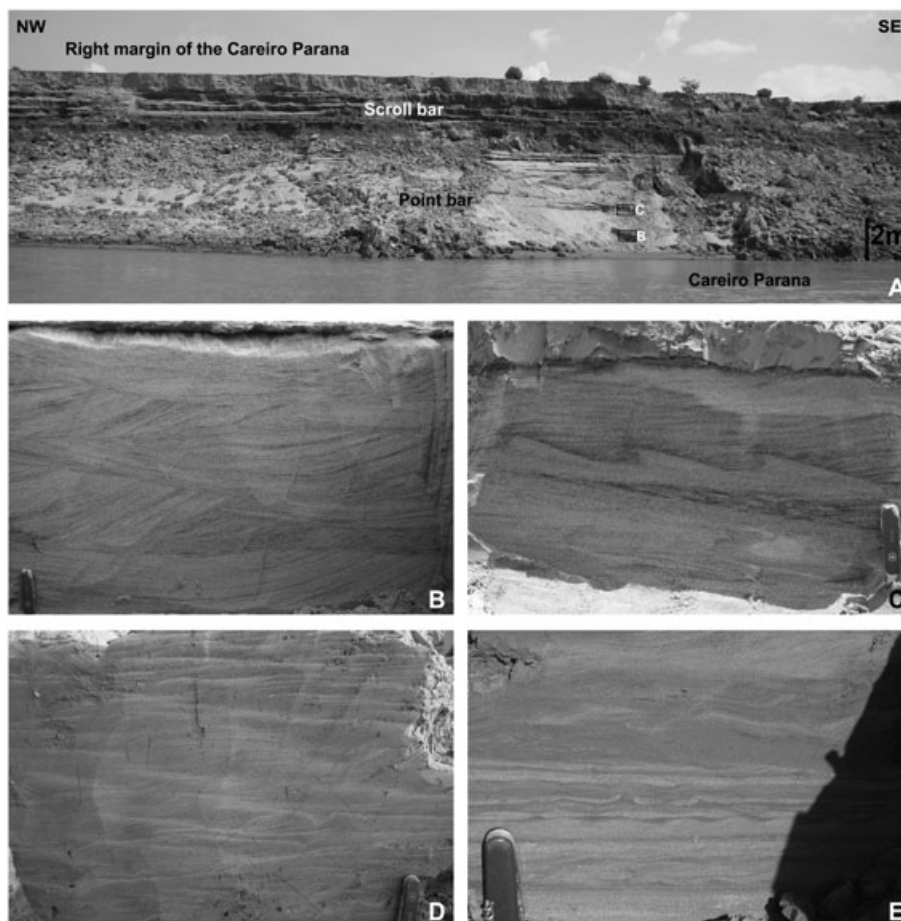


Figure 8. Scroll bar deposits. (A) Scroll bar developed over point bar. Scroll bar morphology is better observed from a satellite image (D3 in Figure 5 (A)). This section corresponds to profile 10, in Figure 7. (B) Detail of the point bar deposits: medium to fine sand fining upward with the development of trough cross-stratification. (C) Backsets structures terminating updip against an upstream-dipping erosion surface, in the sense of Fielding (2006). Flow direction from left to right. (B) and (C) are located in (A). (D) Climbing ripples. (E) Laminar, flaser and lenticular bedding. (D) and (E) correspond to profile 19 in Figure 7.

Depositional model

The bedrock over which this reach of the Amazon River develops consists of fine to coarse-grained siliciclastic deposits of the Alter do Chão and Novo Remanso Formations (Figure 3(B)). These deposits outcrop in the left margin of the Amazon River and are in contact with the floodplain to the south (Figure 6). However, no data is available regarding the deposits which lie beneath the logs that were described, including their continuity at depth or the presence of the Alter do Chão and Novo Remanso formations (Figure 11).

The planform of the Amazon River between the mouths of the Negro and Madeira Rivers is formed by several interconnected channels. The main channel is characterized by relatively straight reaches with some areas exhibiting an incipient meandering form. In contrast, secondary channels are sinuous with current meander development. The system follows a depositional model that is quite different from the classical anastomosing models described by Smith and Smith (1980) and Makaske (1998) (Figure 11).

In the main channel, fine sandy channel bar deposits develop, which are derived from bed load. Bank erosion in secondary channels as well as reaches of the main channel leads to lateral migration and point-bar accretion. Fine-grained sandy point bars develop in the convex part of the bends and constitute the platform for the development of fine-grained sandy and clayey couplets that form scroll bars by fine traction load and vertical accretion. Periods of subaerial exposure are indicated by intense bioturbation with accumulation of leaves and trunk fragments.

Secondary channels migrate extensively on the floodplain, leading to the development of different sets of scroll bars, and locally, meander cut-offs occur and oxbow lakes are formed. The sets of scroll bars are truncated by each other and by present-day channels. Migration of these secondary channels causes individual bends to migrate towards existing oxbow lakes. Meanders intersect these oxbow lakes, preserving part of their original shape. During flooding, silt and sandy/silty clay accumulate mainly along the concave channel banks forming natural levees in contrast to scroll bar ridges which develop in the convex channel banks. Clay accumulates in the lower parts of the floodplain, forming floodbasin deposits. Eventually, after successive periods of flooding natural levees are breached and develop crevasse channels and consequently fine sandy sediments are deposited on the floodplain in the form of crevasse splays.

The crevasse deposits partially cover the portion of oxbow lakes that were preserved, as well as other oxbow lakes. Part of the original outline of the oxbow lakes is preserved and new lakes are formed with an irregularly rounded geometry. The irregularly rounded as well as the oxbow lakes are isolated from secondary channels or connected to the drainage system by small channels, which dry up during the low water season. Shallow lakes are formed in the swales of the scroll bars during high water stages. During flooding, this complex geometry of lakes, paranás and furos becomes interconnected, improving the availability of organic matter. Once the water level drops, the organic matter concentrates in the lakes and consequently accumulates to form organic-rich clay deposits.

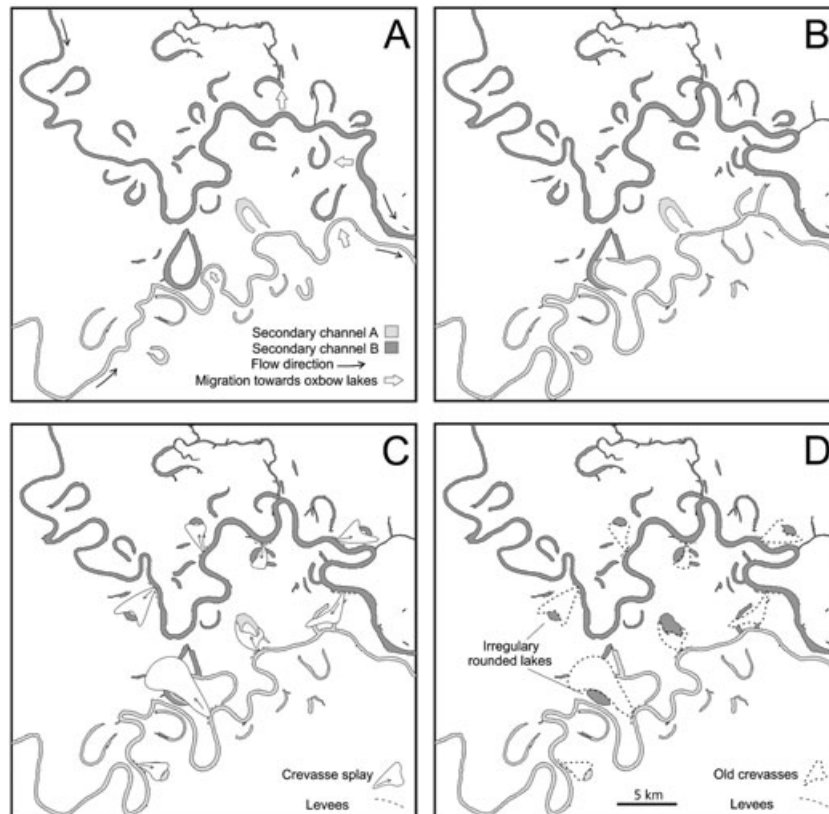


Figure 9. Development of irregularly rounded lakes in the floodplain. (A) Two migrating secondary channels with the development of oxbow lakes. (B) Individual bends in each channel can intersect previously formed oxbow lakes from the same channel or from an adjacent channel. The intersection forms lakes with complex geometry. (C) Crevasse splays can develop and partially bury oxbow lakes or intersected oxbow lakes. (D) As a result lakes develop with an irregularly rounded geometry. The processes in (A), (B) and (C) developed contemporaneously, but here they are separated to illustrate how these lakes are formed.

Meandering secondary channels develop fining upward successions in the convex channel banks. These fining upward successions are formed by sand (point bar deposits) at the base, sand and clay couplets (scroll bar deposits) and covered by clay and organic-rich clays (floodbasin and floodplain lake deposits). Due to the active meandering behavior of secondary channels these fining upward successions are eventually abandoned or isolated from the channels. Erosion in the channel banks in the form of slump blocks eventually expose previously formed fining upward successions. The flooding which results leads to the development of natural levees on top of these older successions, in which silt and sandy/silty clay (natural levee deposits) drape fining upward successions.

Discussion

Relative stability of the system

We discuss our data in relation to other data available for this region (Mertes *et al.*, 1996; Rozo, 2004; Peixoto *et al.*, 2009; Rozo and Soto, 2010), even if there are discrepancies in the image selection process. However, more research must be undertaken to evaluate the best parameters when working with temporal analysis in this type of river.

The percentage of change in the plan view area per year of the Amazon River between the Iça and the Madeira Rivers was initially estimated by Mertes *et al.* (1996) from radar images (1971–1972) and navigation charts of the Brazilian Navy (1979 and 1980). These values vary considerably between the selected locations of analysis, but they show a relatively active area at the confluence with the Jutai River

(Figure 1(B)) reaching up to $2\% \text{ yr}^{-1}$ and a relatively stable area at the confluence with the Negro River with values of $0.2\% \text{ yr}^{-1}$. Recently, percentage change values in the plan view area for specific reaches of the Amazon have been obtained for longer periods of time and using more accurate remote sensing tools (Rozo, 2004; Rozo *et al.*, 2005a; Peixoto *et al.*, 2009; Rozo and Soto, 2010). These values as well as the values that were obtained in this study seem to be in agreement with the data obtained by Mertes *et al.* (1996). However, the Colombian reach of the Amazon River seems to be more stable ($1.4\% \text{ yr}^{-1}$, between 1986 and 2006) (Rozo and Soto, 2010) than the reach of the Solimões River at the confluence with the Japurá River ($1.8\% \text{ yr}^{-1}$, between 1984 and 2005) (Peixoto *et al.*, 2009). In the reach between the confluences of the Negro and Madeira Rivers the percentage change had previously been established at $0.7\% \text{ yr}^{-1}$ between 1986 and 2001 (Rozo, 2004). In the present study a percentage change of $0.6\% \text{ yr}^{-1}$ was calculated based on a longer period of analysis, 31.1 years compared with 15 years for the period between 1986 and 2001. These values indicate that the rate of change in the plan view area of the system per year is almost constant and even slightly lower for the longer period of analysis. The percentage change values per year were also established for the mouth of the Madeira River at $1.4\% \text{ yr}^{-1}$ (1986–2001) (Rozo, 2004) and $1\% \text{ yr}^{-1}$ (1978–2009) in this study, showing a more active system than the reach of the Amazon River studied here.

Migration rates estimated in different reaches of the Amazon River show a clearer decreasing trend in stability from upstream to downstream than the trend of the yearly percentage change in the plan view area of the system. These values allow the section of the Amazon between its source and the mouth of the Madeira River to be divided into three reaches: (1) Upper

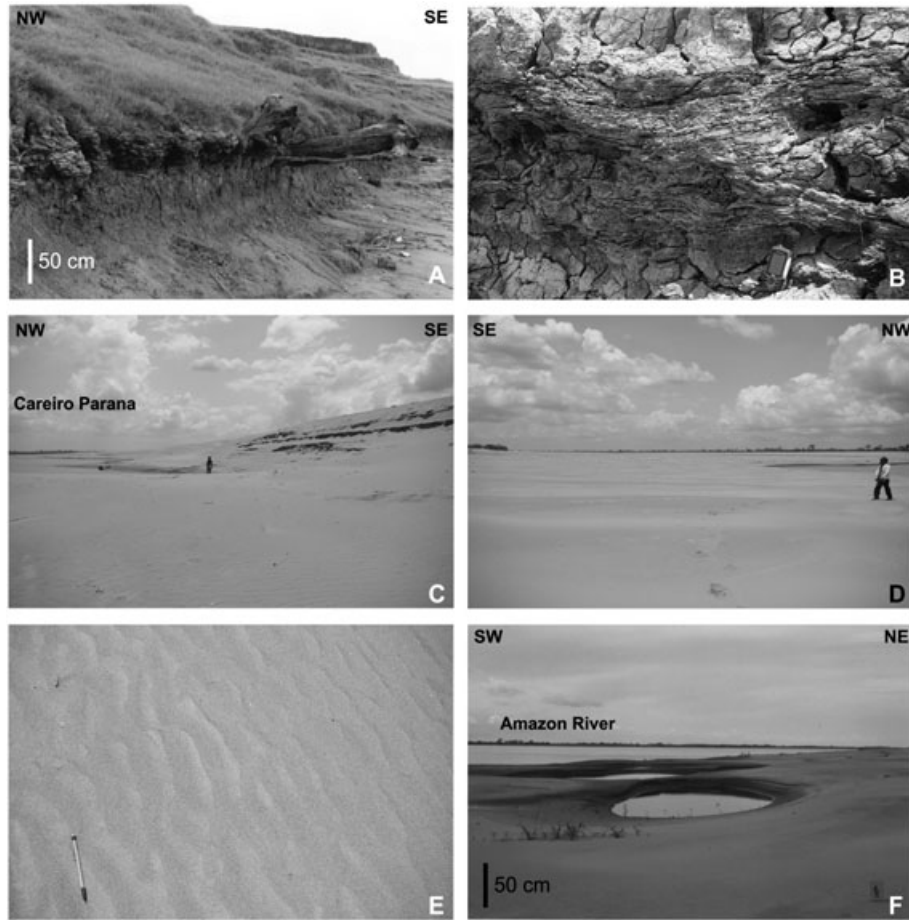


Figure 10. (A) and (B) Organic-rich beds in western Careiro Island. Tree trunks embedded in these deposits can be observed. Floodbasin and natural levee deposition overlay the organic-rich beds. (C), (D) and (E) Sand bars in eastern Careiro Island. Note the magnitude of these sand bars in (C). Dunes in (D) are located above the sand bars, and ripples in (E) are located above dunes. (F) Sand bars in the main channel at the confluence of the Negro and Amazon Rivers. Note the scour in the downstream dune flank.

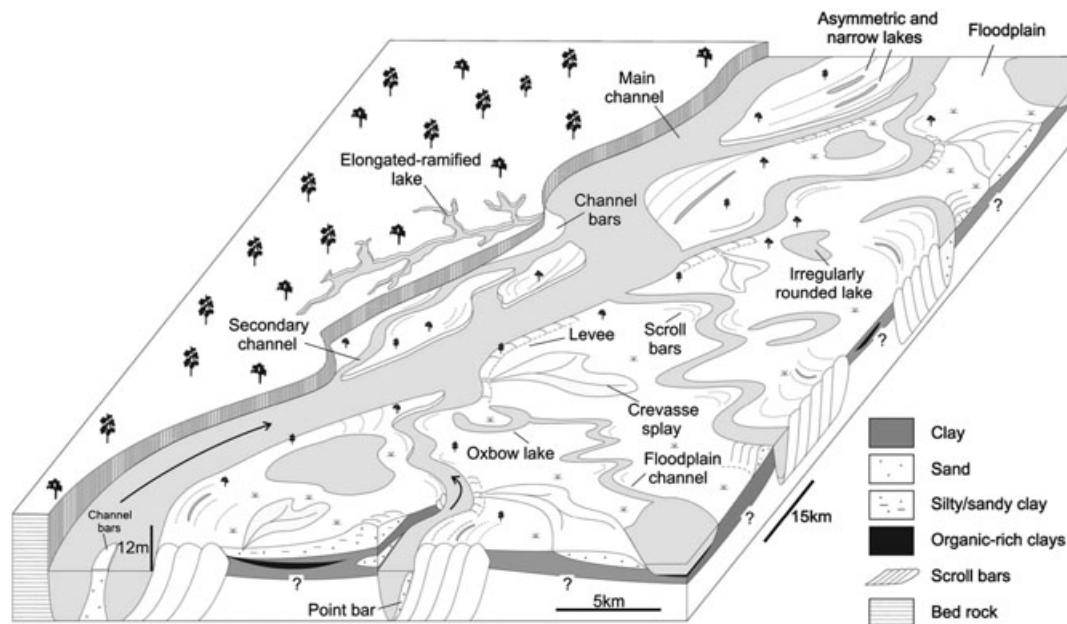


Figure 11. Depositional model and morphologic characteristics of the studied reach of the Amazon River. Note the migration of secondary channels as well as localized migration in the main channel with the development of scroll bars.

Amazon River (the Ucayali River in Peru and Amazonas River in Peru and Colombia, see Figure 1(B)), which corresponds to the more laterally active reach with migration rates of 400 myr^{-1} near Iquitos (Kalliola *et al.*, 1992) and

213 myr^{-1} near Leticia (Rozo and Soto, 2010); (2) the Amazon River between Leticia and Manaus (Solimões River in Brazil, see Figure 1(B)), which represents a less laterally active reach with migration rates of 140 myr^{-1} near Fonte

Boa (Mertes *et al.*, 1996); and (3) a relatively stable reach downstream Manaus (Amazonas River in Brazil, Figure 1 (B)), with maximum migration rates of 60 myr^{-1} .

Genesis and controls of the system

Anastomosing rivers have been described in a variety of climatic and geological settings with considerable differences in spatial scales (Makaske, 2001). Climatic conditions include temperate humid, tropical humid, arid, semi-arid and subarctic, while geological settings include montane, foreland and intracratonic basins. Textural facies models have been proposed mainly for anastomosing rivers in temperate humid and montane settings from western Canada (Smith and Smith, 1980; Makaske, 1998). A preliminary depositional model for a large anastomosing river in tropical humid and intracratonic settings is described in this study (Figure 11). The models for the anastomosing rivers in western Canada and the Amazon are very different in terms of the superficial deposits being generated, which is likely linked to differences in climate, geological setting and spatial scale. However, these models as well as other anastomosing rivers which have been described share several similarities in terms of geomorphology and sedimentary environments.

In the Amazon, alluvial islands with saucer-like morphology are formed by their delimiting natural levees. These islands are very extensive and are typically swampy during most of the year, which is also characteristic of other tropical humid anastomosing rivers such as the Tonlé Sap River in Central Cambodia (Makaske, 2001) and the Magdalena River in Colombia (Smith, 1986). Islands with saucer-like morphology have been identified in all types of anastomosing rivers (Makaske, 2001). However, differences exist in relation to the extent of development of natural levees. Discontinuous levees as in Cooper Creek in central Australia (Rust, 1981) also form in the Amazon River, where they are concentrated mainly along concave banks. These are different from well distributed levee deposits along the channels of the upper Columbia River (Makaske, 1998) and the Alexandra River (Smith and Smith, 1980) in Canada. We suggest that avulsion in the studied reach of the Amazon is responsible for the multichannel pattern along Careiro Island, while downstream mid-channel bar formation and chute cut-offs of the main and secondary channels lead to the development of anastomosis. This is distinctly different from long-lived, rapidly aggrading anastomosing rivers in a humid setting such as the Alexandra, North Saskatchewan, Mistaya, upper Columbia and lower Saskatchewan Rivers where anastomosis is the result of repeated avulsions (Makaske, 2001).

Crevasse splay and organic depositions are also common elements in anastomosing rivers (Makaske, 2001). Crevasse splay deposits in the Amazon are very restricted in the deposits described here, but present-day crevasses at several locations along the system can be observed from satellite imagery. Peat deposits are characteristic of long-lived, rapidly aggrading anastomosing rivers in a humid setting (Makaske, 2001). Organic deposition is very restricted in arid anastomosing rivers such as Cooper Creek, due to reduced plant growth (Rust, 1981). However, extensive peat deposits have been identified in semi-arid conditions in the Okavango River, southwest Africa (Cairncross *et al.*, 1988). The studied reach of the Amazon displays restricted organic deposition, but peat is not found despite the dense forest development.

The stable position of the channels (Smith and Smith, 1980; Rust, 1981; Smith, 1986) and the rarity or absence of meandering features (Smith, 1983; Nanson and Croke, 1992) has been considered a primary characteristic in anastomosing rivers. In

contrast, meandering secondary channels with the development of scroll bars and inclined heterolithic stratification are a distinctive feature in the anastomosing pattern of the Amazon River. Despite climatic differences with the Amazon, meandering characteristics have also been identified in several Australian anastomosing rivers: meandering channels in the Thomson River (Brizga and Finlayson, 1990), a meandering belt with scroll patterns in the Darling River (Bowler *et al.*, 1978), increase in sinuosity with time in the Ovens and King Rivers (Schumm *et al.*, 1996), lateral migration in the Murray River (Nanson and Knighton, 1996) and laterally accreted deposits in Cooper Creek with inclined heterolithic stratification (Gibling *et al.*, 1998). In anastomosing rivers in western Canada, narrow laterally accreting point bars with the development of sets of inclined heterolithic stratification on a small scale were found in the upper Columbia River (Smith, 1983; Thomas *et al.*, 1987). In the lower Saskatchewan River the channels show a tendency towards meandering (Makaske, 2001). In addition, meandering and braided channels may all form part of an anastomosing or anabranching river system (Nanson and Knighton, 1996; Makaske, 2001; Nanson and Gibling, 2003b). Makaske (2001) mentioned that these meandering features are not characteristic in anastomosing rivers, but they may be present.

Multichannel development

The conditions under which multiple channels develop seem to be related to insufficient gradients to move water, and particularly bed load through a single channel system (Nanson and Knighton, 1996; Nanson and Gibling, 2003b). Consequently, a new channel can be formed by a diversion of the flow into the floodplain (i.e. avulsion) (Makaske, 2001; Nanson and Gibling, 2003b); by within-channel deposition (Nanson and Gibling, 2003b) or by a combination of both mechanisms (Makaske *et al.*, 2009). Not only can within-channel deposition form islands that split the flow, generating new channels (Nanson and Gibling, 2003b), but bed aggradation can also act as a primary mechanism of avulsion (Makaske *et al.*, 2009). Avulsion as a primary cause of multiple channel development may be related to downstream and upstream controls. Downstream controls include damming and backtilting (Miall, 1992; Nanson and Gibling, 2003a) and rapidly subsiding setting which is the case in foreland and extensional basins (Makaske, 2001; Nanson and Gibling, 2003b). Upstream controls develop where excessive bed load supply can occur (Abbado *et al.*, 2005; Makaske *et al.*, 2009). High sedimentation rates (Smith, 1983, 1986) may act as upstream or downstream control. The processes associated with avulsion are responsible for creating the multichannel pattern in anastomosing rivers (Makaske, 2001).

It has been suggested that avulsion is responsible for the development of the Careiro Paraná, where the Amazon River progressively abandons its present-day course to the north (Sternberg, 1959). Sternberg (1959) discusses the avulsion of the Careiro Paraná based on oral tradition that suggests a very small channel in the beginning of the 19th century that has since been widening, in contrast to early historical maps from the 18th century that indicate the Paraná as a very wide channel. The lack of accurate data does not allow conclusions to be drawn about the evolution of the Paraná.

In the western part of Careiro Island there is a high concentration of overbank deposition interpreted as natural levee deposits (Figure 7). These levees develop on top of older floodbasin deposits in concave banks, which have been exposed by channel erosion, as noticed earlier by Sternberg (1959). This is indicative of the tendency for overbank deposition in the direction of the flow where the Careiro Paraná is located. Additionally, the eastern part of Careiro Island is geomorphologically

more similar to the floodplain in the southern margin of the river than to the other islands in the system (Figures 6(A) and 2(A)). Islands bound by natural levees with a saucer-like morphology were described as characteristic in the Amazon River (Sternberg, 1959; Baker, 1978) and in fact Careiro Island was described as an example of this morphology. The saucer-like morphology corresponds to the description of floodbasins by Makaske (2001), which are indicative of avulsion and are a key characteristic for distinguishing anastomosing from other multiple channel rivers. This suggests the enclosure of a part of the floodplain, forming Careiro Island, and the development of the Careiro Paraná as an avulsion process leading to the multichannel character in this part of the system.

The other islands in the system seem to have developed as a product of mid-channel bar formation and chute cut-offs of the main and secondary channels rather than from avulsion. These islands do not show similar morphology to the floodplain, as does Careiro Island. The islands, which are products of mid-channel bars, are formed by several sets of scroll bars that migrate in different directions from a central area, which is located towards the upstream part of the islands. Islands formed by this mechanism are Onças, Eva, Jacaré and Soriano. At low water levels, present-day deposition can be observed in the upstream part of Eva and Soriano Islands (see Figure 1(C) for location). Some of these islands also develop lakes on the downstream side of the central area, from where the scroll bars are migrating. Other islands develop wide lakes in the swales associated with the first scroll bars that were formed. The islands, which are a product of chute cut-offs of the main and secondary channels, are isolated from other islands by a chute channel developed on a scroll bar swale. This is evident since the chute channel follows more or less the same orientation as the other narrow lakes that occupied adjacent swales. Islands produced by this mechanism are Terra Nova, Parauacara and Marati, minor islands in front of Novo Remanso and Beija Flor Island (Figure 1(C)). Natural levee deposits develop mainly along concave banks of these islands (Figure 5), but they do not seem to be related with the development of any of the secondary channels downstream of Careiro Island.

Channel migration and islands stability

The temporal analysis indicates that the left margin of the fluvial system, which developed in terraced deposits with steep slopes, has remained relatively unchanged in the last 31.1 years when compared with the right margin, where floodplain deposits occur extensively (Figures 4(A) and 6(A)). Differences in resistance to erosion of the deposits in each margin and slight northward tilting of the basin seem to influence this behavior. Terraced deposits are characterized by locally silicified kaolinitic sandstone from the Alter do Chão Formation, coarse ferruginous sandstone from the Novo Remanso Formation and two ferricretes that were developed at the top of both formations (Rozo *et al.*, 2005b). In contrast, the sediments at the right margin are unconsolidated clay and sand. The terraced deposits are clearly more resistant to erosion than the deposits on the right margin and restrict channel migration toward the left margin. The asymmetric distribution of the floodplain deposits (Figure 6(A)) and the terraced deposits' steep slopes at the left margin (Figure 2(A)) suggest slight northward tilting of the basin. This tilting is probably linked to the ENE-oriented basin depocenters, which show Bouguer anomalies reaching -40 mgal located south of the study area (Figure 6(C)).

The differences in resistance to erosion mentioned above also explain why secondary channels meander, whereas the main channel does not. Terraced deposits in the left margin restrict the migration of the main channel and result in low sinuosity and the present-day ESE direction. In contrast,

secondary channels run almost entirely with both margins on unconsolidated sediments that form the islands and the floodplain. Unconsolidated sediments offer less resistance to erosion by secondary channels, allowing these to develop their meandering planforms. The main channel displays its most sinuous planform directly in front of Marati Island, where its right margin is in contact with the unconsolidated floodplain deposits. A concave erosional bend in the main channel is formed, and followed by a convex depositional bend with scroll bar configuration (Figure 6(A)). Secondary channels develop rectilinear planforms in only two locations, where their left margin is in contact with the terraced deposits. The first location is the Eva Paraná north of Jacaré Island (Figure 6(A)), with a 4 km straight margin following an ESE direction, while the right margin is convex with scroll bar development. The second location is the secondary channel that drains the Preto da Eva River into the Amazon River, it runs straight for 14 km to the ESE.

Vegetation and organic deposits in humid environments have a stabilizing effect on river banks (Smith, 1976; Hickin, 1984; Harwood and Brown, 1993; Huang and Nanson, 1997; Makaske, 2001). Vegetation also seems to be a stabilizing factor in the Amazon River, where a dense and well developed forest covers the islands and the floodplain. Additionally, new depositional areas are colonized by fast growing species. Besides vegetation, the development of ferricretes, as explained above, also acts as a climatic influence on lateral channel stability (Makaske, 2001). Vegetation contributes to the stability of the islands and the floodplain, but the unconsolidated nature and the high proportion of sandy deposits favors the migration of secondary channels. Extensive peat development has been described as a stabilizing factor on channel banks in semi-arid (Cairncross *et al.*, 1988; Stanistreet *et al.*, 1993) and humid temperate anastomosing rivers (Gradzinski *et al.*, 2003). Factors such as very restricted organic deposition and the absence of peat deposits seem to contribute to the relatively less stable channel banks in the Amazon River.

Additionally, stream power is frequently used to study lateral stability in river channels, since it involves two parameters (i.e. slope and discharge) that have been considered to influence channel stability directly (Makaske, 2001). Most anastomosing rivers, when considered as single hydraulic entities and compared with meandering and braided rivers, show lower stream power values (Knighton and Nanson, 1993). Latrubesse (2008) reports values of specific stream power for the Amazon River between 6.6 and 13.6 $W m^{-2}$ with a value of 12.2 $W m^{-2}$ at Jatuarana (30 km downstream of Manaus, see Figure 1(C)). However, these values are in the same range of specific stream power as other large meandering, braided and anastomosing rivers described by Latrubesse (2008). Again, these values are calculated considering the rivers as single hydraulic entities. Individual channels in multichannel systems should be considered separately, because each channel adapts to its discharge independently and consequently discharge distribution over various channels also indicates a reduction in stream power (Makaske, 2001). The tendency of anastomosing rivers to be relatively stable is partially explained by the low stream power in each channel (Makaske, 2001).

Development of the anastomosing pattern

Scroll bar deposits broadly distributed in the islands as well as some parts of the floodplain in the studied reach, were initially considered to belong to a single-channel meandering river that preceded the development of the current anastomosing pattern (Rozo, 2004). The change from single-channel meandering to anastomosing was suggested to have taken place between 6 and 4 ka BP, influenced by climate change from relatively dry to humid conditions (Latrubesse and Franzinelli, 1993; Turcq

et al., 1993; Hooghiemstra, 1995). It was also suggested that the anastomosing pattern could have developed after ~2 ka BP (Rozo, 2004). This assumption is based on radiocarbon dating in two deposits interpreted as point bars to 2.84 ± 0.08 ka BP (Terra Nova Island) (Absy, 1979) and 2.05 ± 0.12 ka BP (Careiro Island) (Sternberg, 1959). These were assumed to belong to a main single-channel meandering system. However, these dates are probably not reliable and of no use for the evaluation of anastomosis in the past. The data presented here clearly establish that the scroll bar deposits have developed at least since 7.5 ± 0.85 ka and are the product of meandering secondary channels as well as localized migration of the main channel in an established anastomosing river. This oldest date was estimated from sediments collected at a depth of 8 m in point bar deposits, over which the scroll bars developed (Profile 10 in Figure 7). Ages of other younger scroll bars vary between 5.5 ± 0.83 and 3.4 ± 0.6 ka.

Recently, Soares *et al.* (2010) dated point bar deposits of the Solimões River near Manacapuru (81 km upstream of the area of study) with ages from 34.5 ± 4.4 to 7.5 ± 0.9 ka, suggesting a mainly meandering fluvial system during that time. The morphology of the scroll bar deposits where these sediments are located is of the same scale as the main present-day channel of the Solimões River, suggesting that these deposits are from the main channel rather than from secondary channels. However, detailed studies of deposits older than those studied here must be undertaken to define the climatic or base-level changes that led to the development of the anastomosing pattern in the Amazon River.

The Amazon River has a consistent pattern of steepening channel gradient, as the river crosses the western structural arches (Figure 3(A)) (Mertes *et al.*, 1996). These authors suggest that subsidence in the basins due to sediment loading or current uplift of the arches is the cause of this behavior. Based on laboratory experiments, Ouchi (1985) demonstrated that meandering rivers, when affected by slow uplift, commonly increase in sinuosity on the downstream side of the uplift, while they adjust to the steeper valley floor. If the upstream slope becomes appreciably flatter, this reach will tend to straighten or anastomose. The Purus arch, which is the closest to the area of study, seems not to have any influence on the development of the anastomosing pattern downstream of Manaus. First, it does not seem to affect the channel pattern of the Amazon River, since the river is not more anastomosing or straight upstream of the arch nor more meandering downstream; and second, according to Ouchi (1985), the pattern of the Amazon River downstream of the arch should be more meandering, but the anastomosing pattern develops in this area.

Conditions for the development of anastomosis are optimal with low gradients and high floodplain aggradation rates, according to the conceptual genetic model for long-lived anastomosis developed by Makaske (2001). The Amazon in the study area has a very low gradient of 2.1 cm km^{-1} (Latrubesse, 2008) and a high average long-term aggradation rate of 1.1 mm yr^{-1} over 7.50 ± 0.85 ka. The sedimentation rate seems to be low when compared with other tropical humid anastomosing rivers such as the Magdalena River (3.8 mm yr^{-1}) (Smith, 1986) or the Solimões River upstream of the area of study (2.3 mm yr^{-1}) (Mertes, 1994). But this value is still high when compared with sedimentation rates of other anastomosing rivers (Makaske, 2001, his table II). Long-lived, rapidly aggrading anastomosing rivers in humid settings generally have higher slopes, while sedimentation rates are in the same range as the value obtained for the Amazon. Additionally, these rivers are the product of repeated avulsions due to continuous, rapid floodplain aggradation (Makaske, 2001). Avulsion does not seem to be common in the studied reach of the Amazon. The

single avulsion process discussed for these reaches of the Amazon is the present-day development of the Careiro Paran, where the coexistence of the main channel of the Amazon and this secondary channel seems to have been in effect since 7.50 ± 0.85 ka. This represents the oldest deposits dated for the Careiro Paran, and indicates a very low rate of abandonment of the older channel. Long-lived, slowly aggrading anastomosing rivers in an arid setting clearly are very different from the Amazon, based on the climatic setting and very low sedimentation rates.

The studied reach of the Amazon seems to pertain to the long-lived, semi-static anastomosing river category (Makaske, 2001, his Figure 7). Apart from the low abandonment rate of the older channel and the independence from high avulsion frequency mentioned above, these systems exist under stable external conditions and are also characterized by low sediment load (Makaske, 2001). In the Amazon there does not seem to be any external control on the development of anastomosis, at least in the last 7.50 ± 0.85 ka. However, the sediment load of the Amazon is higher when compared with other anastomosing rivers (Gupta, 2007, his Table I.1). In the studied reach, suspended load has been calculated at 786 Mt yr^{-1} (Dunne *et al.*, 1988) with bed load being 1% of the suspended load (Mertes, 1985). An abundant supply of fine material may contribute to the stability of the islands and the slow rate of meander development. The size of the river seems to be an important factor as well. Channel abandonment processes seemingly proceed much faster in smaller rivers, where, for example, fallen trees can block complete channels and vegetation development along the banks can relatively soon strangle channel flow and morphodynamics. In contrast, nearly abandoned secondary channels of the Amazon may still be 1 km wide and obviously are able to meander because of substantial bankfull flows. Complete abandonment of these channels probably simply occurs over long periods because channel abandonment processes (often related to vegetation) are not scaled to these large rivers and therefore are relatively less effective. In this context, low abandonment rates seems to apply to all secondary channels of this system, not only to the Careiro area.

Conclusions

The Amazon River between the confluences of the Negro and Madeira Rivers is more stable than reaches upstream and the mouth of the Madeira River. This behavior confirms a general trend where stability increases downstream, and which has been observed in the Amazon from Iquitos to the mouth of the Madeira River. However, active depositional and erosional margins are observed with maximum migration rates of 60 m yr^{-1} and 39 m yr^{-1} , respectively, indicating relative stability for this reach.

The anastomosing pattern in the studied reach of the Amazon River is characterized by:

- relative stability of the system,
- multichannel planform,
- relatively straight main channel,
- sinuous secondary channels with meander development,
- islands with saucer-like and/or scroll bar morphology fixed by trees and shrubs that divide flow up to bankfull,
- steep-sided island margins with height that roughly corresponds to that of the adjacent floodplain,
- discontinuous natural levees concentrated on the concave banks,
- very low gradient (2.1 cm km^{-1})
- and extensively distributed scroll bars.

Scroll bars in the studied reach of the Amazon have developed in a multichannel river system at least since 7.5 ± 0.85 ka. The morphology and sedimentary deposits indicate that these scroll bars are related to subrecent and present-day migration of secondary channels and localized migration of the main channel.

Fining upward successions formed in the convex channel bank by sand and clay couplets (scroll bar deposits) draping sandy point bar deposits and clay and organic-rich clays (flood-basin/floodplain lake deposits) covering the scroll bar deposits characterized the stratigraphy/architecture in the studied reach of the Amazon River. Natural levee deposits develop mainly on the concave channel banks and it is in these areas that previously formed fining upward successions are exposed by lateral channel bank erosion.

Avulsion is inferred to have played a minor role in the formation of this anastomosing system, accounting only for the development of the Careiro Paraná and the enclosure of a part of the floodplain, forming Careiro Island. In contrast, mid-channel bar formation and chute cut-offs of the main and secondary channels are the main formative mechanism of anastomosis in the system.

The meandering planform in secondary channels develops due to the unconsolidated nature of the deposits over which they run almost in their entirety. These unconsolidated deposits are clearly less resistant to erosion than the sandstones and ferricretes (terraced deposits) in the left margin, which restrict the migration of the main channel and result in low sinuosity and the present-day ESE channel trend. Vegetation contributes to the relative stability of the islands and the floodplain, but the unconsolidated nature and high proportion of sandy deposits favors the migration of secondary channels.

A low gradient and high long-term aggradation rate (1.1 mm yr^{-1}) are conditions which favor the development of anastomosis in the studied reach of the Amazon River. Additionally, stable external conditions, low abandonment rate of older channels and independence from high avulsion frequency suggest this system is a long-lived, semi-static anastomosing river *sensu* Makaske (2001). More research is required in order to determine the upstream and downstream continuity of the characteristics described here, and analyze causes for the development of this large anastomosing river.

Acknowledgments—This research was supported by the Graduate Program in Geosciences of the Universidade Federal do Amazonas, the Graduate Program in Geology and Geochemistry of the Universidade Federal do Pará and CNPq-CT-AMAZONIA Proc. 554059/2006-9. Max G. Rozo thanks CAPES and CNPq for awarding the scholarships. We would like to thank Professor Gerald Nanson and Dr Stephen Tooth for their valuable comments, suggestions and insight, and especially Dr Bart Makaske who helped to substantially improve this manuscript. We would like also to thank Roseane Sarges, Luciano Machado and Luiz Saturnino for their help with field work.

References

Abbado D, Slingerland R, Smith ND. 2005. Origin of anastomosis in the upper Columbia River, British Columbia, Canada. In *Fluvial Sedimentology VII*. Special Publication of the International Association of Sedimentologists, **35**, Blum MD, Marriot SB, Leclair SM (eds). Blackwell: Oxford; 3–15.

Absy ML. 1979. A palynological study of Holocene sediments in the Amazon basin. PhD thesis, University of Amsterdam, Amsterdam.

Andrade GOd. 1956. Furos, Parará e Igarapés; análise genética de alguns elementos do sistema potomográfico amazônico. *Boletim Carioca de Geografia* **9**: 15–50.

Araujo JFB, Montalvão RMG, Lima MIC, Fernandez PECA, Cunha FMBd, Fernandes CAC, Basei MAS. 1974. Geologia Folha SA-21-Santarém. In *Levantamento de Recursos Naturais Projeto RadamBrasil*. Departamento Nacional de Produção Mineral: Rio de Janeiro.

Baker VR. 1978. Adjustment of fluvial systems to climate and source terrain in tropical and subtropical environments. In *Fluvial Sedimentology*, Miall AD (ed). Canadian Society of Petroleum Geologists: Calgary; 211–230.

Bemerguy RL, Costa JBS, Hasui Y, Borges MD, Junior AVS. 2002. Structural geomorphology of the Brazilian Amazon Region. In *Contribuições à Geologia da Amazônia* **3**, Klein EL, Vasquez ML, Rosa-Costa LT (eds). Sociedade Brasileira de Geologia Núcleo Norte: Belém; 201–207.

Bowler JM, Stockton E, Walker MJ. 1978. Quaternary stratigraphy of the Darling River near Tilpa, New South Wales. *Proceedings of the Royal Society of Victoria* **90**: 78–88.

Brizga SO, Finlayson BL. 1990. Channel avulsion and river metamorphosis - the case of the Thomson River, Victoria, Australia. *Earth Surface Processes and Landforms* **15**: 391–404.

Cairncross B, Stanistreet IG, McCarthy TS, Ellery WN, Ellery K, Grobicki TSA. 1988. Paleochannels (stone-rolls) in coal seams - modern analogs from fluvial deposits of the Okavango Delta, Botswana, Southern-Africa. *Sedimentary Geology* **57**: 107–118. DOI: 10.1016/0037-0738(88)90020-6.

Caputo MV. 1984. Strigraphy, tectonics, paleoclimatology and paleogeography of northern basins of Brazil, PhD Thesis, University of California, Santa Barbara.

Caputo MV, Rodrigues R, Vasconcelos DNN. 1972. Nomenclatura estratigráfica da Bacia do Amazonas. In *XXVI Congresso Brasileiro de Geologia*. Sociedade Brasileira de Geologia: Belém; 36–46.

Costa JBS, Bemerguy RL, Hasui Y, Borges MD. 2001. Tectonics and paleogeography along the Amazon river. *Journal of South American Earth Sciences* **14**: 335–347.

Cunha PRC, Melo JHG, Silva OB. 2007. Bacia do Amazonas. *Boletim de Geociências da Petrobras* **15**: 227–251.

Dumont JF. 1993. Types of lakes as related neotectonics in Western Amazonia. In *Simpósio Internacional do Quaternário da Amazônia*. PICH/INQUA: Manaus; 99–102.

Dumont JF, Garcia F. 1991. Active subsidence controlled by basement structures in the Marañon Basin of Northeastern Peru. In *Fourth International Symposium on Land Subsidence*. International Association of Hydrological Sciences: Wallingford; 334–350.

Dunne T, Mertes LAK, Meade RH, Richey JE, Forsberg BR. 1988. Exchanges of sediment between the flood plain and channel of the Amazon River in Brazil. *Geological Society of America Bulletin* **110**: 450–467.

Fielding CR. 2006. Upper flow regime sheets, lenses and scour fills: Extending the range of architectural elements for fluvial sediment bodies. *Sedimentary Geology* **190**: 227–240.

Franzinelli E, Igreja HLS. 2002. Modern sedimentation in the Lower Negro River, Amazonas State, Brazil. *Geomorphology* **44**: 259–271.

Gibling MR, Nanson GC, Maroulis JC. 1998. Anastomosing river sedimentation in the Channel Country of central Australia. *Sedimentology* **45**: 595–619.

Gradzinski R, Baryla J, Doktor M, Gmur D, Gradzinski M, Kedzior A, Paszkowski M, Soja R, Zielinski T, Zurek S. 2003. Vegetation-controlled modern anastomosing system of the upper Narew River (NE Poland) and its sediments. *Sedimentary Geology* **157**: 253–276. DOI: 10.1016/S0037-0738(02)00236-1.

Gupta A. 2007. Introduction. In *Large Rivers: Geomorphology and Management*. Gupta A (ed). John Wiley & Sons: Chichester; 1–4.

Harwood K, Brown AG. 1993. Fluvial processes in a forested anastomosing river - flood partitioning and changing flow patterns. *Earth Surface Processes and Landforms* **18**: 741–748. DOI: 10.1002/esp.3290180808.

Hickin EJ. 1984. Vegetation and river channel dynamics. *Canadian Geographer-Geographe Canadien* **28**: 111–126. DOI: 10.1111/j.1541-0064.1984.tb00779.x.

Hooghiemstra H. 1995. Environmental and paleoclimatic evolution in Late Pliocene-Quaternary Colombia. In *Paleoclimatic and Evolution, with Emphasis on Human Origins*, Vrba ES, Denton G, Burckle LH, Partridge TC (eds). Yale University Press: New Heaven; 249–261.

Huang HQ, Nanson GC. 1997. Vegetation and channel variation; A case study of four small streams in southeastern Australia. *Geomorphology* **18**: 237–249. DOI: 10.1016/S0169-555X(96)00028-1.

- Irion G, Junk WJ, Mello JA. 1997. The large central Amazonian river floodplains near Manaus: Geological, climatological, hydrological and geomorphological aspects. In *The Central Amazon Floodplain: Ecology of a Pulsating System*, Junk WJ (ed). Springer: Berlin; 23–46.
- Iriondo M. 1982. Geomorfologia da planície Amazônica. In *IV Simpósio do Quaternário do Brasil*. Sociedade Brasileira de Geologia: Rio de Janeiro; 323–348.
- Junk WJ, Bayley PB, Sparks RE. 1989. The flood pulse concept in river-floodplain systems. In *Proceeding of the International Large River Symposium*. Canadian Special Publications of Fisheries and Aquatic Sciences, **106**, Dodge D (ed). Department of Fisheries and Oceans Canada: Ottawa; 110–127.
- Kalliola R, Salo J, Puhakka M, Rajasilta M, Häme T, Neller RJ, Räsänen ME, Danjoy Arias WA. 1992. Upper Amazon channel migration. *Naturwissenschaften* **79**: 75–79.
- Knighton D, Nanson GC. 1993. Anastomosis and the continuum of channel pattern. *Earth Surface Processes and Landforms* **18**: 613–625.
- Kristler P. 1954. Historical resume of the Amazon Basin. Petrobras/Renor (Internal report 104-A): Belém.
- Latrubesse EM. 2008. Patterns of anabranching channels: The ultimate end-member adjustment of mega rivers. *Geomorphology* **101**: 130–145. DOI: 10.1016/j.geomorph.2008.05.035.
- Latrubesse EM, Franzinelli E. 1993. Reconstrução das condições hidrológicas do passado. *Ciência Hoje* **16**: 40–43.
- Latrubesse EM, Franzinelli E. 2002. The Holocene alluvial plain of the middle Amazon River, Brazil. *Geomorphology* **44**: 241–257.
- Makaske B. 1998. Anastomosing rivers; forms, processes and sediments. *Nederlandse Geografische Studies* 249, Koninklijk Nederlands Aardrijkskundig Genootschap/Faculteit Ruimtelijke Wetenschappen, Universiteit Utrecht, Utrecht.
- Makaske B. 2001. Anastomosing rivers: a review of their classification, origin and sedimentary products. *Earth-Science Reviews* **53**: 149–196.
- Makaske B, Smith DG, Berendsen HJA, de Boer AG, van Nielen-Kiezebrink MF, Locking T. 2009. Hydraulic and sedimentary processes causing anastomosing morphology of the upper Columbia River, British Columbia, Canada. *Geomorphology* **111**: 194–205.
- Mertes LAK. 1985. Floodplain development and sediment transport in the Solimões-Amazon River in Brazil. MSc thesis, University of Washington, Seattle.
- Mertes LAK. 1994. Rates of floodplain sedimentation on the central Amazon River. *Geology* **22**: 171–174. DOI: 10.1130/0091-7613(1994)022 < 0171:rofps > 2.3.co;2.
- Mertes LAK, Dunne T, Martinelli LA. 1996. Channel-floodplain geomorphology along the Solimões-Amazon River, Brazil. *Geological Society of America Bulletin* **108**: 1089–1107.
- Miall AD. 1992. Alluvial Deposits. In *Facies Models: Response to Sea Level Change*, Walker RG, James NP (eds). Geological Association of Canada: St. John's; 119–142.
- Moura PA. 1944. O relevo da Amazônia. In *Amazônia Brasileira*. Instituto Brasileiro de Geografia e Estatística – IBGE: Rio de Janeiro; 14–23.
- Murray AS, Wintle AG. 2000. Luminescence dating of quartz using an improved single-aliquot regenerative-dose protocol. *Radiation Measurements* **32**: 57–73.
- Nanson GC. 1980. Point-bar and floodplain formation of the meandering Beaton River, Northeastern British-Columbia, Canada. *Sedimentology* **27**: 3–29.
- Nanson GC, Croke JC. 1992. A genetic classification of floodplains. *Geomorphology* **4**: 459–486.
- Nanson GC, Gibling MR. 2003a. Rivers and alluvial fans. In *Encyclopedia of Sediments and Sedimentary Rocks*, Middleton GV (ed). Kluwer Academic Publishers: Dordrecht; 568–582.
- Nanson GC, Gibling MR. 2003b. Anabranching Rivers. In *Encyclopedia of Sediments and Sedimentary Rocks*, Middleton GV (ed). Kluwer Academic Publishers: Dordrecht; 9–11.
- Nanson GC, Knighton D. 1996. Anabranching rivers: their cause, character and classification. *Earth Surface Processes and Landforms* **21**: 217–239.
- Ouchi S. 1985. Response of alluvial rivers to slow active tectonic movement. *Bulletin of the Geological Society of America* **96**: 504–515.
- Pärrsinen MH, Salo JS, Räsänen ME. 1996. River floodplain relocations and the abandonment of Aborigine settlements in the Upper Amazon Basin: A historical case study of San Miguel de Cunibos at the Middle Ucayali River. *Geoarchaeology* **11**: 345–359.
- Peixoto JMA, Nelson BW, Wittmann F. 2009. Spatial and temporal dynamics of river channel migration and vegetation in central Amazonian white-water floodplains by remote-sensing techniques. *Remote Sensing of Environment* **113**: 2258–2266. DOI: 10.1016/j.rse.2009.06.015.
- Rossetti DD, de Toledo PM, Goes AM. 2005. New geological framework for Western Amazonia (Brazil) and implications for biogeography and evolution. *Quaternary Research* **63**: 78–89. DOI: 10.1016/j.yqres.2004.10.001.
- Rozo JMG. 2004. Evolução Holocênica do Rio Amazonas entre a Ilha do Careiro e a foz do Rio Madeira. MSc thesis, Universidade Federal do Amazonas, Manaus.
- Rozo MG, Soto CC. 2010. Quantification of change and migration rates in the Amazon River. In *45 Congresso Brasileiro de Geologia*. Sociedade Brasileira de Geologia: Belém.
- Rozo JMG, Nogueira ACR, Carvalho A. 2005a. Análise multitemporal do sistema fluvial do Amazonas entre a ilha do Careiro e a foz do rio Madeira. In *XII Simpósio Brasileiro de Sensoriamento Remoto*. Instituto Nacional de Pesquisas Espaciais: Goiânia; 1875–1882.
- Rozo JMG, Nogueira ACR, Horbe AMC, Carvalho A. 2005b. Depósitos Neogênicos da Bacia do Amazonas. In *Contribuições à Geologia da Amazônia 4*, Horbe AMC, Souza VS (eds). Sociedade Brasileira de Geologia Núcleo Norte: Manaus; 201–207.
- Rust BR. 1981. Sedimentation in an arid-zone anastomosing fluvial system - Cooper's Creek, central Australia. *Journal of Sedimentary Petrology* **51**: 745–755.
- Santos FAM. 2000. Growth and leaf demography of two *Cecropia* species. *Revista Brasileira de Botânica* **23**: 133–141.
- Schumm SA, Erskine WD, Tilleard JW. 1996. Morphology, hydrology, and evolution of the anastomosing Owens and King Rivers, Victoria, Australia. *Geological Society of America Bulletin* **108**: 1212–1224. DOI: 10.1130/0016-7606(1996)108 < 1212:MHAEOT > 2.3.CO;2.
- Smith DG. 1976. Effect of vegetation on lateral migration of anastomosed channels of a glacier meltwater river. *Geological Society of America Bulletin* **87**: 857–860. DOI: 10.1130/0016-7606(1976)87 < 857:eovlm > 2.0.co;2.
- Smith DG. 1983. Anastomosed fluvial deposits: modern examples from Western Canada. In *Modern and Ancient Fluvial Systems, Special Publication of the International Association of Sedimentologists* **6**, Collinson J, Lewin J (eds). Blackwell: Oxford; 155–168.
- Smith DG. 1986. Anastomosing river deposits, sedimentation rates and basin subsidence, Magdalena River, northwestern Colombia, South America. *Sedimentary Geology* **46**: 177–196.
- Smith DG, Smith ND. 1980. Sedimentation in anastomosed river systems: examples from alluvial valleys near Banff, Alberta. *Journal of Sedimentary Petrology* **50**: 157–164.
- Soares EAA, Tatumi SH, Ricominni C. 2010. OSL age determinations of Pleistocene fluvial deposits in Central Amazonia. *Anais da Academia Brasileira de Ciências* **82**: 1–9.
- Stanistreet IG, Cairncross B, McCarthy TS. 1993. Low sinuosity and meandering bedload rivers of the Okavango fan - channel confinement by vegetated levees without fine sediment. *Sedimentary Geology* **85**: 135–156. DOI: 10.1016/0037-0738(93)90079-k.
- Sternberg HOR. 1950. Vales tectônicos na Planície Amazônica? *Revista Brasileira de Geografia* **4**: 3–26.
- Sternberg HOR. 1959. Radiocarbon dating as applied to a problem of Amazonian morphology. In *XVIII Congrès International de Géographie*. Union géographique internationale: Rio de Janeiro; (2) 399–424.
- Taylor G, Woodyer KD. 1978. Bank deposition in suspended-load streams. In *Fluvial Sedimentology*, Miall AD (ed). Canadian Society of Petroleum Geologists: Calgary; 257–275.
- Thomas RG, Smith DG, Wood JM, Visser J, Calverley-Range EA, Koster EH. 1987. Inclined heterolithic stratification - terminology, description, interpretation and significance. *Sedimentary Geology* **53**: 123–179.
- Turcq B, Suguio K, Martin L, Flexor JM. 1993. Registros milenares nos sedimentos dos lagos da serra do Carajás. *Ciência Hoje* **16**: 31–35.
- Wanderley Filho JR. 1991. A Evolução estrutural da bacia do Amazonas e sua relação com o embasamento. MSc thesis, Universidade Federal do Pará, Belém.
- Wohl EE. 2007. Hydrology and Discharge, In *Large Rivers: Geomorphology and Management*, Gupta A (ed). John Wiley & Sons: Chichester; 29–41.

3 RECENT FLUVIAL DYNAMICS OF THE COLOMBIAN AMAZON RIVER*

Max G. Rozo¹, Carlomagno Soto Castro², Afonso C. R. Nogueira¹

¹ *Instituto de Geociências, Universidade Federal do Pará, CP 1611, 66.075-900, Belém/PA, Brasil*

² *Organization for Tropical Studies- OTS, Puerto Viejo, Costa Rica*

* Submitted to Remote Sensing of Environment

Abstract

An analysis of fluvial dynamics of the Colombian Amazon River, was carried out for a period of 19.9 years. Remote sensing image processing techniques were applied to Landsat images acquired on July 19, 1986; November 14, 1994; July 20, 2001 and June 24, 2006. These images were selected from a database of 44 Landsat images based on minimal daily water level variations while providing the longest temporal span. The images were processed using the Brazilian software SPRING with the method of unsupervised classification *Isoseg*, to distinguish between land and water categories. Subsequent visual evaluation was made to classify land categories into recent deposition and islands. Finally the areas of the main channel, islands and recent deposition, as well as the areas of erosion and deposition were estimated using ArcMap. Geomorphologic characteristics were examined, based on remote sensing data. The analysis revealed a depositional tendency of the system between 1986 and 2006, with a period where erosion was more intense than deposition between 1994 and 2001. Percent change in the plan view area of the system ($1.4\% \text{ yr}^{-1}$) and the maximum migration rates (125 m yr^{-1}) suggest that reach of the Amazon is less active than reaches upstream and the specific reach downstream between the confluences of the Jutai and Japurá Rivers. Variations in discharge, evaluated through a hydrological analysis, seem to be responsible for deposition and erosion dynamics found from remote sensing analysis in the Colombian Amazon River. Characteristics such as the multichannel platform, the sinuous main and secondary channels with meander development, lateral activity of the channel margins, islands dominated by scroll bar morphology, the absence of islands with saucer-like morphology and extensively distributed scroll bars on the river floodplain suggest a

multichannel meandering pattern for this reach of the Amazon, that corresponds to a laterally active anabranching river.

Keywords: Amazon River, remote sensing, temporal analysis, anabranching laterally active pattern.

Introduction

Large rivers are defined in terms of their drainage basin, length, the volume of sediment transported and water discharge (Potter 1978). Depending on the criteria used, different classification systems exist for these rivers (Inman and Nordstro 1971; Potter 1978; Meade 1996; Gupta 2007). It appears that relying solely on specific subjective, quantitative values for river classification is problematic in the case of large systems in general. Although it is difficult to define criteria for large rivers (Inman and Nordstro 1971; Potter 1978; Meade 1996; Gupta 2007), it is well established that such rivers are the major conveyors of sediments from the continents to the oceans. Syvitski et al. (2005) have estimated that approximately 21Gt yr^{-1} of sediments were supplied by large rivers to oceanic basins, mostly as suspended load. The transit of such amounts of sediments is also associated with the diversity of landscapes and fluvial facies. Large rivers are characterized by wide floodplains where sediment is stored temporarily and remobilized from time to time. These systems are also characterized by the presence of different channel patterns, from single sinuous channels to anastomosing reaches.

The Amazon River is the largest river in the world in terms of mean annual discharge ($175,000\text{ m}^3\text{ s}^{-1}$) and drainage area ($6,915,000\text{ km}^2$) (Wohl 2007). Recent estimations indicate a mean annual discharge of $209,000\text{ m}^3\text{ s}^{-1}$ (Latrubesse 2008) and mean annual sediment discharge at Obidos gauging station of 754 Mt yr^{-1} (Martinez et al. 2009). The Amazon is more than 6,000 km long and runs from the Andes in Peru to the Atlantic Ocean in Brazil (Figure 1A). In Peru, the river is known as the Amazonas below the junction of the Marañon and Ucayali Rivers (Figure 1B). In Colombia, the river runs for no more than 100 km and it is also known as the Amazonas. After entering Brazil the river is denominated Solimões and the name Amazonas is not used until the junction with the Negro River at Manaus (Figure 1B). Here we refer to the Amazon as the entire fluvial system.

The Amazon River follows a generally increasing trend in stability between the Iça and Madeira Rivers (Figure 1B) (Mertes et al. 1996). River stability has been evaluated using satellite images and based on the percentage of change in the plan view area per year. Change

in the plan view area values between $2\% \text{ y}^{-1}$ and $0.2\% \text{ y}^{-1}$ were found at the confluence with the Jutáí River and the confluence with the Negro River, respectively (Mertes et al. 1996). Recently, percent change values in the plan view area of the Amazon have been estimated at $1.8\% \text{ y}^{-1}$ at the confluence with the Japurá River (Peixoto et al. 2009) and at $0.6\% \text{ y}^{-1}$ between the confluences of the Negro and Madeira Rivers (Rozo et al. 2012). These values are in agreement with the generally increasing trend in stability demonstrated by Mertes et al. (1996). Differences between estimates are related to more accurate remote sensing tools and longer periods of time analyzed used by Peixoto et al. (2009) and Rozo et al. (2012). Maximum migration rates estimated in different reaches of the Amazon River reflect a similar increasing stability trend from upstream to downstream. Migration rates of 400 m yr^{-1} (Kalliola et al. 1992) and 213 m yr^{-1} (Rozo and Soto 2010) have been reported in the Upper Amazon River in the Iquitos area (Peru) and near Leticia (Colombia), respectively (Figure 1B). In the Brazilian Amazon River, rates of 140 m yr^{-1} (Mertes et al. 1996) and 60 m yr^{-1} (Rozo et al. 2012) were reported for the reaches near Fonte Boa and Manaus, respectively (Figure 1B).

These quantifications of the percentage of change in the plan view area per year and migration rates are in agreement with the channel pattern classifications of different reaches of the Amazon. Kalliola et al. (1992) describe some reaches in Peru with predominantly meandering and even straight patterns. Baker (1978) refers to the Solimões River as having both meandering and anastomosing patterns. A predominantly anastomosing pattern was also attributed to the Brazilian Amazon River (Mertes et al. 1996; Latrubesse and Franzinelli 2002; Rozo 2004), mainly based on its multichannel pattern and relatively stability. In the Amazon River downstream the confluence with the Negro River, the anastomosing pattern has been characterized by the development of islands with saucer-like morphology due to bounded natural levees (Sternberg 1959; Rozo et al. 2012). The saucer-like morphology corresponds to Makaske's (2001) description of floodbasins, which are indicative of avulsion and are a key characteristic for distinguishing anastomosing from other multiple channel rivers. This morphology was also recognized by Baker (1978) in the Solimões River. Rozo et al. (2012) identified meandering secondary channels as well as localized migration of the main channel in the anastomosing pattern of the Amazon River downstream Manaus. The meandering features in the form of scroll bars were also identified by others in different anastomosing reaches of the Amazon (Mertes et al. 1996; Latrubesse and Franzinelli 2002). In this context, it is clear that the Amazon, with its meandering secondary channels, is different

from many other anastomosing rivers (e.g. Makaske 1998, 2001) than have laterally stable, non-meandering channels.

Recently, Latrubesse (2008) described the Amazon River, as a whole, as predominantly anabranching. The term anabranching is applied to any type of multiple channel pattern, whereas anastomosing rivers are a low-energy type with cohesive or organic-rich floodplains (Nanson and Knighton 1996). From the available remote sensing data and field descriptions of the Amazon (Sternberg 1959; Baker 1978; Latrubesse and Franzinelli 2002; Rozo 2004; Latrubesse 2008; Rozo et al. 2012) it is clear that the Brazilian Amazon is anastomosing as understood by Makaske (2001) and it is also anabranching *sensu* Nanson and Knighton (1996).

To our knowledge, no research has yet been published which explains the behavior of the Colombian Amazon River, and specifically whether this reach of the Amazon develops meandering features as do the upper reaches, or whether it shares the characteristic main anastomosing pattern with meandering secondary channels of the Amazon River in Brazil. Therefore, in the present study the plan view changes of the Colombian Amazon River between 1986 and 2006 (Figure 1C) are quantified and its geomorphologic characteristics examined, based on remote sensing data. Also, a hydrological analysis based on discharge is presented to determine whether changes in the river's plan view are a direct response to variations in discharge.

Study area

The reach of the Amazon River studied here is located upstream of the confluence with the Javari River, in the Colombian section of the river (Figure 1C). The area includes an upstream reach of the Amazon River in Peruvian territory, as well as a reach downstream in Brazil where the towns of Tabatinga and Benjamin Constant are located. In this reach, the Amazon River is a multichannel system with both the main and secondary channels exhibiting a meandering planform (Figure 1C). The channels are straight and sinuous, with sinuosity varying from 1.02 to 1.72 in the main channel and from 1.03 to 3.08 in secondary channels. The width of the river varies from 1 to 12 km, with variation in the main channel varying from 1 to 4.4 km. At Nazareth (Figure 1C) the mean annual discharge is $34,757 \text{ m}^3 \text{ s}^{-1}$. The slope of the water's surface at Teresina (22 kilometers downstream the area of study, see Figure 1B) is 3.8 cm km^{-1} , decreasing to 3.4 cm km^{-1} at the confluence with the Iça River (Putumayo River in Colombia) and bed size material is medium sand with a $D_{50} = 0.3 \text{ mm}$ (Latrubesse 2008).

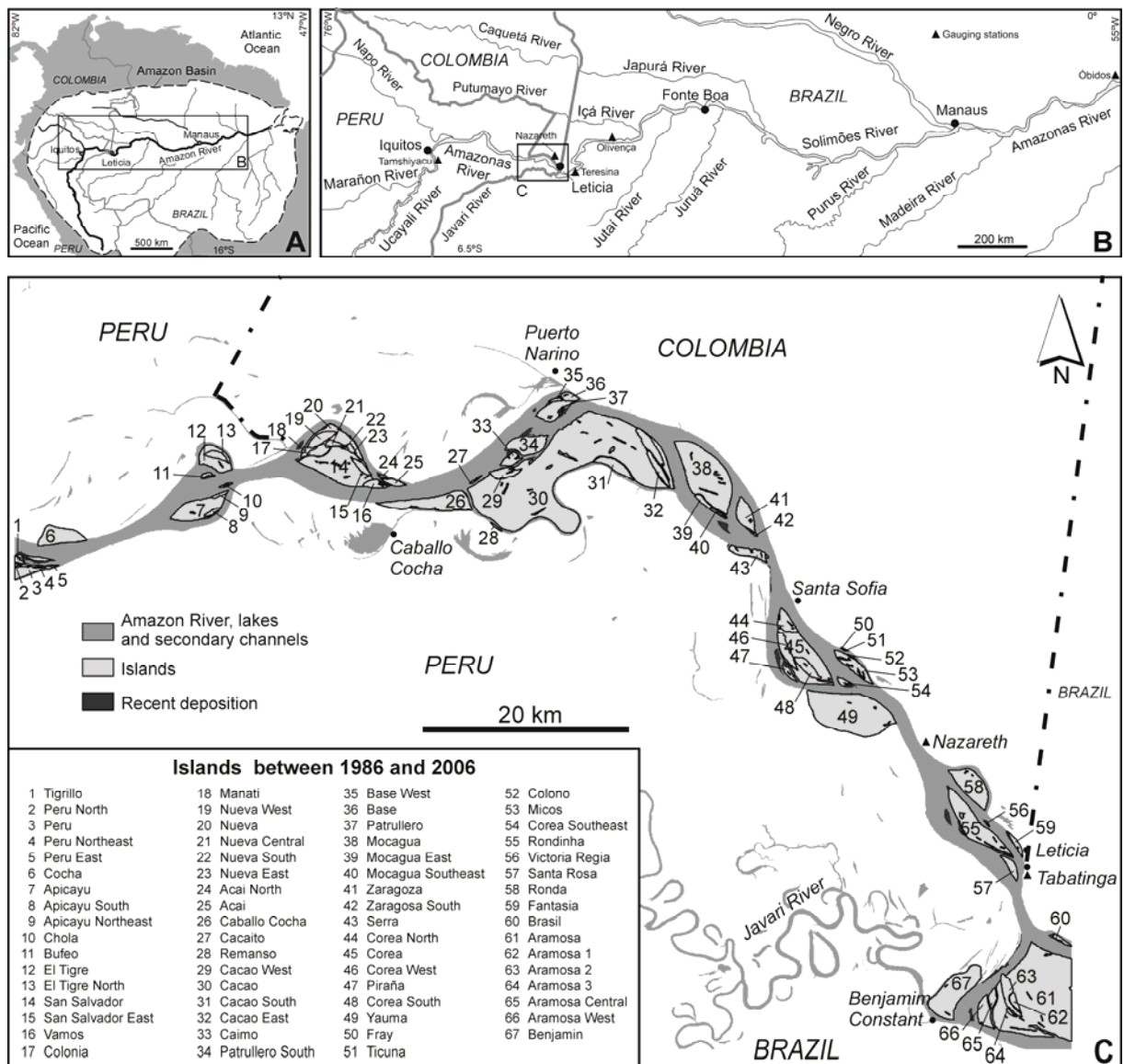


Figure 1. Location map of the Colombian Amazon River. A) Amazon Basin. B) Regional map of the Amazon River between Iquitos, Peru and Manaus, Brazil. We refer to the Ucayali-Amazonas-Solimões system as the Amazon River. Locations of gauging stations considered in the hydrological analysis are indicated. C) Studied reach of the Amazon River. This map was generated based on the Landsat image June 24 2006. Islands not present at that time were added to the map in order to show the location of all islands studied.

A seasonal flood pulse controls water dynamics of the Amazon, with the high level reached in June and the low water stage occurring around December (Junk et al. 1989). Precipitation is responsible for the mean amplitude of the annual water-level fluctuations which, in the central Amazon region, can reach 10 m (Irion et al. 1997).

Materials and methods

Most temporal analyses of areas along the Amazon River used Landsat imagery with a spatial resolution of 30 m (Rozo 2004; Peixoto et al. 2009; Rozo et al. 2012). Also, Landsat images with spatial resolution of 80 m resized to 30 m have been used by Rozo et al. (2012) and radar images with a 16 m spatial resolution were used by Mertes et al. (1996). Water level fluctuations between the images selected for analysis are more variable among different authors: 82 cm (Rozo 2004), 1 to 2.9 m (Peixoto et al. 2009) and 12 cm (Rozo et al. 2012). Images were selected by Mertes et al. (1996) from the low water season without considering actual water level fluctuations.

In this study, Landsat images (WRS-2, path 004, Row 063) with spatial resolution of 30 meters were first selected from three different databases: 1) Earth Resources Observation and Science Center (EROS) from the United States Geological Survey, 2) Global Land Cover Facility (GLCF) from the National Aeronautics and Space Administration (NASA) and the University of Maryland and 3) Image Generation Division (DGI) from the National Institute for Space Research (INPE), Brazil. A visual evaluation of the cloud cover was undertaken for the images available, and 44 images were selected based on minimal or absent cloud cover near or over the main channel.

The water level on the acquisition date of each of the 44 images was obtained to choose images with minimal daily water level variation. Daily water level data of the Amazon River, measured at the Tabatinga gauging station (Figure 1C), were obtained from Brazil's National Water Agency (ANA). Only water level variations equal to or less than 52 cm were considered (Table 1). This criterion was chosen because it gave enough images to cover a broad time interval. Another consideration was to select images acquired during the dry season, which allows better detection of changes in fluvial dynamics. Four Landsat images were selected as shown in Table 1, covering nearly 20 years between July 19, 1986 to June 24, 2006. Images taken on November 14, 1994 and July 20, 2001 were selected based on water level variations and to document the behavior of the system for the periods 1986-1994, 1994- 2001 and 2001-2006.

Daily water discharge data from four different gauging stations were obtained to analyze the relationship between hydrological patterns and the results of the temporal analysis. Selected stations include: Tamshiyacu in Peru, upstream of the area of study; Nazareth in Colombia, inside the area of study; Teresina and Olivença in Brazil downstream the area of study (Figure 1B). Discharge data from the stations in Peru and Brazil were obtained from Brazil's National Water Agency (ANA) and discharge for the Colombian

station was obtained from the National University of Colombia in Leticia. Water discharge data was not available for Tabatinga station, from which water level data was obtained. Some gaps in water discharge data existed: data were not available for Nazareth in 1986, 1987 and the July-August period in 1988; Teresina stopped recording data in October 1997, that is why the data for this station was omitted for further analysis; and data were not available for Olivença between May and August 1990. Discharge values for Tamshiyacu calculated before and after December 2005 showed large differences, and this was also the case for water levels. For these reasons, data reported after December 2005 was not used in this analysis.

Table 1. Landsat data used in this study. Water level and time variation between image acquisition dates are also indicated. The Landsat images were obtained from: (1)<http://glovis.usgs.gov/>; (2) <http://glcf.umiacs.umd.edu/index.shtml>; and (3) <http://www.dgi.inpe.br/CDSR/>. Water levels were obtained from Agência Nacional de Águas in Brazil.

Dataset	Image source	Acquisition date	Water level (cm)	Water level variation (cm)			Time variation (years)		
				19-Jul-86	14-Nov-94	20-Jul-01	19-Jul-86	14-Nov-94	20-Jul-01
5 (TM)	2	19-Jul-86	708	0	14	22	0	8.3	15
7 (ETM+)	2	14-Nov-94	694	14	0	36	8.3	0	6.7
7 (ETM+)	1	20-Jul-01	730	22	36	0	15	6.7	0
5 (TM)	3	24-Jun-06	678	30	16	52	19.9	11.6	4.9

Image processing

The images used for analysis were already georeferenced, with a maximum root mean square error (RMSE) of 50 m (Tucker et al. 2004). This corresponds to ± 50 m (1.7 pixels) in each migration rate calculated between each of the periods. For migration rates in m yr^{-1} this error is $\pm 6 \text{ m yr}^{-1}$ (1986-1994), $\pm 7 \text{ m yr}^{-1}$ (1994-2001), $\pm 10 \text{ m yr}^{-1}$ (2001-2006) and $\pm 3 \text{ m yr}^{-1}$ (1986-2001). The error varies in each calculated area, but follows the following trend: $1 \text{ km}^2 \pm 0.1 \text{ km}^2$, $5 \text{ km}^2 \pm 0.3 \text{ km}^2$, $20 \text{ km}^2 \pm 1.1 \text{ km}^2$, and for 50 km^2 2.6 km^2 .

Images were processed using the Georeferenced Information Processing System (SPRING) 4.1 developed by the National Institute for Space Research (INPE) in Brazil. Segmentation and classification were applied during image processing. The method of segmentation was based on a region growing algorithm applied to color compositions R(5)G(4)B(3). Following segmentation, an extraction of the attributes of the regions was carried out. We used the classifier Isoseg. The areas classified by the system, following an unsupervised procedure, were grouped into two predefined classes: water and land. This process allowed the delimitation by region of the water bodies and the non flooded land. Classified images were subjected to a procedure of vector generation from the matrix format of the classified image. Digital processing of the images provided the contours of the fluvial

system of the Colombian Amazon River, including some areas in Peru and Brazil. These data were organized as information layers inside of a SPRING project.

Editing and river dynamics quantification

The classified images were exported as shapefiles into ArcMap. There, manual corrections were made based on the elimination of clouds and shadows and to correct any errors which had occurred during the classification process. A visual post-classification process was carried out to separate land areas inside the main channel that were devoid of any vegetation cover. These areas, defined as recent deposition, correspond to emerged areas where vegetation has not yet become established; they are generally covered by water at bank full discharge. In this analysis, areas of recent deposition are visible because the images were recorded at low water stages. When the recent deposition is colonized by vegetation, it becomes an island or part of an island, or it can also be attached to the floodplain. Finally, the plan view area of the channels, islands and recent deposition was calculated. These areas were compared between 1986-1994, 1994-2001, 2001-2006 and 1986-2006, to determine the percentage of change in the plan view area of each geoform.

The identification of pixel class-change for each of the four periods (1986-1994, 1994-2001, 2001-2006 and 1986-2006) was carried out. Over these time periods, the following changes were recognized: (1) Deposition: changes from water to islands, water to recent deposition and water to floodplain; (2) Erosion: changes from floodplain to water, recent deposition to water and islands to water; (3) Erosion/deposition: changes from floodplain to recent deposition, and islands to recent deposition. In this category, areas from the floodplain and islands were eroded first before new sediments were deposited. (4) Changes between land categories: from floodplain to islands, recent deposition to islands, recent deposition to floodplain and islands to floodplain; (5) No change.

For the time periods considered, the plan view areas of each category (change or no change) were calculated. The percentage of change in each category was estimated with respect to the total plan view area between the banks over which the change occurred (total area of change and no change). The sum of percent change for the categories of deposition and erosion provided a percent change in the plan view area of the system. This value was also divided by the number of years over which the change occurred, giving a percent change in the plan view area of the system per year (Mertes et al. 1996). Land change categories were not added to the percent change in the plan view area of the system since islands may be excised parts of the floodplain or vice versa and recent deposition can become islands or

floodplain, representing a change in the geoform classification but not a real erosional or depositional change. Migration rates in meters per year were calculated at specific locations where there is an evident tendency for the river to erode or deposit.

Shuttle Radar Topographic Mission (SRTM) digital elevation data with 90 m of spatial resolution was obtained from the Consultative Group on International Agricultural Research - Consortium for Spatial Information (CGIAR-CSI). This SRTM image, as well as Landsat images were used to interpret geomorphology in the area.

Discharge related to erosion and deposition patterns

For each gauging station, monthly water discharge was calculated using available data. Mean monthly water discharge was calculated between July 1986 and June 2006, for each of the stations, as well. The variation (g') in monthly discharge (f) with respect to mean monthly discharge (Q_{mean}) over the period of study for each station was plotted as $g' = f - Q_{\text{mean}}$ (Figures 8, 9 and 10). For each subperiod of study (July 1986 – November 1994, November 1994 – July 2001 and July 2001 – June 2006) the mean variation, standard deviation and extreme events were calculated and normal distributions plotted. Variation in monthly water discharge with respect to mean monthly discharge was plotted against time, and compared with erosion and deposition periods obtained from the temporal analysis (Figures 8, 9 and 10).

Results

Temporal analysis

The temporal analysis of the Colombian portion of the Amazon River shows its evolution between 1986 and 2006. Changes in the channel, islands and areas of recent deposition are evident from a simple visual evaluation of maps generated on the four dates of comparison used in this analysis. Figure 2 shows the changes for the overall period. More specific variations in the channel, islands and recent deposition between 1986-1994, 1994-2001 and 2001-2006, are presented in Figures 3, 4 and 5 respectively. Table 2 also shows the evolution of islands which were accreted, formed, eroded or remained the same at each date. This table clearly shows the accretion and emergence of new islands toward 2006.

Channel changes between July 19, 1986 and November 14, 1994

Over this 8.3 year period, the plan view area of the channels in the studied reach was reduced by 1.5%, while the plan view area of the islands was increased by 8.1% (Table 2); these

processes represent net deposition in the system. The change in the plan view area of recent deposition by -41.9% indicates erosion. However, these areas could become colonized by vegetation and consequently become islands, parts of islands, or part of the floodplain, and thus would not contribute to a real erosional process. Comparing the total plan view area of the islands, channels and recent deposition between 1986 and 1994 (Table 2), 5.4 km² is lost by the channels (through deposition inside them), 27.2 km² is accreted to islands and 6.9 km² is lost by recent deposition. We observed more deposition than erosion.

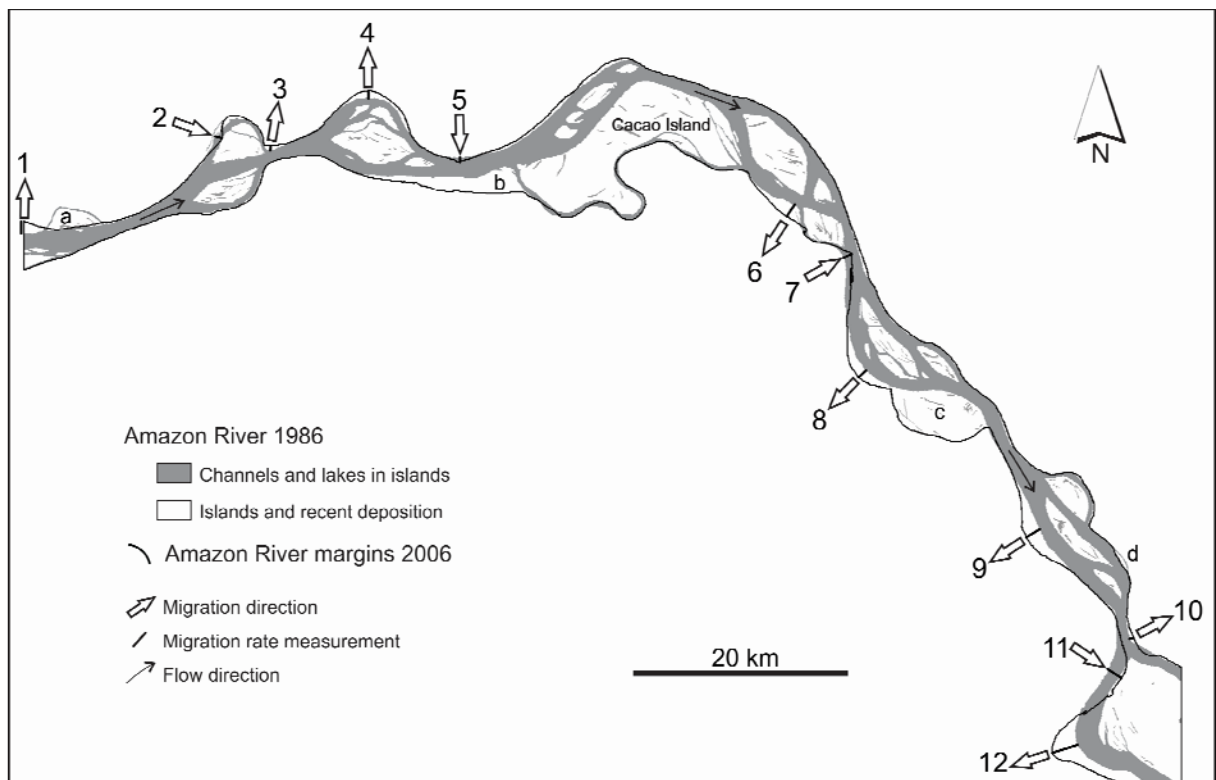


Figure 2. Amazon River margin changes between 1986 and 2006. Sites where maximum migration rates were recorded are indicated and specific values of migration are shown in Table 4. Areas not considered as channel migration are: (a) Cocha Island, that was accreted to the floodplain by 2001; (b) Caballo Cocha Island, which was isolated from the floodplain by 2001; (c) Yauma Island, which by 2006 was being accreted to the floodplain, with a channel to the south that still remains active during high water stages; (d) Fantasia island, which was accreted to the floodplain by 2006.

The changes in the plan view area of the islands show a tendency for deposition towards 1994 (Table 2). Lateral accretion of existing islands corresponds to 17.3 km² and new islands amount to 18 km². In contrast, plan view area partially eroded from existing islands is 8 km² and 0.1 km² of islands was fully eroded by 1994. Of the 38 islands present in 1986, 23 increased in plan view area with a maximum increase of 205% (Base Island) while five islands suffered reductions in area with a maximum rate of 54% at Peru Northeast Island.

Table 2. Percent change in the plan view area of islands, channels and recent deposition in the Colombian Amazon River. The plan view area at each date and for each island is indicated, as well as the total plan view area of islands, channels and recent deposition. Location of the islands is indicated in Figure 1C.

Feature	Plan view area (km ²)				Percent change in the plan view area			
	1986	1994	2001	2006	1986-1994	1994-2001	2001-2006	1986-2006
Peru	2.00	2.02	2.39	2.47	1.2	5.9	3.0	10.3
Peru East	0.24	0.24			0.7			
Peru North	0.13	0.10	0.09	0.11	-24.3	-7.8	14.6	-20.0
Peru Northeast	0.45	0.20			-54.5			
Tigrillo				0.64				
Caiman			0.57	0.72			26.1	
Caiman East				0.02				
Cocha	6.12	6.64			8.5			
Apicayu	6.92	8.30	8.47		11.4	2.1		
Apicayu South	0.52			9.10			1.9	22.2
Apiyacu Northeast		0.60	0.46			-23.5		
Chola				0.07				
Bufeo				0.16				
El Tigre	8.80	8.76	7.77	6.42	-13.7	-11.4	-17.3	-36.8
El Tigre North	1.35							
San Salvador	14.29							
San Salvador East	1.23	18.55	19.03	18.10	8.8	1.7	-4.9	6.1
Vamos	1.53							
Nueva South		0.17						
Nueva	0.93	1.52			62.5			
Nueva East	0.52	0.84	7.54		60.0	36.1		
Nueva West		2.45		10.53			12.6	298.5
Nueva Central		0.74						
Colonia	1.19	1.28	1.66		8.2	29.0		
Manati			0.16					
Acai				1.06				
Acai North				0.16				
Caballo Cocha			11.30	10.58			-6.4	
Remanso			0.25					
Boto	0.12							
Cacaito		0.74	0.19			-73.8		
Cacao	97.86	105.43	105.82	108.61	2.3	0.4	0.5	5.3
Cacao East	5.24							
Cacao West			2.28					
Cacao South	2.87	3.12	3.20	3.20	8.7	2.3	0.0	11.2
Caimo				1.70				
Patrullero	3.77	5.39	4.95	4.92	42.9	-8.2	-0.5	30.4
Patrullero South		6.20	4.66	6.03		-24.8	29.3	
Base	0.38	1.15			204.9			
Base West		0.32						
Mocagua	23.64	23.93	24.15	23.73	1.2	0.9	-1.7	0.4
Mocagua South		0.74						
Mocagua SE		0.33	1.55	1.39		44.1	-10.5	
Zaragoza	2.34	2.69	3.69	4.03	15.1	37.0	9.1	72.1
Zaragoza South				0.13				
Serra	7.10	7.43	5.03	2.85	4.6	-32.4	-43.3	-59.8
Corea	7.81	10.74			6.3			
Corea South	2.30		18.42	19.58		12.4	6.3	58.4
Corea North	2.25	2.82			25.0			
Corea West		2.83						
Corea Southeast		0.52		0.64				
Piraña				0.84				
Ticuna				0.01				
El Colono				0.04				
Fray				0.06				
Micos	3.80	3.88	3.98	3.64	2.2	2.5	-8.4	-4.1
Yauma	29.69	28.89	28.41	28.68	-2.7	-1.6	0.9	-3.4
Ronda	8.14	8.60	8.40	8.57	5.6	-2.3	2.1	5.3
Rondina	8.38	9.92	10.86	12.35	18.4	9.5	13.8	47.4
Victoria Regia				0.11				
Fantasia	0.46	1.00	0.97		116.8	-2.6		
Santa Rosa	2.01	2.18	1.53	1.65	8.8	-30.0	8.0	-17.7
Brasil				0.63				
Aramosa	54.05							
Aramosa 1	0.99	61.82	58.58	59.10	5.9	-5.2	0.9	1.3
Aramosa 2	3.02							
Aramosa 3	0.28							
Aramosa Central		0.42	0.97	1.11		130.6	13.5	
Aramosa West		1.96	3.44	3.37		75.7	-1.9	
Benjamin	20.98	15.41	14.50	13.90	-26.5	-5.9	-4.1	-33.7
Islands	333.71	360.89	365.27	371.03	8.1	1.2	1.6	11.2
Channels	356.49	351.14	359.80	353.70	-1.5	2.5	-1.7	-0.8
Recent deposition	16.57	9.62	13.09	14.63	-41.9	36.0	11.8	-11.7

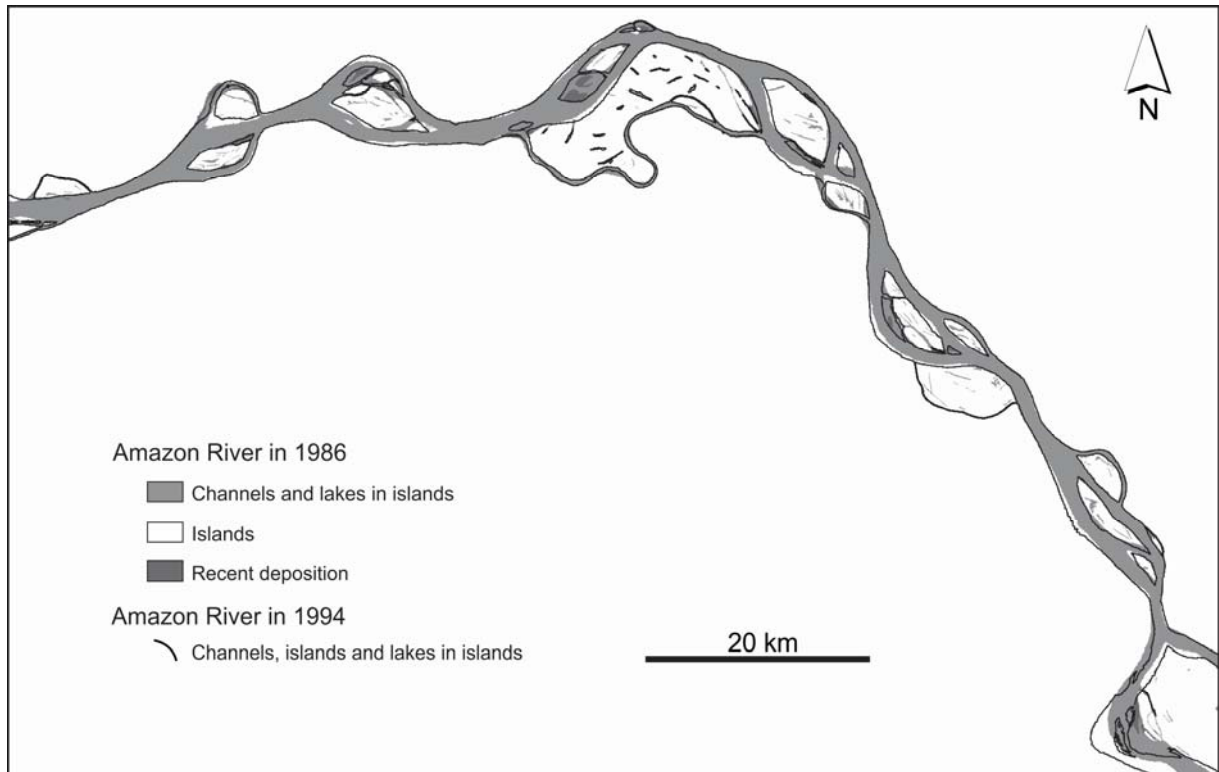


Figure 3. Temporal analysis of the Colombian Amazon River between July 19, 1986 and November 14, 1994. Channels, lakes within islands, islands and recent deposition contours are compared between these two dates.

Nine islands were accreted to other islands by 1994 with a usually greater increase in the plan view area of the resulting island. Only the accreted El Tigre and El Tigre North Islands had smaller resulting areas by 1994. During this period, 13 new islands appeared in the system while only Boto Island was completely eroded.

The percent change in the plan view area of the Amazon River system for this period was 16.4% ($2\% \text{ yr}^{-1}$). Areas which remained unchanged amount to 81.7%, and 1.9% of the area was found to change between land categories (Table 3). The categories grouped under erosion correspond to 7.6% of the change in the plan view area while deposition adds up to 8.7%. Areas that were eroded before deposition took place represent 0.1% of the change. This detailed pixel to pixel analysis shows that the main process acting over the period is deposition. Plan view areas covered by water in 1986 which were occupied by islands in 1994 represent the largest category of change for the period (6%). Other important changes over this period include the floodplain and island plan view areas which were eroded, at 4% and 3.2%, respectively. Based on the pixel class-change analysis it is possible to decipher whether plan view areas of recent deposition were accreted to islands/floodplain or eroded. Indeed, 1.6% of the change in the plan view area corresponds to recent deposition that was colonized

by vegetation and converted to islands, 0.2% of the area was converted to floodplain and only 0.4% of the area was actually eroded.

Channel changes between November 14, 1994 and July 20, 2001

Over this period (6.7 years) the plan view area of the channels changed by 2.5% (Table 2), indicating that the main process acting in the system was erosion that lead to an increase in the plan view area of the channels. In contrast, the 1.2% and 36% increase in the plan view area of islands and recent deposition, respectively, indicate deposition. Comparing the plan view area of channels, islands and recent deposition between 1994 and 2001 from Table 2, it can be seen that 8.7 km^2 was eroded by the channels. The plan view area on which deposition took place, forming or accreting islands, is 4.4 km^2 and the area gained by recent deposition is 3.5 km^2 . This small difference of 0.8 km^2 indicates more erosion than deposition.

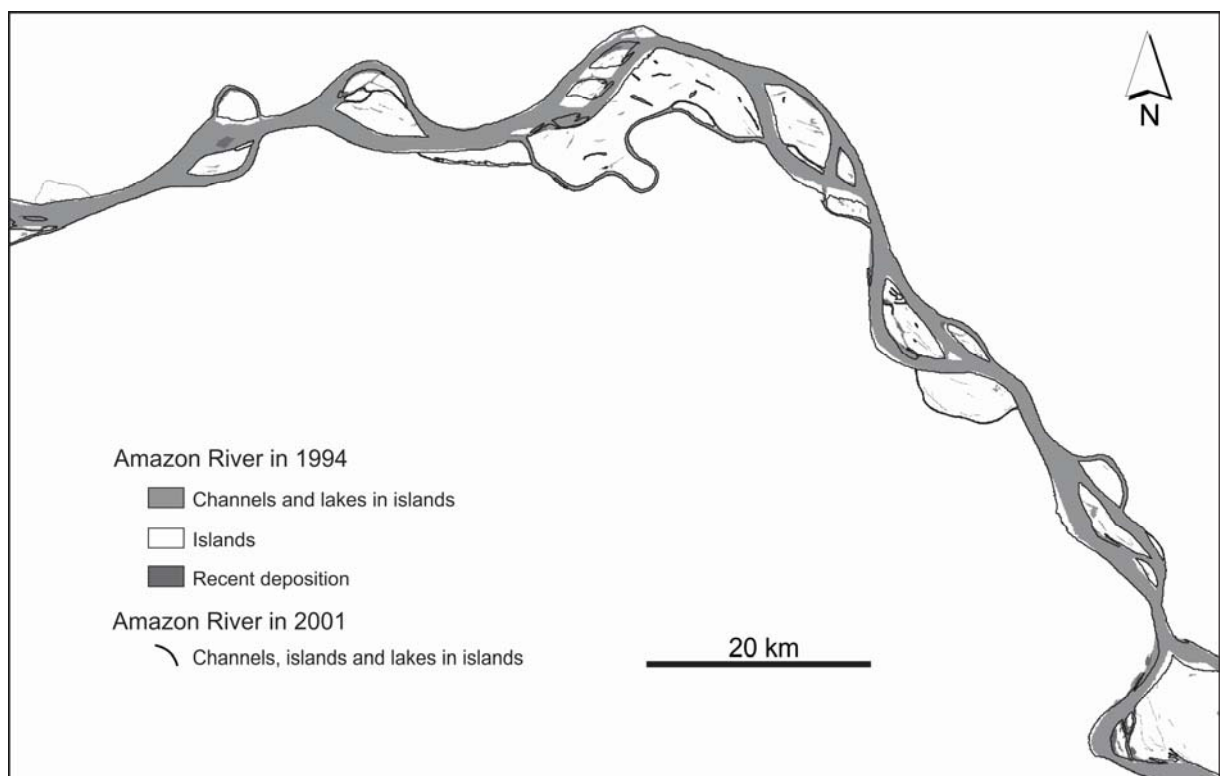


Figure 4. Temporal analysis of the Colombian Amazon River between November 14, 1994 and July 20, 2001. Channels, lakes within islands, islands and recent deposition contours are compared between these two dates.

Based on the plan view area of islands shown in Table 2, over this period 10.2 km^2 accumulated by lateral accretion and 3.3 km^2 was gained with new islands. Partial erosion of existing islands amounts to 11.6 km^2 and islands completely eroded amount to 2.2 km^2 . This

indicates that the plan view area which was eroded (0.3 km^2) is greater than the area of deposition. Cocha Island was accreted to the floodplain and Caballo Cocha Island was isolated from it, changes representing -6.6 km^2 and 11.3 km^2 , respectively. These two islands represent land changes and do not indicate erosion or deposition. Of the 41 islands present in the system in 1994, 15 saw their plan view area increase while 13 were partially eroded. The greatest increase is seen at Aramosa Central Island (130.6%) and the greatest eroded area is at Cacaito Island (-73.8%). Eight islands were accreted to other islands, with an increase in the plan view area of the resulting islands. By 2001, four islands had been entirely eroded, four new islands were created, one was accreted to the floodplain and one island became isolated from the floodplain.

The percent change in the plan view area of the system during this period corresponds to 12.5% ($1.9\% \text{ yr}^{-1}$), with 84.3% of the areas not changing and changes between land categories amounting to 3.2% (Table 3). The categories of erosion correspond to 6.5% and deposition to 5.8%. Areas which underwent erosion and deposition over this period represent 0.2% of the change in the plan view area. Changes in plan view area from islands to water represent the largest category of change with 3.7%, followed by water to islands at 3.2% and floodplain to water at 2.4%. These data indicate that the main process acting over this period is erosion.

Channel changes between July 20, 2001 and June 24, 2006

The comparison between 2001 and 2006 represents an interval of 4.9 years. The plan view area of the channels was reduced by 1.7%, while the area of islands and recent deposition were increased by 1.6% and 11.8%, respectively. These values indicate net deposition over this period. Comparing the plan view areas of channels, islands and recent deposition over this period, 6.1 km^2 was lost by the channels, 5.8 km^2 was accreted or constitutes new islands and 1.5 km^2 was gained by recent deposition.

The comparison of the plan view area of islands over this period (Table 2) indicates deposition up to 14 km^2 . The increase in area of existing islands amounts to 7.7 km^2 , and new islands cover 6.3 km^2 . The loss in plan view area amounts to 7.2 km^2 , with 6.8 km^2 corresponding to partial erosion of existing islands and 0.4 km^2 to islands that were completely eroded by 2006. Fantasia Island was accreted to the floodplain, with an area amounts of 1 km^2 . Of the 33 islands existing in 2001, 16 had a greater plan view area and four were accreted to other islands, with an increase in the area of the resulting island. Channel erosion was responsible for the reduction in plan view area of 10 islands and the complete

disappearance of 2 islands. Only one island was accreted to the floodplain. By 2006, 15 new islands were added to the system.

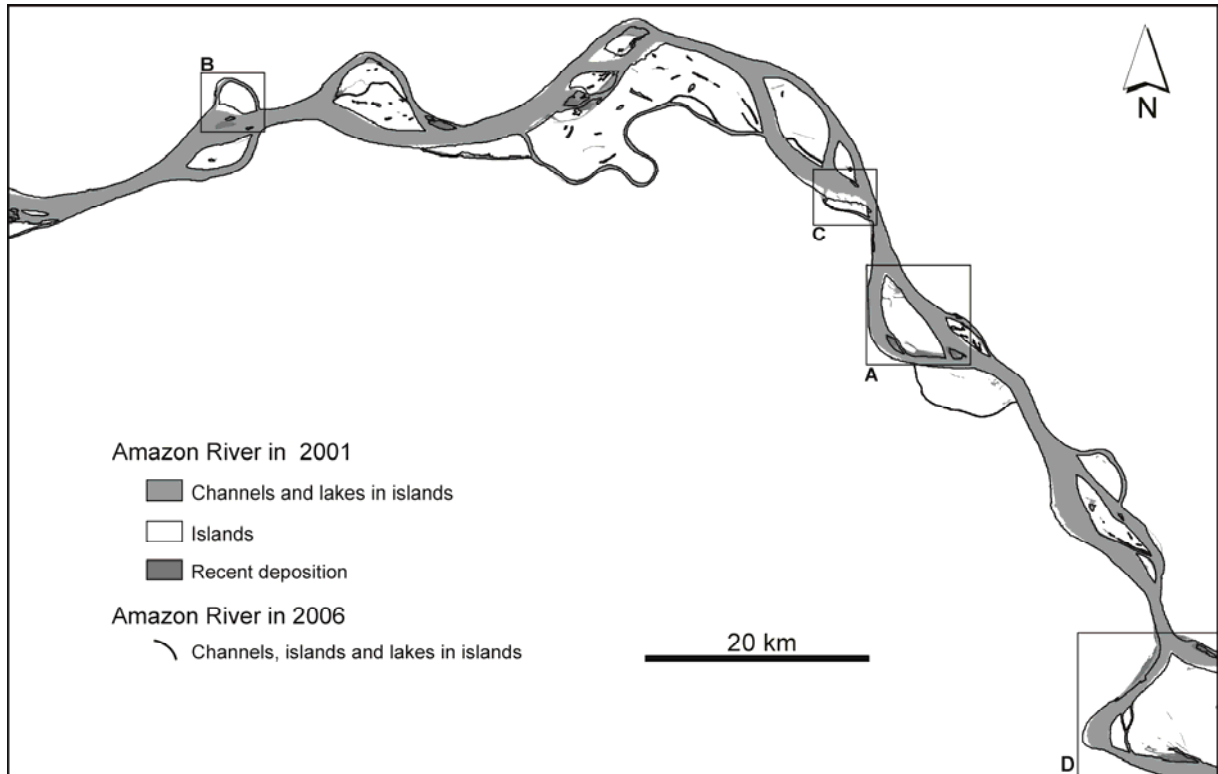


Figure 5. Temporal analysis of the Colombian Amazon River between July 20, 2001 and June 24, 2006. Channels, lakes within islands, islands and recent deposition contours are compared between these two dates. Boxes A, B, C and D indicate islands with more significant plan view changes between 1986 and 2006 and are detailed in Figure 6.

The percent change in the plan view area of the system over this period is 9.9%, with an annual rate of 2% (Table 3). Plan view areas which did not change amount to 88.7% and 1.5% of the area represents changes between land categories. Areas of the floodplain and islands which were eroded and where recent deposition then took place correspond to 0.1%. The erosion categories comprise 4.5% of change in the plan view area, while deposition corresponds to 5.4%, clearly showing the depositional tendency. The most important changes between 2001 and 2006 are the erosion of existing islands (2.6%), island areas gained from water (2.5%) and recent deposition converted to islands by vegetation development (1.7%).

Area variation between July 19, 1986 and June 24, 2006

The comparison between 1986 and 2006 currently represents the largest possible temporal interval (19.9 years) to evaluate fluvial dynamics of the Colombian Amazon River (Table 1). The plan view of the channels changed by -0.8%, a reduction which indicates a depositional

process. The increase in the plan view area of the islands by 11.2% also indicates deposition, with a greater area in 2006 than in 1986. In contrast, the change in the plan view area of recent deposition by -11.7% suggests erosion (Table 2). However, this reduction in the area of recent deposition could indicate colonization by vegetation which transformed areas into islands or parts of islands, or into parts of the floodplain. Information regarding with the processes undergone by these areas is only available from the pixel-class analysis. Comparing the plan view areas of the channels, islands and recent deposition between 1986 and 2006 (Table 2), it can be seen that the area lost by channels amounts to 2.8 km² (deposition inside the channels), 37.3 km² became new islands or was accreted to them and 1.9 km² was lost by recent deposition. More deposition than erosion is observed over this period.

Table 3. Percent change in the plan view area of: each category of the pixel class-change analysis; the river system and the system per year. The time periods over which the changes occurred correspond to 8.3 years (1986-1994), 6.7 years (1994-2001), 4.9 years (2001-2006) and 19.9 years (1986-2006). The plan view area of each category of change is also indicated.

Categories	From	To	From 19-Jul-86 to 14-Nov-94				From 14-Nov-94 to 20-Jul-01					
			Area of change (km ²)	Percent change in the plan view area of			Area of change (km ²)	Percent change in the plan view area of				
				each category	the system	the system /year		each category	the system	the system /year		
Deposition	Water	Islands	43.9	6.0	8.7	16.4	2.0	23.8	3.2	5.8	12.5	1.9
	Water	Recent Deposition	8.9	1.2				11.3	1.5			
	Water	Floodplain	10.4	1.4				8.1	1.1			
Erosion	Floodplain	Water	29.2	4.0	7.6	16.4	2.0	18.1	2.4	6.5	12.5	1.9
	Recent deposition	Water	3.0	0.4				3.1	0.4			
	Islands	Water	23.0	3.2				27.2	3.7			
Erosion/ deposition	Floodplain	Recent Deposition	0.3	0.0	0.1	16.4	2.0	0.2	0.0	0.2	12.5	1.9
	Islands	Recent Deposition	0.2	0.0				1.4	0.2			
Land change	Floodplain	Islands	0.4	0.1	1.9	16.4	2.0	11.2	1.5	3.2	12.5	1.9
	Recent deposition	Islands	11.6	1.6				5.5	0.7			
	Recent deposition	Floodplain	1.8	0.2				0.9	0.1			
	Islands	Floodplain	0.0	0.0				6.4	0.9			
No change			594.2	81.7	81.7			627.1	84.3	84.3		
Total plan view area between the banks over which the change occurred			727.0			744.3						

Categories	From	To	From 20-Jul-01 to 24-Jun-06				From 19-Jul-86 to 24-Jun-06					
			Area of change (km ²)	Percent change in the plan view area of			Area of change (km ²)	Percent change in the plan view area of				
				each category	the system	the system /year		each category	the system	the system /year		
Deposition	Water	Islands	18.8	2.5	5.3	9.9	2.0	73.2	9.6	13.9	27.1	1.4
	Water	Recent Deposition	12.8	1.7				10.7	1.4			
	Water	Floodplain	7.3	1.0				21.8	2.9			
Erosion	Floodplain	Water	11.9	1.6	4.5	9.9	2.0	51.9	6.8	12.8	27.1	1.4
	Recent deposition	Water	2.3	0.3				3.6	0.5			
	Islands	Water	19.4	2.6				42.1	5.5			
Erosion/ deposition	Floodplain	Recent Deposition	0.0	0.0	0.1	9.9	2.0	1.1	0.1	0.4	27.1	1.4
	Islands	Recent Deposition	0.6	0.1				1.7	0.2			
Land change	Floodplain	Islands	0.0	0.0	1.5	9.9	2.0	10.7	1.4	3.9	27.1	1.4
	Recent deposition	Islands	8.5	1.1				10.8	1.4			
	Recent deposition	Floodplain	1.5	0.2				1.4	0.2			
	Islands	Floodplain	1.0	0.1				6.5	0.9			
No change			656.7	88.7	88.7			525.1	69.0	69.0		
Total plan view area between the banks over which the change occurred			740.7			760.7						

A visual comparison of the islands present in 1986 and 2006 shows the depositional tendency by 2006 (Table 2). The plan view area of islands shows an area of deposition up to

50.9 km², with 32 km² corresponding to an increase in the area of existing islands and 18.9 km² consisting of new islands formed over this period. The eroded areas amount to 17.5 km², with 16.6 km² attributed to the partial erosion of existing islands and 0.9 km² to islands which were completely eroded by 2006. Areas accreted to the floodplain amount to 6.6 km², and areas isolated from the floodplain correspond to 10.6 km². In 1986 there were 38 islands in the system; by 2006 13 of them had a greater area, in part due to new depositional areas around them and also by the accretion of 13 existing islands. The loss of island area during this period is due to seven islands which decreased in size and three which were completely eroded. By 2006, 20 new islands had emerged in the system. Cocha and Fantasia Islands were accreted to the floodplain and Caballo Cocha Island was isolated from the floodplain.

Islands that visually displayed more drastic change from 1986 to 2006 are shown in Figure 6. In 2006 Corea Island area had increased by 58.4% from its initial area; this increase is mainly due to the accretion of Corea South, Corea North and Corea West Islands. El Tigre Island was reduced in size by 36.8%, despite the fact that El Tigre North Island was accreted by 1994. Serra Island was eroded by 59.8%. Aramosa Island increased in size by only 1.3%, however its shape suffered an obvious change. Other islands which were considerably changed include Nueva island, which increased in size by 298.52% mainly due to accretion of other islands, and Patrullero, Zaragoza and Rondinha Islands which increased in size by 30.42%, 72.10% and 47.41%, respectively.

The percent change in the plan view area of the system between 1986 and 2006 amounts to 27.1% with an annual rate up to 1.4% (Table 3). The areas that did not change over the period amount to 69%, and change between land categories amounts to 3.9%. The pixel class-change analysis indicates a 14.3% change for the depositional categories and 12.8% for the erosional categories, corroborating a depositional period. Areas which were first eroded and where recent deposition then took place represent 0.4% of the change. The main category of change for this period corresponds to areas of water that were occupied by accreting or forming islands, with 9.6%. The channels were responsible for the erosion of areas of the floodplain, which amounts to 6.8% and erosion of islands amounting to 5.5% of the change in the plan view area. In the case of recent deposition, through the pixel class-change analysis it can be established that 1.4% of the change in the plan view area represents areas colonized by vegetation and converted to islands. The plan view area which became vegetated and was transformed into floodplain amounts to 0.2%, and only 0.5% of the area was actually eroded (Table 3).

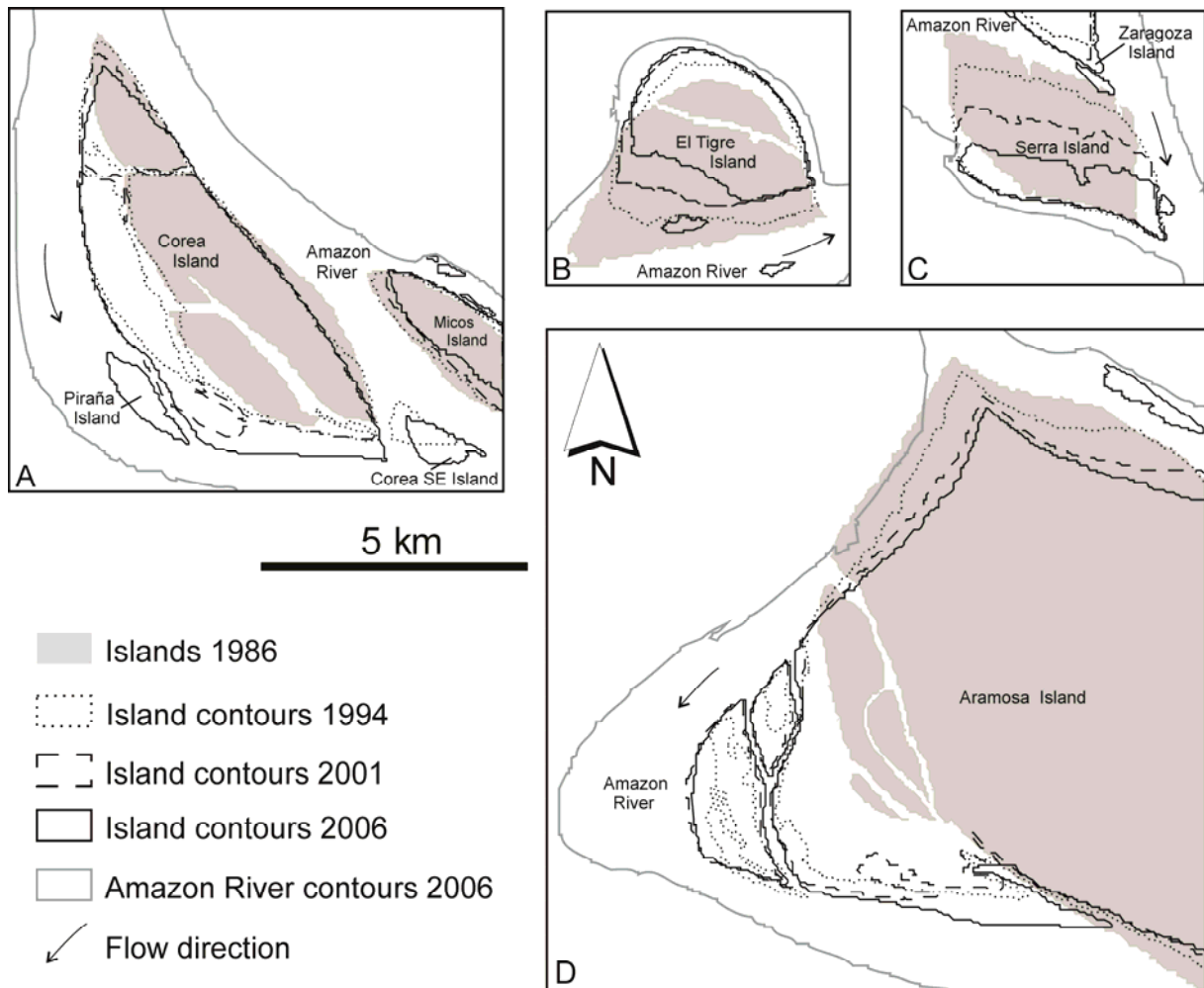


Figure 6. Islands with more significant plan view changes between 1986 and 2006. See Figure 5 for location. (A) Corea Island significantly increased in area on the right margin. Erosion on the right margin of Micos Island since 1994 is also observed. Southeast Corea Island was present in 1994 and 2006, however eroded by 2001, and Pirafña Island was formed by 2006. (B) El Tigre Island has considerably eroded on its upstream side, with deposition along the convex side of its secondary channel. (C) Serra Island was drastically eroded upstream. In contrast, Zaragoza Island has been gaining area since 1994. (D) Aramosa Island grew in area by only 1.3%, however it can be seen how the shape of the island changed by 2006. Note that the right channel of the Amazon River upstream Aramosa Island was completely developed by 2006 in an area occupied by Aramosa Island in 1986.

Migration rates of the margins of the Amazon River

Migration rates of the Amazon River's margins were estimated at the locations shown in Figure 2. Migration values in meters and meters per year, over the four periods of analysis, are indicated in Table 4. The most active areas where migration rates were calculated occur on the left margin upstream of Cacao Island, and on the right margin downstream of the same island (Figure 2). On the right margin are also localized the maximum migration rates for erosion and deposition. Erosion of the margins is the predominant process, with eight

locations showing maximum erosion rates compared with three locations showing maximum depositional rates. Only one location, the left margin of the Amazon River to the west of Vamos Island underwent erosion and later deposition. In each of the periods studied, the largest migration rates are erosional (Table 4).

Table 4. Migration rates of the margins of the studied reach of the Amazon River. The locations are numbered from upstream to downstream and organized by maximum rates of erosion and deposition over the 1986-2006 period. See Figure 2 for the specific location of each site.

Margin		Location		Migration rates						Process		
				1986-1994		1994-2001		2001-2006			1986-2006	
				(m)	(m yr ⁻¹)	(m)	(m yr ⁻¹)	(m)	(m yr ⁻¹)		(m)	(m yr ⁻¹)
Right	12	East of Benjamin Island	1771	213	198	30	509	104	2479	125	Erosion	
	9	West of Rondinha Island	402	48	693	104	422	86	1517	76		
	6	SW of Mocaqua Island	399	48	603	90	327	67	1329	67		
Left	1	North of Peru Island	497	60	217	32	370	76	1085	55		
Right	8	Southwest of Corea Island	279	34	417	62	291	59	987	50		
Left	4	North of Nueva Island	497	60	84	13	116	24	697	35		
	3	East of El Tigre Island	186	22	229	34	86	18	502	25		
	10	North of Aramosa Island	205	25	145	22	26	5	376	19		
Right	5	West of Vamos Island	16	2	-	-	-	-	-	-		
Right	11	NW of Aramosa Island	761	92	369	55	341	70	1471	74		Deposition
	7	South of Serra Island	403	49	80	12	348	71	830	42		
Left	2	West of El Tigre Island	349	42	106	16	201	41	656	33		
	5	West of Vamos Island	-	-	220	33	224	46	428	22		

Areas which were not considered for migration measurements are islands accreted to or isolated from the floodplain. Indeed, these do not represent channel migration (erosion or deposition) over the period of analysis. These areas are shown in Figure 2 and include: Cocha and Fantasia Islands which were accreted to the floodplain by 2001 and 2006 respectively; Caballo Cocha Island that was isolated from the floodplain by 2001 and Yauma Island, which by 2006 was being accreted to the floodplain, with a channel to the south that still remains active during high water stages.

The maximum migration rate recorded here is 213 m yr⁻¹, for an erosional area located on the right margin to the east of Benjamin Island over the 1986-2001 period (site 12, Figure 2). This location is also the most active erosional area over the periods 2001-2006 (104 m yr⁻¹) and 1986-2006 (125 m yr⁻¹). During the 1994-2001 period the most active erosional area is the right margin of the Amazon to the west of Rondinha Island with 104 m yr⁻¹ (site 9, Figure 2). For deposition, the maximum migration rate is 92 m yr⁻¹ on the Amazon River's right margin to the Northwest of Aramosa Island over the 1986-1994 period (site 11, Figure 2). This location is also the most active depositional area over the period 1994-2001 (55 m yr⁻¹)

and 1986-2006 (74 m yr^{-1}). Between 2001 and 2006 the most active depositional area is the right margin to the south of Serra Island with 71 m yr^{-1} (site 7, Figure 2).

Geomorphologic units

The geomorphologic analysis of the study area defined four units which are: a) Terraces b) Scroll bars; c) Floodplain; and d) Channel bars (Figure 7).

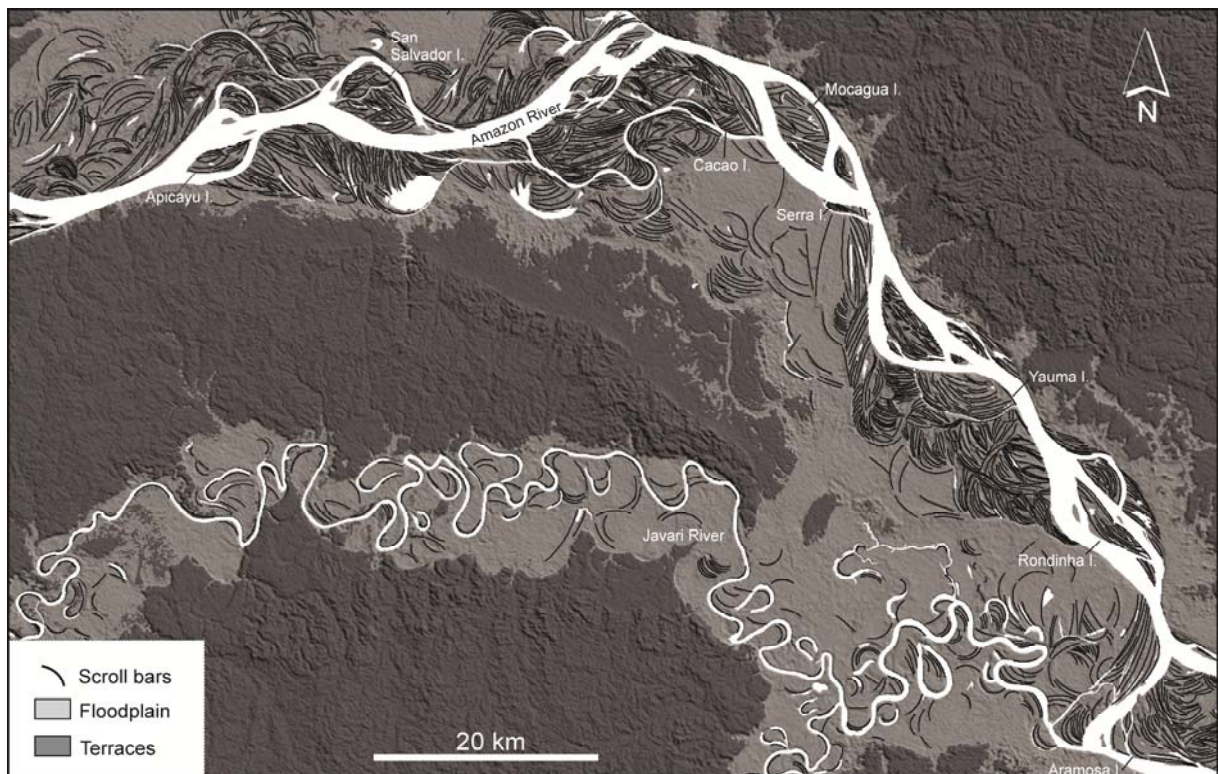


Figure 7. Morphology of the area. Terraces represent higher elevations (100 – 160 m.a.s.l) and the floodplain lower areas (80 – 100 m.a.s.l.). Note the terraces controlling the development of the floodplain and scroll bars on the right margin upstream Apicayu Island and on the left margin downstream Cacao Island. This map was generated based on interpretation of the Landsat images used in the temporal analysis, and a SRTM image.

Terraces

This unit represents the *Terciario Inferior Amazonico* and *Terciario Superior Amazonico* deposits. The *Terciario Inferior Amazonico* deposits (Huguett et al. 1979) is also referred to as the Pebas Formation (Khobzi et al. 1980) and in Brazil it is correlated to the Solimões Formation (Rego 1930). Morphologically, it is characterized by elevations between 100 and 120 m.a.s.l., a relief with a medium degree of erosion and dendritic drainage pattern. The *Terciario Superior Amazonico* deposits (Huguett et al. 1979) correlates with the Iça

Formation (Maia et al. 1977) in Brazil. In morphological terms it is characterized by elevations between 120 and 160 m.a.s.l., a low degree of erosion and sub-trellis drainage.

Scroll bars

The islands in the system, together with most of the right bank and portions of the left margin of the Amazon River, are composed of scroll bars (Figure 7). Ridge-and-swale morphology is characteristic in these areas with the development of narrow lakes and minor secondary channels that follow the swales (Figure 7). These scroll bars represent present-day and ancient lateral accretion of the main and secondary channels. Linked to present day-channels, scroll bar sets are up to 3.2 km wide in the main channel (right margin of the Amazon River, northwest of Aramosa Island, Figure 7) and in secondary channels are up to 2.8 km wide at Yauma Island. Some sets are truncated by the main and secondary channels as well. The sets are also separated by successive reactivation surfaces that record changes in migration direction. In some areas of the floodplain, scroll bars are linked to abandoned meanders where oxbow lakes are still preserved, partially or completely filled with sediments (Figure 7).

The scroll bars clearly show migration of secondary channels as well as the main channel (Figure 7). The left margin of the Amazon River in front of Apicayu Island shows an extensive set of scroll bars product of the migration of the main channel towards the southeast. South of Serra Island on the right margin there is another set of scroll bars indicating the migration of the main channel towards northeast. Northwest of Aramosa Island the Amazon develops an extensive scroll bar set migrating southeast. These three areas represent locations where some of the maximum depositional migration rates have been obtained and correspond to sites 2, 7 and 11 respectively, from Figure 2. Scroll bar sets on the islands which originate from migration of the main channel are observed at Rondinha Island, where a set of scroll bars indicates migration to the southwest and on the opposite side of the channel a maximum erosional rate of migration is found (site 9, Figure 2 and Figure 7). Scroll bar sets inside islands due to migration of secondary channels are observed at: San Salvador Island, where a scroll bar set indicates migration to the north and a maximum migration rate on erosion is found on the opposite side of the secondary channel (site 4, Figure 2 and Figure 7); and at the southern end of Mocagua Island where a scroll bar set migrating slightly to the southwest develops, which follows the erosion on the other side of the secondary channel (site 6, Figure 2). Other secondary channels develop extensive scroll bars sets as in the case of the channel south of Cacao Island (Figure 7). In the area of Yauma Island several sets of scroll

bars can be observed, where the secondary channels that formed them are not longer active, with the exception of the channel that outlines the south of Yauma Island (Figure 7).

Floodplain

This unit is characterized by a mostly flat surface with elevation between 80 and 100 m.a.s.l. It represents a large part of the right margin of the Amazon River downstream of Cacao Island and the left margin upstream the same island. Other areas are part of this unit but are more restricted than the others indicated above, due the proximity of the terraces to the channels (Figure 7). The floodplain of the Javari River, embedded between terrace deposits, can be also observed in Figure 7. On the floodplain of the Amazon River, completely and partially sediment-filled oxbow lakes are present, with the preservation of the original contour from which they were formed. Some oxbow lakes are truncated by the migration of other channels. Oxbow lakes are very common on the floodplain of the Javari River. Individual bends of the Javari River migrate in the direction of existing oxbow lakes formed from the same river. Meanders intersect the existing oxbow lakes, preserving part of their original shape (Figure 7). The oxbow lakes on the floodplain of the Amazon and Javari Rivers are isolated from channels or connected to the drainage system by small channels, which dry up during the low water season.

Channel bars

The present-day channel bars of the Amazon River emerge at low water during the dry season and extend up to 1.9 km long and 0.8 km wide. These bars represent downstream accretion elements in the fluvial system, in contrast to scroll bars that indicate lateral accretion. Channel bars and unvegetated areas being accreted laterally correspond to recent deposition areas from the temporal analysis.

Discharge related to the erosion and deposition periods

The Tamshiyacu gauging station had a mean monthly discharge of $23,817 \text{ m}^3 \text{ s}^{-1}$ between July 1986 and June 2006. The variation in monthly discharge with respect to the mean monthly discharge, over this period, is from $14,473$ to $-13,588 \text{ m}^3 \text{ s}^{-1}$ with predominance of discharge variation greater than mean discharge between July 1986 and November 1994. From November 1994 to June 2006 the variation in discharge tends to be lower than mean discharge (Figure 8). A normal distribution of variation of the monthly discharge with respect to the mean monthly discharge, over the period July 1986 – November 1994 (Figure 8), shows a

mean value of $652 \text{ m}^3 \text{ s}^{-1}$, a positive value which indicates predominance of monthly discharge above mean discharge. Extreme events with respect to mean discharge, over this period, indicate that the probability of occurrence of discharge variation greater than $10,000 \text{ m}^3 \text{ s}^{-1}$ is greater than events with discharge variation lower than $-10,000 \text{ m}^3 \text{ s}^{-1}$. Over the periods November 1994 – July 2001 and July 2001 – June 2006 the results are opposite those of the previous period. Over these periods normal distributions show a mean value of variation between monthly and mean discharge of -335 and $-828 \text{ m}^3 \text{ s}^{-1}$, respectively, and higher probability of occurrence of extreme events lower than mean discharge (Figure 8).

The Nazareth gauging station had a mean monthly discharge from July 1986 to June 2006 of $34,908 \text{ m}^3 \text{ s}^{-1}$, with variation of the monthly discharge with respect to mean monthly discharge between $29,851$ and $-21,626 \text{ m}^3 \text{ s}^{-1}$. Between July 1986 and November 1994, the first four years where discharge data is available show a greater number of values below mean discharge when compared with values above mean discharge, and a considerable increase in values above mean discharge towards the end of this period (Figure 9). Over the November 1994 – July 2001 period, a significant increase in values above mean discharge is observed. The last period (July 2001 – June 2006) starts with higher values of discharge variation than mean discharge but from the end of 2003 the values are lower than mean discharge (Figure 9). Normal distributions for the periods of July 1986 – November 1994 and July 2001 – June 2006 indicate a mean variation in monthly discharge with respect to the mean discharge of -759 and $-282 \text{ m}^3 \text{ s}^{-1}$, which indicates the predominance of discharge variation lower than mean discharge. Extreme events ($\geq 20,000 \text{ m}^3 \text{ s}^{-1}$ and $\leq -20,000 \text{ m}^3 \text{ s}^{-1}$) for discharge variation over these periods indicate a higher probability of occurrence of values lower than mean discharge (Figure 9). In contrast, between November 1994 and July 2001 the mean value of discharge variation ($852 \text{ m}^3 \text{ s}^{-1}$) and the probability of occurrence of extreme events of discharge higher than mean discharge indicate that variation above mean discharge is characteristic (Figure 9).

The mean monthly discharge for the Olivença station was $47,100 \text{ m}^3 \text{ s}^{-1}$ between July 1986 and June 2006 with variation between monthly discharge and mean monthly discharge from $34,593$ to $-31,828 \text{ m}^3 \text{ s}^{-1}$ (Figure 10). An overview of the variation in monthly discharge with respect to mean discharge from Figure 10 shows a predominance of lower variation values from July 1986 to July 2001, in contrast to higher variation values from July 2001 to June 2006. The discharge variation data is very similar between values above and below mean discharge, specifically between July 1986 and July 2001. Normal distributions for monthly and mean discharge variation over July 1986 – November 1994 and November 1994 – July

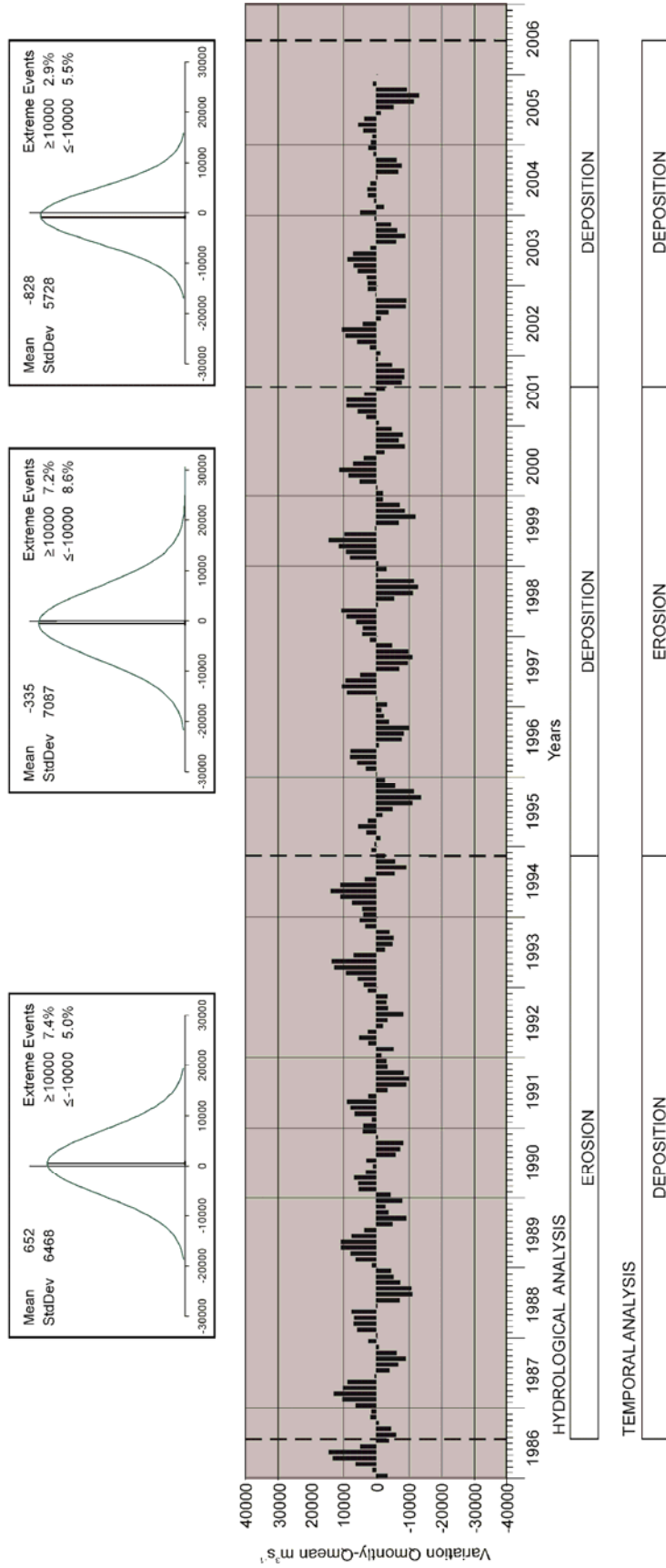


Figure 8. Variation in monthly discharge with respect to mean monthly discharge ($23,817 \text{ m}^3 \text{ s}^{-1}$) for Tamshiyacu gauging station over the period 1986-2006. For each sub period of analysis, normal distributions of the Qmonthly – Qmean variation are indicated in the upper part. Results of the hydrological and temporal analyses for erosion or deposition periods are indicated at the bottom for comparison. Dashed lines indicate the limits of each sub period. Location of Tamshiyacu gauging station is indicated in Figure 1B.

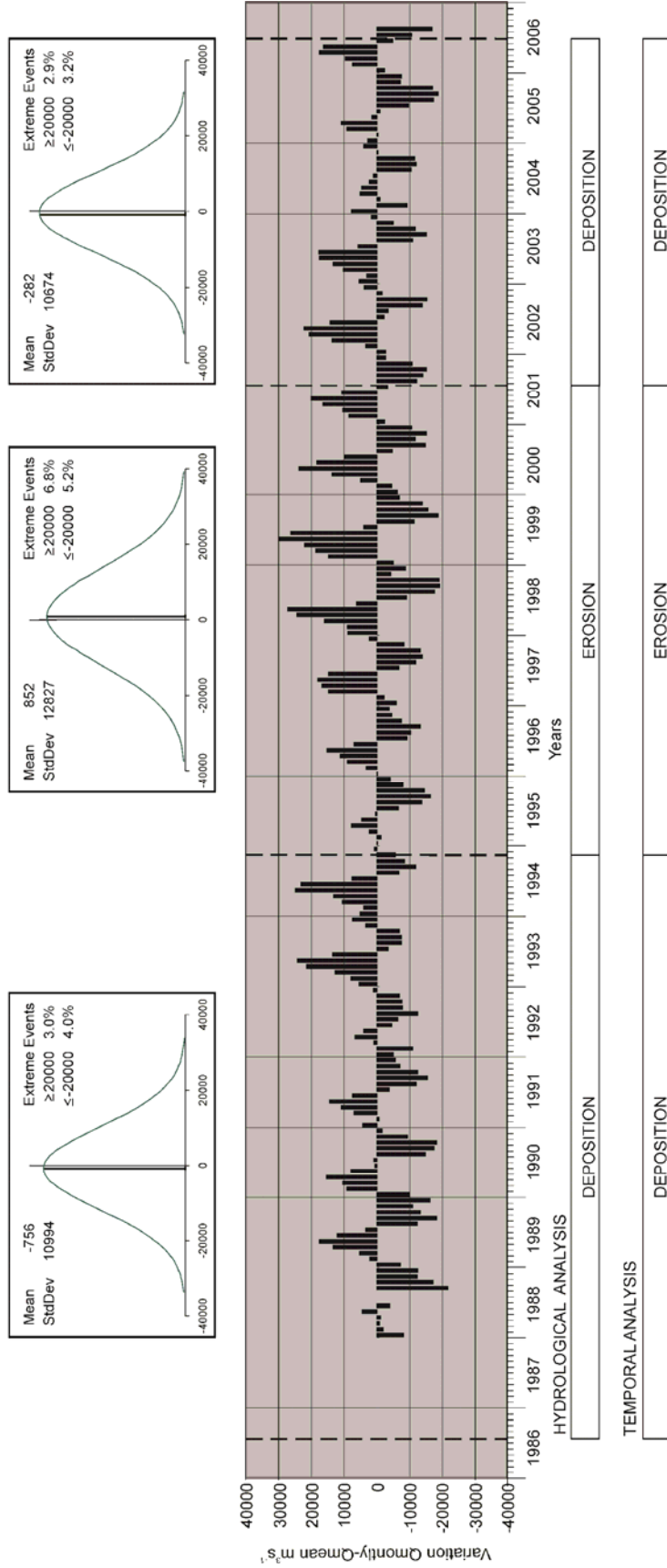


Figure 9. Variation in monthly discharge with respect to mean monthly discharge ($34,908 \text{ m}^3 \text{ s}^{-1}$) for Nazareth gauging station over the period 1986-2006. For each sub period of analysis, normal distributions of the Qmonthly – Qmean variation are indicated in the upper part. Results of the hydrological and temporal analyses for erosion or deposition periods are indicated at the bottom for comparison. Dashed lines indicate the limits of each sub period. Location of Nazareth gauging station is indicated in Figures 1B and 1C.

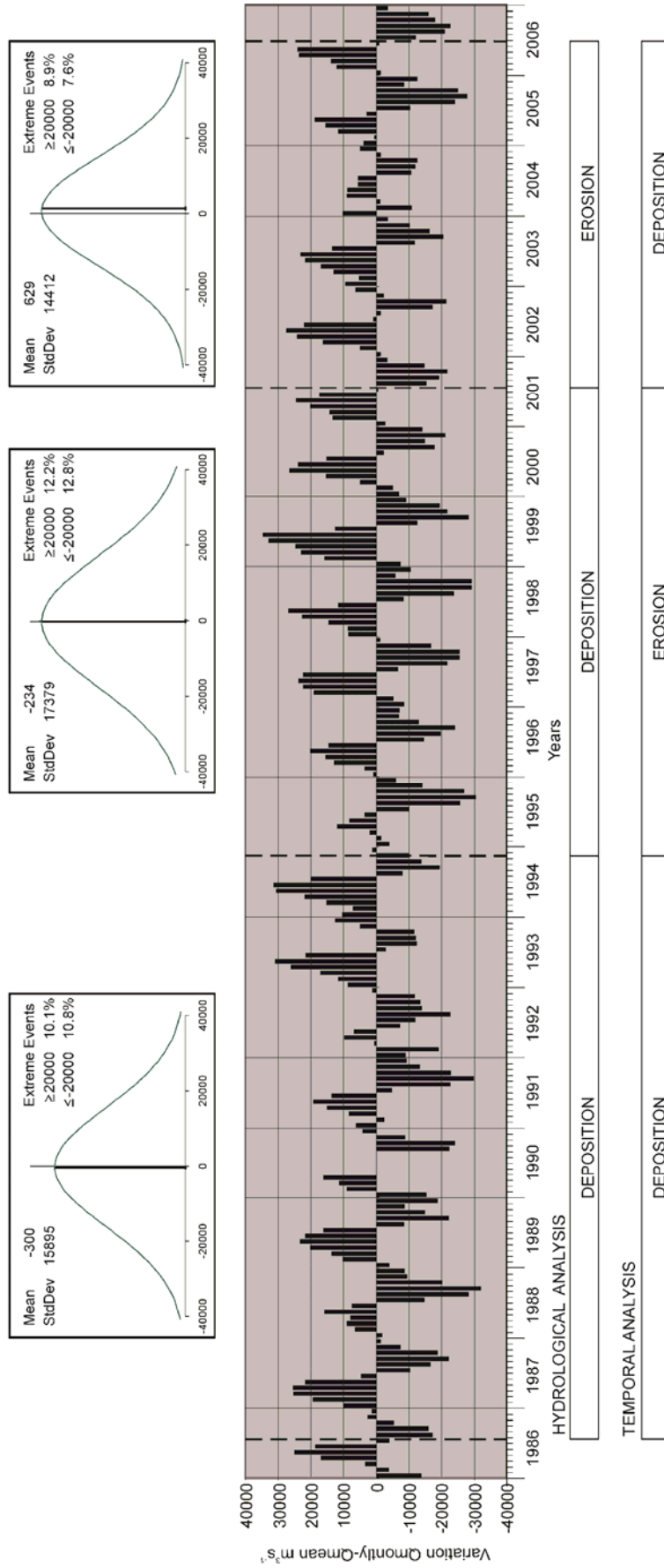


Figure 10. Variation in monthly discharge respect to mean monthly discharge ($47,100 \text{ m}^3 \text{ s}^{-1}$) for Olivença gauging station over the period 1986-2006. For each sub period of analysis, normal distributions of the Qmonthly - Qmean variation are indicated in the upper part. Results of the hydrological and temporal analyses for erosion or deposition periods are indicated in the bottom. Dashed lines indicate the limits of each sub period. Location of Olivença gauging station is indicated in Figure 1B.

2001 indicate mean values lower than mean discharge. The probability of occurrence of extreme events, over these two periods, also indicates the predominance of events with lower than average discharge. The last period (July 2001 – June 2006), in contrast to the two previous periods, shows data that indicate the predominance of discharge variation higher than mean discharge (Figure 10).

Discussion

Fluvial dynamics of the Colombian Amazon River

We discuss our data in relation to other data available for this region (Mertes et al. 1996; Rozo 2004; Peixoto et al. 2009; Rozo et al. 2012), even if there are discrepancies in the image selection process. Mertes et al. (1996) indicate that their values are considered of low accuracy due to the use of a variety of different mapping techniques that result in evident variations in the channel. Here we compared Landsat data at the same spatial resolution, selected based on very minimal water level variations and that were processed and edited following the same techniques. However, result accuracy still depends on the scale used. Additionally, more research must be undertaken to evaluate the best parameters when working with temporal analysis in this type of river.

The percentage of change in the plan view area per year of the Amazon River between the Iça and the Madeira Rivers (Figure 1B) was initially estimated by Mertes et al. (1996) from radar images (1971-1972) and navigation charts of the Brazilian Navy (1979 and 1980). These values vary considerably between the selected locations of analysis, but they show a relatively active area at the confluence with the Jutáí River reaching up to $2\% \text{ y}^{-1}$ and a relatively stable area at the confluence with the Negro River with values of $0.2\% \text{ y}^{-1}$. Recently, percent change values in the plan view area for specific reaches of the Amazon have been obtained for longer periods of time and using more accurate remote sensing tools. In the reach between the confluences of the Negro and Madeira Rivers, the percent change has been established at $0.7\% \text{ y}^{-1}$, over 15 years (1986 – 2001) (Rozo 2004) and $0.6\% \text{ y}^{-1}$, over 31.1 years (1986 – 2001) (Rozo et al. 2012). In the reach of the Solimões River at the confluence with the Japurá River a percent change in the plan view area of the system of $1.8\% \text{ y}^{-1}$ was calculated between 1984 and 2005 (21 years) (Peixoto et al. 2009). These values seem to be in concordance with data obtained by Mertes et al. (1996). However, the data obtained here shows that the Colombian Amazon River seems to be less active than the reach downstream between the confluences of the Jutáí and Japurá Rivers. The Colombian Amazon

River has a lower percentage of change in the plan view area ($1.4\% \text{ y}^{-1}$) than the reach at the confluence with the Japurá River ($1.8\% \text{ y}^{-1}$) (Peixoto et al. 2009). These two values were estimated over almost the same number of years, 21 and 19.9 respectively. The value for the Jutai River ($2\% \text{ y}^{-1}$) calculated over 8 years (Mertes et al. 1996) is more suitable for comparison with the values obtained for the other periods studied in the Colombian Amazon River, which are between 1.9 and $2\% \text{ y}^{-1}$ over 8.3 and 4.9 years (Table 3). However, it is best to consider longer periods of time to more accurately understand the behavior of the system. The Colombian reach of the Amazon River shows a less active behavior when analyzed over longer periods of time.

Migration rates estimated in different reaches of the Amazon River show a similar trend in upstream to downstream stability than the trend in the yearly percent change in the plan view area of the system. These values allow the section of the Amazon between its source and the mouth of the Madeira River to be divided into three reaches: 1) Upper Amazon River (The Ucayali River and Amazonas River in Peru, see Figure 1B), which corresponds to the more laterally active reach with migration rates of 400 m yr^{-1} near Iquitos (Kalliola et al. 1992); 2) the Colombian Amazon River and the Solimões River in Brazil, see Figure 1B, which represents a less laterally active reach with migration rates of 125 m yr^{-1} near Leticia and 140 m yr^{-1} near Fonte Boa (Mertes et al. 1996); and 3) a relatively stable reach downstream of Manaus (Amazonas River in Brazil, see Figure 1B), with maximum migration rates of 60 m yr^{-1} (Rozo et al. 2012). Rozo and Soto (2010) indicated a maximum migration rate of 213 m yr^{-1} for the Colombian Amazon River however this rate is calculated over 8.3 years while the maximum rate indicated here (125 m yr^{-1}) is estimated over a longer period of time, 19.9 years (Table 4).

Island dynamics in the system from 1986 to 2006 (Table 2) clearly show a tendency of new islands emerging and accretion of existing islands to other islands towards 2006. Island dynamics follow the erosion and deposition periods identified from the pixel-class analysis. The number of islands in the system had increased by 1994 and also towards 2006, and decreased by 2001. The same tendency is seen with the number of islands which increased in area as well as islands that emerged over each period. In contrast, the number of islands whose plan view area was reduced and that were fully eroded increased by 2001 and decreases toward 2006. In the case of the actual area deposited or eroded in the islands over each of the periods analyzed, the tendency is similar. The area of newly formed islands decreased by 2001 and increased toward 2006. The area accreted laterally to other islands decreases by 2001 and also towards 2006. However, if the total area accreted and generated are compared,

they follow the same general trend, with a decrease in area towards 2001 which corresponds to the erosional period and an increase in area by 2006, which follows the depositional period. In the case of the area partially eroded from islands and the area that corresponds to fully eroded islands, there is an increase by 2001 and a decrease towards 2006.

Island dynamics in the system also indicate how islands can increase in plan view area, a process which does not only result from new areas being accreted to existing islands. The mechanisms that were observed in the reach of the Colombian Amazon River are: 1) Accretion of new areas of recent deposition that subsequently are colonized by vegetation; 2) Accretion of existing islands due to deposition that overlaps the area between islands. In some cases the area between islands is a secondary channel, which is abandoned due to channel migration and becomes partially or completely filled with sediments; and 3) Sediment that fill lakes in islands. Similar processes occur when islands are accreted to the floodplain; in this case new sediments are deposited between an island and the floodplain and subsequently colonized by vegetation. In the opposite case, when an area is detached from the floodplain forming an island, a new secondary channel is formed or an abandoned channel is reactivated.

The temporal analysis indicates that the right margin of the fluvial system upstream of Cacao Island, and the left margin downstream of the same island have remained relatively unchanged between 1986 and 2006. In contrast, maximum migration rates and significant channel changes are found on the opposite margins (Figure 2). Differences in the ability of the deposits in each margin to resist erosion seem to influence this behavior. Terraces are characterized mostly by claystones and sandstones from the *Terciario Inferior* and *Superior* deposits (Huguett et al. 1979). In contrast, the sediments on the floodplain and scroll bars are unconsolidated clay and sand. The right margin upstream of Apicayu Island developed on terraces controlling river migration and forcing the river to erode the floodplain and previously formed scroll bars on the opposite margin, where these deposits occur extensively (Figures 2 and 7). On the right margin between Apicayu and Cacao Islands, floodplain and scroll bar deposits occur but are confined due to the proximity of the terraces to the river. On the left margin downstream of Cacao Island, the terraced deposits control river migration in contrast to the right margin, where an extensive floodplain with previous phases of river migration is evident (Figure 7). Terraces are clearly more resistant to erosion than the floodplain and scroll bar deposits and restrict channel migration.

Discharge related to the erosion and deposition periods

A classical balance model for aggradation and degradation of alluvial channels based on an equation by Lane (1955) and discussed by Blum and Tornqvist (2000) established the relationship between these processes and sediment supply and stream power. When sediment supply exceeds the transport capacity of the discharge regime aggradation takes place, and degradation occurs in the opposite condition (Blum and Tornqvist 2000). If there is no variation in sediment supply, aggradation or degradation will depend on stream power changes. Stream power is a result of density of the water, acceleration of gravity, discharge and slope. Density of the water and acceleration of gravity are constant values and on the Colombian Amazon reach the value of slope has been established at 0.00038 (Latrubesse 2008). This leads us to assume that changes in discharge would directly affect aggradation and degradation in the system. Erosion (aggradation) and deposition (degradation) were established here for the Colombian Amazon River based on the temporal analysis, where the periods between 1986-1994 and 2001-2006 were depositional and the period 1994-2001 was erosional.

From 1986 to 1994, discharge data from the Nazareth gauging station inside the area of study (Figure 1) indicates that most of the monthly discharge values are below the mean monthly discharge (Figure 9). The negative value for the mean of the variation in monthly discharge with respect to the mean monthly discharge indicates that over this period discharge decreases, tipping the aggradation – degradation balance model (Blum and Tornqvist 2000) to aggradation. This corroborates the depositional period obtained between 1986 and 1994 from the temporal analysis. Hydrological analysis between 1994 and 2001 shows that most of the discharge data are above the mean monthly discharge, with a positive value for the mean of the variation in monthly discharge with respect to the mean monthly discharge indicating erosion. This is also in agreement with the data obtained for this period from the temporal analysis (Figure 9). Hydrological analysis for the last period of study that is from 2001 to 2006 indicates deposition which is also corroborated by the temporal analysis. Missing discharge data between 1986 and 1994 does not seem to influence the hydrological analysis since same results were obtained from temporal analysis in this station.

Discharge data analyzed for the two other gauging stations, Tamshiyacu and Olivença, do not agree with the deposition and erosion periods obtained from the temporal analysis. In the case of Tamshiyacu station, hydrological data indicates opposite deposition and erosion for the periods 1986-1994 and 1994-2001 when compared with the data from the temporal analysis (Figure 8). The only period that shows an agreement is 2001-2006, which is a

depositional period. Hydrological analysis of discharge data at the Olivença gauging station shows that only the period from 1986 to 1994, which indicates deposition, agrees with results from the temporal analysis (Figure 10). The discharge differences between the three gauging stations seem to be related to variations in climatic conditions in the drainage areas of these stations.

The Tamshiyacu gauging station is located 381 km upstream of the area of study, in a reach between the confluences of the Marañón and Ucayali Rivers and the mouth of the Napo River (Figure 1). At Tamshiyacu the Amazon River drains an area of 720,000 km² which corresponds to the southwestern most area of the Amazon Basin. This catchment area includes the sources of the Amazon in the Andes mountain range. The Amazon River at Nazareth station drains an area of 874,000 km², which is 21% greater than at Tamshiyacu. This percentage includes the catchment area of the Napo River which corresponds to part of the northwestern Amazon Basin. At the Olivença gauging station the Amazon drains 16% more area than at Nazareth. This 16% corresponds to lowland areas of the Amazon forest, which are mainly located in the southwestern part of the Amazon Basin.

Analyzing the climatic conditions in the drainage areas of the gauging stations mentioned here, would help determine the factors that influence discharge variations between these three stations. However, the restricted amount of available information, and time required to process and validate a database from Peru, Ecuador, Colombia and Brazil would make difficult to develop such analysis. Similarly, a comparison of sediment supply and stream power data to determine what triggers bed aggradation or degradation in the area, following the balance model in Blum and Tornqvist (2000), would be difficult. In Brazil sediment influx rates of the Amazon River have been established from hydrological data at the gauging stations downstream of the Olivença station (Dunne et al. 1988; Meade 1994). However, no data is available on sediment influx rates in the Amazon River in Peru and Colombia, nor is specific data about sediment supply variation related to the periods of erosion/deposition studied here. In Colombia and Peru, only scattered data is available on granulometric bedload analysis and suspended sediment, from unpublished government reports. In this context more research is needed especially to define climatic conditions that trigger discharge variations and consequently erosional and depositional processes in the Amazon River.

Implications of channel pattern classification

Alluvial islands with saucer-like morphology due to bounding by natural levees have been described in the Amazon River (Sternberg 1959; Baker 1978; Rozo et al. 2012). The saucer-like morphology corresponds to the description of floodbasins by Makaske (2001), which are indicative of avulsion and are a key characteristic for distinguishing anastomosing from other multiple channel rivers.

The stable position of channels (Smith and Putnam 1980; Rust 1981; Smith 1986) and the rarity or absence of meandering features (Smith 1983; Nanson and Croke 1992) have been considered primary characteristics in anastomosing rivers. However, meandering features have also been identified in the anastomosing Amazon River (Sternberg 1959; Baker 1978; Mertes et al. 1996; Latrubesse and Franzinelli 2002; Rozo 2004; Rozo et al. 2012). Despite climatic differences with the Amazon, meandering characteristics have also been identified in several Australian anastomosing rivers (Bowler et al. 1978; Brizga and Finlayson 1990; Nanson and Knighton 1996; Schumm et al. 1996; Gibling et al. 1998) and in some anastomosing rivers in western Canada (Smith 1983; Thomas et al. 1987; Makaske 2001). In addition, meandering and braided channels may all form part of a broader anastomosing river system (Makaske 2001), as well as part of anabranching rivers (Nanson and Knighton 1996; Nanson and Gibling 2003). Makaske (2001) mentioned that these meandering features are not characteristic in anastomosing rivers, but they may still be present.

The morphology of the Colombian Amazon River shows dominant meandering features with extensively distributed scroll bars generated by the migration of the main and secondary channels. The islands in the system are formed by several sets of scroll bars that migrate in different directions from a central area, which is located towards the upstream part of the islands. Some of these islands also develop lakes on the downstream side of the central area, from where the scrolls bars are migrating. Other islands develop wide lakes in the swales of what correspond to the first scroll bars that were formed. However, narrow lakes which follow the swales dominate this landscape. Islands with saucer-like morphology were not identified in the Colombian Amazon River. The islands in the studied reach seem to have developed as a product of within-channel deposition rather than from avulsion, which leads to the development of the multichannel pattern. The situation is particularly different in the Amazon River between the confluences of the Negro and Madeira Rivers, where not only is avulsion responsible for the multichannel pattern, but within-channel deposition also leads to the development of anastomosis (Rozo et al. 2012).

The dominant meandering characteristics in the Colombian Amazon River indicate that this reach is distinct from the Amazon River in Brazil, where anastomosing patterns have been suggested (Sternberg 1959; Baker 1978; Mertes et al. 1996; Latrubesse and Franzinelli 2002; Rozo 2004; Rozo et al. 2012). However, this Colombian reach is an example of the meandering reaches in the Solimões River in Brazil recognized by Baker (1978). The morphologic characteristics and temporal analysis suggest that this reach of the river has a meandering, multichannel pattern which corresponds to a laterally active anabranching river following the multichannel river classification of Nanson and Knighton (1996). However, field research must be undertaken to characterize the sedimentology of this part of the fluvial system and describe its channel pattern in more detail.

The percentage of change in the plan view area per year and migration rates discussed above also suggest a change from meandering to anastomosing from upstream to downstream. The Upper Amazon River (i.e. the Ucayali and Amazonas Rivers in Peru, see Figure 1B) displays an active meandering system. The Colombian Amazon River and the Solimões River in Brazil (see Figure 1B) represent a less laterally active meandering pattern and a relatively stable anastomosing reach downstream Manaus.

Conclusions

The percent change in the plan view area of the system and the maximum migration rates obtained for the reach of the Colombian Amazon River are relatively low when compared with values found upstream and in the reach between the confluences of the Jutái and Japurá Rivers. This indicates that the reach of the Amazon that was studied here is less active than reaches upstream and the specific reach downstream of the Jutái–Japurá confluences. Furthermore, it shows a relatively different trend in stability as compared with the Amazon between Iquitos and the mouth of the Madeira River, with an increase in stability from Iquitos to the mouth of the Javará River, a decrease towards the mouth of the Japurá River and again an increase toward the confluence with the Madeira River.

Deposition in the Colombian Amazon predominated between 1986 and 2006, however erosion was more intense than deposition between 1994 and 2001. Island dynamics follow the same depositional tendency as the system as a whole, with more new islands forming, a greater total island area and accretion of existing islands to other islands towards 1994 and 2006. In contrast, decrease in the area of islands and a rise in island erosion was found by 2001.

Variations in discharge, registered at the Nazareth gauging station, seem to be responsible for deposition and erosion dynamics found from remote sensing analysis in the Colombian Amazon River. Discharge variation at Tamshiyacu (Peru) and Olivença (Brazil) gauging stations, upstream and downstream of the area of study, respectively, suggest patterns of erosion and deposition which differ from those found in the Colombian Amazon River. This indicates that different hydrological regimes in the drainage areas that do not overlap between these three gauging stations influence variations in discharge, and consequently erosion and deposition dynamics.

Characteristics such as the multichannel platform, the sinuous main and secondary channels with meander development, lateral activity of the channel margins, islands dominated by scroll bar morphology, the absence of islands with saucer-like morphology and extensively distributed scroll bars on the river floodplain suggest a multichannel meandering pattern for this reach of the Amazon, that corresponds to a laterally active anabranching river. However, more research is required, especially involving sedimentological data to better characterize the system in the context of meandering or anastomosing multichannel rivers. Also, causes for its development must be studied.

A temporal analysis based on remote sensing data provides important basic information about the dynamics of fluvial systems in the Holocene. Extreme care must be taken in the selection of images to be used for comparison, including minimizing errors induced by variations in water level, adjusting the resolution of the images to be compared and processing techniques. However, the accuracy of the results will depend on the required scale. Additionally, more research must be undertaken to evaluate the best parameters when working with temporal analysis in Amazonian Rivers.

Acknowledgments

This research was supported by the Graduate Program in Geology and Geochemistry of the Universidade Federal do Pará. Max G. Roza thanks CNPq for awarding a scholarship. We would like to thank Prof. Santiago Duque for providing hydrological information from Colombia and Prof. André Roy for his valuable comments and suggestions which helped to substantially improve this manuscript.

References

- Baker, V.R. (1978). Adjustment of fluvial systems to climate and source terrain in tropical and subtropical environments. In A.D. Miall (Ed.), *Fluvial Sedimentology* (pp. 211-230). Calgary: Canadian Society of Petroleum Geologists
- Blum, M.D., & Tornqvist, T.E. (2000). Fluvial responses to climate and sea-level change: a review and look forward. *Sedimentology*, 47, 2-48
- Bowler, J.M., Stockton, E., & Walker, M.J. (1978). Quaternary stratigraphy of the Darling River near Tilpa, New South Wales. *Proceedings of the Royal Society of Victoria*, 90, 78-88
- Brizga, S.O., & Finlayson, B.L. (1990). Channel avulsion and river metamorphosis - the case of the Thomson River, Victoria, Australia. *Earth Surface Processes and Landforms*, 15, 391-404
- Dunne, T., Mertes, L.A.K., Meade, R.H., Richey, J.E., & Forsberg, B.R. (1988). Exchanges of sediment between the flood plain and channel of the Amazon River in Brazil. *Geological Society of America Bulletin*, 110, 450-467
- Gibling, M.R., Nanson, G.C., & Maroulis, J.C. (1998). Anastomosing river sedimentation in the Channel Country of central Australia. *Sedimentology*, 45, 595-619
- Gupta, A. (Ed.) (2007). *Large Rivers: Geomorphology and Management*. Chichester: John Wiley & Sons
- Huguett, A., Galvis, J., & Ruge, P. (1979). Geologia In, *La Amazonia Colombiana y sus recursos - Proyecto Radargrametrico del Amazonas* (pp. 29-92). Bogotá: Instituto Geografico Agustin Codazzi
- Inman, D.L., & Nordstro, C.E. (1971). Tectonic and morphologic classification of coasts. *Journal of Geology*, 79, 1-7
- Irion, G., Junk, W.J., & Mello, J.A. (1997). The large central Amazonian river floodplains near Manaus: Geological, climatological, hydrological and geomorphological aspects. In W.J. Junk (Ed.), *The central Amazon floodplain: Ecology of a pulsating system* (pp. 23-46). Berlin: Springer
- Junk, W.J., Bayley, P.B., & Sparks, R.E. (1989). The flood pulse concept in river-floodplain systems. In D. Dodge (Ed.), *Proceeding of the International Large River Symposium, Canadian Special Publications of Fisheries and Aquatic Sciences* (pp. 110-127). Ottawa: Department of Fisheries and Oceans Canada
- Kalliola, R., Salo, J., Puhakka, M., Rajasilta, M., Häme, T., Neller, R.J., Rasänen, M.E., & Danjoy Arias, W.A. (1992). Upper Amazon channel migration. *Naturwissenschaften*, 79, 75-79
- Khobzi, J., Kroonenberg, S., Faivre, P., & Weeda, A. (1980). Aspectos geomofologicos de la Amazonia y la Orinoquia Colombianas. *Revista CIAF*, 5, 97-126
- Lane, E.W. (1955). The importance of fluvial morphology in hydraulic engineering. *American Society of Civil Engineers Proceedings*, 81, 1-17
- Latrubesse, E.M. (2008). Patterns of anabranching channels: The ultimate end-member adjustment of mega rivers. *Geomorphology*, 101, 130-145
- Latrubesse, E.M., & Franzinelli, E. (2002). The Holocene alluvial plain of the middle Amazon River, Brazil. *Geomorphology*, 44, 241-257
- Maia, R.G.N., Godoy, H.K., Yamaguti, H.S., Moura, P.A., Costa, F.S.F., Holanda, M.A., & Costa, J.A. (1977). *Projeto Carvão no Alto Solimões* Final report, Companhia de Pesquisa de Recursos Naturais - Departamento Nacional de Produção Mineral, Manaus
- Makaske, B. (1998). Anastomosing rivers; forms, processes and sediments. *Nederlandse Geografische Studies* 249. Utrecht: Koninklijk Nederlands Aardrijkskundig Genootschap/Faculteit RuimtelijkeWetenschappen, Universiteit Utrecht

- Makaske, B. (2001). Anastomosing rivers: a review of their classification, origin and sedimentary products. *Earth-Science Reviews*, 53, 149-196
- Martinez, J.M., Guyot, J.L., Filizola, N., & Sondag, F. (2009). Increase in suspended sediment discharge of the Amazon River assessed by monitoring network and satellite data. *CATENA*, 79, 257-264
- Meade, R.H. (1994). Suspended sediments of the modern Amazon and Orinoco rivers. *Quaternary International*, 21, 29-39
- Meade, R.H. (1996). River-sediment inputs to major deltas. In J.D. Milliman, & B.U. Haq (Eds.), *Sea-level Rise and Coastal Subsidence: Causes, Consequences and Strategies* (pp. 63-85). Dordrecht Kluwer Academic Publishers
- Mertes, L.A.K., Dunne, T., & Martinelli, L.A. (1996). Channel-floodplain geomorphology along the Solimões-Amazon River, Brazil. *Geological Society of American Bulletin*, 108, 1089-1107
- Nanson, G.C., & Croke, J.C. (1992). A genetic classification of floodplains. *Geomorphology*, 4, 459-486
- Nanson, G.C., & Gibling, M.R. (2003). Anabranching Rivers. In G.V. Middleton (Ed.), *Encyclopedia of Sediments and Sedimentary Rocks* (pp. 9 -11). Dordrecht: Kluwer Academic Publishers
- Nanson, G.C., & Knighton, D. (1996). Anabranching rivers: their cause, character and classification. *Earth Surface Processes and Landforms*, 21, 217-239
- Peixoto, J.M.A., Nelson, B.W., & Wittmann, F. (2009). Spatial and temporal dynamics of river channel migration and vegetation in central Amazonian white-water floodplains by remote-sensing techniques. *Remote Sensing of Environment*, 113, 2258-2266
- Potter, P.E. (1978). Significance and origin of big rivers. *Journal of Geology*, 86, 13-33
- Rego, L.F.d.M. (1930). *Notas sobre a geologia do território de Acre e da Bacia do Javari*. Manaus: Cezar and Cavalcante
- Rozo, J.M.G. (2004). *Evolução Holocênica do Rio Amazonas entre a Ilha do Careiro e a foz do Rio Madeira* MSc Thesis, Universidade Federal do Amazonas, Manaus
- Rozo, M.G., Nogueira, A.C.R., & Truckenbrodt, W. (2012). The anastomosing pattern and the extensively distributed scroll bars in the middle Amazon River. *Earth Surface Processes and Landforms*. Accepted article
- Rozo, M.G., & Soto, C.C. (2010). Quantification of change and migration rates in the Amazon River. In, *45 Congresso Brasileiro de Geologia*. Belém: Sociedade Brasileira de Geologia
- Rust, B.R. (1981). Sedimentation in an arid-zone anastomosing fluvial system; Cooper's Creek, central Australia *Journal of Sedimentary Petrology*, 51, 745-755
- Schumm, S.A., Erskine, W.D., & Tilleard, J.W. (1996). Morphology, hydrology, and evolution of the anastomosing Ovens and King Rivers, Victoria, Australia. *Geological Society of America Bulletin*, 108, 1212-1224
- Smith, D.G. (1983). Anastomosed fluvial deposits: modern examples from Western Canada. In J.D. Collinson, & J. Lewin (Eds.), *Modern and Ancient Fluvial Systems. Special Publication of the International Association of Sedimentologist* 6 (pp. 155-168). Oxford: Blackwell
- Smith, D.G. (1986). Anastomosing river deposits, sedimentation rates and basin subsidence, Magdalena River, northwestern Colombia, South America. *Sedimentary Geology*, 46, 177-196
- Smith, D.G., & Putnam, P.E. (1980). Anastomosed river deposits; modern and ancient examples in Alberta, Canada. *Canadian Journal of Earth Science*, 17, 1396-1406

- Sternberg, H.O.R. (1959). Radiocarbon dating as applied to a problem of Amazonian morphology. In, *XVIII Congrès International de Géographie* (pp. 399-424). Rio de Janeiro: Union Géographique Internationale
- Syvitski, J.P.M., Vorosmarty, C.J., Kettner, A.J., & Green, P. (2005). Impact of Humans on the Flux of Terrestrial Sediment to the Global Coastal Ocean. *Science*, 308, 376-380
- Thomas, R.G., Smith, D.G., Wood, J.M., Visser, J., Calverley-Range, E.A., & Koster, E.H. (1987). Inclined Heterolithic Stratification - Terminology, Description, Interpretation and Significance. *Sedimentary Geology*, 53, 123-179
- Tucker, C.J., Grant, D.M., & Dykstra, J.D. (2004). NASA's global orthorectified landsat data set. *Photogrammetric Engineering and Remote Sensing*, 70, 313-322
- Wohl, E.E. (2007). Hydrology and Discharge. In A. Gupta (Ed.), *Large Rivers: Geomorphology and Management* (pp. 29-41). Chichester: John Wiley & Sons

4 THE MEANDERING PATTERN OF THE AMAZON RIVER DURING THE LATE PLEISTOCENE*

Max G. Rozo¹, Afonso C. R. Nogueira¹, Isaac Daniel Rudnitzki¹

¹ *Instituto de Geociências, Universidade Federal do Pará, CP 1611, 66.075-900, Belém/PA, Brasil*

* Submitted to Quaternary Research

Abstract

Channel pattern characteristics of the Amazon River prior to Holocene conditions have been scarcely described. It has been suggested a main meandering channel pattern developed during Late Pleistocene based on point bar deposits found in the western Amazonas sedimentary basin. It has also been indicated that the Iça Formation, which represents Pliocene – Pleistocene deposition in the Solimões sedimentary basin developed from a single-channel meandering pattern with straight reaches. Sedimentary processes were studied using field data, clay and heavy minerals analyzed and optically stimulated luminescence (OSL) dates were obtained from the Iça Formation in the Coari area to define the characteristics of the fluvial system which existed when these sediments accumulated, and to understand the mechanisms controlling the development of the river during that time. Additionally, recent deposition was also studied to understand present-day depositional conditions. The age of the deposits described as the Iça Formation in the Coari area is between 38 ± 4 and 133.8 ± 20.9 ka BP which indicates its Upper Pleistocene age. A main sea level drop during the Late Pleistocene (130 - 18 ka) had a direct influence on deposition of the Iça Formation in the Coari area, with the development of at least three fluvial terraces indicated by the ages obtained. During this time the system was characterized by incision with a more energetic main channel, indicated by thick fluvial channel deposits and less energetic secondary channels that developed extensive point bars over older deposits. Sea level rise and resulting stability from ~6 ka BP suggest a vertically and rapidly aggrading system in the Late Holocene, as indicated by the thick floodplain deposits in the area. The Amazon River was already established in the Late Pleistocene, at least over the last 133.8 ± 20.9 ka BP as a multichannel meandering river, with flow to the East.

Keywords: Amazon River, meandering multichannel system, Iça Formation, Late Pleistocene.

Introduction

The present-day morphological features of the Amazon River have been discussed in relation to the channel pattern which best describes this large fluvial multichannel system (Baker, 1978; Kalliola et al., 1992; Latrubesse and Franzinelli, 2002; Mertes et al., 1996; Rozo, 2004; Rozo et al., 2012a; Rozo et al., 2012b; Sternberg, 1959). Basically, the Amazon River is characterized by a meandering multichannel river pattern in Peru (Kalliola et al., 1992) and Colombia (Rozo et al., 2012b), a multichannel river with meandering and anastomosing reaches in Brazil upstream the confluence with the Negro River (Solimões River) (Baker, 1978) and an anastomosing river with meandering secondary channels downstream Manaus (Rozo et al., 2012a). These determinations have mostly been made using remote sensing data, which allowed the interpretation of saucer-like morphology in the anastomosing reaches and scroll bar patterns in the meandering ones, as well as punctual field descriptions of the river deposits. The saucer-like morphology corresponds to the description of floodbasins by Makaske (2001), and represents a key characteristic for distinguishing anastomosing from other multiple channel rivers. Scroll bars are a distinctive characteristic of single-channel meandering rivers, but laterally migrating channels with the development of scroll morphology can be present in multichannel rivers (Bowler et al., 1978; Brizga and Finlayson, 1990; Nanson and Knighton, 1996; Taylor and Woodyer, 1978). The Amazon River has also been described as predominantly anabranching (Latrubesse, 2008). The term anabranching is applied to any type of multiple channel pattern (Nanson and Knighton, 1996).

Channel pattern characteristics of the Amazon River prior to present-day conditions have been scarcely described, with few studies addressing the subject (Motta, 2008; Soares, 2007). In contrast, a broad discussion about the origin of the Amazon River as a transcontinental eastward flow has occurred in recent years (Campbell et al., 2006; Figueiredo et al., 2009; Hoorn et al., 1995; Hoorn et al., 2010; Latrubesse et al., 2010; Latrubesse et al., 2007; Rossetti et al., 2005; Wilkinson et al., 2010). However, no agreement on the exact time when this event took place and very scarce sedimentologic data on the deposits of central Amazonia characterized this discussion. Thus the development of the Amazon River as it is currently known can be ascribed to any time between the Late Miocene to Late Pleistocene.

To our knowledge, no research has yet been undertaken to understand the characteristics of the Amazon River during the Pleistocene. Soares et al. (2010) suggested a main meandering channel pattern developed during Late Pleistocene based on the oldest (65.2 ± 8.8 ka) point bar deposits found in the western Amazonas sedimentary basin. It has also been discussed that the Iça Formation, which mainly represents Pliocene – Pleistocene deposition in the Solimões sedimentary basin (Rossetti et al., 2005), developed from a single-channel meandering pattern with straight reaches (Motta, 2008). However, the characteristics of this meandering system are poorly understood because its identification is only based on the presence of point bar deposits. Additionally, little is known about how this single-channel meandering river evolved into the present-day system, and which were the mechanisms that conditioned this development.

Another issue that remains controversial is whether the sediments that outcrop in the Coari area and that have been attributed to the Iça Formation (Motta, 2008) in fact belong to this formation as described by Maia et al. (1977). Rossetti et al. (2005) restricted the Iça Formation to the western Solimões sedimentary basin and assigned it a Pliocene – Pleistocene age based on its stratigraphic position. The Iça Formation in Brazil seems to correlate with similar fluvial deposits described in other Amazonian regions: *Terciario Superior Amazónico* deposits (Upper Tertiary deposits) in Colombia (Huguett et al., 1979); Candelaria Formation (Leytón and Pacheco, 1989) in Bolivia; Rio Madeira Formation in the Brazilian border with Bolivia (Adamy and Romanini, 1990; Rizzotto et al., 2005) and the Madre de Dios Formation (Oppenheim, 1946) which has also been referred to as the Ucayali Formation (Kummel, 1948). The age of this formation was suggested to be Pliocene-Holocene (Kummel, 1948), Pleistocene-Holocene (Campbell and Romero-Pittman, 1989), Upper Pleistocene (Quadros et al., 2006; Rizzotto et al., 2006) and Miocene-Pliocene (Campbell Jr et al., 2010; Campbell et al., 2001).

In this study, the sedimentology of the deposits that outcrop in the Coari area and that have been attributed to the Iça Formation (Figure 1) are examined to define the characteristics of the fluvial system which existed when these sediments accumulated, and to understand the mechanisms controlling the development of the river during that time. Additionally, recent deposition is also studied to understand present-day depositional conditions. Grain size, clay and heavy mineral analyses were undertaken to support sedimentological descriptions, help differentiate stratigraphic units and allow discussions on the dominant conditions during deposition. Optical stimulated luminescence samples were also collected to determine the age of the sediments in this area.

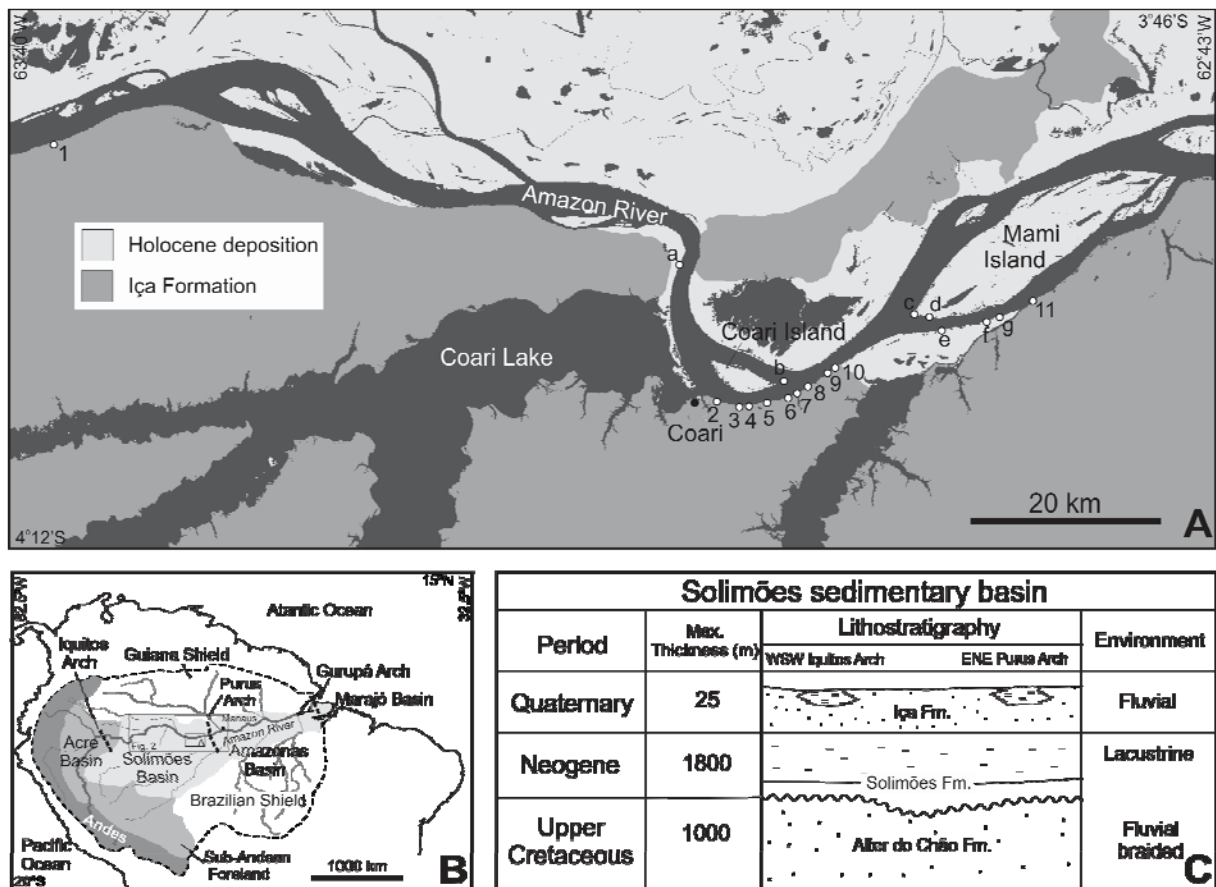


Figure 1 Location map of the Coari area A) Lithostratigraphic units in the study area and location of the stratigraphic profiles. Profiles 1 to 11 correspond to Pleistocene deposition and Profiles (a) to (g) correspond to Holocene deposits. B) Geotectonic units of the Amazon region. C) Stratigraphy of Upper Cretaceous to Quaternary sedimentary deposits in the Solimões sedimentary basin, modified from Wanderley Filho et al. (2007).

Study area

This area is located in the eastern part of the Solimões sedimentary basin (Figure 1B), near the town of Coari (Figure 1A). In this reach, the Amazon River (Solimões River in Brazil) is a multichannel system with an overall meandering appearance (Figure 1A). The floodplain of the Amazon River extends broadly on the left margin. On the right, steep-sided channel margins are locally characterized by slump blocks and great water-depths, up to 24 m near the bank, where older deposits outcrop. This area was selected for study because it represents one of the best outcrops of the sediments overlying the Solimões Formation in the area, and also because it is relatively easily accessible. A seasonal flood pulse controls water dynamics of the Amazon, with a high level by June and low water stage around December (Junk et al., 1989). Precipitation is responsible for the mean amplitude of the annual water-level fluctuations which, in the central Amazon region, can reach 10 m (Irion et al., 1997).

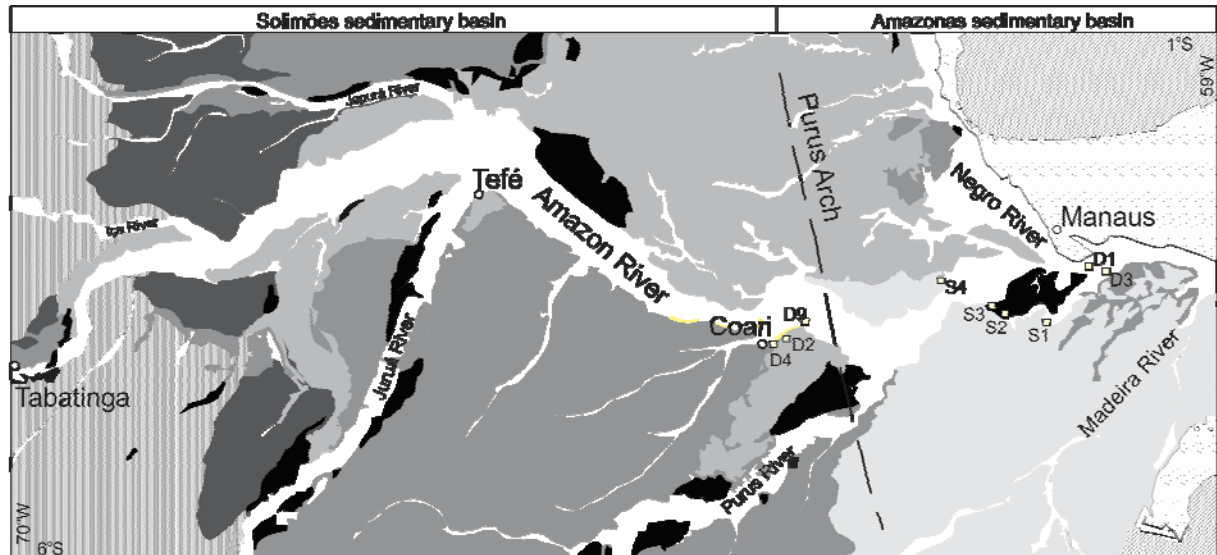
Geological Setting

The Amazon River system developed on an extensive intracratonic depression located between the Guyana Shield in the north and the Central-Brazilian Shield in the south. This depression is subdivided into the Acre, Solimões, Amazonas and Marajó sedimentary basins, which are separated from one another by the Iquitos, Purus and Gurupá arcs, respectively (Caputo, 1984) (Figure 1B). Regionally, Cretaceous and older deposits outcrop to the east of the Negro River while Pliocene and Miocene deposits outcrop west of the Jurúa River (Figure 2). Pleistocene and Holocene deposition is extensively developed between Manaus and the Jurúa River area (Figure 2). In the Coari area two units outcrop mainly along the right river bank, the Solimões and Iça Formations. These formations overlay fine to coarse-grained siliciclastic deposits of the Upper Cretaceous Alter do Chão Formation (Caputo et al., 1972; Kristler, 1954), and are all part of the Solimões sedimentary basin (Figure 1C).

The Solimões series was introduced by Rego (1930) to define Cenozoic sediments that outcrop along the Solimões River. This unit is also known as Pebas, Ramon and Rio Branco Formations in the Acre sedimentary basin and in the sub-Andean basins in Peru and Colombia (Caputo et al., 1971). Maia et al. (1977) subdivided this unit into two formations: a mudstone dominated lower formation denominated Solimões and a sandstone dominated upper formation denominated Iça. However, it is also considered as a single Formation with two units (Caputo, 1984; Eiras et al., 1994; Silva, 1988).

The Solimões Formation is characterized by laminated to massive, light to greenish gray mudstones intercalated with coal layers. Fine to coarse sandstone is also common in this succession (Maia et al., 1977; Nogueira et al., 2003). Overlying the Solimões Formation is the Iça Formation; the contact between these two units marks an unconformity (Figures 5A and 5B). The Iça Formation is characterized by fine to medium sandstones and siltstones with localized yellow to red clay conglomerates. The Solimões Formation has been interpreted as having developed in a continental fluvio-lacustrine environment (Caputo, 1984; Maia et al., 1977), and is also considered to have developed in an extensive lake probably connected to the Atlantic Ocean (Frailey et al., 1988). Meandering channels with marine influence have also been proposed as the depositional environment for this formation in the western part of the basin. This last hypothesis is based on the presence of gypsum layers, carbonatic nodules, fresh water and marine mollusks and sedimentary structures such as tidal rhythmites and flaser and wavy bedding (Gingras et al., 2002; Hoorn, 1993; Hoorn, 1994; Hovikoski et al., 2005; Rasanen et al., 1995). Recently, Latrubesse et al. (2010) have restricted the Solimões Formation to a continental environment dominated by avulsive rivers associated with megafan

systems and flood basins. Also an anastomosing fluvial system has been interpreted in western Amazonia during Late Miocene to the upper Solimões Formation (Gross et al., 2011). The Iça Formation is interpreted as having developed in a fluvial environment (Maia et al 1977).



	Rossetti et al. (2005)	Merles et al. (1986)	Letrubes and Franzinelli (2002)	Soares (2007) Soares et al. (2010)	Rozo et al. (2012)	This study
Holocene	□ Q4 *0.24 - 0.13 ka	Mixed Floodplain	Channel dominated floodplain		Channel bar deposits	Channel bar deposits
	■ Q3 *8.73 - 2.48 ka	Scroll bar Floodplain	Impeded floodplain *0.31±0.05ka *1.3±0.13ka		Floodplain deposits	Floodplain deposits
Pleistocene	□ Undated Unit		Scroll bar deposits	Fluvial terrace 3 *(S3) 7.5±0.90ka *(S2) 34.5 ±4.4ka	Scroll bar deposits *(D1) 9.4±0.60ka *(D3) 7.5±0.85ka	Scroll bar deposits *(D8) 10 ± 2.2ka
	■ Q2 *27.2 ka			Fluvial terrace 2 *(S2) 34.5 ±4.4ka *(S1) 60.7 ±6.6ka		Iça Formation *(D4) 38 ± 4.0ka *(D2) 133.8 ±20.9ka
	■ Q1 *43.7 - 37.4 ka ¹			Fluvial terrace 1 *(S1) 60.7 ±6.6ka *(S4) 85.2 ±8.8ka		
	■ Iça Fm					
Pliocene						
Miocene						
Cretaceous						
Pre-Cretaceous						

*Radiocarbon dating
¹Luminescence dating

Figure 2 Regional geologic map. Units present in the Solimões and western Amazonas sedimentary basins, modified from Rossetti et al. (2005). Units individualized and dated by different authors in the reach of the Amazon River between Tabatinga and the mouth of the Madeira River. See Figure 1B for location.

The age of the Solimões Formation was established based on palynological studies as Paleocene to Pleistocene (Daemon and Contreiras, 1971) and more recently as Miocene (Arai

et al., 2003; Hoorn, 1994). The coal layers correspond to the Miocene to Upper Pliocene based on the presence of ostracods (Caputo, 1984). Recently, the Solimões succession has been positioned in the Upper Miocene in the Coari area (Silveira and Nogueira, 2005). The same age has also been attributed to the uppermost levels of this succession in western Brazilian Amazonia (Latrubesse et al., 2010). The Iça Formation has been attributed to the Pleistocene-Holocene (Caputo, 1984) and Pliocene-Pleistocene (Rossetti et al., 2005)

In the western Amazonas sedimentary basin, Soares (2010) distinguished two Pleistocene and one Holocene-Pleistocene fluvial terraces (Figure 2). Downstream the confluence of the Negro River, Rozo et al. (2012a) recognized three Holocene morphostratigraphic units: 1) Scroll bar deposits; 2) Floodplain deposits in which natural levees, crevasse splay, floodplain lake and floodbasin deposits were characterized and 3) Channel bar deposits (Figure 2).

Methods

Field work was carried out along the Amazon River in the Coari area (Figure 1A), during the low water season in 2009 (October – November). Terraces and recent cutbank exposures were described using standard sedimentological and facies analysis that generated stratigraphic profiles for 18 locations (Figure 1A). Fifty seven samples for grain size, clay and heavy mineral analysis were taken in profiles 3, 5, 8, 9, 10, 11, (a), (b), (c), (e) and (g) (Figures 7 and 8) to support sedimentological descriptions, help with differentiating stratigraphic units and allow discussions on the dominant climate during deposition. Nine samples for optical stimulated luminescence were also collected to determine the age of the sediments (Figures 3 and 4).

The clay fraction ($< 2 \mu\text{m}$) was separated by sedimentation and centrifugation (Brindley and Brown, 1980). Clay fractions were mounted on glass slides and analyses were carried out on three oriented samples (untreated, glycolated and heated at 550°C). X-ray diffraction data (XRD) were obtained using a PANalytical X'pert pro MPD PW 3040/60 diffractometer equipped with Cu $K\alpha$ radiation source and operated at 40 kV/40 mA. All XRD data were collected under the same experimental conditions, in the angular range $3^{\circ} \leq 2\theta \leq 35^{\circ}$ with counting time 47 m 37 s. Relative proportions of clay minerals (smectite and kaolinite) were estimated on the basis of peak intensity measurement (Table 3).

All samples were sieved to obtain the 63 to 125 μm size fraction. Heavy minerals were separated from light mineral by gravity settling using bromoform. Thin sections were prepared for the identification of minerals under the microscope. Heavy minerals

quantification was achieved by counting 300 grains per thin section, excluding opaques. The sum of the hornblende, augite, hyperstene and epidote divided by the sum of zircon, tourmaline and rutile (ZTR) yielded the unstable/stable ratio (Table 4).

Nine optically stimulated luminescence (OSL) dates were determined at the Glass and Dating Laboratory of the Faculty of Technology of São Paulo, Brazil (FATEC–SP). The samples were collected with PVC tubes (60 x 5 cm) in the following profiles and depths: 1 (11.1 and 3 m), 3 (4, 8.1 and 11.4 m), 4 (10.8 m), 8 (7.3 m), 10 (3.2 m) and (d) (7 m) as indicated in Figures 3 and 4. Samples were treated with 20% H₂O₂ for 4 hours, 20% HF for 45 minutes, 20% HCl for 2 hours, and heavy liquid (SPT) treatments. This was followed by sieving to sort out grain sizes between 100 and 160 µm.

The γ -irradiation was carried out using a Co-60 source. Natural radioactive isotope contents were determined with gamma spectroscopy, using an Inspector portable spectroscopy workstation - Canberra, equipped with an NaI(Tl) detector model 802 and lead shield model 727. The data were calibrated with JG-1a, JA-3, JB-2, and JB-3 Japanese soil standard samples. Peak energies used were 238, 295, 352, 1120, 1460, 1760, and 2620 keV. The annual dose was calculated using the activity concentration from ²³²Th, ²³⁸U and ⁴⁰K, determined by gamma spectrometry and Bell's equation. Optically stimulated luminescence (OSL) measurements were recorded with an automated Daybreak Nuclear and Medical system (Model 1100-series). OSL dating of quartz grains was performed using a blue light (470 nm) and detection through ~ 5 mm Hoya U-340 filters. The OSL ages were obtained by the standardized growth curve (SGC) method. Samples D1, D2, D3, D7 and D8 were dated following the multiple-aliquot regenerative-dose (MAR) protocol and samples D4, D5, D6 and D9 were dated by the single-aliquot regenerative-dose (SAR) protocol (Murray and Wintle, 2000). In the MAR protocol used here, using the total regeneration method, all aliquots (with the exception of the natural aliquots, about 10) are bleached to near zero by sunlight exposure during 16 h and then given laboratory doses. In all cases, samples were preheated to 250°C for 10 s prior to measurements, and to 200 °C after the test dose. Following preheating, the OSL shine down curves of the aliquots were measured, the late-light regions were subtracted, and the paleodose values were obtained by direct comparison of the natural OSL with those resulting from artificial irradiation. Tests for dose recovery were performed and the results showed that recovered doses matches given doses. For the paleodose determinations, at least 20 aliquots were measured per sample.

Results

Lithofacies and depositional processes

The facies in the Coari area include mudstones and fine to coarse sandstone of Pleistocene age, as well as Holocene clay and fine to coarse sand in horizontal and inclined beds. Eighteen profiles were described and divided into two correlation sets. The first set corresponds to mudstones and sandstones distributed in 11 profiles (Figures 1, 3 and Table 1). These are located on the right margin of the Amazon River where the Solimões and Iça Formations outcrop. Most of the profiles are located downstream of the town of Coari, with only profile 1 located upstream. The second set corresponds to clay and sand deposits in 7 profiles located mainly downstream of Coari, on the right margin of the river and in the islands, with profile (a) located upstream of Coari (Figures 1, 4 and Table 1). At the base of the profiles, sediments of the Solimões Formation are present which have been interpreted as lacustre-prodelta, delta front and deltaic plain deposits (Figures 3, 5A and 5B) (Vega, 2007).

Pleistocene lithofacies

Massive and even-parallel laminated Mudstone (Mml). This facies consists of massive and subordinate even-parallel laminated mudstone, including minor thin layers of locally wavy fine sandstone. It reaches up to 3.2 m in thickness and is part of fining upward cycles. The predominant process of deposition from suspension was affected by sporadic sandy influx.

Wavy bedded sandstone/mudstone (SMw). Fine to medium sandstone up to 20 cm thick intercalates mudstone of thickness varying from 8 to 20 cm, with characteristic wavy bedding. Subordinate flaser bedding, ripples and clay clasts up to 5 cm in diameter are present. Locally medium sandstone up to 8 cm thick containing mudstone clasts is ferruginized. This facies reaches up to 1.3 m in thickness. These wavy beds are the product of subaqueous dune migration, and lower current activity allows the deposition of fine material by suspension thus filling the troughs.

Inclined heterolithic stratified sandstone/mudstone (SMih). The layers of fine to medium sandstone and mudstone vary from 1 to 50 cm in thickness. The base of this facies is characterized by the presence of ferruginized medium to coarse sandstone varying in thickness between 3 and 51 cm. Flattened clasts of mudstone up to 3 cm in diameter are generally present in this ferruginized sandstone. Organic material is present in some of the deposits overlying the ferruginized sandstone and includes leaves and trunks, the latter being up to 70 cm in length and 25 cm in diameter. Fining upward cycles up to 1.2 m thick can be present in these deposits; some ripples appear in the sandstone. This facies reaches a thickness

of up to 7 m. The inclined heterolithic bedding results from the lateral accretion of point bars in sinuous channels. Mudstone clasts along the medium sandstone register more energetic stages inside the channel with terrigenous and organic detritus influx, as well as reworking of previously deposited mudstones.

Massive siltstone and sandstone (Sm). Siltstone and fine sandstone are organized in coarsening and fining upward cycles. Both cycles are characterized as occurring in the upper part of the profiles. In the case of the coarsening upward cycles, their thickness varies from 20 to 90 cm while the fining upward cycles vary from 1.2 to 4.5 m. This facies reaches up to 4.5 m in thickness. Primary structures could be obliterated since this facies is located in the upper part of the profiles, where weathering processes are more intense. The deposits overlying these sediments have been extremely weathered. The coarsening upward cycles are a result of upper regime flows that promote the influx of sandy material in low energy environments. The fining upward cycles result from sediments deposited under conditions of decreasing depth and velocity with a characteristic decrease in grain size and scale of the hydrodynamic structures up in the sedimentary section (Miall, 1992).

Planar cross bedded sandstone (Sp). Coarse to medium sandstone with sets up to 70 cm thick and which are part of fining upward cycles characterize this facies. It is strongly restricted at the base of each set. Coarse to medium sandstone up to 30 cm thick with flattened mudstone clasts up to 3 cm in diameter are present. These structures result from subaqueous dune migration in a unidirectional lower flow regime. The river bed is eroded and consequently clay clast deposition occurs at the dunes' base.

Trough cross bedded sandstone (St). Sets of coarse to fine sandstone form fining upward cycles or parts of cycles. These vary from 50 cm to 2.4 m in thickness when they are individual fining upward cycles and from 90 cm to 1.2 m when they are part of larger cycles. Some sets do not follow these cycles and can exhibit inclined stratification. Individual troughs have an amplitude of up to 120 cm and a height of 22 cm (Figure 5C). The base of the sets is generally characterized by coarse sandstone up to 10 cm thick with flattened mudstone clasts with diameters up to 3 cm (Figure 5D). At the top of some cycles, even-parallel laminated fine sandstone is common. This facies reaches up to 6.5 m in thickness. These structures result from subaqueous dune migration in a unidirectional lower flow regime. The river bed/bank is eroded and consequently deposition of mudstone clasts occurs at the dunes' base. The even-parallel laminated fine sandstone corresponds to stages of non migration of the dunes that allow the deposition of flat beds, forming even-parallel lamination.

Holocene lithofacies

Massive clay (Cm). This facies can be up to 5 m thick. Subordinate even-parallel lamination and lenticular bedding are present. Thin layers of sand up to 1 cm thick are present as well as sandy clay in some of the intervals; locally this sandstone can reach a thickness of 30 cm. These sediments generally follow the inclination of the scroll bar deposits, and they are more characteristic at the top of the profiles overlying the other facies. The predominant deposition by suspension was affected by sporadic fine sandy influx.

Clay with organic detritus (Co). This facies is composed of dark brown to black clays rich in organic matter. These layers vary from 2 cm to 1 m in thickness and can be intercalated with clay up to 20 cm thick. The diameter of the trunks varies from 8 to 20 cm and their length varies between 70 and 87 cm. They are also oriented perpendicularly to the inclination of the beds, yielding a preferential N-S and NNW-SSE orientation. Fragments of leaves are up to 4 cm long. In areas where poor access impeded our description, these deposits can be up to 2 m thick. This facies is formed during flooding when abundant organic detritus is available and once the water level drops, organic matter concentrates in the lakes.

Inclined heterolithic stratified sand/clay (SCih). Fine sand is characteristic in this facies, with layers from 10 to 60 cm and clay from 18 to 80 cm thick. Ripples are common in the fine sand. The inclined heterolithic bedding results from lateral accretion in sinuous channels.

Planar cross bedded sand (Sp). Several fining upward cycles from coarse to fine sand with planar cross bedding (Figure 6D), which follow the present-day direction of the flow (N70E) are present at the base of this facies. The fining upward cycles vary from 6 to 14 cm thick. At the top of the planar cross bedding sets, coarse to fine sand following cycles fining upward with cross-laminae are present. These last sets are between 5 and 9 cm thick. At the top of these sediments, dunes are present with wavelengths up to 8.3 m and height up to 30 cm (Figure 6C). Individual sets of cross laminae up to 9 cm thick are also present in coarse sand, and contain very fine pebbles up to 3 mm in diameter at the base of the sets. This facies result from the migration of straight crested dunes in the present-day channel.

Rippled sand (Sr). This facies is composed of fine and coarse sand between 25 and 90 cm thick. It occurs at the base of the profiles. The top of these deposits can be undulated and ferruginized following a dune configuration. This facies results from the migration of current ripples.

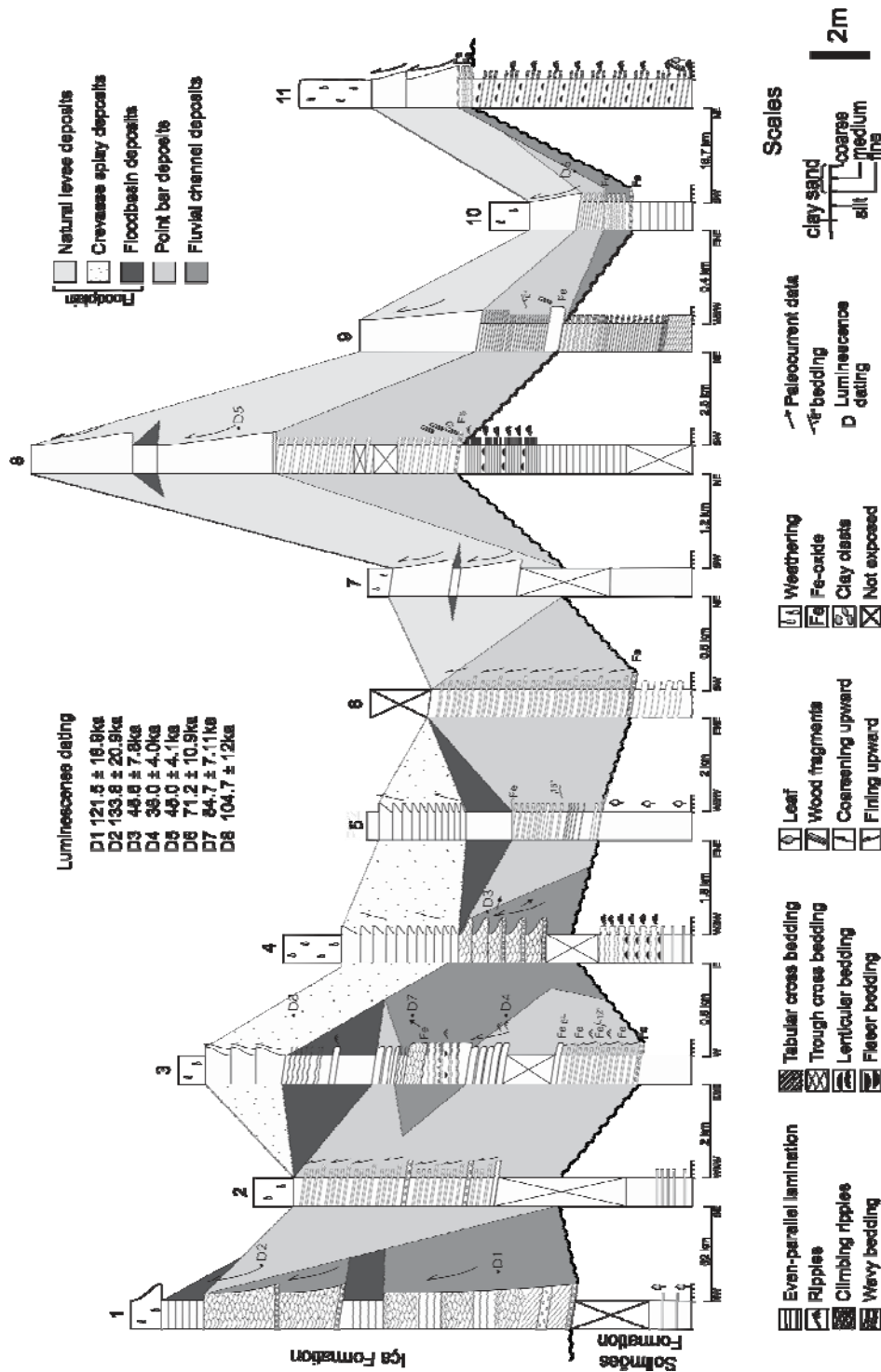


Figure 3 Pleistocene fluvial deposits. On the Coari area, channel and point bar deposits are more common than floodplain deposits. Location of logs indicated in Figure 1A. The depth at which the samples for OSL dating were collected is indicated in profiles 1, 3, 4, 8 and 10. Note that ages of the deposits are older in the upper part of the profiles when compared with the ages obtained in the lower parts.

Table 1. Sedimentary lithofacies

Epoch	Lithofacies	Lithology	Sedimentary structures	Process
Holocene	Cm	Clay, minor sandy clay	Massive and subordinate even-parallel lamination and lenticular bedding	Deposition by suspension with eventual sandy influx.
	Co	Clay	Massive with organic detritus	During flooding abundant organic detritus is available and once the water level drops, the organic matter concentrates in the lakes.
	SCih	Sand and clay	Inclined heterolithic stratification Ripples	Lateral accretion in sinuous channels.
	Sp	Sand	Planar cross bedding	Migration of straight crested dunes in the present-day channel.
	Sr	Sand	Ripples	Migration of current in the present-day channel.
Pleistocene	Mml	Mudstone	Massive and subordinate even-parallel lamination	Deposition by suspension with eventual sandy influx
	SMw	Sandstone and mudstone	Wavy bedding, subordinate flaser bedding, and ripples	Subaqueous dune migration, decrease in current activity allows the deposition of fine material by suspension filling the troughs.
	SMih	Sandstone and mudstone	Inclined heterolithic stratification	Lateral accretion in sinuous channels
	Sm	Siltstone and sandstone	Massive with coarsening and fining upward cycles	Coarsening upward cycles result from influx of sandy material in low energy environments. Fining upward cycles result from sediments deposited under conditions of decreasing depth and velocity.
	Sp	Sandstone	Planar cross bedding	Subaqueous dune migration in a unidirectional lower flow regime.
	St	Sandstone	Trough cross bedding and subordinate even-parallel lamination	Subaqueous dune migration in a unidirectional lower flow regime.

Lithofacies Association

The facies in the Coari area are grouped into four associations for Pleistocene deposition and five associations for Holocene deposition (Table 2).

Pleistocene lithofacies association

Fluvial channel deposits This facies association is characteristic of the base and middle parts of the Pleistocene deposition, varying laterally to point bar deposits (Figure 3). It follows fining upward cycles and is composed of trough cross bedded, coarse to fine sandstone and minor basal mudstone clasts (facies St). The trough cross beds indicate paleocurrents with azimuth values of 19° (Profile 3, Figure 4) and from 115 ° to 155 ° (Profile 4, Figure 4). In a

minor proportion, planar cross bedded coarse to medium sandstone (facies Sp) and intercalated wavy bedded medium to fine sandstone and mudstone (facies SMw) are present at the base of these deposits. The bedding geometry is tabular with a few inclined layers. The thickness of this association is between 1 and 6.5 m. The fining upward cycles generally end in massive and flat-laminated mudstone facies (Mml).

Holocene

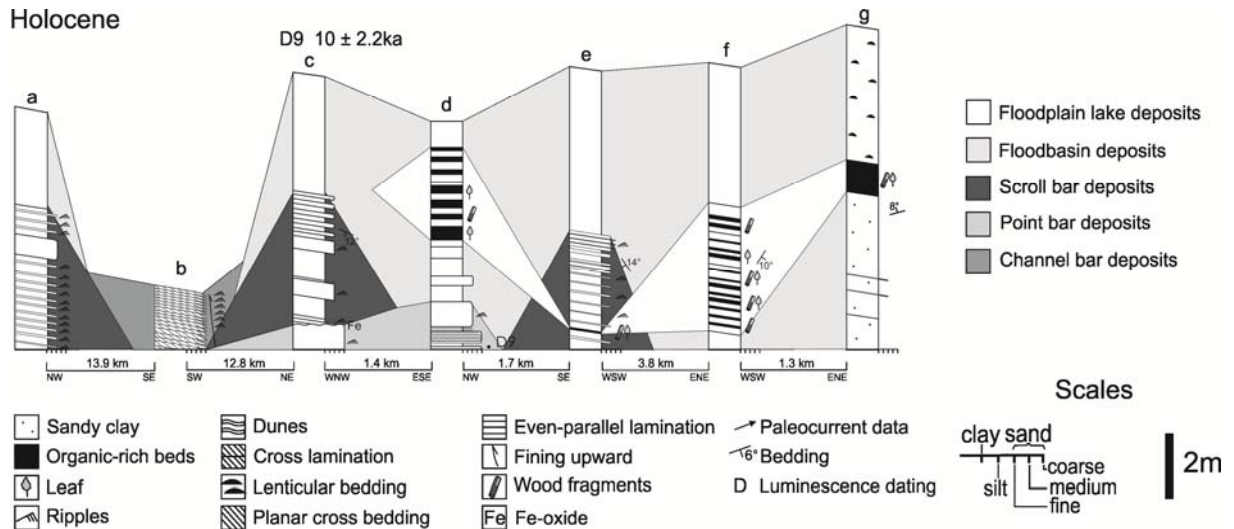


Figure 4 Holocene fluvial deposits. On the Coari area, floodplain deposits are more common than deposits associated to the channels. Location of logs indicated in Figure 1A. The depth at which a sample for OSL dating was collected is indicated in profiles (d).

Fining upward cycles, associated with trough cross stratification suggest deposition inside the channel. The presence of mudstone clasts indicates periods of bank erosion (Figure 5D). The clasts were transported and redeposited together with medium to coarse sandstone. Overlying these cycles, massive and flat-laminated mudstone (facies Mml) is present. Other structures are present mainly in the coarser sediments, such as planar cross bedding (facies Sp), wavy bedding, flaser bedding and ripples (facies SMw). These structures indicate different stages of within-channel deposition related to decreasing depth and velocity toward laterally accreted deposits.

Point bar deposits This association is characteristic of the base and middle sections of the Pleistocene deposits (Figures 3 and 5E). It is composed of fine to medium sandstone and mudstone with inclined heterolithic stratification (facies SMih). The bedding geometry is inclined and highly variable in the profiles described: N6E 12SE (lower part) and NS 6W (upper part) (profile 3); N80E 16NW (profile 5) and N70E 6SE (profile 9) (Figure 3). The thickness of this association is between 1 and 7 m. Individual layers of sandstone vary in thickness between 1 and 50 cm, and mudstone between 1 and 34 cm. It is characterized at its

base by medium to coarse ferruginized sandstone, with flattened clasts of mudstone. Organic material is present in some of the deposits overlying the ferruginized sandstone.

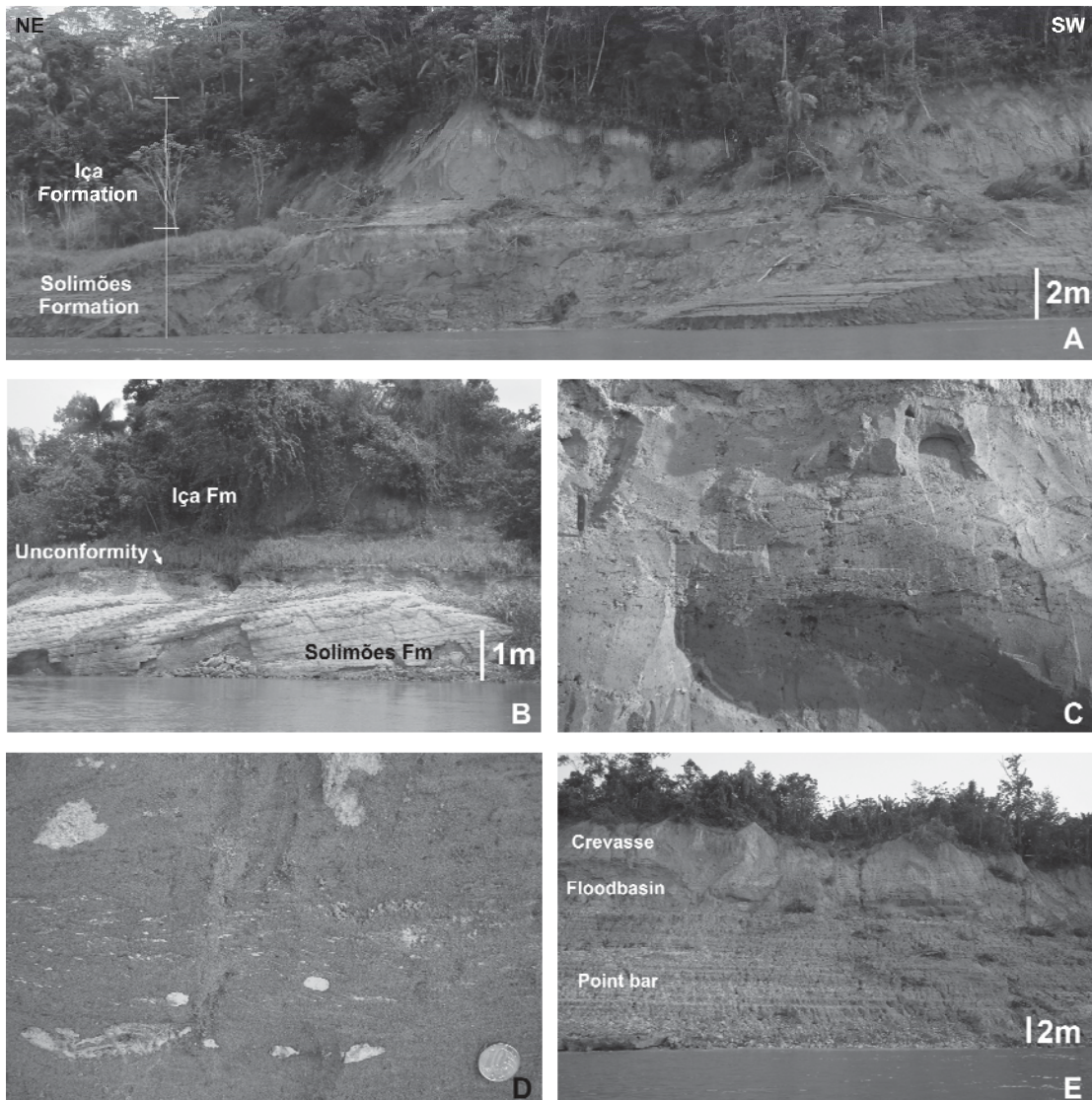


Figure 5 The Iça Formation in the Coari area. A) Typical outcrop of the Solimões and Iça Formations in the area. The Solimões Formation has a characteristic grey colour while the Iça Formation is reddish. B) Detail of the unconformity between the Solimões and Iça Formations, note the ferruginized surface that marks the contact. C) Trough cross stratification in the Iça deposits, note the mudstone clasts in the base of each set. D) Typical mudstone clasts at the base of the point bar and channel deposits in the Iça Formation. E) Overview of the point bar, floodbasin and crevasse splay deposits in profile 3, Figure 3. At the base of these deposits the Solimões Formation outcrops.

The presence of fining upward cycles characterizes its laterally accreted origin. The base of this set is marked by the presence of mudstone clasts indicating periods of erosion during which previously deposited mudstone was eroded, transported and deposited along medium to coarse sandstone. Organic material (trunks and leaves) is present in the mudstone overlying the base of this set. This indicates a change in the depositional conditions, from a

high energy environment that is able to erode mudstone and deposit it along coarser material, followed by a low energy environment which deposits clay along with trunks and leaves.

Floodbasin deposits This facies association is very restricted and mainly localized toward the upper part of the profiles (Figures 3 and 5E). It consists of massive and subordinate even-parallel laminated mudstone with minor thin layers of locally wavy fine sandstone (facies Mml). The bedding geometry is generally tabular and locally inclined (up to 25°). Mudstone layers vary between 30 cm and 1.6 m in thickness while fine sandstone layers vary between 1 and 15 cm. The thickness of this association varies from 30 cm to 3.2 m. This facies is part of fining upward cycles. This association characterized by massive and secondary even-parallel laminated mudstone at the top of fluvial channel, point bar and natural levee deposits suggest its deposition in the floodplain.

Crevasse splay deposits This facies association is characteristic of the upper part of the profiles overlaid by extremely weathered sediments (Figures 3 and 5E). It is exclusively composed of massive sandstone and siltstone forming coarsening upward cycles (facies Sm). The thickness of this association varies from 2.6 to 4 m. This association overlies fluvial channel, point bar and floodbasin deposits which indicates its overbank tendency. Deposition occurs through breaks of natural levees and deposition on the floodplain.

Natural levee deposits This facies association is characteristic of the upper part of the profiles overlaid by extremely weathered sediments (Figure 3). It is exclusively composed of massive sandstone and siltstone forming fining upward cycles (facies Sm). The thickness of this association varies from 1.6 to 4.5 m. It overlies fluvial channel, point bar and floodbasin deposits which indicate its overbank tendency. The fining upward cycles and its position at the top of the profiles suggest deposition as natural levees.

Holocene lithofacies association

Scroll bar deposits The ridge-and-swale morphology is characteristic in these deposits with the development of narrow lakes and minor secondary channels that follow the swales (Figure 6A). This association is composed of fine sand with ripples intercalated with clay following an inclined heterolithic stratification (facies SCih). The beds of this association are oriented from N72W 12SW (profile c) to N24W 14SW (profile e) (Figure 4). The thickness of this association varies from 3.5 to 4.5 m. It is characteristic of the base of the profiles overlying point bar deposits and covered by floodbasin deposits (Figure 4).

Floodbasin deposits This facies association is characteristic of the upper part of the profiles overlying the point bar, scroll bar and floodplain lake deposits (Figure 4). It consists of

massive clay with subordinate even-parallel lamination and lenticular bedding (facies Cm). The bedding geometry is tabular and inclined, following the inclination of underlying scroll bar deposits. In profile (g) the orientation of the beds is N80E 8NW (Figure 4). The thickness of this association varies from 0.8 to 5 m. Sporadic sandy influx is characterized by fine sand layers.

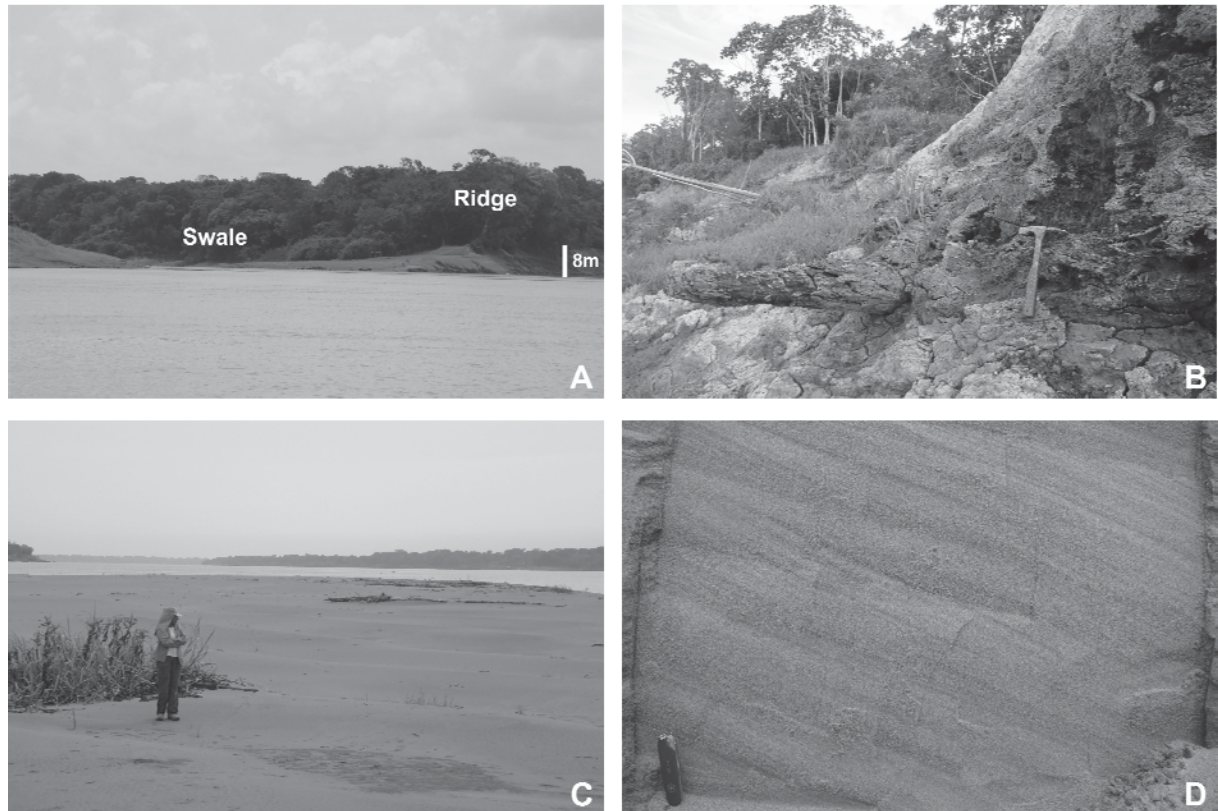


Figure 6 Holocene deposits in the Coari area. A) Morphology of ridge and swales characteristic of scroll bars from the main and secondary channels. B) Organic-rich beds in floodplain lake deposits. Tree trunks embedded in these deposits can be observed. This picture corresponds to Profile (g), Figure 4. C) Present-day sand bars in the Amazon River. Note the magnitude of these sand bars. At the top of these sediments, dunes are present with wavelengths up to 8.3 m and height up to 30 cm. D) Fining upward cycles from coarse to fine sand with planar cross bedding, which follow the present-day direction of the flow.

Floodplain lake deposits This facies association is comprised of clay with organic detritus (facies Co) and intercalated massive clay (facies Cm). This facies association occurs inside floodbasin deposits and locally inside scroll bar deposits (Figure 4). The bedding geometry is tabular and inclined, in profile (f) bedding orientation is N28E 10SE. The thickness of this association varies from 20 cm to 4 m. These sediments contain leaves and trunks, the latter reaching up to 20 cm in diameter and 87 cm in length, oriented perpendicularly to the inclination of the beds (Figure 6B).

Table 2. Sedimentary lithofacies association

Epoch	Lithofacies association	Lithofacies	Interpretation
Holocene	Fine sand with ripples intercalated with clay following inclined heterolithic stratification.	SCih	Scroll bar deposits
	Massive clay with subordinate even-parallel lamination and lenticular bedding	Cm	Floodbasin deposits
	Brown to black clay with organic detritus (leaves and trunks) intercalated with massive clay	Co, Cm	Floodplain lake deposits
	Coarse sand is characteristic of the base of this association, with the presence of planar cross bedding layers. Minor clay layers with thin layers of fine sand are present intercalating the coarse sand. Fine sand with ripples is also present.	Sp, Sr, Cm	Point bar deposits
	Coarse to fine sand with planar cross bedding and cross lamination organized in fining upward cycles, minor fine sandstone with ripples is also present	Sp, Sr	Channel bar deposits
Pleistocene	Trough cross bedded coarse to fine sandstone and minor basal mudstone clasts. In minor proportion planar cross bedded coarse to medium sandstone and intercalated wavy bedded medium to fine sandstone and mudstone. These deposits follow fining upward cycles.	SMw, Sp, St	Fluvial channel
	Fine to medium sandstone and mudstone with inclined heterolithic stratification and secondary fine sandstone with climbing ripples. At the base of this association, medium to coarse ferruginized sandstone with flattened clasts of mudstone overlaid by organic detritus can be present.	Smih	Point bar deposits
	Massive and subordinate even-parallel laminated mudstone with minor thin layers of fine sandstone locally wavy.	Mml	Floodbasin deposits
	Massive sandstone and siltstone with coarsening upward cycles	Sm	Crevasse splay deposits
	Massive sandstone and siltstone with fining upward cycles	Sm	Natural levee deposits

Point bar deposits This facies association is present at the base of profiles (c) and (d) and is overlaid by scroll bar and floodbasin deposits (Figure 4). Coarse sand with planar cross bedding (facies Sp), coarse to fine sand with ripples (facies Sr) and minor massive clay (facies Cm) compose this association. Coarse sand is characteristic of the base of the association with the presence of planar cross bedding layers. Minor clay layers up to 20 cm thick with thin layers of fine sand (up to 1 cm) are present, intercalating the coarse sand. The thickness of this association varies from 80 cm to 1.5 m. The coarse sediment in association with the planar

cross bedding, migrating in the present-day direction of Amazon River flow, suggest point bar deposition over which a scroll bar developed *sensu* Nanson (1980).

Channel bar deposits This facies association is characterized by coarse to fine sand with planar cross bedding and cross lamination organized in fining upward cycles (facies Sp), and minor fine sand with ripples is also present (facies Sr). The geometry of this association is inclined up to 10°. Characteristic fining upward cycles of planar cross bedding and cross lamination are the main components of this facies. The migration of these structures follows the present-day direction of channel flow. These deposits are submersed during the majority of the year, and only visible at very low water levels. These sediments were described in a sand bar located in the downstream extreme of Coari Island, the dimensions of the sandbar are up to 700 m long and 380 m wide. Sand bar surface follows dune morphology (Figure 6C).

Clay and heavy minerals

Kaolinite is present in all of the samples except one (recent deposition) while smectite is absent in five Iça Formation samples and three Solimões Formation samples (Table 3). The relative proportions of these clay minerals vary significantly between the three stratigraphic units present in the area. In the Solimões Formation, the relative proportion of smectite and kaolinite amount to 68% and 32%, respectively. In the Iça Formation smectite and kaolinite each amount to 50%. In recent deposition, the relative proportion of smectite reaches 90% while kaolinite amounts to 10%. The average smectite/kaolinite ratio in the Solimões Formation is 2.2, with values varying from 0 to 6 and a few values greater than 10 (Table 3). In general, S/K values are higher for the Solimões than for the Iça Formation (Figure 7). In the Iça Formation the average S/K ratio is 1 with values between 0 and 3.7 and a few values greater than 4.5. For recent deposition the average S/K ratio is 8.6, with values between 2.7 and 15.9 (Table 3).

In the Solimões Formation, the heavy mineral assemblage is composed of very altered, stable minerals, with a ZTR (Zircon+Tourmaline+Rutile) sum of 196 and unstable/stable ratio of 0.07 (Table 4). The Iça Formation is characterized by a similar heavy mineral assemblage. It is composed of very altered stable minerals, the ZRT sum equals 187 and the unstable/stable ratio is 0.17 (Table 4). The heavy mineral assemblage in recent deposits is composed of unstable species, mostly represented by hypersthene, augite hornblende and epidote. The ZTR sum is 71 while the unstable/stable ratio is 2.87.

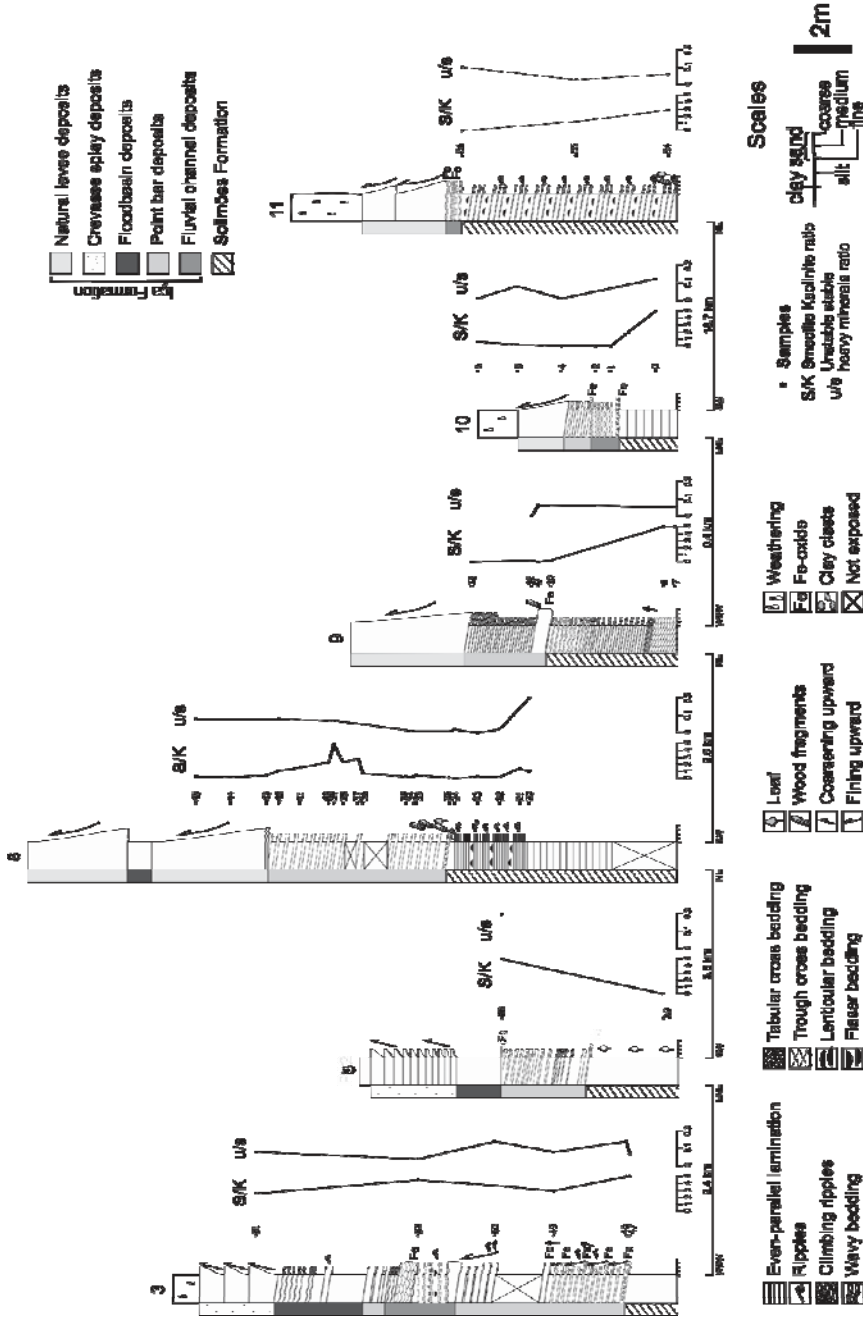


Figure 7 Relationships of clay minerals (smectite – kaolinite ratio) and heavy minerals (unstable – stable ratio) on the deposits of the Solimões and Iça Formations in the Coari Area. In general smectite – kaolinite ratio varies from 0 to 5 with some values out of this range, see Table 3. In general S/K values are higher for the Solimões Formation than for the Iça Formation. The unstable – stable ratio of heavy minerals varies from 0 to 0.2, see Table 4. In general the u/s ratio for tends to be lower for the Solimões Formation than for the Iça Formation.

Table 3. Smectite/kaolinite ratio obtained from X-ray diffractograms of the deposits described in the Coari area. Location of the profiles and samples are indicated in Figures 1A , 7 and 8 respectively. The relationship between the profiles and the S/K ratio is plotted in Figures 7 and 8.

Profile	Formation	Sample	Relative proportion		S/K ratio
			Smectite	Kaolinite	
3	Iça	51	2970.52	1127.43	2.6
		52	3708.99	824.07	4.5
		50	2674.95	727.52	3.7
		49	1417.58	493.65	2.9
		46	4263.6	289.17	14.7
5	Iça	88	2823.89	276.42	10.2
	Solimões	89	0	213.89	0.0
8	Iça	45	353.03	2342.37	0.2
		44	120.07	1809.1	0.1
		43	623.79	1440.53	0.4
		42	1460.99	1345.19	1.1
		41	1425.88	956.24	1.5
		40	2152.78	922.24	2.3
		39	3844.75	792	4.9
		38	2015.14	840.63	2.4
		37	3384.55	1213.74	2.8
		36	969.18	1411.27	0.7
		35	602.01	2786.49	0.2
		34	171.73	963.33	0.2
		33	364.41	934.58	0.4
		25	165.31	1475.17	0.1
	24	0	978.68	0.0	
	Solimões	23	254.93	1478.82	0.2
		22	211.41	1059.3	0.2
21		912.16	652.54	1.4	
20		758.25	772.12	1.0	

Profile	Formation	Sample	Relative proportion		S/K ratio
			Smectite	Kaolinite	
9	Iça	13	0	387.43	0.0
		12	411.92	2006.71	0.2
		9	0	2204.5	0.0
		10	296.07	1659.91	0.2
		8	4151.98	303.36	13.7
Solimões	7	4475.89	62.05	72.1	
	6	723.16	2498.93	0.3	
10	Iça	5	114.03	1677.43	0.1
		4	0	1995.86	0.0
		2	0	823.89	0.0
		1	0	416.88	0.0
Solimões	0	4685.49	470.13	10.0	
11	Solimões	56	0	2458.76	0.0
		55	1206.64	935.15	1.3
		54	1709.83	570.93	3.0
a	Recent	90	1396.63	183.89	7.6
b	Recent	86	3352.49	211.21	15.9
		84	1359.61	128.19	10.6
c	Recent	83	2325.27	295.17	7.9
		82	151.46	55.13	2.7
		81	2606.21	271.8	9.6
		80	3311.17	342.14	9.7
		78	385.44	0	
e	Recent	75	4308.36	363.37	11.9
		74	2881.67	298.66	9.6
		73	3733.28	324.76	11.5
g	Recent	67	5607.95	707.12	7.9
		65	3310.07	655.6	5.0
		64	1899.33	442.79	4.3

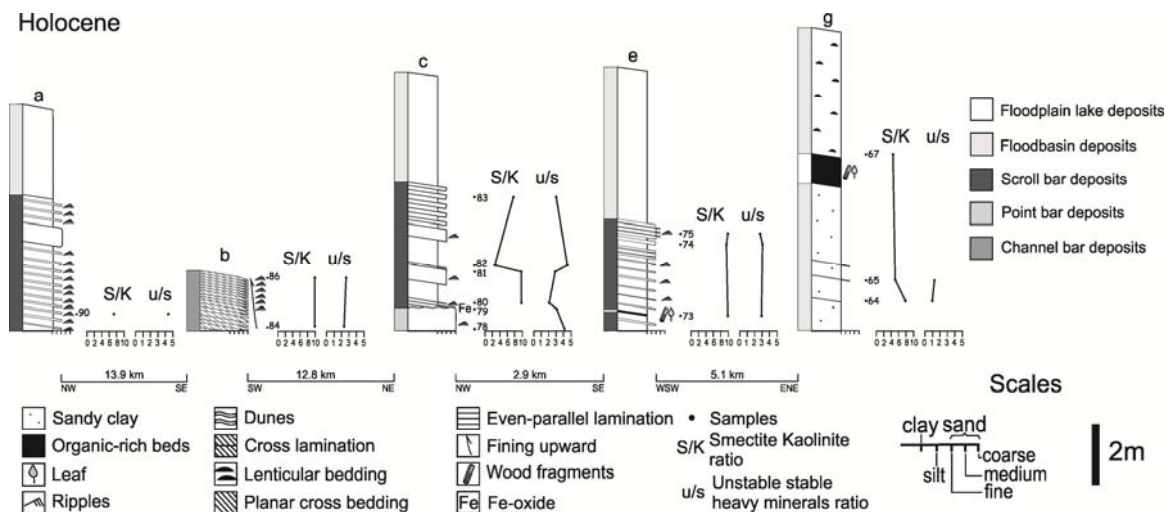


Figure 8 Relationships of clay minerals (smectite – kaolinite ratio) and heavy minerals (unstable – stable ratio) on the Holocene deposits in the Coari Area. In general smectite – kaolinite ratio varies from 0 to 10 with some values out of this range, see Table 3. The unstable – stable ratio of heavy minerals varies from 0 to 5, see Table 4. S/K and u/s ratios are higher than the values for the Solimões and Iça Formations, see Figure 7 and Tables 3 and 4.

Table 4. Distribution of heavy mineral assemblages in the deposits described in the Coari area. Location of the profiles and samples are indicated in Figures 1A, 7 and 8 respectively. The relationship between the profiles and the u/s ratio is plotted in Figures 7 and 8. Unstable heavy minerals include hornblende, augite, hypersthene and epidote. Stable heavy minerals include zircon, tourmaline and rutile (ZTR).

Profile	Formation	Sample	Zircon	Garnet	Sillimanite	Andalucite	Kyanite	Staurolite	Epidote	Tourmaline	Hypersthene	Augite	Hornblende	Muscovite	Rutile	Spinel	Monazite	Total	unstable	stable	u/s ratio	
3	Iça	51	50	0	18	3	43	20	3	121	9	0	4	0	29	0	0	300	16	200	0.08	
		52	69	0	6	3	32	64	6	101	0	0	1	0	18	0	0	300	7	188	0.04	
		50	73	1	7	2	6	20	9	121	15	4	5	0	37	0	0	300	33	231	0.14	
		49	74	44	0	2	11	10	0	103	9	0	8	1	28	10	0	300	17	205	0.08	
		46	98	28	2	0	8	4	13	94	8	3	8	0	30	4	0	300	32	222	0.14	
5	Iça	47	111	27	0	0	11	7	9	99	4	0	3	0	28	1	0	300	16	238	0.07	
		88	13	31	4	2	14	30	37	58	43	25	33	1	0	0	8	0	299	138	71	1.94
8	Iça	45	67	0	0	8	31	24	3	115	7	0	8	0	37	0	0	300	18	219	0.08	
		42	54	14	0	3	27	17	1	145	10	0	6	0	20	3	0	300	17	219	0.08	
		39	46	3	0	2	62	16	1	131	7	0	6	0	19	7	0	300	14	196	0.07	
		36	59	1	0	7	66	13	5	124	4	1	0	0	19	1	0	300	10	202	0.05	
		34	33	1	0	6	108	10	2	128	0	0	0	0	0	12	0	0	300	2	173	0.01
9	Iça	25	51	1	0	13	89	40	0	81	2	0	0	2	21	0	0	300	2	153	0.01	
		24	51	2	0	2	120	5	2	95	1	0	0	0	22	0	0	300	3	168	0.02	
		23	140	2	0	0	44	29	0	50	0	0	0	0	3	0	0	268	0	193	0.00	
		22	149	1	0	0	25	34	1	60	0	2	2	2	0	24	2	0	300	5	233	0.02
		20	64	6	0	0	36	44	11	93	5	10	10	10	0	11	10	0	300	36	168	0.21
10	Iça	12	37	1	0	0	86	108	1	51	0	0	0	3	12	1	0	300	1	100	0.01	
		9	86	1	0	0	89	35	5	72	7	0	0	0	4	1	0	300	12	162	0.07	
11	Solimões	7	20	1	0	0	73	36	2	134	0	6	2	2	2	22	0	300	10	156	0.06	
		6	87	0	0	0	55	59	2	71	0	0	0	0	26	0	0	300	2	184	0.01	
		5	124	0	0	0	34	17	19	93	0	0	0	0	11	2	0	300	19	228	0.08	
		4	132	1	0	0	21	36	2	81	0	1	0	0	1	20	4	0	299	3	233	0.01
		0	61	5	0	0	40	34	3	99	0	11	5	24	5	24	5	13	0	300	19	165
a	Recent	56	57	39	0	1	18	9	0	122	11	2	7	0	30	4	0	300	20	209	0.10	
		55	87	15	7	2	14	40	4	109	2	1	0	0	17	2	0	300	7	213	0.03	
		54	75	3	6	0	23	43	4	120	7	0	2	0	17	0	0	300	13	212	0.06	
b	Recent	90	7	5	1	0	4	14	49	43	93	52	29	0	0	3	0	300	223	50	4.46	
		86	20	13	0	0	0	20	31	49	87	46	26	0	2	6	0	300	190	71	2.68	
c	Recent	84	35	12	0	0	4	15	23	40	113	24	29	0	4	1	0	300	189	79	2.39	
		83	20	22	0	0	2	26	34	40	57	53	43	0	2	1	0	300	187	62	3.02	
		82	14	17	2	0	2	9	20	27	86	83	29	0	7	4	0	300	218	48	4.54	
		81	15	14	2	0	7	23	26	40	74	60	25	0	8	5	0	299	185	63	2.94	
		80	16	4	0	0	3	27	26	63	47	72	30	0	5	7	0	300	175	84	2.08	
e	Recent	79	31	15	1	0	0	9	27	30	97	63	20	0	7	0	0	300	207	68	3.04	
		78	29	9	5	0	3	14	25	22	76	76	38	0	1	1	0	299	215	52	4.13	
		75	17	9	3	0	8	26	43	49	45	38	57	0	1	3	0	299	183	67	2.73	
		74	17	6	1	0	9	30	26	42	69	44	47	0	2	7	0	300	186	61	3.05	
		73	13	5	3	0	18	32	11	45	66	53	44	0	1	9	0	300	174	59	2.95	
g	Recent	65	32	2	8	0	5	24	0	79	41	56	42	1	3	7	0	300	139	114	1.22	
		64	18	2	8	2	4	28	3	99	39	36	30	7	2	22	0	300	108	119	0.91	

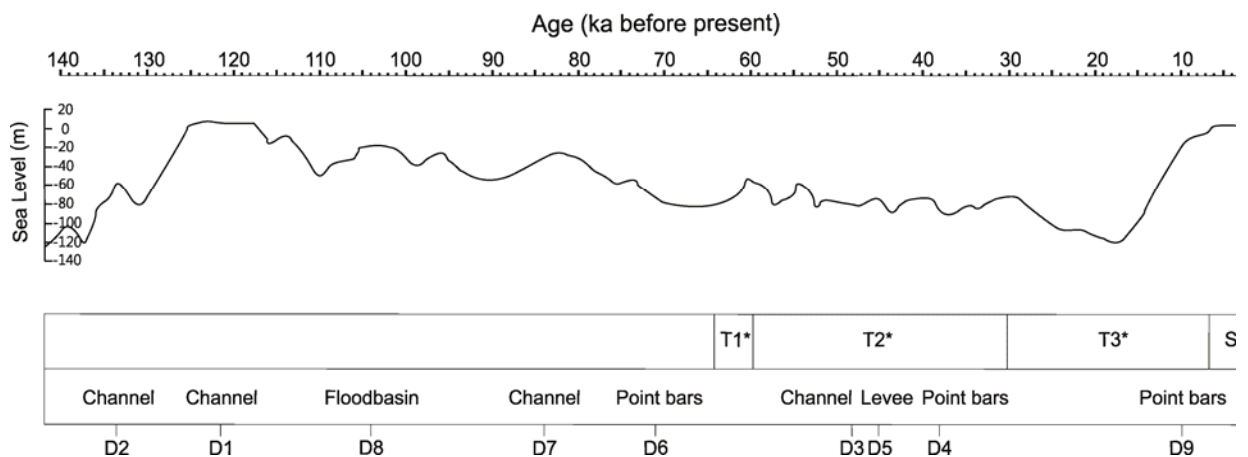


Figure 9 Sea level variation in the last 140 ka. Sea level curve by Chappell et al. 1996. D1-D9 ages obtained here related to the deposits described. T1-T3 Fluvial terraces individualized by Soares (2007) in the western Amazonas sedimentary basin. Scroll bar (S) and floodplain (F) deposits in the Manaus area (Rozo et al., 2012). Ages get younger with the general sea level drop from 130 to 18 ka.

Discussion

Age of the Iça Formation

Pleistocene deposition in the Solimões sedimentary basin is represented by the Iça Formation (Maia et al., 1977) (Figure 2C). This formation has been considered as part of the Solimões Formation (Caputo, 1984; Eiras et al., 1994; Silva, 1988), and consequently it has been restricted to the Solimões sedimentary basin. Recently, Rossetti et al. (2005) identified six units overlying the Solimões Formation: (1) the Iça Formation with an estimated Plio-Pleistocene age based on its stratigraphic position; (2) three Pleistocene units: deposits Q1 (43.7 – 37.4 ka BP), deposits Q2 (27.1 ± 0.2 ka BP) and a third undated unit; and (3) two Holocene units: Q3 (6.73 ± 0.1 – 2.48 ± 0.04 ka BP) and recent deposition (0.24 ± 0.08 – 0.13 ± 0.04 ka BP). The Iça Formation is restricted to the western Solimões sedimentary basin and the Pleistocene units are distributed extensively from the Jurúa River to Manaus with deposition in the western Amazonas sedimentary basin (Figure 2). Updated geological maps from the Brazilian geological survey (CPRM, 2010) show all Pleistocene deposition grouped into the Iça Formation, extending from the Solimões sedimentary basin to the western Amazonas sedimentary basin, indicating that sedimentation in the Pleistocene overlaps the two basins, at least near the Purus Arch.

Soares (2007) and Soares et al. (2010) show two Pleistocene terraces (65.2 ± 8.8 ka – 60.7 ± 6.6 ka) and (60.7 ± 6.6 ka – 34.5 ± 4.4 ka) and a Pleistocene-Holocene terrace (34.5 ±

4.4 ka – 7.5 ± 0.9 ka) for the western Amazonas sedimentary basin (Figure 2). The two Pleistocene terraces seem to be correlated with an undated unit indicated by Rossetti et al. (2005) (Figure 2). In this study, we obtained dates between 38 ± 4 and 133.8 ± 20.9 ka for sediments we have interpreted as the Iça Formation in the Coari area and an age of 10 ± 2.2 ka in the lower part of the deposits we have considered as Holocene. Additionally, the deposits we described as the Iça Formation in the Coari area are similar in lithology to what has been described as the Iça Formation by Rossetti et al. (2005). This situation is similar to the several Late Pleistocene deposits described by Rossetti et al. (2005) which in the Coari area are younger than 10 ± 2.2 ka. The ages obtained here as well as the dating obtained by Soares (2007) and Soares et al. (2010) are in disagreement with the model presented by Rossetti et al. (2005). This difference in ages is probably due to the fact that the more recently determined ages were obtained from luminescence methods while the previously measured dates are based on radiocarbon. Radiocarbon dating may give uncertain ages when samples are contaminated with young organic matter, especially in the case of samples older than 50 ka because these contain a very low amount of their original ^{14}C (Irion et al., 2005). Additionally, the radiocarbon ages obtained by Rossetti (2005) suggest that western lowland Brazilian Amazonia has been formed in the past 40 ka (Irion et al., 2005). Large discrepancies in the distribution and ages of Pleistocene deposition in the area still exist which would likely be clarified by a detailed study and dating of what has been referred to as the Iça Formation in the western Solimões sedimentary basin.

Another important point in this discussion is to consider how the Iça Formation in Brazil has been described and dated in other Amazonian countries. In Colombia this formation is referred to as the *Terciario Superior Amazónico* deposits (Upper Tertiary deposits) to differentiate it from the *Terciario Inferior Amazónico* (Lower Tertiary deposits) which is correlated to the Solimões Formation (Huguett et al., 1979). In lithologic terms, the Lower Tertiary deposits are mudstone dominated and the Upper Tertiary deposits developed a basal conglomerate and sandstone dominates the sequence. The lithology is not different from the described Solimões and Iça Formations in Brazil, however the age established based on the stratigraphic position does not correspond to the estimated dates in Brazil. In Bolivia, the Iça Formation correlates to what was described as the Candelaria Formation (Leytón and Pacheco, 1989) while at the Brazilian border with Bolivia it correlates to the Rio Madeira Formation (Adamy and Romanini, 1990; Rizzotto et al., 2005). The age of the Rio Madeira Formation has been attributed as Upper Pleistocene (Quadros et al., 2006; Rizzotto et al., 2006). In Peru, what correlates to the Iça Formation in lithologic terms is the Madre de Dios

Formation (Oppenheim, 1946) which has been referred to also as the Ucayali Formation (Kummel, 1948). The age of this formation was suggested to be Pliocene-Holocene (Kummel, 1948) and also Pleistocene-Holocene (Campbell and Romero-Pittman, 1989). Campbell et al. (2001) dated two volcanic ash samples in the lower and upper members of the Madre de Dios Formation with ages of 9.01 ± 0.28 Ma and 3.12 ± 0.02 Ma respectively, indicating a Miocene-Pliocene age for these deposits (Campbell et al., 2001). Recently Campbell et al. (2010) obtained magnetostratigraphic data from the Madre de Dios Formation and correlated it with the previously obtained radiometric dates corroborating the Miocene-Pliocene age. The controversy still exists if the deposits described here as the Iça Formation and dated as Upper Pleistocene are in fact the Miocene-Pliocene Madre de Dios Formation. However, studies indicating an Upper Miocene age for the Solimões Formation in the Coari area (Silveira and Nogueira, 2005) and in western Brazilian Amazonia (Latrubesse et al., 2010) indicate that the Iça Formation in the Coari area is younger than Upper Miocene.

Environmental conditions during the Quaternary

The evolution of the Amazon rainforest itself during the Quaternary has been controversial (Colinvaux et al., 2000; Colinvaux et al., 2001; Haffer and Prance, 2001; Hooghiemstra, 2001). Two hypotheses have been discussed widely based on palynological evidence (Colinvaux et al., 1996; Hooghiemstra and van der Hammen, 1998; Kastner and Goñi, 2003; van der Hammen, 1972; van der Hammen, 1974; van der Hammen and Absy, 1994). The first hypothesis states that during some periods the climate was cooler and drier than it is today, and such drier climatic phases caused a fragmentation of the Amazonian rainforest into forest refugia isolated by savannas (Haffer, 1969). These climatic changes should have modified the discharge and erosion – deposition dynamics of the Amazon River and its tributaries. (Irion et al., 1997). The second hypothesis claims a rain forest covered the entire Amazon basin permanently during the Quaternary (Colinvaux, 1979).

In the Amazon, Quaternary sea level changes have been related to changes in slope and river levels, that also affected the erosion – deposition dynamics in the river system (Irion et al., 1997). Irion et al. (1997) state that during warm periods, when sea level was higher than today, large areas of western lowland Amazonia were covered with fluvial sediments forming terraces several meters above the recent ones. These terraces are currently inactive and not inundated during the high water season. But, during cold Pleistocene periods when sea level was low, the rivers of central Amazonia incised deeply into the sediment deposits. This agrees

with the model proposed by Fisk (1944) and discussed by Blum and Tornqvist (2000) for valley development during an individual eustatic cycle.

In the terraces individualized by Soares (2007) and Soares et al. (2010), the oldest is at a higher topographic elevation and more distant from the main river compared with the younger terrace which is at a lower topographic elevation and linked to present-day lateral migration of the main river. The age of the oldest terrace does not correspond to the highest sea level during the last glacial period, following the eustatic sea-level curve of Chappell et al. (1996) (Figure 9). However, the ages of these terraces follow a relative sea level variation from high to low, from approximately 65 to 18 ka, (Figure 9) which would still form older terraces in higher topographic elevations according to the model of Fisk (1944).

In the Coari area we found the older deposits at higher topographic elevation while the younger occur in the lower part of the profiles (Profiles 1 and 3, Figure 3). Additionally, the oldest channel deposits with ages between 133.8 ± 20 ka and 121.5 ± 18.9 ka correlate to the highest sea level between 130 and 10 ka (Figure 9). From around 120 ka the ages obtained here decrease together with the topographic position from where sediments were taken for dating (Profiles 1 and 3, Figure 3). This coincides with channel incision related to a general sea level drop from 120 to 18 ka (Figure 9) and shows the direct influence of sea level variations during that time in the deposition of the Coari area. In profile 8 (Figure 3) a relatively younger age (45 ± 4.1 ka) is found at a higher topographic elevation when compared with the other dates obtained in the area, however the deposits from the location where this age was obtained are interpreted here as natural levees. Fisk (1944) linked incision to glacial cycles, and aggradation to interglacials periods. However, the eustatic sea-level curve obtained by Chappell et al (1996) shows several sea level drops and rises throughout the overall sea level drop between 120 and 18 ka (Figure 9). This suggest several periods of incision and deposition over this period, which explains the formation of at least three fluvial terraces in the Coari area.

Holocene deposition in the Amazon River between Manaus and the mouth of the Madeira River shows older ages at the base of the profiles with younger ages upward from 7.5 ± 0.85 ka to 3.4 ± 0.60 in deposits interpreted as point and scroll bars, respectively (Rozo et al., 2012a). Additionally, younger ages (0.31 ± 0.05 ka and 1.3 ± 0.13 ka) for floodplain deposits covering the point – scroll bar deposits mentioned above have been obtained (Latrubesse and Franzinelli, 2002). This relation with older deposits at the base and younger deposits at the top of the profiles and the high average long-term aggradational rates (1.1 mm yr^{-1}) (Rozo et al., 2012a) are in concordance with the sea level rise and consequent sea level

stability existing in the last 10 ka. This also emphasizes the primary control of sea level in Amazon River deposition during the Quaternary. In the Coari area, sea level stability influence is evident in the thickening of floodbasin deposits and the presence of floodplain lake deposits during the Holocene, compared with the very thin floodbasin deposits and absence of floodplain lake deposits during Late Pleistocene (Figures 3 and 4).

Clay minerals (smectite/kaolinite ratio) allowed a clear differentiation between the three units present in the Coari area: the Solimões Formation, the Iça Formation and recent deposition (Table 3, Figs 7 and 8). Clay mineral analysis in the area had previously been carried out on different individualized units along the Amazon River (Rossetti et al., 2005). Rossetti et al. (2005) did not consider the Iça Formation deposits for analysis due to their high degree of alteration, which is indicated by their red and white colour. Although the smectite – kaolinite ratio obtained here for what we consider to be the Iça Formation shows a different unit from the Solimões Formation and recent deposition, it does not allow any conclusions to be drawn about the climatic conditions during deposition. The weathering event that strongly affected the Iça Formation sediments in the Coari area probably started between 6 and 4 ka BP, related to climate change from relatively dry to humid conditions (Hooghiemstra, 1995; Latrubesse and Franzinelli, 1993; Turcq et al., 1993). Clay minerals analyzed by Rossetti et al. (2005) do not seem to correlate with the deposits described here (Figure 2), with only deposits Q2 and the Iça Formation described here with S/K ratio of 1.5 and 1, respectively.

The unstable/stable heavy mineral ratio also allowed a clear differentiation between the main units present in the Coari area (Table 4, Figures 7 and 8). Comparing the ZTR index in percentage terms and the relation of unstable to stable heavy minerals with previously obtained data in the area, several relationships are evident. The ZTR index and the u/s ratio of the Iça Formation described here and by Rossetti et al. (2005) suggest the same unit, with a ZTR index of 62% and 55% and u/s ratios of 0.2 and 0.3, respectively. This indicates that the similarities between the Iça Formation described in the western Solimões sedimentary basin and the one described here in the Coari area cover more than just lithology. Motta (2008) found a lower ZTR index in his upper and lower Iça Formation units individualized in the Coari area, with values of 25% and 26% and u/s ratios of 0.6 and 0.7, respectively. In contrast, data obtained for present-day sediments of the Amazon River (Solimões River in Brazil) here and by Motta (2008) show similar ZTR index (24% and 23%, respectively) and u/s ratio (2.9 and 2.2, respectively). As mentioned above, Motta (2008) individualized two units for the Iça Formation in the Coari area, the upper and lower Iça Formation. This separation was made based on the comparison of other indices derived from heavy mineral

data, Andalusite/ZTR+Andalusite and Mica/ZTR+Mica. This individualization probably correlates with what was mentioned before about the age of the Iça Formation in the Coari area, with the upper Iça Formation as an older terrace and the lower unit as a younger terrace of the Amazon River.

Sediments of the Iça Formation have been suggested to originate from basic igneous Andean rocks and acid igneous and metamorphic rocks derived from the Amazonian Craton, based on heavy mineral assemblages (Rossetti et al., 2005). Following detailed heavy mineral identification, zircon morphology analysis and the study of rock fragments in Iça deposits, Motta (2008) attributed the provenance of this Formation to igneous and metamorphic sources associated to the Amazonian Craton. Recent deposition originates mainly from Andean sources, the reworking of Neogene deposits in the Solimões sedimentary basin and also likely sediment from the Acre Basin (Motta, 2008).

Quaternary fluvial characteristics of the Amazon River

Scroll bar deposits broadly distributed in the islands as well as some parts of the floodplain in the reach of the Amazon River between the confluences of the Negro and Madeira Rivers, were initially considered to belong to a single-channel meandering river that preceded the development of the current anastomosing pattern (Rozo, 2004). The change from single-channel meandering to anastomosing was suggested to have taken place between 6 and 4 ka BP, influenced by climate change from relatively dry to humid conditions documented by several authors (Latrubesse and Franzinelli, 1993; Turcq et al., 1993; Hooghiemstra, 1995). It was also suggested that the anastomosing pattern could have developed after ~2 ka BP (Rozo, 2004). This assumption is based on radiocarbon dating in two deposits interpreted as point bars to 2.84 ± 0.08 ka BP (Terra Nova Island) (Absy, 1979) and 2.05 ± 0.12 ka BP (Careiro Island) (Sternberg, 1959). These were assumed to belong to a main single-channel meandering system. Recently, Rozo et al. (2012a) clearly established that the scroll bar deposits have developed at least since 7.5 ± 0.85 ka and are the product of meandering secondary channels as well as localized migration of the main channel in an established anastomosing river.

Soares et al. (2010) dated point bar deposits of the Amazon River upstream Manaus (Figure 2) with ages from 34.5 ± 4.4 to 7.5 ± 0.9 ka, suggesting a mainly meandering fluvial system during that time. These deposits correlate with the scroll bar deposits described by Rozo et al. (2012a), since they develop swale and ridge morphology and are linked to the

present-day migration of the river system. This suggests that the current conditions in the Amazon have existed since 34.5 ± 4.4 ka. However, the present-day channel pattern of the Amazon upstream of the confluence with the Negro River is different from the reach downstream the same confluence. Upstream this confluence the river develops a multichannel meandering pattern, where scroll bars are linked mainly to the main channel with small anastomosing reaches indicated by the presence of islands with saucer-like morphology. Downstream the confluence with the Negro River, the Amazon is anastomosing with meandering secondary channels forming extensive scroll bars. The anastomosing pattern in both reaches is mainly identified by the presence of saucer-like islands. The saucer-like morphology corresponds to the description of floodbasins by Makaske (2001), which is a key characteristic for distinguishing anastomosing from other multiple channel rivers. Additionally, the other two terraces described and dated by Soares (2007) and Soares et al. (2010) (from 65.2 ± 8.8 to 34.5 ± 4.4 ka) are interpreted as point bar deposits suggesting that the meandering characteristics extended to at least 65.2 ± 8.8 ka.

The Iça Formation is interpreted as having developed in a fluvial environment (Caputo, 1984; Maia et al., 1977; Rossetti et al., 2005) and specifically in a meandering system (Motta, 2008). Meandering characteristics were extensively recognized in our sedimentary facies analysis where different types of meandering environments were identified in the Late Pleistocene as well as in the Holocene deposits (Table 2). This is in concordance with the Late Pleistocene deposits linked to meandering channels identified by Soares (2007) and Soares et al. (2010). Additionally, our data indicates the development of low energy secondary channels that smoothly eroded underlying sediments (Solimões Formation), indicated by the presence of mudstone clasts at the base and the subsequent development of inclined heterolithic stratification on point bar deposits (Figure 3). Although mudstone clasts are also found at the base of the deposits interpreted as fluvial channel, the facies associated to the latter deposits indicate a more energetic environment linked to a main channel. Rozo et al. (2012a) identified scroll and point bar deposits in the Amazon River downstream Manaus *sensu* Nanson (1980). Coarse sediments with trough cross stratification and slightly convex-up morphology represent the point bar which is overlaid by inclined heterolithic stratification, representing the scroll bar. In the Coari area the inclined heterolithic stratification is related to point bars since no morphology can be linked to the deposits except for the Holocene deposition. This leads us to assume that the deposits interpreted as channel can be also interpreted as point bar in the main channel, which make them very different from the point bar of the secondary channels. In the point bar deposits we suggest are from

secondary channels, there is no coarse sandy base which would also suggest relatively shallow, low energetic meandering secondary channels.

The data presented here indicates an incisive fluvial multichannel meandering system during the Late Pleistocene, with similar conditions to what corresponds to the present-day Amazon River in the Colombian reach (Rozo et al., 2012b). We compare the fluvial system in the Coari area during the Late Pleistocene with the conditions of the Colombian Amazon River because the latter do not develop a present-day anastomosing pattern, which is partially found on the present-day Amazon River between the confluences of the Iça and Negro River (Solimões River in Brazil). Additionally, paleocurrent data obtained here as well as extensive data collected by Motta (2008) in the Coari area indicate a paleoflux of the Amazon River in the Late Pleistocene to the East. The high variability in paleocurrent data from NE to SE (Motta, 2008) and the variation in the bedding of the inclined heterolithic stratification evidences the meandering multichannel characteristics.

Conclusions

The age of the deposits described as the Iça Formation in the Coari area is between 38 ± 4 and 133.8 ± 20.9 ka BP. This clearly indicates its Upper Pleistocene age. Additionally, these deposits correspond in lithology to what has been considered as the Iça Formation in the western Solimões sedimentary basin and correlates to the Late Pleistocene deposits in the western Amazonas sedimentary basin. This suggests a single unit overlying older deposits in both sedimentary basins, with deposition taking place at least over the last 133.8 ± 20.9 ka BP.

A main sea level drop during the Late Pleistocene (130 - 18 ka) had a direct influence on deposition of the Iça Formation in the Coari area, with the development of at least three fluvial terraces indicated by the ages obtained. Additionally, the sea level rise and resulting stability during the Holocene have influenced sedimentation and conditioned the development of the present-day channel pattern of the Amazon River.

The Amazon River during 130 – 18 ka BP was a system characterized by incision with a more energetic main channel, indicated by thick fluvial channel deposits and less energetic secondary channels that developed extensive point bars over older deposits. Sea level rise and the resulting sea level stability from ~6 ka BP suggest a vertically and rapidly aggrading system in the Late Holocene, as indicated by the thick floodplain deposits in the area.

The Amazon River was already established in the Late Pleistocene, at least over the last 133.8 ± 20.9 ka BP as a multichannel meandering river, with flow to the East. The system

was probably similar to the present-day Colombian Amazon River, which does not develop saucer-like morphology that is characteristic of anastomosing rivers, and common in the Brazilian reaches of the Amazon.

Acknowledgments

This research was supported by the Graduate Program in Geology and Geochemistry of the Universidade Federal do Pará and CNPq-CT-AMAZONIA Proc. 554059/2006-9. Max G. Rozo thanks CNPq for awarding a scholarship. We would like to acknowledge the help of Roseane Sarges and Luciano Machado with field work, and Luiz Saturnino with processing clay and heavy mineral samples, Prof. Romulo Angelica helped with clay mineral analysis and Anderson Mendes with heavy mineral analysis.

References

- Absy, M. L. (1979). "A palynological study of Holocene sediments in the Amazon basin." Unpublished PhD thesis, University of Amsterdam.
- Adamy, A., and Romanini, S. J. (1990). Geologia da Região Porto Velho - Abunã. Estados de Rondônia e Amazonas. DNPM/CPRM (Report), Brasília.
- Arai, M., Nogueira, A. C. R., Silveira, R. R., and Horbe, A. M. C. (2003). Considerações Cronoestratigráficas e Paleoambientais da Formação Solimões com Base em Palinomorfos, Região de Coari, Estado do Amazonas. In "Simposio de Geologia da Amazonia, 8." Sociedade Brasileira de Geologia - Núcleo Norte, Manaus.
- Baker, V. R. (1978). Adjustment of fluvial systems to climate and source terrain in tropical and subtropical environments. In "Fluvial Sedimentology." (A. D. Miall, Ed.), pp. 211-230. Canadian Society of Petroleum Geologists, Calgary.
- Blum, M. D., and Tornqvist, T. E. (2000). Fluvial responses to climate and sea-level change: a review and look forward. *Sedimentology* **47**, 2-48.
- Bowler, J. M., Stockton, E., and Walker, M. J. (1978). Quaternary stratigraphy of the Darling River near Tilpa, New South Wales. *Proceedings of the Royal Society of Victoria* **90**, 78-88.
- Brindley, G. W., and Brown, G. (1980). "Crystal structures of Clay Minerals and Their X-Ray identification." Mineralogical Society, London.
- Brizga, S. O., and Finlayson, B. L. (1990). Channel avulsion and river metamorphosis - the case of the Thomson River, Victoria, Australia. *Earth Surface Processes and Landforms* **15**, 391-404.
- Campbell Jr, K. E., Prothero, D. R., Romero-Pittman, L., Hertel, F., and Rivera, N. (2010). Amazonian magnetostratigraphy: Dating the first pulse of the Great American Faunal Interchange. *Journal of South American Earth Sciences* **29**, 619-626.
- Campbell, K. E., Frailey, C. D., and Romero-Pittman, L. (2006). The Pan-Amazonian Ucayali Peneplain, late Neogene sedimentation in Amazonia, and the birth of the modern Amazon River system. *Palaeogeography Palaeoclimatology Palaeoecology* **239**, 166-219.
- Campbell, K. E., Heizler, M., Frailey, C. D., Romero-Pittman, L., and Prothero, D. R. (2001). Upper Cenozoic chronostratigraphy of the southwestern Amazon Basin. *Geology* **29**, 595-598.

- Campbell, K. E., and Romero-Pittman, L. (1989). Geología del cuaternario del Departamento de Madre de Dios (Perú). *Boletín de la Sociedad Geológica del Perú* **79**, 53-61.
- Caputo, M. V. (1984). "Strigraphy, tectonics, paleoclimatology and paleogeography of northern basins of Brazil." Unpublished PhD thesis, University of California.
- Caputo, M. V., Rodrigues, R., and Vasconcelos, D. N. (1971). Litoestratigrafia da Bacia Amazônica. Petrobras/Renor, Manaus.
- Caputo, M. V., Rodrigues, R., and Vasconcelos, D. N. N. (1972). Nomenclatura estratigráfica da Bacia do Amazonas. In "XXVI Congresso Brasileiro de Geologia." pp. 36-46. Sociedade Brasileira de Geologia, Belém.
- Chappell, J., Omura, A., Esat, T., McCulloch, M., Pandolfi, J., Ota, Y., and Pillans, B. (1996). Reconciliation of late Quaternary sea levels derived from coral terraces at Huon Peninsula with deep sea oxygen isotope records. *Earth and Planetary Science Letters* **141**, 227-236.
- Colinvaux, P. A. (1979). The ice-age Amazon. *Nature* **278**, 399-400.
- Colinvaux, P. A., De Oliveira, P. E., and Bush, M. B. (2000). Amazonian and Neotropical plant communities on glacial timescales: the failure of the aridity and refuge hypotheses. *Quaternary Science Reviews* **19**, 141-169.
- Colinvaux, P. A., Irion, G., Rasanen, M. E., Bush, M. B., and Nunes de Mello, J. A. S. (2001). A paradigm to be discarded: geological and paleoecological data falsify the Haffer & Prance refuge hypothesis of Amazonian speciation. *Amazoniana* **16**, 609-646.
- Colinvaux, P. A., Oliveira, P. E., Moreno, J. E., Miller, M. C., and Bush, M. B. (1996). A long pollen record from lowland Amazonia: forest and cooling in glacial times. *Science* **274**.
- CPRM. (2010). Carta Geológica do Brasil ao Milionésimo. CPRM- Serviço Geológico do Brasil.
- Daemon, R. F., and Contreiras, C. J. A. (1971). Zoneamento palinológico da Bacia do Amazonas. In "Congresso Brasileiro de Geologia, 25." pp. 79-88. Sociedade Brasileira de Geologia, São Paulo.
- Eiras, J. F., C.R., B., E.M., S., Gonzaga, F. G., J.G.F., S., and L.M.F., D. (1994). Bacia do Solimões. *Boletim de Geociências da Petrobrás* **8**, 17-45.
- Figueiredo, J., Hoorn, C., van der Ven, P., and Soares, E. (2009). Late Miocene onset of the Amazon River and the Amazon deep-sea fan: Evidence from the Foz do Amazonas Basin. *Geology* **37**, 619-622.
- Fisk, H. N. (1944). Geological Investigation of the Alluvial Valley of the Lower Mississippi River. Mississippi River Commission, Vicksburg.
- Frailey, C. D., Lavina, E. L., Rancy, A., and Souza F., J. P. d. (1988). A Proposed Pleistocene/Holocene Lake in the Amazon Basin and its Significance to Amazonian Geology and Biogeography. *Acta Amazonica* **18**, 119-143.
- Gingras, M. K., Rasanen, M., and Ranzi, A. (2002). The significance of bioturbated inclined heterolithic stratification in the southern part of the Miocene Solimoes Formation, Rio Acre, Amazonia Brazil. *Palaios* **17**, 591-601.
- Gross, M., Piller, W. E., Ramos, M. I., and Douglas da Silva Paz, J. (2011). Late Miocene sedimentary environments in south-western Amazonia (Solimões Formation; Brazil). *Journal of South American Earth Sciences* **32**, 169-181.
- Haffer, J. (1969). Speciation in Amazonian forest birds. *Science* **165**, 131-137.
- Haffer, J., and Prance, G. T. (2001). Climatic forcing of evolution in Amazonia during the Cenozoic: on the refuge theory of biotic differentiation. *Amazoniana* **16**, 579-607.
- Hooghiemstra, H. (1995). Environmental and paleoclimatic evolution in Late Pliocene-Quaternary Colombia. In "Paleoclimatic and Evolution, with Emphasis on Human

- Origins." (E. S. Vrba, G. Denton, L. H. Burckle, and T. C. Partridge, Eds.), pp. 249-261. Yale University Press.
- Hooghiemstra, H. (2001). The continuing debate on the history of the Amazonian rain forest. *Amazoniana* **16**.
- Hooghiemstra, H., and van der Hammen, T. (1998). Neogene and Quaternary development of the neotropical rain forest: the forest regugia hypothesis, and a literature overview. *Earth Science Reviews* **44**, 147-183.
- Hoorn, C. (1993). Marine incursions and the influence of Andean tectonics on the Miocene depositional history of northwestern Amazonia - results of a palynostratigraphic study. *Palaeogeography Palaeoclimatology Palaeoecology* **105**, 267-309.
- Hoorn, C. (1994). An Environmental reconstruction of the Paleo-Amazon River System (Middle-Late Miocene, NW Amazonia). *Palaeogeography Palaeoclimatology Palaeoecology* **112**, 187-238.
- Hoorn, C., Guerrero, J., Sarmiento, G. A., and Lorente, M. A. (1995). Andean tectonics as a cause for changing drainage patterns in Miocene northern South America. *Geology* **23**, 237-240.
- Hoorn, C., Wesselingh, F. P., Hovikoski, J., and Guerrero, J. (2010). The development of the Amazonian mega-wetland (Miocene; Brazil, Colombia, Peru, Bolivia). In "Amazonia, Landscape and Species Evolution: A Look into the Past." (C. Hoorn, and E. P. Wesselingh, Eds.), pp. 123-142. Wiley-Blackwell, London.
- Hovikoski, J., Rasanen, M., Gingras, M., Roddaz, M., Brusset, S., Hermoza, W., and Pittman, L. R. (2005). Miocene semidiurnal tidal rhythmites in Madre de dios, Peru. *Geology* **33**, 177-180.
- Huguett, A., Galvis, J., and Ruge, P. (1979). Geologia In "La Amazonia Colombiana y sus recursos - Proyecto Radargrametrico del Amazonas." Instituto Geografico Agustin Codazzi, Bogota.
- Irion, G., Junk, W. J., and Mello, J. A. (1997). The large central Amazonian river floodplains near Manaus: Geological, climatological, hydrological and geomorphological aspects. In "The central Amazon floodplain: Ecology of a pulsating system " (W. J. Junk, Ed.), pp. 23-46. Ecological Studies. Springer, Berlin.
- Irion, G., Räsänen, M., de Mello, N., Hoorn, C., Junk, W., and Wesselingh, F. (2005). D. Rossetti, P. Mann de Toledo, A.-M. Góes, New geological framework for Western Amazonia (Brazil) and implications for biogeography and evolution, Quaternary Research 63 (2005) 78-89. *Quaternary Research* **64**, 279-280.
- Junk, W. J., Bayley, P. B., and Sparks, R. E. (1989). The flood pulse concept in river-floodplain systems. In "Proceeding of the International Large River Symposium, Canadian Special Publications of Fisheries and Aquatic Sciences." (D. Dodge, Ed.), pp. 110-127. Department of Fisheries and Oceans Canada, Ottawa.
- Kalliola, R., Salo, J., Puhakka, M., Rajasilta, M., Häme, T., Neller, R. J., Räsänen, M. E., and Danjoy Arias, W. A. (1992). Upper Amazon channel migration. *Naturwissenschaften* **79**, 75-79.
- Kastner, T. P., and Goñi, M. A. (2003). Constancy in the vegetation of the Amazon basin during the late Pleistocene: evidence from the organic matter composition of Amazon deep sea fan sediments. *Geology* **31**, 291-294.
- Kristler, P. (1954). Historical resume of the Amazon Basin. Petrobras/Renor (Internal report 104-A), Belém.
- Kummel, B. (1948). Geological reconnaissance of the Contamana region, Peru *Geological Society of America Bulletin* **59**, 1217-1266.

- Latrubesse, E. M., Cozzuol, M., da Silva-Caminha, S. A. F., Rigsby, C. A., Absy, M. L., and Jaramillo, C. (2010). The Late Miocene paleogeography of the Amazon Basin and the evolution of the Amazon River system. *Earth-Science Reviews* **99**, 99-124.
- Latrubesse, E. M., da Silva, S. A. F., Cozzuol, M., and Absy, M. L. (2007). Late Miocene continental sedimentation in southwestern Amazonia and its regional significance: Biotic and geological evidence. *Journal of South American Earth Sciences* **23**, 61-80.
- Latrubesse, E. M., and Franzinelli, E. (1993). Reconstrução das condições hidrológicas do passado. *Ciência Hoje* **16**, 40-43.
- Latrubesse, E. M., and Franzinelli, E. (2002). The Holocene alluvial plain of the middle Amazon River, Brazil. *Geomorphology* **44**, 241-257.
- Leytón, D. F., and Pacheco, Z. J. (1989). "Geología del cuaternario-terciario aflorante en el Río Madre de Dios (Departamentos de Plando, La Paz, Beni)." Sociedad Geológica Boliviana.
- Maia, R. G. N., Godoy, H. K., Yamaguti, H. S., Moura, P. A., Costa, F. S. F., Holanda, M. A., and Costa, J. A. (1977). Projeto Carvão no Alto Solimões, pp. 137. Companhia de Pesquisa de Recursos Naturais - Departamento Nacional de Produção Mineral, Manaus.
- Makaske, B. (2001). Anastomosing rivers: a review of their classification, origin and sedimentary products. *Earth-Science Reviews* **53**, 149-196.
- Mertes, L. A. K., Dunne, T., and Martinelli, L. A. (1996). Channel-floodplain geomorphology along the Solimões-Amazon River, Brazil. *Geological Society of American Bulletin* **108**, 1089-1107.
- Miall, A. D. (1992). Alluvial Deposits. In "Facies Models: Response to Sea Level Change." (R. G. Walker, and N. P. James, Eds.), pp. 119-142. Geological Association of Canada, St. John's.
- Motta, M. B. (2008). "Proveniência da Formação Iça e de sedimentos do Rio Solimões, entre os municípios de Tefé e Manacapuru, Amazonas." Unpublished MSc thesis, Universidade Federal do Amazonas.
- Murray, A. S., and Wintle, A. G. (2000). Luminescence dating of quartz using an improved single-aliquot regenerative-dose protocol. *Radiation Measurements* **32**, 57-73.
- Nanson, G. C. (1980). Point-bar and floodplain formation of the meandering Beatton River, Northeastern British-Columbia, Canada. *Sedimentology* **27**, 3-29.
- Nanson, G. C., and Knighton, D. (1996). Anabranching rivers: their cause, character and classification. *Earth Surface Processes and Landforms* **21**, 217-239.
- Nogueira, A. C. R., Arai, M., Horbe, A. M. C., Silveira, R. R., and Silva, J. S. (2003). A Influência Marinha nos Depósitos da Formação Solimões na Região de Coari (AM): Registro da Transgressão Miocênica na Amazônia Ocidental. In "Simpósio de Geologia da Amazônia, 8." Sociedade Brasileira de Geologia - Núcleo Norte, Manaus.
- Oppenheim, V. (1946). Geological reconnaissance in southeastern Peru. *Bulletin of American association of Petroleum Geologists* **30**, 254-264.
- Quadros, M. L. E. S., Rizzotto, G. J., Oliveira, J. G. F., and Castro, J. M. R. (2006). Depósitos fluviais da Formação Rio Madeira, Pleistoceno Superior da Bacia do Abunã, Rondônia. In "IX Simpósio de Geologia da Amazônia." Belém.
- Rasanen, M. E., Linna, A. M., Santos, J. C. R., and Negri, F. R. (1995). Late Miocene tidal deposits in the Amazonian foreland basin. *Science* **269**, 386-390.
- Rego, L. F. d. M. (1930). "Notas sobre a geologia do território de Acre e da Bacia do Javari." Cezar and Cavalcante, Manaus.
- Rizzotto, G. J., Cruz, N. M. C., Oliveira, J. G. F., Quadros, M. L. E. S., and Castro, J. M. R. (2006). Paleoambiente e o registro fóssilífero Pleistocênico dos sedimentos da Formação Rio Madeira. In "IX Simpósio de Geologia da Amazônia." Belém.

- Rizzotto, G. J., Oliveira, J. G. F., Quadros, M. L. E. S., Castro, J. M. R., Cordeiro, A. V., Adamy, A., Melo, J. H. G., and Dantas, M. E. (2005). Projeto Rio Madeira. Levantamento de informações para subsidiar o estudo de viabilidade do aproveitamento hidrelétrico (AHE) do Rio Madeira. AHE Jirau: relatório final. CPRM (Report), Porto Velho.
- Rossetti, D. F., de Toledo, P. M., and Goes, A. M. (2005). New geological framework for Western Amazonia (Brazil) and implications for biogeography and evolution. *Quaternary Research* **63**, 78-89.
- Rozo, J. M. G. (2004). "Evolução Holocênica do Rio Amazonas entre a Ilha do Careiro e a foz do Rio Madeira." Unpublished MSc thesis, Universidade Federal do Amazonas.
- Rozo, M. G., Nogueira, A. C. R., and Truckenbrodt, W. (2012a). The anastomosing pattern and the extensively distributed scroll bars in the middle Amazon River. *Earth Surface Processes and Landforms*. Accepted article.
- Rozo, M. G., Soto, C. C., and Nogueira, A. C. R. (2012b). Recent fluvial dynamics of the Colombian Amazon River. *Remote sensing of environment*. Submitted article
- Silva, L. L. (1988). A Estratigrafia da Formação Solimões: Uma análise crítica. In "Congresso Brasileiro de Geologia, 35." pp. 725-737. Sociedade Brasileira de Geologia, Belém.
- Silveira, R. R., and Nogueira, A. C. R. (2005). Cronoestratigrafia e Paleoambiente dos Depósitos do Mioceno Superior da Bacia do Solimões, Centro-oeste da Amazônia. In "Congresso Internacional do PIATAM, 1." pp. 98. Finep/Petrobrás, Manaus.
- Soares, E. A. A. (2007). "Depositos Pleistocenos da Região de Confluência dos rios Negro e Solimões, Amazonas." Unpublished PhD thesis, Universidade de São Paulo.
- Soares, E. A. A., Tatum, S. H., and Ricominni, C. (2010). OSL age determinations of Pleistocene fluvial deposits in Central Amazonia. *Anais da Academia Brasileira de Ciências* **82**, 1-9.
- Sternberg, H. O. R. (1959). Radiocarbon dating as applied to a problem of Amazonian morphology. In "XVIII Congrès International de Géographie." pp. 399-424. Union Géographique Internationale, Rio de Janeiro.
- Taylor, G., and Woodyer, K. D. (1978). Bank deposition in suspended-load streams. In "Fluvial Sedimentology." (A. D. Miall, Ed.), pp. 257-275. Canadian Society of Petroleum Geologists, Calgary.
- Turcq, B., Suguio, K., Martin, L., and Flexor, J. M. (1993). Registros milenares nos sedimentos dos lagos da serra do Carajás. *Ciência Hoje* **16**, 31-35.
- van der Hammen, T. (1972). Changes in vegetation and climate in the Amazon Basin and surrounding areas during the Pleistocene. *Geologie en Mijnbouw* **51**, 641-643.
- van der Hammen, T. (1974). The Pleistocene changes of vegetation and climate in tropical South America. *Journal of Biogeography* **1**, 3-26.
- van der Hammen, T., and Absy, M. L. (1994). Amazonia during the last glacial. *Palaeogeography, Palaeoclimatology, Palaeoecology* **109**, 247-261.
- Vega, A. (2007). "Reconstituição Paleoambiental dos depósitos Miocenos na Região centro oriental da bacia do Solimões." Unpublished MSc thesis, Universidade Federal do Amazonas.
- Wilkinson, M. J., Marshall, L. G., Lundberg, J. G., and Kreslavsky, M. H. (2010). Megafan environments in northern South America and their impact on Amazon Neogene aquatic ecosystems. In "Amazonia, Landscape and Species Evolution: A Look into the Past." (C. Hoorn, and E. P. Wesselingh, Eds.), pp. 162-184. Wiley-Blackwell, London.

REFERÊNCIAS

- Abbado D., Slingerland R., Smith N.D. 2005. Origin of anastomosis in the upper Columbia River, British Columbia, Canada. *In: M. D. Blum, S.B. Marriot, S.M. Leclair. (eds.) Fluvial Sedimentology VII. Special Publication of the International Association of Sedimentologists*, 35, Blackwell, Oxford, pp.: 3-15.
- Absy M.L. 1979. A palynological study of Holocene sediments in the Amazon basin. PhD Thesis, University of Amsterdam.
- Adamy A. & Romanini S.J. 1990. *Geologia da Região Porto Velho - Abunã. Estados de Rondônia e Amazonas*. Brasília, DNPM/CPRM, Relatório.
- Andrade G.O.d. 1956. Furos, Paranas e Igarapés; análise genética de alguns elementos do sistema potomográfico Amazônico. *Boletim Carioca de Geografia*, 9:15-50.
- Arai M., Nogueira A.C.R., Silveira R.R., Horbe A.M.C. 2003. Considerações Cronoestratigráficas e Paleoambientais da Formação Solimões com Base em Palinomorfos, Região de Coari, Estado do Amazonas. *In: SBG, Simp. Geol. Amazonia*, 8.
- Araujo J.F.B., Montalvão R.M.G., Lima M.I.C., Fernandez P.E.C.A., Cunha F.M.B.d., Fernandes C.A.C., Basei M.A.S. 1974. *Geologia Folha SA-21-Santarém. Levantamento de Recursos Naturais Projeto RadamBrasil*. Rio de Janeiro, DNPM, Relatório.
- Baker V.R. 1978. Adjustment of fluvial systems to climate and source terrain in tropical and subtropical environments. *In: A. D. Miall (ed.) Fluvial Sedimentology*, Canadian Society of Petroleum Geologists, p.: 211-230.
- Bemerguy R.L., Costa J.B.S., Hasui Y., Borges M.D., Junior A.V.S. 2002. Structural geomorphology of the Brazilian Amazon Region. *In: E. L. Klein, M. L. Vasquez, L. T.Rosa-Costa (eds.) Contribuições à Geologia da Amazônia*, 3, Sociedade Brasileira de Geologia Nucleo Norte, p.: 201-207.
- Blum M.D. & Tornqvist T.E. 2000. Fluvial responses to climate and sea-level change: a review and look forward. *Sedimentology*, 47:2-48.
- Bowler J.M., Stockton E., Walker M.J. 1978. Quaternary stratigraphy of the Darling River near Tilpa, New South Wales. *Proceedings of the Royal Society of Victoria*, 90:78-88.
- Brindley G.W. & Brown G. 1980. *Crystal structures of Clay Minerals and Their X-Ray identification*. Mineralogical Society, London, 495 pp.
- Brizga S.O. & Finlayson B.L. 1990. Channel avulsion and river metamorphosis - the case of the Thomson River, Victoria, Australia. *Earth Surf. Process. Landf.*, 15:391-404.
- Cairncross B., Stanistreet I.G., McCarthy T.S., Ellery W.N., Ellery K., Grobicki, T.S.A. 1988. Paleochannels (stone-rolls) in coal seams - modern analogs from fluvial deposits of the Okavango delta, Botswana, southern-Africa. *Sedimentary Geology*, 57:107-118.
- Campbell Jr, K.E., Prothero D.R., Romero-Pittman L., Hertel F., and Rivera N. 2010. Amazonian magnetostratigraphy: Dating the first pulse of the Great American Faunal Interchange. *Journal of South American Earth Sciences*, 29:619-626.
- Campbell K.E., Frailey C.D., Romero-Pittman L. 2006. The Pan-Amazonian Ucayali Peneplain, late Neogene sedimentation in Amazonia, and the birth of the modern Amazon River system. *Palaeogeography Palaeoclimatology Palaeoecology*, 239:166-219.
- Campbell K.E., Heizler M., Frailey C.D., Romero-Pittman L., Prothero D.R. 2001. Upper Cenozoic chronostratigraphy of the southwestern Amazon Basin. *Geology*, 29:595-598.
- Campbell K.E. & L. Romero-Pittman 1989. Geología del cuaternario del Departamento de Madre de Dios (Perú). *Boletín de la Sociedad Geológica del Perú*, 79:53-61.

- Caputo M.V. 1984. Strigraphy, tectonics, paleoclimatology and paleogeography of northern basins of Brazil. PhD Thesis, University of California, 583 p.
- Caputo M.V., Rodrigues R., Vasconcelos D.N. 1971. *Litoestratigrafia da Bacia Amazônica*. Manaus, Petrobras/Renor, Relatório.
- Caputo M.V., Rodrigues R., Vasconcelos D.N.N. 1972. Nomenclatura estratigráfica da Bacia do Amazonas. In: SBG, Congresso Brasileiro de Geologia, 26, Atas, p. 36.
- Chappell J., Omura A., Esat T., McCulloch M., Pandolfi J., Ota Y., Pillans B. 1996. Reconciliation of late Quaternary sea levels derived from coral terraces at Huon Peninsula with deep sea oxygen isotope records. *Earth and Planetary Science Letters*, **141**: 227-236.
- Colinvaux P.A. 1979. The ice-age Amazon. *Nature*, **278**:399-400.
- Colinvaux P.A., De Oliveira P.E., Bush, M.B. 2000. Amazonian and Neotropical plant communities on glacial timescales: the failure of the aridity and refuge hypotheses. *Quaternary Science Reviews*, **19**:141-169.
- Colinvaux P.A., Irion G., Rasanen M.E., Bush M.B., Nunes de Mello J.A.S. 2001. A paradigm to be discarded: geological and paleoecological data falsify the Haffer & Prance refuge hypothesis of Amazonian speciation. *Amazoniana*, **16**:609-646.
- Colinvaux P.A., Oliveira P.E., Moreno J.E., Miller M.C. Bush, M.B. 1996. A long pollen record from lowland Amazonia: forest and cooling in glacial times. *Science*, **274**: 85-88.
- Costa J.B.S., Bemerguy R.L., Hasui Y., Borges M.D. 2001. Tectonics and paleogeography along the Amazon river. *Journal of South American Earth Sciences*, **14**: 335-347.
- CPRM 2010. *Carta Geológica do Brasil ao Milionésimo*. CPRM- Serviço Geológico do Brasil.
- Daemon R.F. & Contreiras C.J.A. 1971. Zoneamento palinológico da Bacia do Amazonas. In: SBG, Congresso Brasileiro de Geologia, 25, Atas, p. 79.
- Dumont J.F. 1993. Types of lakes as related neotectonics in Western Amazonia. In: PICH/INQUA, Simpósio Internacional do Quaternário da Amazônia, Atas, p. 99.
- Dumont J.F. & Garcia F. 1991. Active subsidence controlled by basement structures in the Marañon Basin of Northeastern Peru. In: International Association of Hydrological Sciences, International Symposium on Land Subsidence, 4, Atas, p. 334.
- Dunne T., Mertes L.A.K., Meade R.H., Richey J.E. Forsberg B.R. 1988. Exchanges of sediment between the flood plain and channel of the Amazon River in Brazil. *Geol. Soc. Am. Bull*, **110**:450-467.
- Eiras J.F., Becker C.R., Souza E.M., Gonzaga F.G., Silva J.G.F., Daniel L.M.F. 1994, Bacia do Solimões. *Boletim de Geociências da Petrobras*, **8**:17-45.
- Fielding C.R. 2006. Upper flow regime sheets, lenses and scour fills: Extending the range of architectural elements for fluvial sediment bodies. *Sedimentary Geology*, **190**:227-240.
- Figueiredo J., Hoorn C., van der Ven P., Soares E. 2009. Late Miocene onset of the Amazon River and the Amazon deep-sea fan: Evidence from the Foz do Amazonas Basin. *Geology*, **37**:619-622.
- Fisk H.N. 1944. *Geological Investigation of the Alluvial Valley of the Lower Mississippi River*. Vicksburg, Mississippi River Commission, Relatório.
- Frailey C.D., Lavina E.L., Rancy A., Souza F. J.P.d. 1988. A Proposed Pleistocene/Holocene Lake in the Amazon Basin and its Significance to Amazonian Geology and Biogeography. *Acta Amazonica*, **18**:119-143.
- Franzinelli E. & Igreja H.L.S. 2002. Modern sedimentation in the Lower Negro River, Amazonas State, Brazil. *Geomorphology*, **44**:259-271.

- Gibling M.R., Nanson G.C., Maroulis J.C. 1998. Anastomosing river sedimentation in the Channel Country of central Australia. *Sedimentology*, **45**:595-619.
- Gingras M.K., Rasanen M., Ranzi A. 2002. The significance of bioturbated inclined heterolithic stratification in the southern part of the Miocene Solimoes Formation, Rio Acre, Amazonia Brazil. *Palaios*, **17**:591-601.
- Gradzinski R., Baryla J., Doktor M., Gmur D., Gradzinski M., Kedzior A., Paszkowski M., Soja R., Zielinski T., Zurek S. 2003. Vegetation-controlled modern anastomosing system of the upper Narew River (NE Poland) and its sediments. *Sedimentary Geology*, **157**:253-276.
- Gross M., Piller W.E., Ramos M.I., Douglas da Silva Paz J. 2011. Late Miocene sedimentary environments in south-western Amazonia (Solimões Formation; Brazil). *Journal of South American Earth Sciences*, **32**:169-181.
- Gupta A. (Ed.) 2007. *Large Rivers: Geomorphology and Management*. John Wiley & Sons, Chichester, 689 pp.
- Haffer J., 1969. Speciation in Amazonian forest birds. *Science*, **165**:131-137.
- Haffer J. & Prance G.T. 2001. Climatic forcing of evolution in Amazonia during the Cenozoic: on the refuge theory of biotic differentiation. *Amazoniana*, **16**:579-607.
- Harwood K. & Brown A.G. 1993. Fluvial processes in a forested anastomosing river - flood partitioning and changing flow patterns. *Earth Surf. Process. Landf.*, **18**:741-748.
- Hickin E.J. 1984. Vegetation and river channel dynamics. *Can. Geogr.-Geogr. Can.*, **28**:111-126.
- Hooghiemstra H. 1995. Environmental and paleoclimatic evolution in Late Pliocene-Quaternary Colombia. In: E. S. Vrba, G. Denton, L. H. Burckle and T. C. Partridge (eds) *Paleoclimatic and Evolution, with Emphasis on Human Origins*. Yale University Press, p.: 249-261.
- Hooghiemstra H. 2001. The continuing debate on the history of the Amazonian rain forest. *Amazoniana*, **16**:653-656.
- Hooghiemstra H. & van der Hammen T. 1998. Neogene and Quaternary development of the neotropical rain forest: the forest regugia hypothesis, and a literature overview. *Earth Science Reviews*, **44**:147-183.
- Hoorn C., 1993. Marine incursions and the influence of Andean tectonics on the Miocene depositional history of northwestern Amazonia - results of a palynostratigraphic study. *Palaeogeography Palaeoclimatology Palaeoecology*, **105**: 267-309.
- Hoorn C., 1994. An Environmental reconstruction of the Paleo-Amazon River System (Middle-Late Miocene, NW Amazonia). *Palaeogeography Palaeoclimatology Palaeoecology*, **112**: 187-238.
- Hoorn C., Guerrero J., Sarmiento G.A., Lorente M.A. 1995. Andean tectonics as a cause for changing drainage patterns in Miocene northern South America. *Geology*, **23**:237-240
- Hoorn C., Wesselingh F.P., Hovikoski J., Guerrero J. 2010. The development of the Amazonian mega-wetland (Miocene; Brazil, Colombia, Peru, Bolivia). In: C. Hoorn & E. P. Wesselingh (eds.) *Amazonia, Landscape and Species Evolution: A Look into the Past*. Wiley-Blackwell, p.: 123-142.
- Hovikoski J., Rasanen M., Gingras M., Roddaz M., Brusset S., Hermoza W., Pittman L.R. 2005. Miocene semidiurnal tidal rhythmites in Madre de Dios, Peru. *Geology*, **33**:177-180.
- Huang H.Q. & Nanson G.C. 1997. Vegetation and channel variation; A case study of four small streams in southeastern Australia. *Geomorphology*, **18**:237-249.
- Huguett A., Galvis J., Ruge P. 1979. *Geologia La Amazonia Colombiana y sus recursos - Proyecto Radargrametrico del Amazonas*. Bogotá, Instituto Geografico Agustin Codazzi, Relatório.

- Inman D.L. and C.E. Nordstro, 1971. Tectonic and morphologic classification of coasts. *Journal of Geology*, **79**: 1-7.
- Irion G., Junk W.J., Mello J.A. 1997. The large central Amazonian river floodplains near Manaus: Geological, climatological, hydrological and geomorphological aspects. *In*: W. J. Junk (ed.) *The central Amazon floodplain: Ecology of a pulsating system*. Springer, p.: 23-46.
- Irion G., Räsänen M., de Mello N., Hoorn C., Junk W., Wesselingh F. 2005. D. Rossetti, P. Mann de Toledo, A.M. Góes, New geological framework for Western Amazonia (Brazil) and implications for biogeography and evolution, *Quaternary Research* 63 (2005) 78-89. *Quaternary Research*, **64**:279-280.
- Iriondo M. 1982. Geomorfologia da planície Amazônica. *In*: SBG, Simpósio do Quaternário do Brasil, 4, *Atas*, p. 323.
- Junk W.J., Bayley P.B., Sparks R.E. 1989. The flood pulse concept in river-floodplain systems. *In*: D. Dodge (ed.) *Proceeding of the International Large River Symposium, Canadian Special Publications of Fisheries and Aquatic Sciences*. Department of Fisheries and Oceans Canada, p.: 110-127.
- Kalliola R., Salo J., Puhakka M., Rajasilta M., Häme T., Neller R.J., Räsänen M.E., Danjoy Arias W.A. 1992. Upper Amazon channel migration. *Naturwissenschaften*, **79**:75-79.
- Kastner T.P. & Goñi M.A. 2003. Constancy in the vegetation of the Amazon basin during the late Pleistocene: evidence from the organic matter composition of Amazon deep sea fan sediments. *Geology*, **31**:291-294.
- Khobzi J., Kroonenberg S., Faivre P., Weeda A. 1980. Aspectos geomofologicos de la Amazonia y la Orinoquia Colombianas. *Revista CIAF*, **5**:97-126.
- Knighton D. & Nanson G.C. 1993. Anastomosis and the continuum of channel pattern. *Earth Surf. Process. Landf.*, **18**:613-625.
- Kristler P. 1954. *Historical resume of the Amazon Basin*. Belém, Petrobras/Renor, Relatório.
- Kummel B. 1948. Geological reconnaissance of the Contamana region, Peru. *Geological Society of America Bulletin*, **59**; 1217-1266.
- Lane E.W. 1955. The importance of fluvial morphology in hydraulic engineering. *American Society of Civil Engineers Proceedings*, **81**:1-17
- Latrubesse E.M. 2008. Patterns of anabranching channels: The ultimate end-member adjustment of mega rivers. *Geomorphology*, **101**:130-145.
- Latrubesse E.M., Cozzuol M., da Silva-Caminha S.A.F., Rigsby C.A., Absy M.L., Jaramillo C. 2010. The Late Miocene paleogeography of the Amazon Basin and the evolution of the Amazon River system. *Earth-Science Reviews*, **99**:99-124.
- Latrubesse E.M., da Silva S.A.F., Cozzuol M., Absy M.L. 2007. Late Miocene continental sedimentation in southwestern Amazonia and its regional significance: Biotic and geological evidence. *Journal of South American Earth Sciences*, **23**:61-80.
- Latrubesse E.M. & Franzinelli E. 1993. Reconstrução das condições hidrológicas do passado. *Ciência Hoje*, **16**:40-43.
- Latrubesse E.M. & Franzinelli E. 2002. The Holocene alluvial plain of the middle Amazon River, Brazil. *Geomorphology*, **44**:241-257.
- Leytón D.F. & Pacheco Z.J. 1989. *Geología del cuaternario-terciario aflorante en el Río Madre de Dios (Departamentos de Plando, La Paz, Beni)*. Sociedad Geológica Boliviana, 352 pp.
- Maia R.G.N., Godoy H.K., Yamaguti H.S., Moura P.A., Costa F.S.F., Holanda M.A., Costa J.A. 1977. Projeto Carvão no Alto Solimões. Manaus, CPRM/DNPM, Relatório, 137p.
- Makaske B. 1998. Anastomosing rivers; forms, processes and sediments. *Nederlandse Geografische Studies*, 249. Utrecht, Koninklijk Nederlands Aardrijkskundig Genootschap/Faculteit Ruimtelijke Wetenschappen, Universiteit Utrecht.

- Makaske B. 2001. Anastomosing rivers: a review of their classification, origin and sedimentary products. *Earth-Science Reviews*, **53**:149-196.
- Makaske B., Smith D.G., Berendsen H.J.A., de Boer A.G., van Nielen-Kiezebrink M.F., Locking T. 2009. Hydraulic and sedimentary processes causing anastomosing morphology of the upper Columbia River, British Columbia, Canada. *Geomorphology*, **111**:194-205.
- Martinez J.M., Guyot J.L., Filizola N., Sondag F. 2009. Increase in suspended sediment discharge of the Amazon River assessed by monitoring network and satellite data. *CATENA*, **79**:257-264.
- Meade R.H. 1994. Suspended sediments of the modern Amazon and Orinoco rivers. *Quaternary International*, **21**:29-39.
- Meade R.H. 1996. River-sediment inputs to major deltas. In: J. D. Milliman & B. U. Haq (eds.) *Sea-level Rise and Coastal Subsidence: Causes, Consequences and Strategies*. Dordrecht Kluwer Academic Publishers. p.: 63-85
- Mertes L.A.K. 1985. Floodplain development and sediment transport in the Solimões-Amazon River in Brazil. MSc Thesis, University of Washington. 108 p.
- Mertes L.A.K. 1994. Rates of floodplain sedimentation on the central Amazon River. *Geology*, **22**:171-174.
- Mertes L.A.K., Dunne T., Martinelli L.A. 1996. Channel-floodplain geomorphology along the Solimões-Amazon River, Brazil. *Geological Society of American Bulletin*, **108**:1089-1107.
- Miall A.D. 1992. Alluvial Deposits. In: R. G. Walker & N. P. James (eds.) *Facies Models: Response to Sea Level Change*. Geological Association of Canada, p.: 119-142.
- Motta M.B. 2008. Proveniência da Formação Iça e de sedimentos do Rio Solimões, entre os municípios de Tefé e Manacapuru, Amazonas. Dissertação de Mestrado, Departamento de Geociências, Universidade Federal do Amazonas. 112 p.
- Moura P.A. 1944. O relevo da Amazônia. In: *Amazônia Brasileira*. IBGE, p.: 14-23
- Murray A.S. & Wintle A.G. 2000. Luminescence dating of quartz using an improved single-aliquot regenerative-dose protocol. *Radiation Measurements*, **32**:57-73.
- Nanson G.C. 1980. Point-bar and floodplain formation of the meandering Beatton River, Northeastern British-Columbia, Canada. *Sedimentology*, **27**:3-29.
- Nanson G.C. & Croke J.C. 1992. A genetic classification of floodplains. *Geomorphology*, **4**:459-486.
- Nanson G.C. & Gibling M.R. 2003. Anabranching Rivers. In: G. V. Middleton (ed.) *Encyclopedia of Sediments and Sedimentary Rocks*. Kluwer Academic Publishers, p.: 9-11.
- Nanson G.C. & Gibling M.R. 2003. Rivers and alluvial fans. In: G. V. Middleton (ed.) *Encyclopedia of Sediments and Sedimentary Rocks*. Kluwer Academic Publishers, p.: 568-582.
- Nanson G.C. & Knighton D. 1996. Anabranching rivers: their cause, character and classification. *Earth Surf. Process. Landf.*, **21**:217-239.
- Nogueira A.C.R., Arai M., Horbe A.M.C., Silveira R.R., Silva J.S. 2003. A Influência Marinha nos Depósitos da Formação Solimões na Região de Coari (AM): Registro da Transgressão Miocênica na Amazônia Ocidental. In: SBG, Simp. Geol. Amazônia, 8.
- Oppenheim V. 1946. Geological reconnaissance in southeastern Peru. *Bulletin of American association of Petroleum Geologists*, **30**:254-264.
- Ouchi S. 1985. Response of alluvial rivers to slow active tectonic movement. *Bulletin of the Geological Society of America*, **96**:504-515.
- Pärssinen M.H., Salo J.S., Räsänen M.E. 1996. River floodplain relocations and the abandonment of Aborigine settlements in the Upper Amazon Basin: A historical case

- study of San Miguel de Cunibos at the Middle Ucayali River. *Geoarchaeology*, **11**:345-359.
- Peixoto J.M.A., Nelson B.W., Wittmann F. 2009. Spatial and temporal dynamics of river channel migration and vegetation in central Amazonian white-water floodplains by remote-sensing techniques. *Remote Sensing of Environment*, **113**:2258-2266.
- Potter P.E. 1978. Significance and origin of big rivers. *Journal of Geology*, **86**:13-33.
- Quadros M.L.E.S., Rizzotto G.J., Oliveira J.G.F., Castro J.M.R. 2006. Depósitos fluviais da Formação Rio Madeira, Pleistoceno Superior da Bacia do Abunã, Rondônia, *In*: SBG, Simp. Geol. Amazônia, 9.
- Rasanen M.E., Linna A.M., Santos J.C.R., Negri F.R. 1995. Late Miocene tidal deposits in the Amazonian foreland basin. *Science*, **269**:386-390.
- Rego L.F.d.M. 1930. *Notas sobre a geologia do território de Acre e da Bacia do Javari*. Cezar and Cavalcante, Manaus, 45 pp.
- Rizzotto G.J., Cruz N.M.C., Oliveira J.G.F., Quadros M.L.E.S., Castro J.M.R. 2006. Paleoambiente e o registro fóssilífero Pleistocênico dos sedimentos da Formação Rio Madeira, *In*: SBG, Simp. Geol. Amazônia, 9.
- Rizzotto G.J., Oliveira J.G.F., Quadros M.L.E.S., Castro J.M.R., Cordeiro A.V., Adamy A., Melo J.H.G., Dantas M.E. 2005. *Projeto Rio Madeira. Levantamento de informações para subsidiar o estudo de viabilidade do aproveitamento hidrelétrico (AHE) do Rio Madeira. AHE Jirau*. Porto Velho, CPRM, Relatório final.
- Rossetti D.F., de Toledo P.M., Goes A.M. 2005. New geological framework for Western Amazonia (Brazil) and implications for biogeography and evolution. *Quat. Res.*, **63**:78-89.
- Rozo J.M.G. 2004. Evolução Holocênica do Rio Amazonas entre a Ilha do Careiro e a foz do Rio Madeira. Dissertação de Mestrado, Departamento de Geociências, Universidade Federal do Amazonas. 93 p.
- Rozo J.M.G., Nogueira A.C.R., Carvalho A. 2005. Análise multitemporal do sistema fluvial do Amazonas entre a ilha do Careiro e a foz do rio Madeira. *In*: INPE, Simpósio Brasileiro de Sensoriamento Remoto, 12, *Atas*, p. 1875.
- Rozo J.M.G., Nogueira A.C.R., Horbe A.M.C., Carvalho A. 2005. Depósitos Neogênicos da Bacia do Amazonas. *In*: A. M. C. Horbe & V. S. Souza (eds.) *Contribuições à Geologia da Amazônia*, 4, Sociedade Brasileira de Geologia Núcleo Norte, p.: 201-207.
- Rozo M.G., Nogueira A.C.R., Truckenbrodt, W. 2012. The anastomosing pattern and the extensively distributed scroll bars in the middle Amazon River. *Earth Surface Processes and Landforms*, (Aceito ainda sem data de publicação).
- Rozo M.G. & Soto C.C. 2010. Quantification of change and migration rates in the Amazon River. *In*: SBG, Congresso Brasileiro de Geologia, 45.
- Rozo M.G. Soto C.C., Nogueira A.C.R. 2012. Recent fluvial dynamics of the Colombian Amazon River (submetido). *Remote sensing of environment*.
- Rust B.R. 1981. Sedimentation in an arid-zone anastomosing fluvial system; Cooper's Creek, central Australia *Journal of Sedimentary Petrology*, **51**:745-755.
- Santos F.A.M. 2000. Growth and leaf demography of two Cecropia species. *Revista Brasileira de Botânica*, **23**:133-141.
- Schumm S.A., Erskine W.D., Tilleard J.W. 1996. Morphology, hydrology, and evolution of the anastomosing Ovens and King Rivers, Victoria, Australia. *Geol. Soc. Am. Bull.*, **108**:1212-1224.
- Silva L.L. 1988. A Estratigrafia da Formação Solimões: Uma análise crítica. *In*: SBG, Congresso Brasileiro de Geologia, 35, *Atas*, p. 725

- Silveira R.R. & Nogueira A.C.R. 2005. Cronoestratigrafia e Paleoambiente dos Depósitos do Mioceno Superior da Bacia do Solimões, Centro-oeste da Amazônia. *In: Finep/Petrobrás, Congresso Internacional do PIATAM, 1, Atas, p. 98.*
- Smith D.G. 1976. Effect of vegetation on lateral migration of anastomosed channels of a glacier meltwater river. *Geol. Soc. Am. Bull.*, **87**:857-860.
- Smith D.G. 1983. Anastomosed fluvial deposits: modern examples from Western Canada. *In: J. D. Collinson & J. Lewin (eds.) Modern and Ancient Fluvial Systems. Special Publication of the International Association of Sedimentologist, 6, Blackwell, p.: 155-168.*
- Smith D.G. 1986. Anastomosing river deposits, sedimentation rates and basin subsidence, Magdalena River, northwestern Colombia, South America. *Sedimentary Geology*, **46**:177-196.
- Smith D.G. & Putnam P.E. 1980. Anastomosed river deposits; modern and ancient examples in Alberta, Canada. *Canadian Journal of Earth Science*, **17**:1396-1406.
- Smith D.G. & Smith N.D. 1980. Sedimentation in anastomosed river systems: examples from alluvial valleys near Banff, Alberta. *Journal of Sedimentary Petrology*, **50**: 157-164.
- Soares E.A.A. 2007. Depósitos Pleistocenos da Região de Confluência dos rios Negro e Solimões, Amazonas. Tese de doutorado, Instituto de Geociências, Universidade de São Paulo. 205 p.
- Soares E.A.A., Tatum S.H., Ricominni C. 2010. OSL age determinations of Pleistocene fluvial deposits in Central Amazonia. *Anais da Academia Brasileira de Ciências*, **82**:1-9.
- Stanistreet I.G., Cairncross B., McCarthy T.S. 1993. Low sinuosity and meandering bedload rivers of the Okavango fan - channel confinement by vegetated levees without fine sediment. *Sedimentary Geology*, **85**:135-156
- Sternberg H.O.R. 1950. Vales tectônicos na Planície Amazônica? *Revista Brasileira de Geografia*, **4**:3-26.
- Sternberg H.O.R. 1959. Radiocarbon dating as applied to a problem of Amazonian morphology. *In: Union Géographique Internationale, Congrès International de Géographie*, 18, *Atas*, p. 399.
- Syvitski J.P.M., Vorosmarty C.J., Kettner A.J., Green P. 2005. Impact of Humans on the Flux of Terrestrial Sediment to the Global Coastal Ocean. *Science* **308**:376-380.
- Taylor G. & Woodyer K.D. 1978. Bank deposition in suspended-load streams. *In: A. D. Miall (ed.) Fluvial Sedimentology. Canadian Society of Petroleum Geologists*, p.: 257-275.
- Thomas R.G., Smith D.G., Wood J.M., Visser J., Calverley-Range E.A., Koster E.H. 1987. Inclined Heterolithic Stratification - Terminology, Description, Interpretation and Significance. *Sedimentary Geology*, **53**:123-179.
- Tucker C.J., Grant D.M., Dykstra J.D. 2004. NASA's global orthorectified landsat data set. *Photogrammetric Engineering and Remote Sensing*, **70**:313-322.
- Turcq B., Suguio K., Martin L., Flexor J.M. 1993. Registros milenares nos sedimentos dos lagos da serra do Carajás. *Ciência Hoje*, **16**:31-35.
- van der Hammen T. 1972. Changes in vegetation and climate in the Amazon Basin and surrounding areas during the Pleistocene. *Geologie en Mijnbouw*, **51**:641-643.
- van der Hammen T. 1974. The Pleistocene changes of vegetation and climate in tropical South America. *Journal of Biogeography*, **1**:3-26.
- van der Hammen T. & Absy M.L. 1994. Amazonia during the last glacial. *Palaeogeography, Palaeoclimatology, Palaeoecology*, **109**:247-261.
- Vega A. 2007. Reconstituição Paleoambiental dos depósitos Miocenos na Região centro oriental da bacia do Solimões. Dissertação de Mestrado, Departamento de Geociências, Universidade Federal do Amazonas.

- Wilkinson M.J., Marshall L.G., Lundberg J.G., Kreslavsky M.H. 2010. Megafan environments in northern South America and their impact on Amazon Neogene aquatic ecosystems. *In: C. Hoorn & E. P. Wesselingh (eds.) Amazonia, Landscape and Species Evolution: A Look into the Past.* Wiley-Blackwell, p.: 162-184.
- Wohl E.E. 2007. Hydrology and Discharge. *In: A. Gupta (ed.) Large Rivers: Geomorphology and Management.* John Wiley & Sons, p.: 29-41.



UNIVERSIDADE FEDERAL DO PARÁ
INSTITUTO DE GEOCIÊNCIAS
PROGRAMA DE PÓS-GRADUAÇÃO EM GEOLOGIA E GEOQUÍMICA



PARECER

Sobre a Defesa Pública da Tese de Doutorado de JOSÉ MAX GONZÁLEZ ROZO

A banca examinadora da tese de doutorado de JOSÉ MAX GONZÁLEZ ROZO intitulada "O SISTEMA FLUVIAL SOLIMÕES-AMAZONAS DURANTE O HOLOCENO" composta pelos Professores Doutores Afonso César Rodrigues Nogueira (Orientador-UFPA), José Cândido Stevaux (UEM), Ana Maria Góes (USP) (UFPA), Antônio Emídio de Araújo Santos Júnior (UFPA) e Arnaldo de Queiroz da Silva (UFPA), após a apresentação oral e arguição do candidato, emite o seguinte parecer:

O candidato apresentou contribuição relevante ao conhecimento sobre as características morfoestratigráficas e sedimentológicas dos grandes rios tropicais desde o Pleistoceno. Destaca-se a abordagem integrada utilizando diversas ferramentas para embasar o modelamento dos depósitos relacionados aos sistemas fluviais amazônicos. O documento está bem apresentado na forma de três artigos, dos quais um já está publicado e ressalta-se que a conclusão da tese ocorreu em 36 meses. A apresentação oral foi clara, bem estruturada e de conteúdo relevante e notou-se um incremento da pesquisa em relação ao texto. Além disso, o candidato demonstrou capacidade de síntese em apresentar no tempo estipulado o conteúdo da sua tese.

Na arguição o candidato defendeu sua tese e respondeu satisfatoriamente as várias questões gerais e específicas apresentadas, demonstrando maturidade científica.

Com base no exposto, a banca examinadora decidiu por unanimidade aprovar a tese de doutorado com distinção.

Belém, 3 de setembro de 2012.

Prof. Dr. Afonso César Rodrigues Nogueira (Membro-UFPA)

Prof. Dr. José Cândido Stevaux (Membro-UEM)

Prof. Dr. Ana Maria Góes (Membro-USP)

Prof. Dr. Antônio Emídio de Araújo Santos Júnior (Membro-UFPA)
Prof. Dr. Arnaldo de Queiroz da Silva (Membro-UFPA)